Effects of Exercise on Adipose Tissue Remodeling

by

Cheehoon Ahn

A dissertation submitted in partial fulfillment
of the requirements for the degree of
Doctor of Philosophy
(Movement Science)
in the University of Michigan
2023

Doctoral Committee:

Professor Jeffrey Horowitz, Chair
Associate Professor Dave Bridges
Professor Gregory Cartee
Associate Professor Jacob Haus

Cheehoon Ahn

ahnchi@umich.edu

ORCID iD: 0000-0003-4140-125X

Dedication

This dissertation is dedicated to my family

Acknowledgments

First and foremost, I am deeply indebted to my advisor, Jeff Horowitz, for believing in me, always being open, and not only serving as an inspirational figure in the world of science but also as a shining role model for compassion and kindness. I will never forget the first time we met as strangers during the orientation day lunch session where I instantly knew that this is where I belong. That's how our journey began and it was one of the best decisions that I made in my life to learn from you. I have learned so much from you, and even though we will soon be parting ways, you will always remain my mentor.

I would like to extend my sincere appreciation to my dissertation committee members. Thank you, Greg Cartee, for providing wise and thoughtful guidance, and warm words. Thank you, Jake Haus, I appreciate your critical thinking and the feedback you provided, which encouraged me to strive for excellence. Thank you, Dave Bridges, although our communication was not frequent, I was always influenced by your work, which were fundamental to my research.

I am extremely grateful for every past and current member of the Substrate Metabolism Lab, who played a significant role in my journey. Thanks to Ben Ryan for teaching me everything I needed to know as a graduate student and for always acting professionally, which I greatly admired. You are the role model of a postdoc. Thanks to Alison Ludzki for consistently providing positive energy. Thanks to Pallavi Varshney for providing comprehensive instruction in every detail, greatly benefiting my capacity. Thanks to Michael Schleh for fostering excellent teamwork that allowed us to make progress, even in the midst of a pandemic. You are not only a great friend but also a mentor to me. Thanks to Tao Zhang for always being cooperative and a good friend. Thanks to Suzette Howton for understanding my concerns regarding subject recruitment and making efforts to accommodate me. Thanks to Thomas Rode for offering exceptional technical assistance and creating a humorous working environment that I will miss a lot.

Lastly, thanks to all the undergraduate members who readily assisted me whenever I needed it.

I am grateful to my friends in the doctoral suite: Jeongjin Kim, Seongeun Kwak, James Shadiow, Corey Mazo, and Alex Ahn. I enjoyed every moment spent with you all and the numerous scientific discussions we had over the last four years. I am grateful that most of you are moving on to new chapters, and we will stay in touch.

Thanks to Xiting Yang, who holds great importance in my life. I am excited about our upcoming journey.

Finally, a heartfelt thank you to my family, who always believed in me and provided endless support and enthusiasm throughout my studies. Thanks to my parents, Hyesook and Kwangseog, for shaping who I am and for always being by my side. Thanks to my brother, Chiwon, for having my back.

Table of Contents

List of Tables

List of Figures

Abstract

An excessive amount of fat in abdominal subcutaneous adipose tissue (aSAT) is a hallmark of obesity that often exhibits low capillary density, fibrotic extracellular matrix, immune cell infiltration, and dysregulated metabolic function. These abnormalities in aSAT are linked to excessive release of fat into the bloodstream, which can cause insulin resistance and systemic inflammation. Therefore, strategies to remodel aSAT structure and metabolic function for healthful fat storage hold high clinical interest. Regular exercise is recommended to treat obesity-induced health complications but the direct effects of exercise on aSAT are poorly understood. The aim of this dissertation were to assess the direct effects of exercise on aSAT morphology and factors regulating aSAT morphology, metabolic function, and inflammation. In Project 1, a total of 45 healthy adults who exercise regularly performed a single session of either low- (LOW), moderate- (MOD), or high- (HIGH) intensity exercise (n=15 in each group). aSAT samples were collected before and 1.5 hours after exercise. Transcriptomic analysis revealed a robust upregulation in the global “inflammatory response” pathway in all groups (adjusted $p<1e^{-07}$), yet HIGH induced more extensive inflammatory responses than both LOW and MOD. Conversely, ribosomal and oxidative phosphorylation pathways were upregulated after MOD and LOW, but not HIGH. Of the few overlapping differentially expressed genes, we found the most robust changes in some core clock genes (adjusted $p<0.0001$). Findings from Project 1 suggest changes in the inflammatory, circadian clock, ribosomal, and oxidative phosphorylation gene sets shortly after acute exercise may be important contributors to exercise-induced aSAT adaptations. In Project 2, aSAT samples were collected from 36 adults with obesity before and after 12 weeks of moderate-intensity continuous training (MICT; 70%HR_{max}, 45 min; n=17) or high-intensity interval training (HIIT; 90%HR_{max}, 10×1min; n=19), maintaining their body weight throughout. MICT and HIIT induced similar modifications in aSAT structure (reduced adipocyte size, increased Col5a3, increased capillary density, all $P\leq0.05$) and altered protein abundance of factors

that regulate structural remodeling (reduced MMP9; increased ANGPTL2; both $P \leq 0.02$), lipid and oxidative metabolism (increased HSL, CD36, and COX4; $P < 0.03$), and key proteins involved in the MAPK pathway when measured the day after the last exercise session. These findings from Project 2 indicate that exercise training may induce some early structural and metabolic adaptations in aSAT even without weight loss. In Project 3, aSAT was collected from 16 adults with overweight/obesity who exercise regularly for at least 2 years (EX) and 16 well-matched sedentary/non-exercisers (SED) who were tightly pair-matched for adiposity. Compared with SED, aSAT collected from EX had greater capillary density and a lower abundance of Col6a and macrophages ($P < 0.05$). Global proteomics analysis revealed ribosomal, mitochondrial, and lipogenic proteins were upregulated, whereas complement and proteasomal proteins were downregulated in EX vs. SED (FDR<0.1). Phosphoproteomics indicated a greater abundance of phosphoproteins involved in protein translation, lipogenesis, and direct regulation of transcripts in EX vs. SED ($P < 0.01$). Findings from Project 3 suggest that regular exercise in adults with overweight/obesity favorably remodels the aSAT structure and proteomic profile in ways that may lead to improved lipid storage capacity, which can contribute to preserved cardiometabolic health. Overall, the projects in this dissertation demonstrate regular exercise may induce robust structural and functional adaptations in aSAT that may contribute to improved/sustained cardiometabolic health. My dissertation projects also shed light on potential molecular mechanisms that may mediate the exercise effects on aSAT.

Chapter 1

Statement of the Problem

Obesity has become the largest risk factor for cardio-metabolic disease in the U.S. and its prevalence is rapidly increasing globally (1, 2). The excessive amount of body fat mass that is the hallmark of obesity often consists of large fat cells, with a relatively low capillary density, a highly fibrotic extracellular matrix (ECM), altered immune cell profiles, and dysregulated lipid metabolism, which are all highly linked with cardiometabolic health complications, including insulin resistance and systemic inflammation (3). Although obesity-related health complications are commonly attributed to visceral adiposity, abnormalities in subcutaneous adipose tissue can also have a tremendous impact on metabolic health. For example, excessive systemic fatty acids are tightly linked with insulin resistance that is common in obesity – and the vast majority of these fatty acids are released from abdominal subcutaneous adipose tissue (aSAT) (4, 5). Importantly, this high rate of fatty acid release from aSAT is largely responsible for lipid accumulation in other tissues, including visceral adipose tissue (6). Altered macrophage population and cytokine production (i.e. increased pro-inflammatory macrophages and cytokines) from aSAT in obesity are also now considered a very important contributor to elevated systemic inflammation and whole-body insulin resistance (7). Therefore, clinical and/or pharmacological strategies targeting aSAT fatty acid storage capacity and inflammation in aSAT hold high promise as effective therapeutic approaches to treat obesity-related health complications.

Regular exercise is a first-line therapeutic approach to treat obesity-related metabolic health complications such as insulin resistance, cardiovascular disease, and type 2 diabetes (8-10). While much of the work examining the effects of exercise on metabolic health has focused on adaptations in skeletal muscle mitochondria and oxidative capacity – increasing muscle oxidative capacity, per se, is often found to do rather little to improve insulin sensitivity or other key markers of metabolic health (11, 12). Therefore, interventions specifically targeting increases in muscle oxidative capacity may

not be particularly effective. Alternatively, recent findings from our lab and others suggest that exercise may modify aSAT in ways that can improve fatty acid storage capacity and attenuate inflammation (13-15). For example, preliminary data from our lab suggests serum collected immediately after a session of exercise accelerated the rate of adipogenesis, measured *in vitro,* which may lead to improved lipid storage capacity (13). Others have reported increased angiogenesis (14) and attenuated fibrosis and inflammation after exercise training (15). However, surprisingly little is known about both acute and chronic effects of exercise on the structural and functional aspects of aSAT (e.g., adipogenesis, angiogenesis, ECM remodeling, inflammation) that may improve metabolic health. Expanding our understanding of the impact of exercise on adaptations to the structure and function of aSAT may help optimize exercise protocols for improving metabolic health in obesity, and may also help identify novel signaling pathways in aSAT that may lead to alternative approaches for treating and/or preventing obesity-related diseases.

Long-term adaptations to exercise training are largely a consequence of the accrual of acute responses to each exercise session (e.g., changes in gene expression, and cellular signaling) (16). Emerging evidence from our lab and others suggests that a session of exercise can induce a wide range of transcriptional modifications in aSAT that may regulate angiogenesis, adipogenesis, and inflammation (17-19). In addition, macrophage phenotype in aSAT has been found to be altered in a few hours after a single session of exercise (17, 20) suggesting exercise provides a potent stimulus to rapidly trigger cell signals to change macrophage profiles within aSAT. Therefore, characterizing the transcriptional and post-translational responses in aSAT after a session of exercise will advance our understanding of how the accumulation of repeated sessions of exercise (i.e., exercise training) may translate into robust modifications to the structure and function of aSAT in the long term. Importantly, acute responses to exercise within skeletal muscle and the cardiovascular system can vary greatly depending on the intensity of exercise being performed (21), and the same appears to be true in aSAT (22, 23). Recent findings from our lab indicate that a single session of exercise at high-intensity induced distinct transcriptional modifications in aSAT related to inflammation, metabolism, and adipogenesis compared with a session of moderate-intensity exercise (18). How these

transcriptional responses translate into functional modifications (i.e., protein expression and post-translational modification) and whether these modifications are held at a wider range of exercise intensity (i.e., low to high-intensity exercise) are unexplored. Comparing the acute effects of low-, moderate-, and high-intensity exercise on aSAT will further expand our understanding of the effect of exercise on factors that regulate aSAT remodeling and inflammation. The overall objectives of Project 1 of my dissertation were to compare exercise-induced transcriptional and post-translational responses in aSAT 90 min after low-, vs. moderate-, vs high-intensity exercise. *The specific aims of Project 1 of my dissertation were to compare the acute effects of low-, moderate-, and high-intensity exercise on: (1) aSAT transcriptome regulating aSAT remodeling and metabolism; (2) post-translational modifications to factors regulating aSAT remodeling and inflammation (e.g., phosphorylation of metabolic and cellular signaling proteins); and (3) circulating aSAT cytokine abundance.*

Because the accrual of signaling events after each session of exercise underlies much of the adaptations due to exercise training, a logical next step of my dissertation was to determine whether/how these acute responses to exercise assessed in Project 1 may translate into structural and/or functional adaptations in aSAT after exercise training. Very little is known about exercise-induced adaptations to the structure and function of aSAT in human subjects. The few available studies in this area have focused primarily on adaptations to “conventional” moderate-intensity continuous training (MICT) and almost nothing is known about aSAT adaptations to high-intensity interval training (HIIT), which has garnered considerable attention due to its time efficiency and distinct physiological responses compared with MICT (24, 25). A recent murine study reported a greater effect on circulating adipokine levels and adipocyte size in HIIT vs. MICT, providing some evidence to suggest HIIT may induce more robust adaptations in aSAT (26). However, to my knowledge, no previous studies comprehensively examined structural and functional adaptations in aSAT in response to MICT vs. HIIT in human subjects with obesity. The overall objectives of Project 2 of my dissertation were to compare the effects of 12 weeks of HIIT vs. MICT (without weight loss) on aSAT structure/morphology and lipid metabolism, and molecular factors involved in aSAT remodeling and metabolic function in adults with obesity. *The specific aims of Project 2 were to compare the effects of 12*

weeks of HIIT vs. MICT in adults with obesity on: (1) *aSAT structure/morphology (i.e. capillarization, ECM composition, and adipocyte size); (2) systemic fatty acid mobilization (i.e. fatty acid rate of appearance (Ra) in plasma); and (3) protein abundance of molecular factors that regulate tissue remodeling (i.e. angiogenic and adipogenic transcription factors/markers, ECM remodeling regulators, inflammatory activation, lipolytic and esterific enzymes, and mitochondrial markers).*

In Project 2 of my dissertation, measuring longitudinal adaptions in subjects after a few months of exercise training has the advantage of assessing relatively early training-induced adaptations in aSAT. However, some adaptations in aSAT may take several months or even years to manifest meaningfully (27). Although there are important limitations associated with cross-sectional studies, a cross-sectional design provides an opportunity to examine structural and functional characteristics of aSAT (e.g., capillarization, ECM fibrosis) from individuals who have been habitual exercisers for several years vs. those who have never been regular exercisers. In addition, based on preliminary findings from our lab, we contend habitual exercise may innately reprogram the regulation of angiogenesis and ECM remodeling in aSAT. Therefore, in addition to comparing "static" measures of aSAT capillarization and ECM composition using standard histology and immunoblot techniques, I propose to conduct *ex vivo* analyses of aSAT angiogenic capacity and nascent tissue development, via 3-dimensional tissue culture techniques (i.e., "organoid (i.e., spheroid)" culture). The primary objectives of Project 3 of my dissertation are to compare the structure/morphology and remodeling capacity of aSAT samples collected from adults who have been regular exercisers for many years vs. a well-matched cohort of non-exercisers.

The specific aims of Project 3 of my dissertation were to collect aSAT samples from adults who exercise regularly and a well-matched cohort of non-exercisers to compare (1) aSAT structure/morphology (i.e. capillarization, ECM composition, adipocyte size, macrophage profile, and innervation); (2) aSAT proteomes; (3) angiogenic capacity of aSAT by ex vivo angiogenesis assay; (4) the development of adipocytes and ECM in adipose spheroids cultured from aSAT stromal cells; and (5) cardiometabolic health outcomes (i.e., insulin sensitivity, blood lipid profile, and systemic inflammatory profile).

In summary, the projects outlined in my dissertation proposal addressed the following specific aims:

PROJECT 1:

Specific Aim 1: Compare the acute effects of low-, moderate-, and high-intensity exercise on aSAT transcriptome that regulate metabolic function and remodeling of aSAT.

Specific Aim 2: Compare the acute effects of low-, moderate-, and high-intensity exercise on post-translational modifications on key proteins involved in metabolism, cellular signaling, and inflammation in aSAT.

Specific Aim 3: Compare the acute effects of low-, moderate-, and high-intensity exercise on the circulating cytokine abundance.

PROJECT 2:

Specific Aim 1: Compare the effects of 12 weeks of HIIT vs. MICT without weight loss on aSAT structure/morphology in adults with obesity.

Specific Aim 2: Compare the effects of 12 weeks of HIIT vs. MICT without weight loss on systemic lipid metabolism in adults with obesity.

Specific Aim 3: Compare the effects of 12 weeks of HIIT vs. MICT without weight loss on factors that regulate changes in aSAT structure and lipid metabolism in adults with obesity.

PROJECT 3:

Specific Aim 1: Compare aSAT structure/morphology and factors involved in regulating tissue remodeling between well-matched regularly exercising vs. non-exercising adults with overweight/obesity.

Specific Aim 2: Compare aSAT proteomes that are involved in metabolism and aSAT remodeling between well-matched regularly exercising vs. non-exercising adults with overweight/obesity.

Specific Aim 3: Compare the angiogenic capacity of aSAT, using an *ex vivo* angiogenesis assay between well-matched regularly exercising vs. non-exercising adults with overweight/obesity.

Specific Aim 4: Compare the structure and gene expression in adipose spheroids cultured from aSAT samples collected from well-matched exercising vs. non-exercising adults with overweight/obesity.

These dissertation projects were designed to test the overall hypothesis that exercise induces structural and metabolic adaptations in aSAT that may help improve adipose tissue function and attenuate inflammation, which can further lead to improved cardiometabolic health. Findings from these projects greatly expand our understanding of exercise as a therapeutic strategy to treat metabolic health complications and also may provide novel targets for pharmaceutical interventions.

Chapter 2

Review of Literature

2.1 INTRODUCTION

Over 1.9 billion adults worldwide are currently categorized as overweight and more than 650 million of them are obese (28). This is an alarming issue given that obesity is associated with numerous cardiometabolic health diseases such as Type 2 diabetes (T2D), cardiovascular diseases (CVD), and nonalcoholic fatty liver diseases (NAFLD) (2, 29, 30). Excessive fat mass (i.e., adipose tissue) is the hallmark phenotypical characteristic observed in obesity (31). Increased adipose tissue mass is a major underlying cause of obesity-related cardiometabolic health complications, such as insulin resistance because it is the main source of exacerbated inflammation and excess amounts of mobilized fatty acids that lead to the accumulation of ectopic fats in other important organs (32-34). Although intra-abdominal adipose tissue (i.e. visceral adipose tissue) has been linked with cardiometabolic health complications, almost 90% of total fatty acids mobilized into the systemic circulation are derived from abdominal subcutaneous adipose tissue (aSAT) which is the largest adipose tissue depot that stores lipids (35). Therefore, aSAT is an important target to treat obesity-related cardiometabolic health complications.

aSAT stores excess dietary intake in the form of intracellular triglycerides within “white adipocytes”, which are specialized cells characterized by a unilocular lipid droplet that comprises the most volume of the cells (36). Because adipocytes in human adult aSAT are almost exclusively white adipocytes (37), ‘adipocytes’ and ‘white adipocytes’ will be used interchangeably throughout the chapter. These adipocytes are also capable of synthesizing triglycerides from fatty acyl precursors (i.e., de novo lipogenesis) and liberating fatty acids into the system in times of energy demand (38, 39). While adipocytes occupy most of the aSAT in volume, their cell numbers take up 10~20% of total cells in aSAT indicating the presence of other types of cells (40). Adipose tissue is a very

heterogeneous tissue that consists of diverse cells and structural components such as endothelial cells that build up the capillaries, immune cells (e.g., macrophages, T-cells, etc), fibroblasts, and adipogenic progenitor cells that integrate to maintain metabolic homeostasis and create unique tissue milieu. Importantly, the abundance, polarization, and phenotype of these cells change in response to different metabolic perturbations (e.g. caloric excess or deficit) (3, 41). As such, aSAT function and even its structure can be modified during weight loss or gain. For example, fibrosis in aSAT can be modified by the production/degradation of collagenous proteins secreted from adipocytes and fibroblasts and inflammatory status of aSAT can be modified by immune cell infiltrations (42, 43). Both the number and size of adipocytes can increase (33) while the sprouting of capillaries is promoted to support the expanding adipocytes (44). An effective interplay between these cells and structural components in aSAT is crucial because there is strong evidence that dysregulations in aSAT remodeling may be central to reduced fatty acid storage capacity and exacerbated tissue inflammation that further leads to excess fatty acid spillover to other metabolic organs (i.e., skeletal muscle and liver) and systemic inflammation (32, 45).

Unfortunately, the vast majority of individuals with obesity experience cardiometabolic health complications such as obesity-related insulin resistance (46), and abnormalities in aSAT structure and function appear to be important contributing factors (47, 48). These structural characteristics and functional dysregulations of aSAT in obesity include hypertrophic adipocytes, lower capillarization, ECM fibrosis, infiltration of pro-inflammatory immune cells, and reduced mitochondrial abundance and oxidative capacity (3, 49). These features can negatively influence the capacity of aSAT to effectively store fatty acids into safer neutral lipids and sensitivity to important hormones (i.e., insulin, catecholamines, etc) that regulate fatty acid mobilization (50, 51). Thus, approaches targeting aspects of aSAT structure and function possess high clinical advantages to combat obesity-related health complications. However, to date, no pharmacological treatments to normalize aSAT dysregulation have been developed.

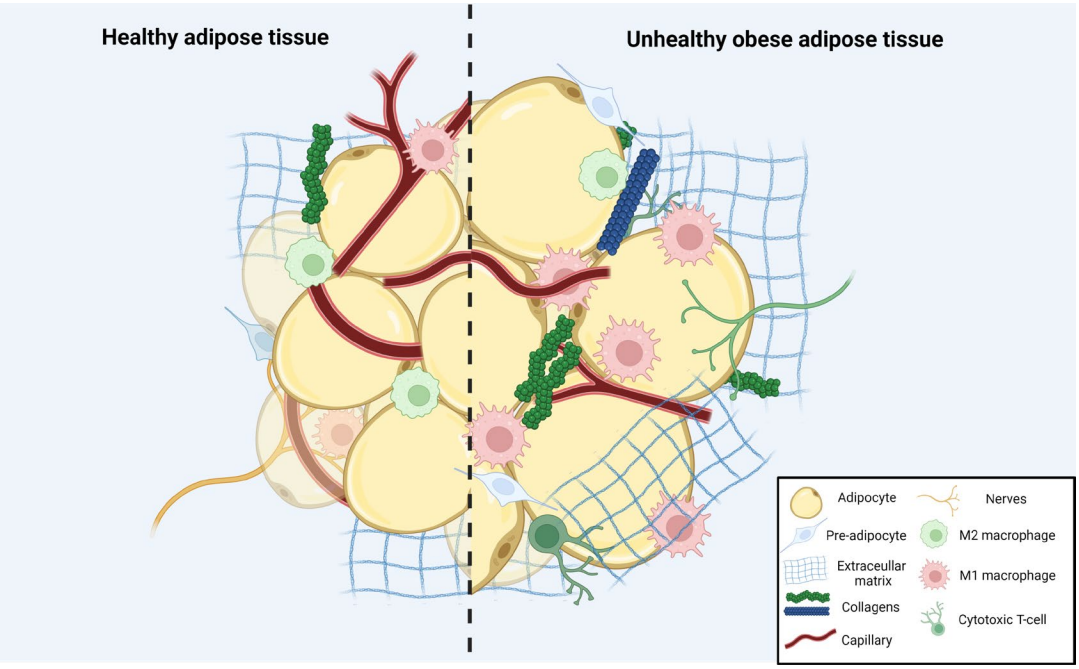

Figure 2-1 Snapshot of healthy vs. unhealthy obese adipose tissue.

Compared with healthy adipose tissue, unhealthy obese adipose tissue is present with hypertrophic adipocytes, relatively less capillarization and innervation, more fibrosis, and more abundance of pro-inflammatory immune cells (e.g., M1 macrophages, cytotoxic T cells) that may lead to lower fatty acid storage capacity and augmented systemic inflammation.

Exercise induces robust adaptations in the cardiovascular system and skeletal muscle that can improve cardiometabolic health. For example, exercise can improve cardiovascular health by increasing cardiac output, reducing arterial stiffness, and inducing skeletal muscle adaptations by increasing mitochondrial oxidative capacity and vascularization (9, 52). There is some evidence demonstrating exercise may improve metabolic health by inducing adaptations in aSAT – but very little is known about the effects of exercise on aSAT. Some of the available evidence indicated that 6 months of aerobic training increased gene expressions of mitochondrial oxidative phosphorylation in aSAT in healthy men (53). In addition, transplantation of subcutaneous white adipose tissue from exercise-trained donor mice improved glucose tolerance and induced vast modifications in gene expressions involved in metabolism in sedentary mice, suggesting a direct relationship between adipose tissue modifications and exercise-induced health improvements (54). Importantly, the interpretations of the direct effects of exercise on aSAT remodeling are confounded from these studies because even a small degree of weight/fat loss can largely impact adipose tissue physiology (8). For example, aSAT

structure and function were reported to be altered after exercise training (e.g., smaller adipocytes, reduced inflammation, and improved responsiveness to catecholamines) but the effects of exercise could not be distinguished from the potent effects of weight loss in these studies (55-58). Recent evidence from our lab has reported that even a single session of exercise may upregulate angiogenic and inflammatory transcriptional responses in aSAT suggesting exercise may directly trigger cues to remodel aSAT (17, 18). Therefore, understanding the acute and chronic adaptations of aSAT remodeling in response to exercise is necessary because it may help optimize exercise to treat obesity-related metabolic health complications and reveal novel signaling pathways that may be pharmaceutically applied to treat obesity-related diseases.

This review will provide background on major cellular and structural components in aSAT and their regulation, and the regulation of fatty acid metabolism in aSAT. It will also describe how aSAT structure and fatty acid metabolism are altered in obesity and how they are associated with obesity-related cardiometabolic health complications. This review will then conclude by outlining how exercise may lead to a remodeling of aSAT that could lead to improved fatty acid storage capacity and attenuated inflammation.

2.2 ADIPOSE TISSUE STRUCTURE AND REMODELING

Effective remodeling of aSAT structure is important for metabolic health

Increased aSAT mass in obesity is often associated with poor metabolic health outcomes such as insulin resistance and systemic inflammation (33, 34). However, not all individuals with obesity experience insulin resistance (48). Interestingly, these ‘metabolically healthy’ individuals with obesity have distinct aSAT characteristics compared with ‘metabolically unhealthy’ individuals with obesity, which suggests a healthier remodeling of aSAT in response to caloric excess may attenuate/prevent poor metabolic health outcomes (48, 59). aSAT from these metabolically healthy individuals with obesity often features smaller adipocytes, higher capillarization, less fibrosis, and less pro-inflammatory immune cell infiltrations (48, 59, 60). These metabolically favorable adaptations in aSAT are believed to increase the fatty acid storage capacity that can safely sequester fatty acids within adipocytes thus reducing the spillover of fatty acids to the system that may lead to ectopic fat accumulation in other organs (i.e., skeletal muscle

and liver) (32). The cellular (i.e., adipocytes, immune cells, and other stromal vascular cells) and structural (i.e., vasculature, ECM proteins, and nerve fibers) components of aSAT are interconnected and closely interplay to maintain metabolic homeostasis (3, 41).

Dysregulations in aSAT remodeling in obesity, on the other hand, can lead to reduced fatty acid storage capacity and exacerbated local inflammation that subsequently leads to insulin resistance and systemic inflammation (3, 49). Hypertrophic adipocytes, lower capillarization, fibrosis, pro-inflammatory immune cell infiltration, and lower nerve innervation are typically observed in dysregulated aSAT remodeling (3, 49, 61). Importantly, these cellular and structural maladaptations often develop in an integrated fashion. For example, hypoxic signals from hypertrophic adipocytes with suboptimal capillarization can induce transcription of fibrotic ECM protein genes, leading to the development of fibrosis which in turn exacerbates the inflammatory status of aSAT (62). This section will outline the major components that consist of aSAT structure, describe how they are altered in obesity, and how their alterations are associated with poor metabolic health.

Adipocyte hypertrophy and adipogenesis

During periods of overeating and weight gain, adipose tissue expansion occurs mostly through the enlargement of existing mature adipocytes (i.e. hypertrophy) although differentiation of existing precursor cells to new mature adipocytes (i.e. hyperplasia) is also possible. Increased adipocyte size, which is very commonly observed in obesity, has been traditionally reported to be associated with poor metabolic health outcomes such as insulin resistance (63). In contrast, smaller adipocyte size has been reported to be positively associated with insulin sensitivity and lower susceptibility to diabetes in individuals with obesity (59, 64, 65). Although available research does not definitively elucidate whether there is a causal relationship between adipocyte size and metabolic health, accumulating evidence strongly supports the concept so-called “adipose tissue expandability hypothesis” first suggested by Dr. Vidal-Puig’s group, which generally states that the reduced capacity of adipocytes to sequester fatty acids leads to the accumulation of fatty acids in other metabolically important organs such as skeletal muscle and liver, creating lipotoxic ectopic fats that are central to systemic metabolic disturbances (33, 66). Moreover, liberated free fatty acids can also directly initiate

inflammatory signaling in adipocytes that leads to the secretion of pro-inflammatory cytokines and infiltrations of immune cells (67).

In contrast to adipocyte hypertrophy, increasing evidence indicates that adipocyte hyperplasia could contribute to healthier adipose tissue remodeling in obesity because of the increased capacity to sequester fatty acids within newly generated adipocytes (68, 69). Overexpression of adiponectin in adipose tissue in mouse models induced significant weight gain and hyperplastic adipose tissue expansion and yet these mice were protected from diabetic phenotypes such as insulin resistance, systemic hyperglycemia, and hyperlipidemia (70). Ten weeks of adipogenic cocktail injection to induce hyperplastic expansion of subcutaneous white adipose tissue in mice during a high-fat diet (HFD) improved metabolic profiles (i.e., higher insulin sensitivity and reduced hepatic ectopic fat) even with higher fat mass compared with the control HFD group (71). By using a lineage-tracing technique that enabled permanent tracking of adipocyte proliferation in the “AdipoChaser” mouse, Dr. Philipp Scherer's group demonstrated that new adipocytes can emerge from the differentiation of precursor cells in an obesogenic environment (72). Unfortunately, in vivo assessment of adipogenesis in humans is still at the stage of infancy. Allister et al attempted to track triglyceride synthesis, de novo lipogenesis, and adipocyte proliferation in aSAT by incorporating deuterated water consumption in insulin-sensitive and insulin-resistant individuals with overweight/obesity (73). Four weeks of deuterated water administration revealed that the rates of adipocyte proliferation were not different in insulin-sensitive vs. resistant individuals with overweight/obesity (0.6% vs. 0.7%/day respectively) (73). From this study, it is unknown why the adipocyte proliferation rates were not different between two groups with distinct metabolic profiles. Perhaps, a robust change in adipocyte differentiation requires a longer period to occur or metabolic triggers (i.e., excess caloric intake). More work is warranted to characterize adipogenic capacity in human aSAT in different metabolic perturbations (i.e., excess energy intake and exercise) to fully understand whether/how fatty acid storage capacity could be enhanced through adipogenesis in human aSAT .

Adipogenesis, the production of new smaller mature adipocytes, is achieved by the differentiation of adipocyte precursor cells (APC) (i.e., pre-adipocyte) in adipose stromal that are committed to adipocyte lineage (68, 74). Typical markers of the adipocyte

lineage include platelet-derived growth factor α and β (PDGFRα and PDGFRβ) which are highly expressed on perivascular mural cells in adipose tissue (68). These fibroblast-like progenitor cells enter the commitment step (i.e. early differentiation) driven by bone morphogenetic protein 2 and 4 (BMP2 and BMP4) which phosphorylate transcription factors SMAD1/5/8, allowing nuclear translocation of ZNF423 to further induce transcription of peroxisome proliferator-activated receptor gamma (PPARγ), which is the master regulator of adipogenesis (74). Both canonical and noncanonical WNT (wingless-type mouse mammary tumor virus integration site family) signaling have been identified to regulate the expression of PPARγ and CCAAT enhancer-binding protein alpha (CEBPα) (75), another important adipogenic transcription factor that positively coordinates with PPARγ. With the action of PPARγ and CEBPα, the committed “pre-adipocytes” undergo vast morphological changes, forming unilocular lipid droplet that mostly consists of neutral lipids and express markers of mature adipocytes such as fatty acid-binding protein 4 (FABP4), perilipins, and lipolytic enzymes (74).

Impaired adipogenesis is associated with obesity and poor metabolic health (i.e. insulin resistance) (76, 77). Precursor cells isolated from aSAT in individuals with obesity exhibited reduced adipogenic capacity compared with those from lean individuals when cultured in vitro (78). Interestingly, cultured preadipocytes from the obese group expressed a high level of mitogen-activated protein 4 kinase 4 (MAPK4K4), which is known to suppress PPARγ activity, indicating impaired adipogenesis may be associated with inflammation (78). High throughput genomic sequencing of PPARγ in aSAT collected from patients with and without T2D identified sets of mutations in the genome, coupled with a seven-fold increased risk of T2D, suggesting that reduced adipogenic capacity may have a direct relationship with insulin resistance and increased risk of T2D (79).

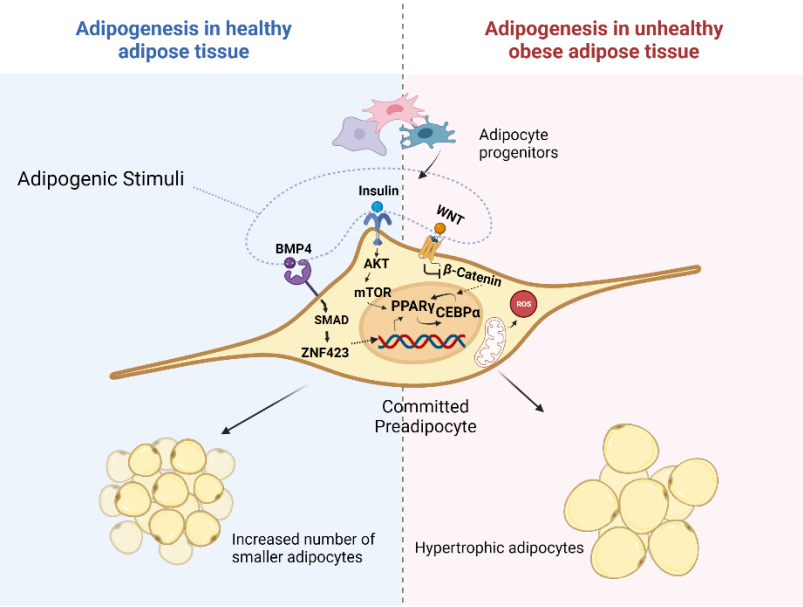

Figure 2-2 Adipogenesis in healthy vs. unhealthy obese adipose tissue

APCs can enter the commitment step in response to different adipogenic stimuli (e.g., BMP4, insulin, WNT, etc) and become pre-adipocytes. These adipogenic stimuli lead to increased expression of key adipogenic transcription factors such as PPARγ and CEBPα which facilitates differentiation into mature adipocytes. Adequate production of reactive oxygen species (ROS) by mitochondria can also promote adipogenesis. The adipogenic potential of obese insulin-resistant adipose tissue has been reported to be downregulated, leading to hypertrophic growth of existing mature adipocytes instead of hyperplastic expansion.

Adipose tissue capillarization and angiogenesis

aSAT is highly vascularized where each adipocyte is in contact with an extensive capillary network (44). Adipose vasculature not only provides essential nutrients, oxygen, growth factors, and hormones to the cells, but also participates in tissue remodeling by supporting the infiltration of immune cells, the release of cytokines and adipokines, and the removal of waste products or necrotic cells (44, 80). Tang et al reported that PDGFRβ^{+} APCs in adipose stromal that have high adipogenic potential were mainly derived from the mural compartments of adipose vasculature, supporting the notion that capillaries may also function as an important source for adipogenesis (80). Moreover, the structural crosstalk between the adipocytes and the capillaries is now found to be much more complex, such that the arteriolar differentiation and remodeling of perivascular extracellular matrix precede the adipogenic process during embryonic development,

while in the later stage of tissue expansion, the mature adipocytes drive the angiogenic process that expands and maintains the capillary network (81).

Angiogenesis in aSAT is the formation of new blood vessels by the sprouting/splitting of capillaries in response to pro-angiogenic stimuli (82). Early investigations posed hypoxia as an important driver for angiogenesis in aSAT where the hypertrophic expansion of adipocytes creates increased demand for oxygen following excess energy intake (83). Hypoxia-inducible factor -1 and -2 alpha (HIF-1α and HIF-2α) are the major transcription factors that mediate the hypoxic response that is hydroxylated and subsequently degraded by oxygen-sensing prolyl hydroxylase enzymes (PHD-1,2,3) at normal oxygenation (44). In a condition where the oxygen demand exceeds the supply, as is often the case during the active expansion of adipose tissue, PHDs are inhibited leaving HIF-α to function as a 'pro-angiogenic' stimulator to induce increased capillarization (44). However, administration of HIF-1α to mice models with established obesity (i.e., ob/ob) did not induce an angiogenic response in white adipose tissue but instead promoted the accumulation of fibrotic extracellular matrix (ECM) proteins and augmented inflammation (62), leading to the conclusion that hypoxic response via HIF-1α may not be enough to elicit enough angiogenesis and there could be other pathways that mediate angiogenesis in adipose tissue. Among many other angiogenic factors, vascular endothelial growth factor (VEGF) which is secreted from both mature adipocytes and stromal cells is considered the master regulator of angiogenesis and is the most largely studied pro-angiogenic modulator (84). VEGFα is known to bind a tyrosine receptor VEGFR2 while VEGFβ has been reported to bind VEGFR1 inducing signaling cascades that promote endothelial cell growth (85, 86). Overexpression of VEGFα from multiple murine studies revealed that induction of VEGFα attenuated markers of hypoxia and induced the growth of neovasculature in adipose tissue that was further translated into improved glucose tolerance and reduced inflammation which suggests that pro-angiogenic stimulation may be metabolically beneficial (87-89). Angiopoetin 1 and 2 (ANGPTL-1 and -2), important functional partners of VEGF, have been reported to bind endothelial cell tyrosine receptor, Tie-2, which further activates TWIST1 to function as a transcription factor (44, 90). Although the exact function of these family proteins is not yet completely understood, it appears that while ANGPTL-1 enhances VEGF activity and

contributes to vascular development as an agonist for Tie-2, ANGPTL-2 antagonizes Tie-2 and promotes destabilization of the vessel structure and elicits pro-angiogenesis when VEGF is present (44).

The rate of aSAT expansion (i.e., adipocyte hypertrophy) often exceeds the rate of angiogenesis in response to repeated excess energy intake, which leaves the tissue in low capillary density (91). As the rate-limiting step for healthy aSAT expansion, angiogenic capacity is often compromised in obesity (i.e., reduced protein expression of angiogenic factors) and impaired angiogenesis is tightly associated with dysregulated tissue remodeling and poor metabolic health (44, 49, 92). For example, reduced oxygen and nutrient supply due to lower capillarization may lead to adipocyte death that recruits adipose tissue macrophages (ATMϕ) that create crown-like structures (CLS) and further augment inflammation (49). Accumulation of HIF-1α in the long term fails to induce angiogenesis but instead increases the production of pro-inflammatory cytokines such as TNF-α, IL-6, and MCP-1, exacerbating local inflammatory status by recruiting pro-inflammatory M1 macrophages (93). Despite the ongoing debate about whether human adipose tissue is truly hypoxic in obesity and if the hypoxia caused by obesity is sufficient to drive angiogenesis, it seems evident that capillary density (both when expressed as the number of capillaries per adipose area and adipocytes) is relatively lower in adipose tissues in obesity, which is closely linked to insulin resistance and exacerbated local inflammation.

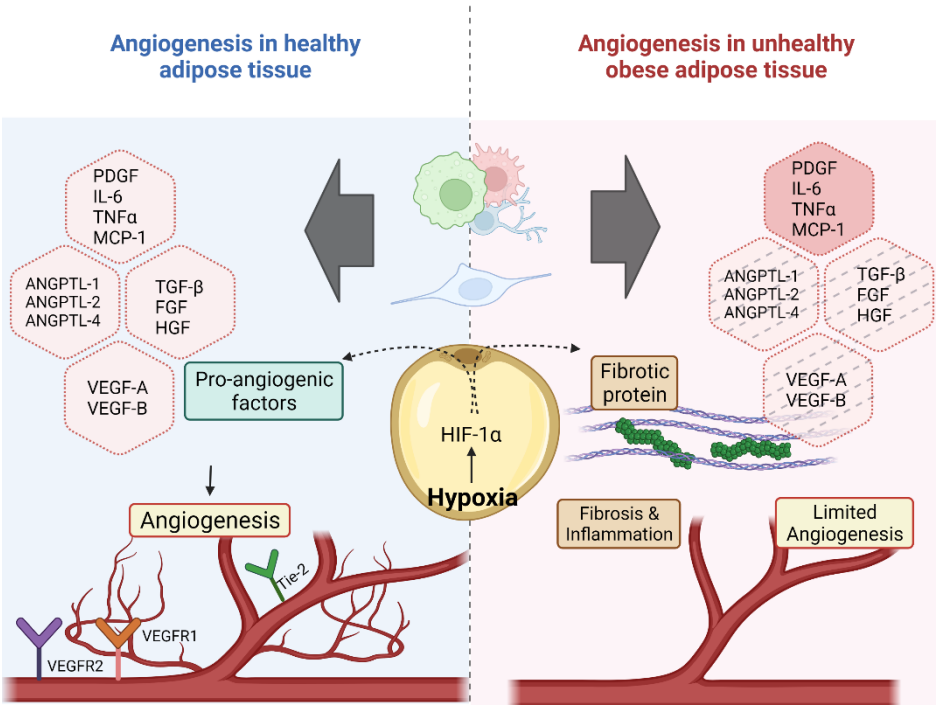

Figure 2-3 Angiogenesis in healthy vs. unhealthy obese adipose tissue

During the expansion of adipose tissue, adipocytes and stromal vascular cells (e.g., pre-adipocytes and immune cells) secrete pro-angiogenic factors that facilitate the formation of new capillaries. In unhealthy obese adipose tissue, the rate of angiogenesis often fails to catch up with the rate of tissue expansion, which results in lower capillary density. This further leads to impairments in angiogenic potential and production of fibrotic ECM proteins and pro-inflammatory factors that may contribute to adipose tissue dysfunctions.

Adipose tissue ECM composition and remodeling

Adipose tissue ECM is mostly comprised of structural proteins such as collagens and fibronectins that provide mechanical support for the tissue but are also heavily involved in cellular signalings for cell migration, repair, survival, and development (94-96). While Type I collagen (Col1), which is cross-linked in triple-helical fibers, is the most abundant fibrillary protein that forms the ECM network, Type IV collagen (Col4), heparin sulfate proteoglycans, and laminins form the basement membrane that surrounds the adipocytes. (96-98). Type V and VI collagens (Col5 and Col6) feature more 'micro-fiber' characteristics that link the Col1 fibers (96). Col6 is the most largely studied collagen type in adipose tissue because of its high abundance in adipose tissue and tight association with adipose tissue function (99, 100). Other than collagens, a variety of proteins such as osteopontin, hyaluronan, and elastin also contribute to the complex network of ECM (42).

The nature of structural ECM proteins in aSAT is not static-but rather keeps being actively remodeled via continuous production from adipocytes and stromal cells and degradation by ECM gelatinases (42). Matrix metalloproteinases (MMPs) are the main gelatinases (i.e., endopeptidases) that are secreted as zymogens and activated in extracellular space, which degrade collagenous ECM proteins via proteolytic cleavage (101). These MMPs are endogenously inhibited by tissue inhibitors of metalloproteinases (TIMPS) that bind to MMPs to regulate their activity (102). Specific subtypes and their roles of MMPs and TIMPs in ECM remodeling in human aSAT have not been fully defined, but it has been strongly suggested that the balance between these endogenous ECM modifiers plays an important role in regulating aSAT remodeling and metabolic homeostasis, especially in the context of obesity (96, 101). Other than the structural ECM proteins (e.g., collagens) and their enzymatic regulators (i.e., MMPs, TIMPs), there are also non-structural matricellular proteins in aSAT ECM (e.g., Secreted protein, acidic and rich in cysteine (SPARC), Thrombospondins (THBS), integrins, etc) that characteristically contain binding sites for structural proteins and cell surface receptors and participate in various cellular signaling processes although the discussion of their specific roles is out of the scope of this review (detailed review provided by (42, 96)).

Excess deposition of ECM proteins (i.e. fibrosis) in aSAT is one of the hallmarks consistently observed in obesity (103, 104). Numerous histological and transcriptional evidence show increased collagen abundance in adipose tissue both in *ob/ob* mice and individuals with obesity, and altered expression of MMPs and TIMPs (99, 105-108). The mechanisms underlying the development of fibrosis in obesity have been tightly linked to impaired angiogenesis and augmented inflammation (62, 104). In response to the prolonged nutrient flux that creates a hypoxic state in adipose tissue, the accumulated HIF1-α fails to induce angiogenic responses but instead alternatively activates transcription of ECM collagen genes, leading to the deposition of fibrous ECM proteins (62). This HIF1-α induction also upregulates some key inflammatory genes that include macrophage inflammation factor 1 (MIF1) and IL-6, contributing to the low-grade inflammation (more details regarding inflammation provided in “Adipose tissue inflammation” section) that in turn also activates the transcription of ECM genes (109). Another study that linked adipose tissue inflammation to fibrosis was conducted by

Spencer et al., from which co-culture of human adipocytes and macrophages revealed that transforming growth factor β (TGFβ), secreted from infiltrated adipose macrophages facilitates the accumulation of Col6 and plasminogen activator inhibitor-1 (PAI-1), another ECM regulator that inhibits fibrinolysis (110). Whether metabolic functions in aSAT are impacted by fibrosis remains to be fully elucidated. Khan et al demonstrated that genetic ablation of Col6a reduced ECM stability in adipose tissue and contributed to the massive expansion of adipocytes when the mice were challenged with HFD (105). However, interestingly, these mice exhibited normal glucose metabolism despite increased adipose tissue mass leading the authors to conclude that reduced ECM deposition allows adipocytes to expand and safely sequester fatty acids which further leads to reduced lipid-induced insulin resistance (105). Alternatively, it was proposed that some of the receptor molecules on the adipocyte membrane that link ECM (e.g., integrins, CD44, CD36) participate in signaling pathways (e.g., focal adhesion kinase (FAK) and mitogen-activated protein kinases (MAPK)) that induce the transcription of the factors that inhibit angiogenesis, induce cell death, and inflammation which may lead to insulin resistance (42).

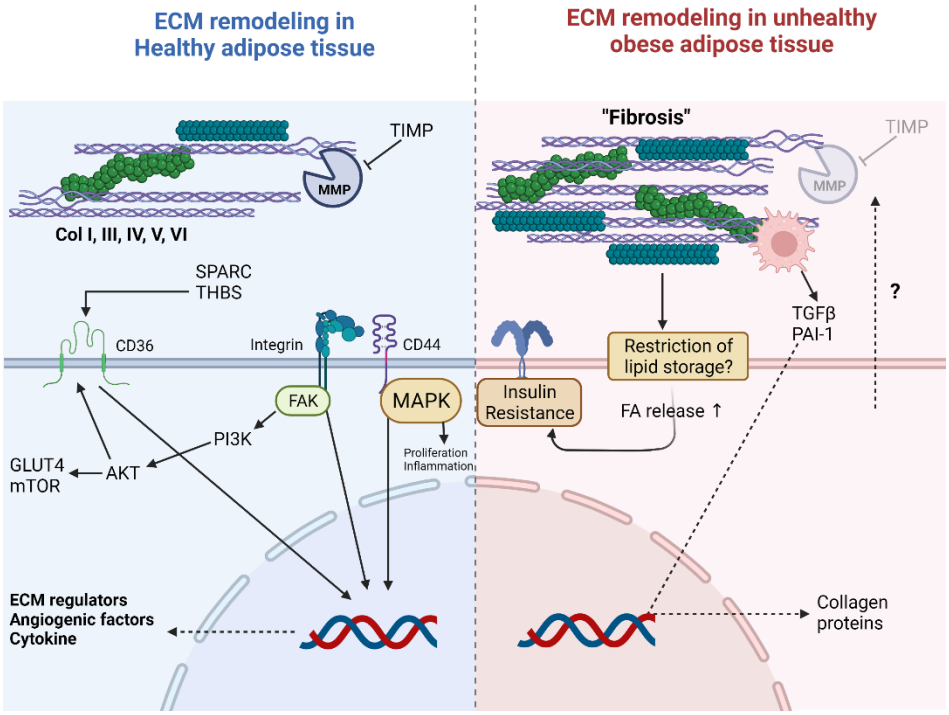

Figure 2-4 ECM remodeling in healthy vs. unhealthy obese adipose tissue

ECM structural proteins provide mechanical support and mediate cellular signals in adipose tissue. The balance of structural proteins is maintained by the interplay between endopeptidases (i.e. MMPs) and their regulators (i.e. TIMPs). In obese insulin-resistant adipose tissue, excessive deposition of ECM collagen proteins (i.e. fibrosis) is commonly observed partially due to augmented production of collagen fibers induced by macrophages and impairment in the axis of MMP-TIMP. In turn, fibrosis may limit the expansion capacity of adipocytes which may result in lipid-induced insulin resistance.

Adipose tissue inflammation

aSAT secretes various adipokines and cytokines to the system, serving as an important endocrine organ that regulates whole-body metabolic homeostasis. In healthy, lean aSAT, an anti-inflammatory phenotype is sustained by a higher abundance of adiponectin, which is known as an insulin-sensitizing adipokine, and expression of many tissue-resident immune cells (e.g., M2 macrophages, eosinophils, regulatory T-cells, and Th2 cell) that secrete anti-inflammatory factors such as IL-4 and -10 that suppress the immune response (43). However, during unhealthy aSAT remodeling triggered by excessive nutritional overload, the infiltration of bone marrow-derived macrophages to aSAT induces the phenotypic switch of ATMϕ from anti-inflammatory M2 type to a more pro-inflammatory M1 type which is the main source of pro-inflammatory cytokines such as TNF-α, IL-1β, and MCP-1 and lead to chronic low-grade systemic inflammation (111). There is strong evidence that points out that the increased level of pro-inflammatory cytokines and hormones in aSAT is mostly attributed to the infiltrated ATMϕ (112, 113). Factors that promote the recruitment of ATMϕ include dead adipocytes, hypoxia, free fatty acids, ER stress, and cellular senescence suggesting that this maladaptive response in aSAT is a classical process that occurs during dysregulated aSAT remodeling (3, 43). However, the immune response in aSAT is certainly a much more complex story than a binary mix of M1 against M2 ATMϕ because some findings report pro-inflammatory M2 macrophages (114), ATMϕ with both phenotypes (115), or even a wider spectrum of ATMϕ types characterized by distinct metabolic activities independent of M1 or M2 types (116). In addition, immune cells other than ATMϕ such as neutrophils, T-cells, and natural killer cells may also serve important roles in regulating inflammation in obesity, adding more complexity to the immune adaptations in aSAT (117).

Infiltration of immune cells is aSAT and the resultant aggravation of inflammation has been long accepted as one of the key underlying causes for the development of insulin resistance (51). The inflammatory cytokines produced by these immune cells can

directly interfere the insulin signaling in adipocytes (118-120). For example, it was demonstrated that TNF-α secreted from ATMϕ can directly interfere with GLUT4 translocation by inhibiting tyrosine phosphorylation of IRS-1 in adipocytes through activation of JNK and p38 MAPK (118, 121). Factors that are highly produced by ATMϕ such as IL-6 and CCL2 were also shown to induce insulin resistance in adipocytes (122, 123). IL-6 particularly was reported to inhibit the interaction of insulin receptor and IRS-1 via JAK-STAT signaling pathways and also inhibit tyrosine phosphorylation of IRS-1 via activation of STAT3. (121).

Although immune cell infiltration, especially macrophage infiltrations in aSAT has been acknowledged as one of the key targets to suppress to normalize dysfunctional adipocytes and improve metabolic health, there is evidence that aSAT inflammation is necessary in aSAT remodeling (124, 125). The abundance of infiltrated macrophages and the expression of pro-inflammatory cytokines were independent of high-fat diet (HFD)-induced insulin resistance in mice at least in the short term (3 days) suggesting a possibility of alternative roles of macrophages in adipose tissue (124). Asterholm et al conducted an elegant study where they designed different mouse models that lack pro-inflammatory potentials in white adipose tissue (125). Upon HFD challenge, a more pronounced reduction of adipogenesis and angiogenesis, and impaired glucose metabolism were observed from these genetically modified mice compared with HFD-fed littermates which led to the conclusion that inflammation is necessary for proper adipose tissue remodeling (125). The finding that ATMϕ in obesity contained an increased level of lipids coupled with increased lysosome biogenesis also suggests a possibility that ATMϕ can sequester fatty acids in cases of nutritional overload (126). In addition, recent evidence suggests an active role of ATMϕ in bioenergetics where they may differentially adapt to utilize glucose or lipids in response to metabolic perturbations and serve as a substrate buffer (well-reviewed by Caslin et al) (127). Although inflammation in aSAT has been mostly studied under the context of impaired metabolic health, these findings propose that more work be conducted to decipher their role in aSAT remodeling which may, in turn, help design aSAT inflammation-oriented therapeutics to treat obesity-related health complications.

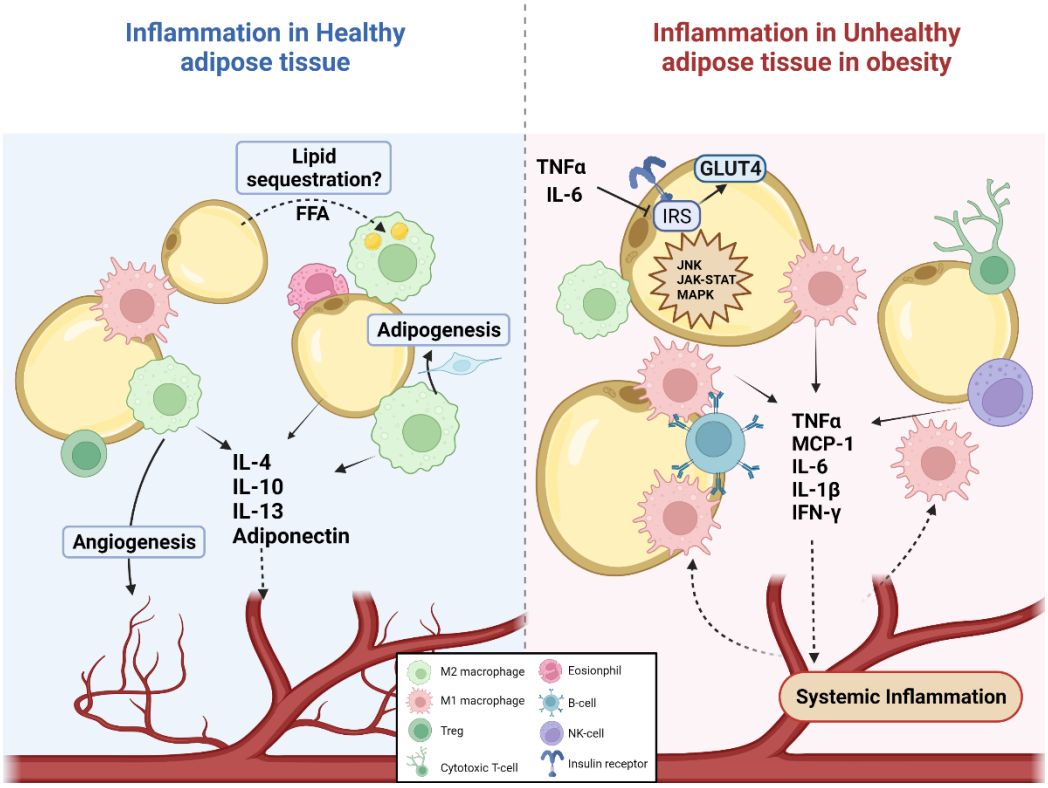

Figure 2-5 Inflammation in healthy vs. unhealthy obese adipose tissue

Immune cells in adipose tissue serve critical roles in maintaining healthy tissue expansion and metabolic homeostasis. In healthy adipose tissue, the abundance of anti-inflammatory immune cells (e.g., M2 ATMϕ and Tregs) is relatively higher than pro-inflammatory immune cells (e.g., M1 ATMϕ, cytotoxic T cells, and B cells) and the cytokines produced from these immune cells contribute to tissue remodeling process (i.e. angiogenesis and adipogenesis). On the other hand, in unhealthy obese adipose tissue, more pro-inflammatory immune cells are infiltrated, which release inflammatory cytokines that cause insulin resistance and systemic inflammation.

Adipose tissue mitochondrial density and oxidative function

Mitochondria in adipocytes serve a critical role in bioenergetics by oxidizing incoming fatty acids and glucose, generating intermediary metabolite (e.g., Acetyl-CoA) for de novo fatty acid synthesis, and esterifying glycerol-3-phosphates and fatty acids into triglycerides (128, 129). In addition to its function regulating substrate flux, mitochondria in adipocytes also play essential roles during adipose tissue remodeling (130, 131). For example, mitochondrial biogenesis and adipocyte differentiation are synchronized by sharing same transcription factors such as PPARγ, CEBPα, cAMP response element-binding protein (CREB), estrogen-related receptor α (ERRα), and peroxisome proliferator-activated receptor gamma coactivator 1-α (PGC-1α), implicating that increased mitochondrial biogenesis is essential during adipocyte development (132-134). This is

supported by the notion that adipocyte mitochondria provide essential substrates (e.g., citrate; the only precursor substrate for cytosolic acetyl-CoA, which is used for fatty acid synthesis) necessary for lipogenesis during adipocyte differentiation (128, 135). Reactive oxygen species (ROS), mainly produced by the electron transport chain in the mitochondria also have the potential to induce PPARγ transcription facilitating adipocyte differentiation (136). Although excessive production of ROS is often associated with cellular dysfunctions and impaired metabolic health (137, 138), an adequate amount of ROS increases glucose uptake and lipid synthesis in adipocytes (139, 140) implying an important role of mitochondria in adipose tissue remodeling and function.

Mitochondrial biogenesis and function in aSAT are often found to be compromised in obesity (131). Heinonen et al compared mitochondrial abundance and activity in aSAT acquired from healthy monozygotic twins who were discordant for body weight (mean BMI difference = 6kg/m^2) and discovered a lower abundance of mitochondrial DNA (mtDNA) and transcriptomes, and downregulated gene and protein expressions of oxidative machinery, confirming impaired mitochondrial biogenesis and reduced respiratory potential in acquired obesity (141). By using high-resolution respirometry, Yin et al revealed lower mitochondrial oxygen consumption in isolated adipocytes from individuals (142). Because mitochondria in adipocytes serve a crucial role in maintaining metabolic homeostasis by balancing substrate oxidation and lipogenesis, there is a tight association between mitochondrial dysfunction and insulin resistance in obesity. Compared with matched insulin-sensitive pairs, insulin-resistant individuals with obesity exhibited downregulated AMPK activity and increased oxidative stress in aSAT despite similar adiposity (143). Mechanistic studies have reported that high flux of glucose and fatty acids leads to mitochondrial dysfunction (e.g., reduced biogenesis, membrane potential, and oxidative capacity) which in turn, leads to excessive production of ROS that impairs insulin-mediated GLUT4 translocation (130). In addition to the direct link between mitochondrial oxidants (i.e., ROS) and insulin signaling, mitochondrial dysfunction may directly alter adipokine secretion (144) and adipogenic capacity (145, 146) which suggests a more extensive role of mitochondria in aSAT function and remodeling.

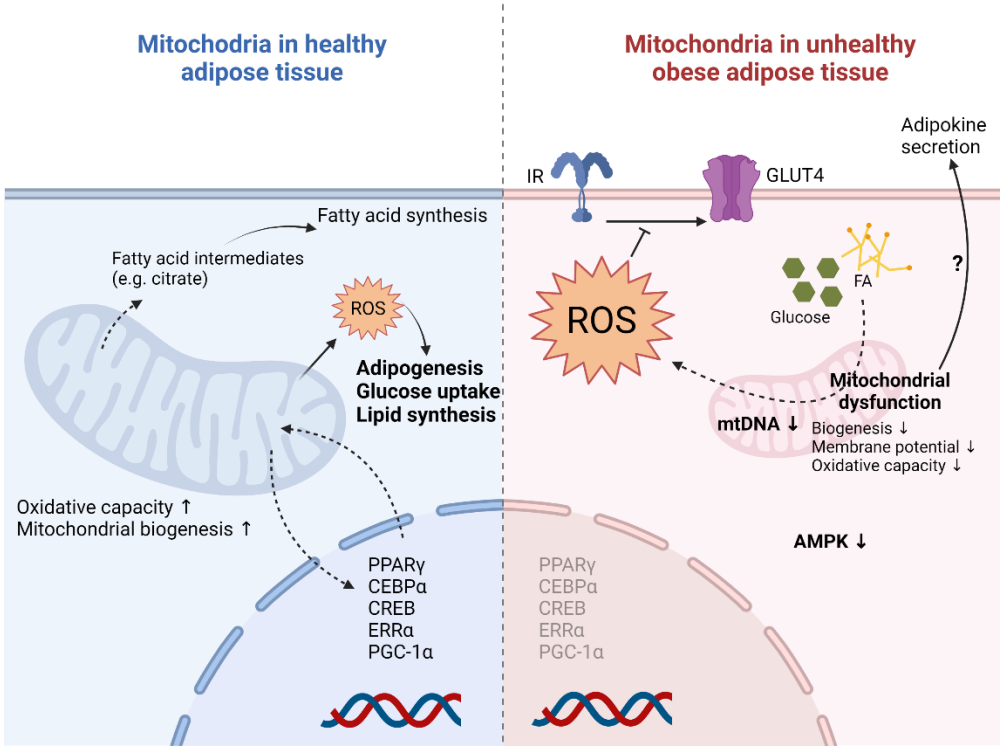

Figure 2-6 Mitochondria in healthy vs. unhealthy obese adipose tissue

Mitochondria in adipose tissue regulates bioenergetics largely through oxidation. It is also an essential player in adipogenesis. The abundance and function of mitochondria in unhealthy obese adipose tissue have been reported to be downregulated. The high flux of substrates induces mitochondrial dysfunction which leads to increased production of ROS and altered adipokine secretion.

Adipose tissue innervation

Since the discovery of leptin, adipose tissue has been accepted as an endocrine organ that can communicate with the central nervous system (CNS) (147). Recent years of research have shed light on another mode of adipose-CNS crosstalk that regulates whole-body metabolism – signaling from localized sensory nerve fibers innervating in adipose tissue to CNS (i.e., afferent pathway) and from CNS to the sympathetic nerves in adipose tissue (i.e., efferent pathway) (61). The arborization of sensory and sympathetic nerves in adipose tissue has been confirmed with histological measurements in rodent models (148-150). It has been reported that adipocytes can activate the sensory nerve fibers by releasing different mediators such as leptin, fatty acids, neurotrophic factors (e.g., neuregulin 4(NRG4), brain-derived neurotrophic factor (BDNF), nerve growth factor (NGF), etc.), VEGF, and inflammatory cytokines (e.g., TNFα, IL-6, IL-1β) that may regulate lipolysis, thermogenesis, and angiogenesis in adipose tissue (61). More recently, it was discovered that sensory nerve fibers in adipose tissue may circumvent

CNS integration and directly function in a paracrine manner by releasing neuropeptides like calcitonin gene-related peptide (CGRP) and Substance-P (151, 152). These factors have been reported to modulate immune cells and vasodilation (151, 152), but further exploration is needed to reveal their exact function in adipose tissue. The role of sympathetic innervation in adipose tissue has been mostly studied in the context of lipolysis because fatty acid mobilization during fasting more relies on norepinephrine released from sympathetic nerves than from the adrenal gland (153). Other neurotransmitters released from the sympathetic nerves in adipose tissue include neuropeptide Y (NPY) which may regulate angiogenic and adipogenic processes, and ATP, which functions as a co-transmitter that binds to purinergic receptors and participates in various metabolic pathways (e.g., lipolysis, lipogenesis, and inflammation, etc.) (154, 155).

Although there are limited numbers of evidence, existing evidence suggests that adipose tissue innervation may be impaired in obesity (61). Wang et al showed that the arborization of sympathetic innervation in inguinal white adipose tissue is lower in *ob/ob* mice compared with wild types, demonstrating that lower density of sympathetic innervation could be a hallmark of structural maladaptations in adipose tissue in obesity (156). Disruptions in sensory nerve activities in adipose tissue may occur in obesity because the overloading of inflammatory cytokines from adipocytes and immune cells are likely to hyperactivate local sensory nerve fibers and lead to ‘neurogenic inflammation’ (157) although this has not been studied in adipose tissue yet. Also, based on the finding that insulin can inhibit lipolysis and suppress sympathetic outflow by acting on insulin receptors in the brain (158), hyperinsulinemia in obesity may downregulate sympathetic activity and in turn, attenuate catecholamine-mediated lipid metabolism in adipose tissue. However, no work has directly examined the effects of obesity on afferent/efferent innervations in human aSAT, warranting further research.

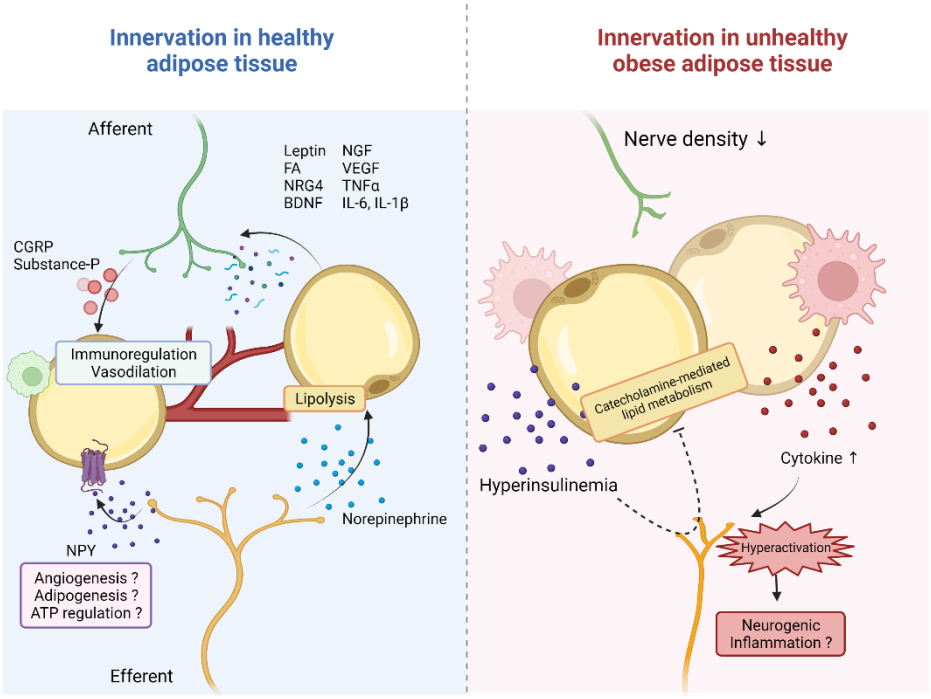

Figure 2-7 Innervation in healthy vs. unhealthy obese adipose tissue

Crosstalk between adipose tissue and CNS through sensory and sympathetic nerves functions to regulate metabolism and tissue remodeling process. At least from adipose tissue in obese mice, the density of innervation has been reported to be lower. This may be a result of neurogenic inflammation caused by pro-inflammatory cytokines.

2.3 ADIPOSE TISSUE FATTY ACID METABOLISM

Fatty acid mobilization and storage in adipose tissue are directly related to metabolic health

The major function of adipose tissue is to store and release fatty acids to help meet energy demands (38). Unfortunately, the imbalance between fatty acid storage and release (i.e., excessive release and reduced storage capacity) that is commonly observed in obesity, underlies the accumulation of ectopic fats in other metabolic organs and the development of lipid-induced insulin resistance. This phenomenon is clearly illustrated in individuals with lipodystrophy which is a genetic disorder resulting in impaired fat storage capacity in subcutaneous adipose tissue, and these patients often experience extraordinarily impaired glucose tolerance despite often appearing to be very lean (159). Given the causal relationship between excessive systemic fatty acid mobilization from aSAT and impaired metabolic health, it is necessary to fully understand how fatty acid metabolism is regulated in aSAT and identify mechanisms that may be targeted to

improve fatty acid storage and reduce excessive release in obesity. The section above discussed various cellular and structural components that are involved in aSAT remodeling. While these aSAT remodeling components may play an important role in regulating fatty acid mobilization by 'shaping' the aSAT into a more metabolically favorable form, the activity of fatty acid mobilization is directly regulated by intracellular signaling networks and neurohumoral signals (38). This section will describe how fatty acid metabolism is controlled (i.e., fatty acid release and fatty acid storage) in aSAT and how it is altered in obesity.

Regulation of fatty acid release

aSAT lipolysis is the hydrolytic cleavage of ester bonds in triglycerides that are stored in the unilocular lipid droplet in adipocytes. This occurs as sequential hydrolysis by lipolytic enzymes (i.e., adipose triglycerides lipase (ATGL), hormone-sensitive lipase (HSL), and monoglyceride lipase (MGL)) that results in the libration of fatty acids (160). Upon stimulation by lipolytic activators such as increased levels of catecholamines (i.e., norepinephrine and epinephrine) binding to lipolysis-inducing β-adrenergic receptors on adipocytes that exceed the binding to lipolysis-inhibiting α-adrenergic receptors, the coupled stimulatory G_s proteins activate adenylyl cyclase (161). Subsequently, intracellular cyclic AMP (cAMP) level is increased which in turn activates protein kinase A (PKA) that phosphorylates lipolytic enzymes and associated proteins (i.e., comparative gene identification-58 (CGI-58), G0/G1 switch gene 2 (G0S2), perililpin (PLIN) that are involved in the hydrolysis of lipid intermediates (161). Phosphorylated CGI-58, which is a positive regulator of ATGL, binds to ATGL and nullifies the inhibitory effect of G0S2 on ATGL leading to translocation of ATGL to lipid droplet surface that previously has been covered with PLIN proteins before the phosphorylation by PKA (161). With the help of ATGL, triacylglycerol is hydrolyzed into diacylglycerol, which is subsequently hydrolyzed into monoacylglycerol and free fatty acids by phosphorylated HSL and MGL respectively (161). Particularly, HSL has been reported to be capable of being serine-phosphorylated by AMPK and extracellular-regulated kinase (ERK) suggesting that HSL activation can occur through different pathways in response to energy-depleting and stressful circumstances (i.e., exercise) (162, 163). This catabolic process is regulated by numerous neurohumoral factors - stimulated by catecholamines, glucagon, cortisol, and natriuretic

peptides and inhibited by insulin and adenosine (38). Although different signaling cascades initiated by these hormones are out of the scope of this review (see more details from (38), the role of insulin should be highlighted given its powerful antilipolytic effect and importance in modulating metabolic health. Briefly, insulin activates phosphodiesterase 3B (PDE-3B), which lowers cAMP concentrations that lead to attenuated PKA activity, thereby exerting antilipolytic effects (164, 165).

Although the lipolytic response to catecholamines is often blunted in obesity, basal lipolysis (i.e., unstimulated) is often very high in obesity. This excessive rate of lipolysis leads to an overall increase in the fatty acid release into the systemic circulation, thereby contributing to ectopic fat-induced insulin resistance in skeletal muscle and liver (166, 167). Arner et al proposed adipose tissue inflammation as the major contributor to the increased basal lipolysis (161). Increased levels of TNFα from aSAT increases phosphorylation of PLIN1 even in the absence of catecholamines, revealing attachable sites on lipid droplets for ATGL and HSL (166, 167). In addition, it was reported that TNFα could alternatively downregulate G0S2, eventually leading to enhanced basal lipolysis (168).

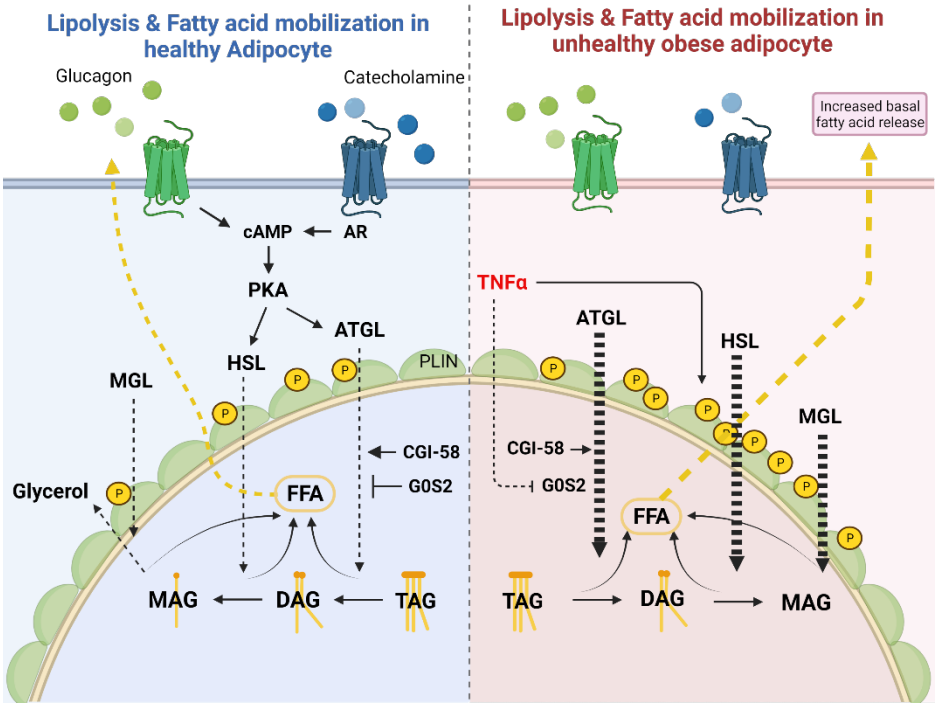

Figure 2-8 Fatty acid mobilization in healthy vs. unhealthy obese adipose tissue

In response to lipolytic signals (i.e. binding of catecholamine or glucagon), lipolytic enzymes function to hydrolyze TAG into glycerol and fatty acids. In unhealthy obese adipose tissue, the basal fatty acid release

is augmented due to the increased access of lipolytic enzymes to lipid metabolites, which is induced by inflammatory factors (e.g. TNFα).

Regulation of fatty acid storage

Most of the energy stored in aSAT is in the forms of neutral lipids (triglycerides being the most abundant form) that are esterified from fatty acids with the addition of glycerol intermediate in adipocytes (39). Lipoprotein lipases (LPL) hydrolyze the triglycerides from VLDL and chylomicrons and help the uptake of fatty acids into adipocytes through fatty acid transport proteins whereas albumin-bound fatty acids can be both directly taken up at the membrane site via diffusion or through the fatty acid transport proteins on adipocytes (169). A portion of fatty acids taken up into the adipocyte also can come from already liberated fatty acids (i.e., re-esterification) (170). The fatty acids are incorporated into triacylglycerol (TAG) via esterification with glycerol-3-p (G3P) which is derived from glycerol or dihydroxyacetone-p that originates from glucose or pyruvate (39). Similar to lipolysis, fatty acid esterification also occurs in sequential steps that involve different key lipogenic enzymes (171). Glycerol-P acyltransferase (GPAT) catalyzes the acylation of fatty acid with G3P forming lysophosphatidic acid (LPA) which is further modified into phosphatidic acid, and then into diacylglycerol (DAG). Formation of TAG from DAG is achieved by the addition of another unit of fatty acid catalyzed by diacylglycerol acyltransferase (DGAT) – a more detailed review on GPAT and DGAT is provided by Coleman et al and Yen et al (171, 172). Insulin stimulates lipid uptake and fatty acid esterification in adipose tissue by activating LPL and DGAT respectively and increases glucose uptake which can be utilized as a precursor for G3P (50, 173). It has been also reported that insulin promotes de novo lipogenesis in adipocytes via the mTOR-sterol regulatory element-binding protein (SREBP1c) pathway (174). On the other hand, it was recently confirmed that catecholamines, which promote fatty acid release by upregulating lipolysis, suppress fatty acid reesterification and instead redirect fatty acids to mitochondria for oxidation through a STAT3-dependent mechanism (175). Other than the sources mentioned above, fatty acids can also be synthesized from intracellular Acetyl-CoA (i.e., De novo lipogenesis) but this will not be discussed in detail here given that the amount of lipid produced by *de novo* lipogenesis contributes only 1~3% of the total fat balance in humans (176).

In obesity, basal LPL activity is upregulated whereas LPL-mediated TAG hydrolysis is downregulated in response to hyperinsulinemia, suggesting impaired insulin-mediated stimulation of LPL activity (177). In agreement with this, many studies have reported reduced post-absorptive fatty acid storage in insulin-resistant individuals with obesity (178-180). In addition to altered LPL action, impairments in the uptake of liberated fatty acids across adipose tissue can also contribute to altered fatty acid storage (181). The net removal of TAG and fatty acids is reduced in obesity despite higher expression of CD36 in adipose tissue, which is suggestive of impaired intracellular fatty acid trafficking by CD36 (181). Moreover, some evidence suggests a reduced lipogenic capacity in obese adipose tissue, as deuterated water tracing revealed that fractional glycerol and triglyceride synthesis, as well as de novo lipogenesis, were reduced in insulin-resistant individuals with obesity compared with well-matched insulin-sensitive individuals with obesity (73, 182). A strong negative correlation between the abundance of lipogenic enzymes such as DGAT1, fatty acid synthase (FASN), and LPL in aSAT and insulin resistance provides additional support that fatty acid storage capacity is impaired by insulin resistance (183).

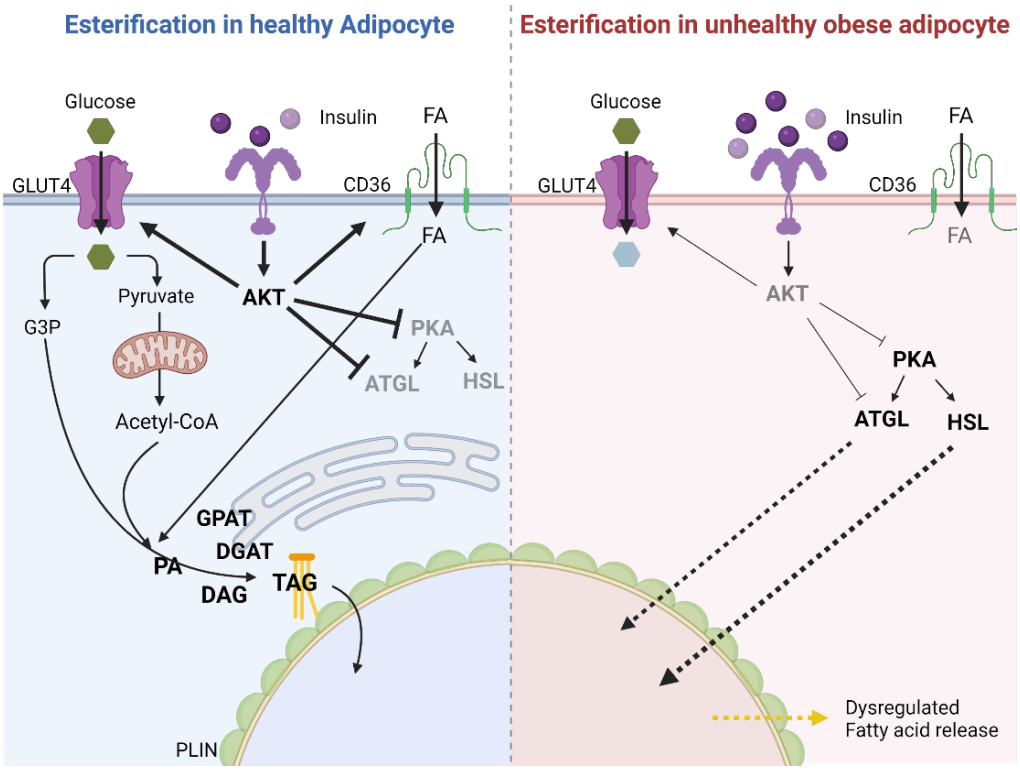

Figure 2-9 Fatty acid esterification in healthy vs. unhealthy obese adipose tissue

Insulin exerts an antilipolytic effect that while it inhibits lipolytic enzymes, promotes the uptake of glucose and fatty acids that provide esterific precursors which form into TAG. In obese insulin-resistant adipose tissue, the impact of insulin is attenuated, leading to dysregulated fatty acid release instead of storage.

2.4 ROLE OF EXERCISE ON ADIPOSE TISSUE STRUCTURE AND METABOLISM

Exercise is well-known to improve metabolic health and is considered a first-line treatment to combat obesity-related metabolic health complications (8-10). Most of the existing literature has explored the effects of exercise centering on functional and structural adaptations in skeletal muscle (52, 184, 185). For example, exercise can acutely increase skeletal muscle glucose uptake both via insulin-dependent and independent pathways (186, 187). In the long term, exercise training induces vast remodeling of skeletal muscle that includes, but is not limited to increased capillarization, mitochondrial density and oxidative capacity, and improved contractile machinery. (52, 188). However, surprisingly little is known regarding both acute and chronic effects of exercise on aSAT structure and function. Our lab recently reported that a session of exercise acutely induced transcriptional modifications in human aSAT that are involved in angiogenesis, fibrosis, and inflammation (17, 18). However, it is largely unknown whether or how these responses to each session of exercise may lead to long-term structural and functional changes in aSAT. This section will illustrate the acute and chronic effects of exercise on adipose tissue remodeling and function that have been previously reported.

Role of exercise on adipose tissue structure and remodeling capacity

A single session of exercise may induce a pro-angiogenic response and modify inflammatory profiles in aSAT (17, 189). Just 15 min of aerobic exercise at 80% VO_2max induced dynamic changes in transcriptomes in aSAT collected 6 hours after exercise from healthy lean male subjects (189). In this study, pathway analysis revealed that gene sets involved in inflammation, immunoregulation, and angiogenesis were significantly differentially expressed after exercise compared with no exercise (189). Similar responses may occur in individuals with higher adiposity, supported by findings from our lab that mRNA expression of VEGFα in aSAT and IL-6 expression from CD14+ immune cells in aSAT were increased after 1 hour of moderate-intensity exercise in adults with overweight/obesity (17). Also, inflammatory gene sets in aSAT were altered 1 hour after

high- vs. moderate-intensity exercise in adults with obesity without significant group differences (18). Interestingly, another recent study from our lab revealed that exercise acutely modifies aSAT cellularity – a decreased abundance of pro-fibrotic CD34hi APCs after 1 hour of moderate-intensity aerobic exercise in adults with obesity – suggesting exercise may rapidly remodel aSAT by regulating specific cell types in aSAT (190). In addition, multi-level omics analyses conducted on blood samples collected after acute exercise revealed that large numbers of molecules involved in inflammation and metabolism were changed (191). Given that aSAT serves as a source for various cytokines and metabolites (192), it is reasonable to speculate that aSAT may be central to these dynamic changes in response to exercise. However, whether these responses translate into functional changes in aSAT and whether it is differentially regulated by different modes of exercise (i.e., intensity, duration) are unknown.

The long-term effect of exercise on adipose tissue structure and function has received considerable attention, especially in the context of adipose tissue 'browning' because of its potential role in improving metabolic health (193). Brown adipose tissue is characterized by multilocular lipid droplets, high mitochondrial density, and increased expression of uncoupling protein 1 (UCP1) which is capable of increasing energy expenditure via non-shivering thermogenesis (194). It has been reported from murine studies that exercise may induce the 'browning' of white adipose tissue, forming into a more metabolically favorable form that can increase energy expenditure (54, 195, 196). However, adipose tissue browning is under-reported in human adipose tissue, and much evidence suggests this may not be the case in human aSAT (37, 197-199). Regardless, there is some evidence that exercise may still remodel white adipose tissue structure which might lead to improvements in metabolic health (14, 15). Kawanishi et al reported that exercise training attenuated the development of adipose tissue fibrosis and inflammation during the HFD diet in mice even without bodyweight differences between sedentary and training groups (15). Aerobic exercise training increased capillary density in aSAT in insulin-sensitive sedentary adults without reduction in fat mass (14). Some studies have reported reduced adipocyte sizes after exercise training but the interpretations of these results are confounded because training resulted in body weight and fat mass loss which could greatly impact adipocyte size independently of exercise

(200-202). This evidence suggests a possibility that exercise may improve metabolic health by remodeling aSAT structure into a more metabolically favorable form. However, few studies comprehensively examined the direct effects of exercise on the structural adaptations of aSAT (i.e., adipogenesis, angiogenesis, ECM remodeling, and inflammatory modification).

Role of exercise on adipose tissue fatty acid metabolism

Fatty acid release is increased during exercise as a result of the combined effects of increased lipolysis, reduced fatty acid reesterification, and increased adipose tissue blood flow (ATBF) (23). Increased pro-lipolytic hormones (e.g., catecholamine and ANP) promote lipolysis by stimulating phosphorylation of lipolytic enzymes (i.e., ATGL, HSL), which primarily drives the increased fatty acid mobilization (38, 203). In addition, insulin is reduced during exercise, thereby attenuating the potent anti-lipolytic effects due to insulin, further augmenting fatty acid mobilization (38). In the past several years, research has revealed candidates of tissue-derived hormones (i.e., myokines and adipokines) other than neurohormonal factors that facilitate lipolysis in response to exercise; IL-6, IL-15, irisin, and GDF15, suggesting that exercise-mediated humoral induction of lipolysis in aSAT is not limited to catecholamines and ANP (204). Although the increase of lipolytic and fatty acid mobilization rates during exercise are typical phenomena across individuals, the magnitude of the increase is influenced by individual anthropometric characteristics (e.g., degree of fitness, adiposity, age, etc.). For example, lipolytic and fatty acid mobilization rate is higher in aerobically trained individuals compared with untrained individuals when exercising at the same relative exercise intensity (205). Conversely, exercise-induced lipolysis and fatty acid mobilization have been reported to be lower in obesity which is attributed to increased sensitivity of antilipolytic α2-adrenergic receptors and perhaps also due to increased ANP clearance (206, 207).

Findings regarding the effects of exercise training on basal lipolysis are equivocal with reports of higher (208), lower (209), or similar (210) basal lipolysis in isolated adipocytes from trained individuals compared with sedentary individuals. However, lipolytic sensitivity to physiological catecholamine concentrations remains unchanged after weeks of exercise training (211). At a molecular level, Riis et al recently reported that ten weeks of endurance training did not alter protein expressions of lipolytic

regulators in aSAT (i.e., ATGL, HSL, CGI-58, G0S2) in healthy men (212). Also, mRNA levels of esterific enzymes (i.e., DGAT1 and GPAT1) were unaffected by training in this study, suggesting that training per se may not induce robust molecular adaptations related to lipolysis and esterification in aSAT (212). Whether this lack of change in lipolytic and esterific enzymes in aSAT after training is also observed in individuals with overweight/obesity is not clear. Although β-adrenergic sensitivity to physiological catecholamine concentration was not different between trained and untrained individuals (211), adipocytes isolated from elite runners exhibited more responsiveness to epinephrine at pharmacological concentrations, which suggests that training may increase the capacity for lipolysis (213).

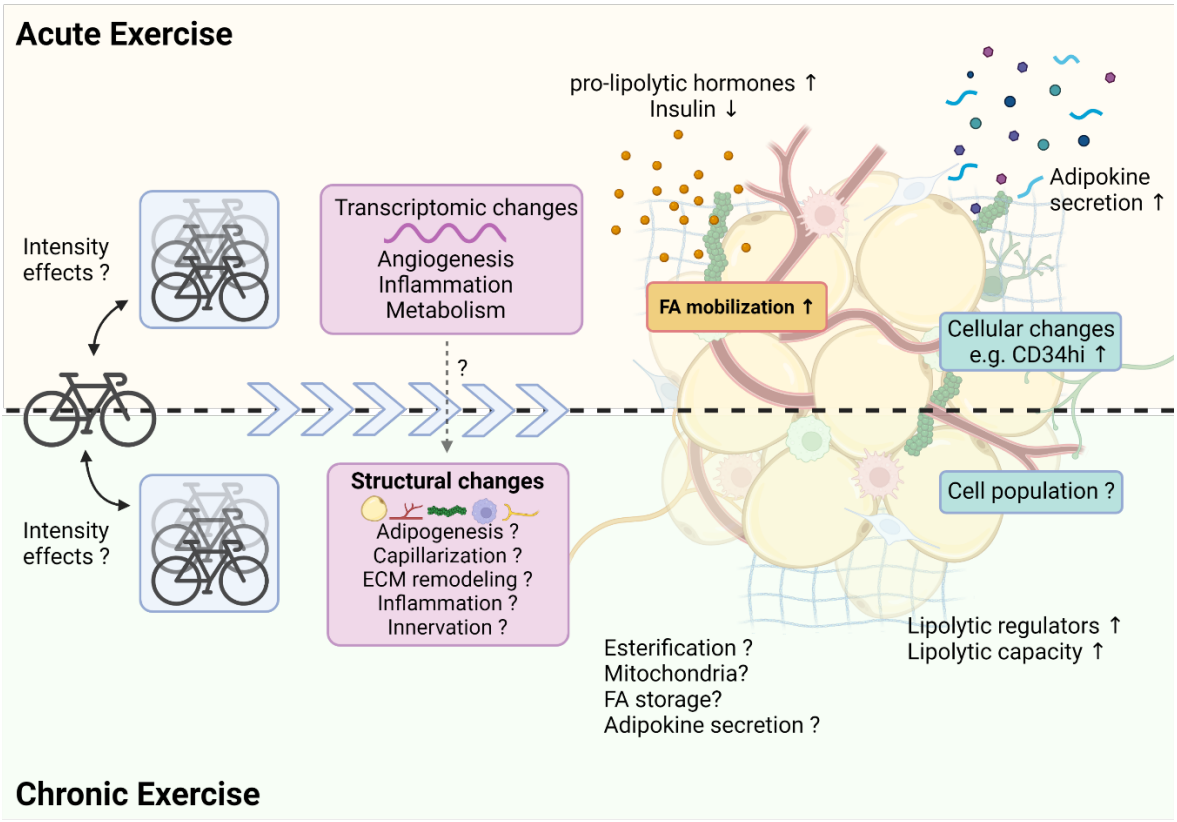

Figure 2-10 Acute and chronic effects of exercise on adipose tissue structure, function, and metabolism

A single session of exercise can alter the expression of genes that are involved in tissue remodeling and metabolism. Chronic exercise may induce structural and functional modifications in adipose tissue that may favorably impact metabolic health. The adaptations in adipose tissue in response to exercise may be exercise intensity-dependent.

2.5 SUMMARY

aSAT undergoes extensive structural and functional remodeling in response to changes in body fat mass (e.g., weight loss/gain) (33). White adipocytes, the main reservoir for fatty acid sequestration, are embedded in ECM with diverse immune cells and stromal vascular cells and communicate with the system through local vasculature and nerves (3, 61). A healthy remodeling achieved by proper interplay between these cellular and structural components is important to maintain fatty acid storage uptake capacity and lower inflammation status (66).

Structural remodeling and fatty acid metabolism in aSAT are often compromised in overweight/obesity and are at the root of the development of obesity-related cardiometabolic health complications (3, 49). Hypertrophic adipocytes, lower capillary and mitochondrial density, ECM fibrosis, pro-inflammatory macrophage infiltration, and lower nerve innervation may contribute to dysregulated fatty acid mobilization and uptake capacity in aSAT, and exacerbated systemic inflammation (3, 49, 61).

Evidence suggests that acute exercise may rapidly induce transcriptions involved in aSAT remodeling (i.e., angiogenesis and inflammation) and even modify aSAT cellularity (214). Despite the limited evidence, some studies suggest that exercise may induce robust structural and functional adaptations in aSAT (i.e., increased capillarization, reduced fibrosis, and altered inflammatory status) in longer-term that may lead to improved fatty acid storage capacity and inflammatory status (204, 214). In addition, these effects of exercise on aSAT may be differentially triggered depending on exercise intensity (204). Therefore, studies should be designed to comprehensively examine the direct effects of exercise on aSAT remodeling and metabolic function with the consideration of different exercise intensities.

Chapter 3

Project 1
The Effects of a Single Session of Low-, Moderate-, or High-Intensity Exercise on Adipose Tissue Transcriptome, Protein Phosphorylation, and Cytokine Production.

3.1 ABSTRACT

Exercise training can improve and maintain cardiometabolic health, in part through exercise-induced adaptations in adipose tissue. Adaptive responses to training are largely due to the accumulation of the transient changes in transcriptional regulation that occur shortly after each session of exercise, but the acute effects of exercise on the adipose tissue transcriptome are still poorly understood. The primary aim of this study was to compare the acute effects of exercise performed at low-, moderate-, or high-intensity on abdominal subcutaneous adipose tissue (aSAT) transcriptome. A total of 45 regularly exercising adults without obesity (BMI 25±2kg/m^2; VO_2max 37±6ml/kg/min) performed a single session of exercise at either low-intensity (LOW; 60min continuous exercise at 30% VO_2peak; n=15), moderate-intensity (MOD; 45min continuous exercise at 65% VO_2peak; n=15), or high-intensity (HIGH; 10x1min intervals at 90% VO_2peak interspersed with 1min active recovery; n=15). aSAT biopsy samples were collected 5-10cm from the umbilicus before exercise and 1.5 hours after exercise, and then processed for RNA sequencing and targeted protein immunoassays. Circulating cytokines were measured from blood samples collected before, during, and after exercise. A total of 17,466 genes were detected by our RNAseq analysis, yet there was a surprisingly small degree of overlap in differentially expressed genes (DEGs) among groups (only 6% of upregulated DEGs and 4% of downregulated DEGs overlapped among three exercise intensities). Despite the small degree of overlapping DEGs, pathway analysis revealed a robust upregulation in the global “inflammatory response” pathway in all groups (adjusted $p<1e^{-07}$), yet HIGH induced more extensive inflammatory responses than both LOW and MOD. Intriguingly, of the few overlapping DEGs, we found the most robust changes in some core clock

genes (e.g., NR1D1, NAMPT, CIART; adjusted $p<0.0001$). Interestingly, ribosomal and oxidative phosphorylation pathways were upregulated after MOD and LOW but not HIGH. Despite the somewhat distinct transcriptomic responses, we found each of the three exercise sessions reduced ERK phosphorylation in aSAT and increased the plasma concentration of pro-(IL1β, IL6, and TNFα) and anti-(IL10) inflammatory cytokines after exercise. Collectively, our data suggest changes in the inflammatory, circadian clock, ribosomal, and oxidative phosphorylation genes shortly after acute exercise may be important contributors to exercise-induced aSAT adaptations in response to regularly performed exercise. Because the three different exercise sessions induced rather distinct transcriptomic responses, exercise intensity and duration may differentially impact aSAT adaptations.

3.2 INTRODUCTION

The cardiometabolic health benefits of regular exercise are well-documented (8, 9); however, the precise mechanisms driving these effects remain incompletely understood. Most studies examining the metabolic benefits of exercise largely focus on adaptations in skeletal muscle, but far less is known about exercise-induced adaptations in adipose tissue that also underlie some of the health benefits of exercise (14, 15). For example, exercise training has been found to increase aSAT capillarization (14), lower pro-inflammatory macrophage infiltration, and reduce the fibrotic composition of the extracellular matrix of adipose tissue (15, 215). Exercise-induced adaptations have also been attributed to an attenuated release of proinflammatory cytokines from aSAT (“adipokines”), and lower systemic inflammation (216). But, how exercise triggers the adaptive response in aSAT, and whether exercise intensity may impact these triggers is unclear.

Adaptations to regular exercise typically result from the accrual of repeated exposure to acute transcriptional changes that occur shortly after each exercise session (217). For example, the increase in mitochondrial density in skeletal muscle in response to training is largely initiated by accumulated transcriptional regulators of mitochondrial biogenesis (e.g., PGC-1α, MEF2, NRFs) and transcripts involved in oxidative phosphorylation (e.g., COX, SDHA) (185, 218, 219). Prior research has also reported an

increased mitochondrial density in aSAT following exercise training (212, 220) perhaps through upregulation of the same genes (195, 221) as observed in skeletal muscle. Additionally, we previously observed a robust increase in the mRNA expression of the key angiogenic transcription factor VEGFA 1 hour after aerobic exercise (17), which might be part of the initial step for enhanced vascularization in aSAT observed with exercise training (14). Hence, identifying early transcriptomic signals that occur in the hours after exercise is critical to understanding the mechanisms underlying the exercise-induced adaptations in aSAT. Importantly, exercise intensity can govern the magnitude of significant metabolic or inflammatory alterations and some preclinical studies report that high-intensity training induced more pronounced adaptations in adipose tissue (e.g., a greater abundance of capillaries and smaller adipocytes, and less pro-inflammatory macrophage infiltration) compared with moderate-intensity training (201, 222). Therefore, the early signaling responses in adipose tissue in response to a session of exercise may be intensity-dependent.

The primary aim of this study was to compare the acute effects of exercise performed at low-, moderate-, or high-intensity on aSAT transcriptome. Importantly, to minimize the impact of introducing novel exercise, particularly when implemented in non-exercising individuals (189), we recruited adults who engage in regular endurance exercise to assess early aSAT response triggered by an acute session of exercise. We hypothesized that 1) a single session of exercise would alter aSAT transcriptome, cytokine production, and protein phosphorylation and 2) the exercise-induced effects would be distinct among three exercise intensities.

3.3 METHOD

Subjects

Of 190 subjects who signed up for the initial screening, a total of 45 healthy subjects [age 18-40 years; body mass index (BMI) 20-30kg/m^2] enrolled and completed the study (Figure 3-1A). All participants were exercising regularly (≥30min, ≥ 3 days/week, moderate to vigorous intensity endurance-type exercise) for at least 2 months and reported having stable body weight for at least 6 months before their experimental measurement. Subjects were not taking any medications or supplements known to affect

their metabolism except for contraceptive medications for some female participants. Subjects also had no history of cardiovascular or metabolic disease. All female participants were premenopausal and not pregnant or lactating. All subjects completed a detailed medical history survey and resting electrocardiogram, which were reviewed by a physician before any testing. Written informed consent was obtained from all subjects before the study. This study conformed to the standards set by the Declaration of Helsinki, except for registration in a database, and was approved by the University of Michigan Institutional Review Board.

Group assignment

Enrolled subjects were assigned to one-of-three exercise treatment groups in a counter-balanced manner. The three exercise treatment groups were:

1) Low-intensity exercise (LOW; 60 min of steady-state exercise at ~30% peak oxygen consumption (VO_2peak); n=15),
2) Moderate-intensity exercise (MOD; 45 min of steady-state exercise at ~65% VO_2peak; n=15)
3) High-intensity exercise (HIGH; 10 x 1 min intervals at ~90% VO_2peak with 1 min of active recovery between intervals; n=15)

Preliminary procedures

Body composition: Body composition was determined by dual-energy x-ray absorptiometry (Lunar DPX DEXA scanner, GE, WI).

Aerobic capacity (VO_2peak): Graded exercise testing was performed on a stationary cycle ergometer (Corvival, Lode, Netherlands) using an incremental exercise protocol starting at 40W and increasing 20W per minute until volitional exhaustion. The rate of oxygen consumption was measured throughout this test using a metabolic cart (Quark CPET, COSMED, Italy) and peak oxygen uptake (VO_2peak) was determined as the highest 30-second average before volitional fatigue. Measurements of respiratory exchange ratio (RER) ≥ 1.2 and maximal heart rate (HR_{max}) ≥ 90% of age-predicted values (i.e., 220-age) were used as secondary indices to help confirm maximal effort during these tests.

The experimental exercise sessions were performed on the same cycle ergometer as VO_2peak was measured.

Exercise familiarization exercise: All participants underwent at least one supervised familiarization exercise session during which they performed the exercise protocol consistent with their group assignment. This familiarization exercise session was completed at least a few days before the experimental trial and was employed to avoid the introduction of novel effects from the experimental exercise session.

Experimental trial

The experimental trial is outlined in Figure 3-1B. After overnight fasting followed by a standardized dinner (30% of estimated total daily energy expenditure) at ~1900h and snack (10% of estimated total daily energy expenditure) at ~2200h, subjects arrived at the clinical facility at 0700h for the experimental trial. Resting metabolic rate was measured by indirect calorimetry (TrueOne 2400, ParvoMedics, USA) following 30min of quiet resting. An intravenous catheter was inserted into the antecubital vein on one arm. At ~0900 h, an aSAT sample was collected by aspiration 5-10cm distal to the umbilicus, as described previously (190). aSAT samples were snap-frozen in liquid nitrogen and stored at −80°C for later quantification of the transcriptome (RNA sequencing) and protein abundance (targeted immunoblots) (see details below). After the pre-exercise biopsy (Pre), a pre-exercise blood sample was collected. Subjects then performed their prescribed exercise session.

Subjects assigned to LOW performed steady-state exercise at 40% heart rate reserve (HRR) (~30% VO_2peak) (223) for 60 min (Figure 3-1B), subjects assigned to MOD performed steady-state exercise at 70% HRR (~65% VO_2peak) for 45 min (Figure 3-1B), and subjects assigned to HIGH performed 10 x 1 min intervals at 90% HRR (~90% VO_2peak) with 1 min of active recovery between intervals (Figure 3-1B). The HIGH exercise session also included a 3 min warm-up and cool-down before and after the interval protocol (total exercise time in HIGH was 25 min). Exercise intensity was monitored by a telemetry heart rate device (Polar, Finland).

Blood samples were collected in the middle (MID) of the exercise session (at ~30” in LOW, at ~22” in MOD, and between the 5th and 6th interval for HIGH). Additional blood samples were collected during the final 30-60 seconds of exercise (End), 1 hour post-exercise (1hPost), and 1h 30min post-exercise (1.5hPost). Blood samples were centrifuged at 3,000 g at 4°C for 15 min. Serum and plasma were aliquoted and stored at −80°C until analysis for circulating factors. After exercise, all subjects quietly rested on a bed for 1h 30min. Then, post-exercise aSAT biopsy samples (Post) were collected in the same manner as the pre-exercise samples but on the opposite side of the umbilicus.

Analytical procedures

RNA-sequencing

RNA was extracted by using a Qiagen Mini RNA extraction kit (74004, Qiagen). Total RNAs were polyA enriched, and directional RNA-seq libraries were prepared using the NEBNext Ultra II RNA library prep Kit. Paired-end sequencing was conducted at a NovaSeq 6000 sequencer at the Oklahoma Medical Research Foundation (OMRF) clinical genomics core. The paired-end RNA-seq reads were mapped to human transcripts annotated in GENCODE v44 (224) using Bowtie (225). Gene level read counts were estimated using rSeq (226, 227).

Bioinformatics

Normalization of gene count data and differentially expressed gene (DEG) analysis was performed by using DESeq2 (228). Adjusted p-value < 0.05 was used as a cutoff for the determination of DEGs. Gene Set Enrichment Analysis (GSEA; Broad Institute) was performed by using the ‘fgsea’ package in R (R, Vienna, Austria). HALLMARK was used to identify enriched core biological gene sets after LOW, MOD, and HIGH as the database for GSEA. KEGG (Kyoto Encyclopedia of Genes and Genomes) was used to identify enriched functional pathways in HIGH vs. LOW, HIGH vs. MOD, or MOD vs. LOW. Adjusted p-value < 0.05 was used as a cutoff for the determination of significantly enriched gene sets or pathways.

Targeted immunoblots

We used capillary electrophoresis-based Western blot (JESS, ProteinSimple, San Jose, CA) to measure the abundance of proteins of interest in aSAT lysates. A portion of each aspirated adipose biopsy sample (~90 mg wet weight) was homogenized in ice-cold 1X RIPA buffer (89901, Thermofisher) with freshly added protease and phosphatase inhibitors (P8340, P5726, and P0044; Sigma) using two 5 mm steel beads (TissueLyser II, Qiagen, CA). Homogenates were rotated at 50 rpm for 60 min at 4°C and then centrifuged at 4°C for 3 x 15 minutes at 15,000g. Protein concentration was assessed using the bicinchoninic acid method (#23225, Thermofisher) after removing the supernatant. Samples were prepared in 4x Laemmli buffer, and heated for 7 minutes at 95°C. Equal amounts of protein (0.16µg) were mixed with the Simple Western sample buffer and fluorescent mix and loaded in capillaries in 12-230 kDa JESS separation module, 25 capillary cartridges (SW-W003). All experiments were performed on the automated JESS device in accordance with the manufacturer's instructions. Primary antibodies used were Hormone-sensitive lipase (HSL, #18381, Cell Signaling Technology), phospho-HSL (Ser565) (pHSL^{S565}, #4137, Cell Signaling Technology), phospho-HSL (Ser660) (pHSL^{S660}, #4126, Cell Signaling Technology), Protein kinase B (AKT, #9272, Cell Signaling Technology), phospho-AKT (Ser473) (pAKT^{S473}, #9271, Cell Signaling Technology), phospho-AKT (Thr308) (pAKT^{T308}, #13038, Cell Signaling Technology), p38 mitogen-activated protein kinase (P38, #9212, Cell Signaling Technology), phospho-P38 MAPK (Thr180/Tyr182) (pP38$^{T180/Y192}$, #9211, Cell Signaling Technology), p44/42 MAPK extracellular signal-regulated kinase (ERK, #4695, Cell Signaling Technology), phospho-p44/42 MAPK (Thr202/Tyr204) (pERK$^{T202/Y204}$, #4376, Cell Signaling Technology), Signal transducer and activator of transcription 3 (STAT3, #12640, Cell Signaling Technology), and phospho-STAT3 (Tyr705) (pSTAT3^{Y705}, #9145, Cell Signaling Technology).

Blood measurements

Plasma concentrations of glucose (TR-15221, ThermoFisher), plasma fatty acids (NC9517309, NC9517311; Fujifilm Medical Systems), and plasma glycerol (F6428, Sigma) were assessed using commercially available kits. Plasma lactate was measured

as previously described (229). Plasma cortisol concentration was assessed using a chemiluminescent immunoassay (Siemens 1000). Epinephrine and norepinephrine (Abnova, Taipei City, Taiwan; KA1877) were measured by ELISA. Plasma concentrations of IL1β, IL10, IL6, IFNγ, and TNFα were measured using a customized Luminex Multiplex kit (HSTCMAG-28SK).

Plasma volume correction

Because of the well-known reduction of plasma volume due to hemoconcentration during exercise (230), we measured calcium (Ca) concentration as the marker for hemoconcentration (231). The concentration of circulating parameters at Mid, End, 1hPost, and 1.5hPost was corrected for plasma volume as follows:

$$[\text{parameter}]_c = [\text{parameter}]_u / (1 + \Delta\text{Ca}(\%)/100)$$

Where ΔCa(%) refers to the percentage change of Ca concentration relative to pre-exercise (Pre) level and c and u sub-indices denote corrected and uncorrected concentration, respectively.

Statistical analyses

A two-way ANOVA linear mixed model was used to compare results from all variables except RNA-sequencing data. Parameters with non-normally distributed residuals were log-transformed before the statistical analysis. Statistical analysis was done by using SPSS (Statistics for Windows, version 26.0; IBM Corp., Armonk, NY) or R. P value < 0.05 was considered statistically significant. Data are presented as mean ± SD unless noted otherwise.

3.4 RESULTS

Subject characteristics and heart rate responses during exercise.

A total of 45 subjects (15 LOW, 15 MID, and 15 HIGH) completed the study. All subjects were healthy, non-obese, and recreationally active (Table 3-1), and as designed, there was no difference in baseline anthropometric characteristics or aerobic fitness among groups (VO_2peak) (Table 3-1). Subjects exhibited a normal range of metabolic health indices, as evidenced by low fasting insulin (5.8 ± 2.9 mU/L), glucose (4.9 ± 0.5 mmol/L), fatty acid (307 ± 151 µmol/L), and triglyceride concentration (0.8 ± 0.4 mmol/L), all of which did not differ among groups (Table 3-1). During the steady-state exercise sessions, average HR was 105±7 bpm during LOW and 140±9 bpm during MOD (representing 40±5% and 69±6% HRR, respectively). During HIGH, average HR during the one-minute high-intensity intervals was 161±13 bpm (86±8% HRR and 90±5% HR_{max}).

Plasma concentrations of epinephrine, norepinephrine, lactate, and cortisol

Before exercise (Pre), plasma concentrations of epinephrine, norepinephrine, lactate, and cortisol were not different among groups (Figure 3-2). Exercise significantly increased plasma epinephrine and norepinephrine concentrations above Pre in all groups (all $p<0.001$), but concentrations of both hormones were more than 2-fold greater in HIGH compared with LOW and MOD at the end of exercise ($p<0.001$), with no difference between LOW and MOD (Figure 3-2A). Similarly, exercise significantly increased plasma lactate concentrations above Pre in all groups (all $P<0.001$), with the highest concentrations found after HIGH ($P<0.001$) vs MOD and LOW; Figure 3-2C). Plasma lactate concentration during MOD was also significantly greater than LOW ($P<0.01$) (Figure 3-2C). Plasma concentrations of epinephrine and lactate returned to pre-exercise levels 1h after exercise (1hPost) in all groups. Plasma norepinephrine concentration also declined to near the pre-exercise level at 1hPost in all groups, however, 1hPost values remained slightly, yet significantly higher than Pre in both LOW and MOD (both $p\leq0.05$), but not in HIGH (Figure 3-2B). In contrast to plasma catecholamine and lactate concentrations, we did not detect a significant change in plasma cortisol concentration during exercise in any of the groups (Figure 3-2D).

Plasma glycerol and fatty acid concentrations

As expected, plasma glycerol concentration increased during exercise compared with Pre in all groups (all $p<0.001$), and concentrations declined to near pre-exercise levels after exercise, but still remained slightly, yet significantly higher than Pre at 1hPost and 1.5hPost (all $p<0.05$). (Figure 3-3A). There were no significant differences in plasma glycerol concentrations among groups (Figure 3-3A). Exercise also increased plasma fatty acid concentrations in LOW and MOD (both $p<0.001$) – but at the end of the exercise, fatty acid concentration was ~50% greater in LOW vs. MOD ($p<0.05$). In contrast to LOW and MOD, exercise significantly reduced plasma fatty acid concentration in HIGH ($p<0.01$) and concentrations after exercise in HIGH were significantly lower than both MOD ($p<0.01$) and LOW ($p<0.001$) (Figure 3-3B).

Acute LOW, MOD, and HIGH induced distinct transcriptomic responses in aSAT.

A total of 17,466 genes were detected by our RNAseq analysis and comparing aSAT samples collected before exercise (Pre) and 1.5h after exercise (Post), we found 1003 differentially expressed genes (DEG) after LOW (397 upregulated and 606 downregulated), 1979 DEGs after MOD (773 upregulated and 1206 downregulated), and 759 DEGs after HIGH (452 upregulated and 307 downregulated) (adjusted $p<0.05$) (Figure 3-4A, B, C). Interestingly, there was a relatively small degree of overlap in DEGs detected among all three exercise groups (20% of LOW, 10% of MOD, and 17% of HIGH for upregulated DEGs and 10% of LOW, 5% of MOD, and 21% of HIGH for downregulated DEGs) and the number of DEGs after MOD was nearly 2-fold and 2.5-fold greater than LOW and HIGH, respectively (Figure 3-4D). To identify the DEGs that were most affected by exercise, we focused on DEGs that were changed more than 2-fold ($|\log_2 FC|>1$) after exercise and discovered 24 DEGs in LOW (15 upregulated and 9 downregulated), 20 DEGs in MOD (16 upregulated and 4 downregulated), and 51 DEGs in HIGH (48 upregulated and 3 downregulated) (Table 3-2). 5 DEGs from this list were found in all groups: NR1D1 (Nuclear Receptor Subfamily 1 Group D Member 1) and CIART (Circadian-Associated Repressor of Transcription), both known to be involved in circadian rhythm (232, 233), were downregulated by exercise and APOL4 (Apolipoprotein L4), KCNK6 (Potassium Two Pore Domain Channel Subfamily K Member 6), and C3orf52

(Chromosome 3 Open Reading Frame 52) were upregulated by exercise (Table 3-2). Interestingly, in addition to NR1D1 and CIART, some other 'core' clock genes such as DBP, PER1 (downregulated), and NAMPT (upregulated), were also significantly altered after exercise in all groups (Figure 3-4H). However, we did not find an exercise effect on BMAL1 or CLOCK, which are the 'master clock' genes that regulate the transcription of other circadian genes (234) (Figure 3-4H). GSEA using the HALLMARK pathways revealed a robust upregulation of inflammation-related pathways (e.g., 'Inflammatory response', 'TNFA signaling via NFkB', 'IL6-JAK-STAT3 signaling', 'IFNγ response') significantly enriched at least from two groups (Figure 3-4E, F, G). However, the types of inflammatory genes and their magnitude of changes after exercise were not the same in LOW vs. MOD vs. HIGH. For example, although the 'Inflammatory response' pathway was globally upregulated after exercise (adjusted $p<1e^{-}07$), the magnitude of individual gene expression changes in LOW, MOD, and HIGH were not the same (Supplementary Figure 3-1). Comparing gene expression changes among the exercise groups, we detected 734 DEGs in HIGH vs MOD (468 greater in HIGH and 266 greater in MOD) and 183 DEGs in HIGH vs. LOW (153 greater in HIGH and 30 greater in LOW) (adjusted $p<0.05$) (Figure 3-5I, J). Surprisingly, we did not detect any DEGs between LOW vs. MOD (Figure 3-4K). We conducted GSEA using KEGG pathways to compare the enriched pathways after HIGH vs. both LOW and MOD and found HIGH induced more extensive inflammatory responses (e.g., regulation of T cell, NK cell, B cell, and chemokine production) compared with both LOW and MOD (Figure 3-4L, M). Interestingly, the 'Ribosome' pathway was enriched both in LOW and MOD compared with HIGH, suggesting a possibility of a more robust upregulation of ribosomal biogenesis after LOW and MOD compared with HIGH (Figure 3-4L, M). Although no specific DEGs were identified in the comparison between LOW and MOD, pathway analysis did reveal some differences between these groups, and 'Ribosome', 'Oxidative phosphorylation', and 'Proteasome' pathways were found to be more enriched in MOD vs. LOW (Figure 3-4N).

Circulating cytokine concentrations are differentially modified by acute exercise and may also be differentially regulated by exercise intensity.

Before exercise, plasma concentrations of IL1β, IL10, IL6, TNFα, and IFNγ were not different among groups (Table 3-3). Exercise significantly increased plasma IL1β, IL10, IL6, and TNFα at End in all groups ($p<0.01$) but IFNγ was not changed by exercise (Table 3-3). While IL1β and IL10 returned to pre-exercise level 1.5h after exercise, IL6 and TNFα remained higher than Pre at 1.5hPost ($p<0.001$ and $p<0.05$, respectively) (Table 3-3). Interestingly, we did not detect any group differences in the cytokines we measured in this study (Table 3-3).

Acute exercise downregulated ERK phosphorylation at 1.5hPost without exercise-intensity specific effect.

Our targeted analysis to assess potential exercise-induced post-translational modifications to some metabolically-relevant proteins revealed that exercise decreased the phosphorylation of ERK in aSAT (expressed as the ratio of protein abundance of $pERK^{T202/Y204}$:total ERK) when measured ~1.5h after exercise in all groups ($p<0.05$) with no differences observed between groups (Figure 3-5A). In contrast, we did not detect an effect of exercise on the phosphorylation of P38 (ratio $pP38^{T180/Y182}$:total P38) or STAT3 (ratio $pSTAT3^{Y705}$:total STAT3) in any of the groups (Figure 3-5B and 5C). Phosphorylation of one of the chief lipolytic enzymes, HSL on either the AMPK regulatory site serine 565 (expressed as $pHSL^{S565}$:total HSL) or the PKA regulatory site, serine 660 ($pHSL^{S660}$:HSL) was not increased in aSAT collected 1.5 hours after any of the exercise sessions (Figure 3-5D). This aligns with the plasma epinephrine concentration, which returned to pre-exercise levels 1 hour after exercise in all groups (Figure 3-2). Similarly, there were no differences in the phosphorylations of AKT ($pAKT^{T308}$:AKT or $pAKT^{S473}$:AKT) in the aSAT samples collected after LOW, MOD, or HIGH (Figure 3-5E).

3.5 DISCUSSION

Among the most novel findings of this study were the distinct alterations in aSAT transcriptome observed 1.5 hours after three different exercise sessions (LOW, MOD, HIGH), all commonly prescribed for maintaining fitness and health. HIGH induced more pronounced upregulations in inflammatory genes than MOD or LOW, while MOD and LOW upregulated ribosomal and oxidative phosphorylation genes. Despite a relatively small degree overlap of differentially expressed genes among the three groups, we found that alteration in circadian clock genes and upregulation of inflammatory genes were largely consistent across three exercise modalities. Overall our data suggests that acute exercise triggers early transcriptomic responses in inflammation, circadian rhythm, ribosome, and oxidative phosphorylation that may be differentially regulated by exercise-intensity. These early modifications in aSAT transcriptome, secretome, and proteome in response to each session of exercise may contribute to the maintenance of adipose tissue function in those who exercise regularly.

Aligning with our present findings, expression of inflammatory genes has been reported to increase in adipose tissue after a session of exercise in both preclinical models (235, 236) and humans (18, 189, 237), suggesting a transient induction of aSAT inflammation may be an intrinsic response to the stress of exercise. Our findings expand on previous work examining the effects of endurance exercise on aSAT inflammation by demonstrating inflammatory gene sets in aSAT increase after a session of exercise at low-, moderate-, and high-intensity. Interestingly, although LOW, MOD, and HIGH all upregulated inflammatory pathways in aSAT, our data suggests that HIGH may have a propensity to induce a more pronounced increase in inflammatory genes compared with MOD and LOW, perhaps at least in part as a consequence of an accumulation of non-esterified fatty acids in adipose tissue during HIGH. Very low adipose tissue blood flow during high-intensity exercise is believed to “trap” fatty acids within the tissue (38, 238), reflected in our study by the low plasma fatty acid concentration during HIGH, and accumulation of fatty acids within the tissue may have contributed to a greater inflammatory response in HIGH (67, 239). Additionally, we found that some specific inflammatory pathways may also be differentially regulated during low-, moderate-, and high-intensity exercise. For example, canonical IL6-JAK-STAT3 signaling was

upregulated after MOD and HIGH, but not in LOW (adjusted p=0.14), suggesting that there could be an intensity threshold for the IL6-JAK-STAT3 signaling to be activated in aSAT. Therefore, while we observed global upregulation of inflammatory gene sets in aSAT after acute exercise, the specific outcome of transcriptomic responses (e.g., types of recruited immune cells, activation of signaling cascades) may differ by exercise intensity.

In addition to the differential regulation of inflammatory genes among different exercise intensities, we found that some other gene sets may also be regulated in an intensity-dependent manner. Our finding that 'ribosome' and 'oxidative phosphorylation' pathways were upregulated by LOW and MOD suggests 45-60 minutes of low-to-moderate continuous intensity endurance exercise (which aligns with most clinical exercise prescriptions for adults with obesity) can trigger cues that could lead to adaptations favoring protein translation capacity and perhaps enhanced capacity to attenuate oxidative stress in aSAT. Unexpectedly, both 'ribosome' and 'oxidative phosphorylation' pathways were significantly downregulated during HIGH, which seems to conflict with the beneficial effects of high-intensity exercise (222, 240). The reasons for the acute downregulation of ribosome and oxidative phosphorylation pathways by HIGH are unclear, but the relatively large increase of inflammatory responses during HIGH may be an important contributor to this finding in samples collected < 2 hours after the exercise session (241, 242). Overall, our data indicate that some acute transcriptomic alterations by exercise are intensity-dependent, which may lead to intensity-specific adaptations in aSAT.

Our novel findings also demonstrate that gene expression of several core clock components (e.g., NR1D1, NAMPT, DBP, PER1, CIART) (243, 244) was significantly altered by acute exercise in all groups. Generally, clock genes exhibit circadian rhythmic expression in peripheral tissues such as adipose tissue, skeletal muscle, and liver, and participate in various biological processes including metabolic regulation and hormone/peptide release (245). It is well documented that lipid mobilization and storage in aSAT are impacted by circadian regulation (246, 247), and the disruption of the circadian rhythm of these processes has been found to be linked to metabolic health complications (248). Interestingly, the gene we found to have the greatest magnitude of

reduction after all exercise sessions in our study was the core clock component, NR1D1, which was recently reported to play a critical role in adipose tissue abnormalities common in obesity (e.g., fibrotic extracellular matrix and macrophage infiltration). Hunter et al. demonstrated that mice with a specific deletion of NR1D1 in white adipose tissue exhibited a large increase in adiposity in response to high fat diet (HFD), yet the markedly elevated fibrosis and macrophage infiltration found within white adipose tissue in response to HFD in littermate controls was not present in the adipose tissue-specific NR1D1 knock-out mice – and these mice were also protected from developing insulin resistance (249). Our finding that exercise increased gene expression of NAMPT, a key enzyme that mediates NAD+ biosynthesis (250), also supports the notion that acute exercise may trigger cues to enhance aSAT lipid storage capacity based on evidence that adipose-specific deletion of NAMPT in mice induced impaired adipogenic capacity and marked extracellular matrix fibrosis in their subcutaneous white adipose tissue (250). Whether the robust reduction in gene expression of NR1D1 and/or the increase in NAMPT expression we observed in aSAT after exercise translates to a change in protein abundance of these factors is not clear, but it is intriguing to consider that changes in NR1D1 and NAMPT expression after each session of exercise may contribute to adaptive responses to help augmenting metabolically favorable lipid storage capacity in aSAT that may be beneficial during periods of weight gain. The downregulation of some other clock genes that we observed after exercise does not align with a recent finding that a session of moderate-to-vigorous exercise (80% VO_2max) increased the mRNA expression of PER1 and PER2 in aSAT after 8 weeks of exercise training in adults with overweight/obesity (251). The reasons for this discrepancy are not clear, but this suggests changes in circadian transcripts after acute exercise may depend on factors such as the degree of adiposity and training-, and/or nutritional-status (251, 252). Interestingly, the expression of ‘master clock’ genes (i.e., BMAL1 and CLOCK) whose transcription is suppressed by NR1D1 and PER (253), did not change after acute exercise in either our study or Dreher et al.(251), which may indicate that the main aSAT clock was stable. Alternatively, it is possible that the exercise-induced transcriptional response of master clock genes is delayed – and we may have not captured the change in our samples collected 1.5h after the exercise session. In addition, although our finding of

exercise-induced alterations in core clock genes is interesting because circadian rhythm is tightly associated with energy homeostasis in aSAT (232), these effects may be driven by the energy deficit induced by exercise, rather than a direct effect of the exercise. However, it was recently reported that 10% weight loss without exercise did not increase mRNA expression of NR1D1 or PER1 in adipose tissue from adults with obesity (252, 254) suggesting the significant alterations in core clock genes we observed may be at least partially mediated by exercise-induced stimuli other than energy deficit (255).

Our findings that plasma concentrations of circulating pro-/anti-inflammatory cytokines were elevated at the end of moderate- and high-intensity exercise aligns with previous studies (256-258). Additionally, here we now report that even low-intensity exercise (30% VO_2peak) is enough to increase the circulating concentration of pro-(IL1β, IL6, TNFα) and anti-(IL10) inflammatory cytokine in regularly exercising adults. Despite distinct exercise stimulus and energy expenditure among LOW, MOD, and HIGH in our study, the effect of exercise on the circulating cytokines we measured were remarkably similar. Interestingly, a previous study reported that the magnitude of increase in circulating cytokines that included IL1β, IL10, IL6, and TNFα was greater immediately after exercise in physically active adults compared with age-matched sedentary cohorts, suggesting that increased immuno-sensitivity may be an important adaptation induced by regular exercise (259). Collectively, our data suggests that both pro- and anti-inflammatory cytokine production can be enhanced by acute exercise, which may not be specifically regulated by exercise intensity per se.

ERK and P38, key signaling proteins in the MAPK pathway that can regulate adipocyte proliferation, lipolytic function, and inflammation in adipose tissue (163, 260, 261), can be modified by exercise and thus mediate exercise-induced metabolic and tissue remodeling effects on adipose tissue (196, 262, 263). Alteration in ERK phosphorylation in response to acute exercise suggests that a session of exercise may rapidly trigger cellular signaling that regulates the growth/proliferation of adipocytes (264). However, because activation of ERK can result in contrasting proliferative outcomes in adipocytes such as upregulated (265) or downregulated (266) differentiation which is believed to be timely regulated (264), further assessment of downstream signaling of ERK is needed to accurately interpret our finding of reduced ERK phosphorylation after acute

exercise. In contrast, we did not observe a difference in the phosphorylation of key lipolytic enzyme HSL or insulin signaling protein AKT, which aligns with our observation that the concentration of epinephrine, a lipolytic stimulator, and insulin, an upstream activator of AKT (data not shown) returned to pre-exercise levels 1.5 hours after exercise. Interestingly, despite the distinct differences in exercise intensity, duration intensity, and energy expenditure among groups, the effect of acute exercise on the phosphorylation of the key metabolic proteins (ERK, P38, STAT3, HSL, AKT) that we measured was remarkably similar. Future research is needed to expand the assessment of phosphorylation on a larger pool of proteomes (i.e., phosphoproteomics) or other post-translational modifications (e.g., protein acetylation and methylation) triggered by a session of exercise performed at different intensities.

We (267) and others (14, 57, 220) have demonstrated the possibility of favorable adaptations in aSAT after months of exercise training (e.g., increased capillarization and mitochondrial density, ECM remodeling, and attenuated macrophage infiltration) yet, the triggering signals for the adaptive responses are not completely understood. As noted above, the reduction in NR1D1 and/or the increase in NAMPT after each session of exercise may be important contributors. Additionally, the acute inflammatory response we observed in aSAT after LOW, MOD, and HIGH may contribute as well. Although chronically elevated inflammation in adipose tissue and systemic circulation is commonly linked with a host of chronic diseases (43, 45, 268), paradoxically, acute inflammatory responses in aSAT may be an important contributor to favorable tissue remodeling to enhance lipid storage capacity (125). For example, in response to just 9 days of an HFD, transgenic mice with an adipose tissue-specific reduction in proinflammatory potential displayed reduced adipogenic capacity and failed to reduce fibrotic content in ECM compared with wild-type mice (125). The transgenic mice also exhibited excessive ectopic lipid deposition and glucose intolerance compared with the wild-type (125), suggesting adipose tissue remodeling in response to inflammatory stimuli may translate to important clinical outcomes. Further evidence supporting the role of acute inflammatory stimuli leading to some favorable remodeling in adipose tissue includes that acute introduction of the bacterial toxin lipopolysaccharide (LPS) promotes adipogenesis in adipose tissue in rats (269) and mice (125). Therefore, while an acute upregulation of

inflammatory responses in aSAT after each session of exercise may contribute to the maintenance of “healthy” aSAT in non-obese subjects like those in the present study, it may also underlie the favorable remodeling of aSAT we observed in adults with obesity in response to exercise training (267).

Although considerable effort was made to control for many aspects of our study, it is important to acknowledge some of the limitations. Firstly, our cross-sectional study design carries the limitations inherent to studies where each subject does not serve as their control. Importantly, we were successful in tightly matching subjects in each group for key factors that could impact the outcomes, such as sex, cardiorespiratory fitness (VO_2peak), body fat mass, and lean mass, enhancing confidence in the interpretations of our findings. Additionally, although our three different exercise treatments (LOW, MOD, and HIGH) represent commonly prescribed exercise programs, the exercise sessions were not matched for the duration or total energy expenditure, which may confound our interpretation of the impact of exercise ‘intensity’. However, an important goal of our study was to compare three distinct exercise modalities that are commonly implemented in clinical/applied settings, which makes matching for exercise duration and/or energy expenditure unfeasible. It is also important to acknowledge that responses to the interval exercise performed in HIGH likely cannot be fully attributed only to the high-intensity intervals, but the non-steady-state nature of this exercise may have impacted the responses as well, but exercise intensity used during HIGH (which mimics common high-intensity interval training (HIIT) prescriptions) cannot be performed continuously for more than a few minutes at most. Another important limitation is related to the timing of the aSAT biopsy. Obviously, collecting only one aSAT sample ~1.5 after exercise does not fully capture the acute effect of exercise on aSAT that can persist or be further altered up to a few days. Therefore, our findings are limited to characterizing the very early responses to exercise performed at low-, moderate- and high-intensity exercise. Follow-up studies in which biopsies are collected at several timepoints over the 24-48h period after exercise will more fully characterize the signaling events that may contribute to aSAT remodeling. Furthermore, while the changes in aSAT gene expression after a session of 3 different exercise treatments we report here are compelling, longitudinal exercise training studies are required to assess whether these responses after each exercise

session translate to proteomic and functional adaptations in aSAT with regularly performed exercise at these intensities.

In summary, our findings indicate that acute exercise can rapidly modify the aSAT transcriptome of pathways related to inflammation, circadian rhythms, protein translation, and mitochondrial biogenesis. Importantly, the magnitude of changes in the expression of some genes and regulation of gene sets of some specific biological pathways were distinctively regulated by different exercise intensities. Specifically, inflammatory response was more pronounced by HIGH compared with LOW and MOD, and ribosomal and oxidative phosphorylation genes were upregulated by MOD and LOW. Moreover, the transcriptomic response in aSAT by exercise may underlie the alterations in phosphorylation of metabolic proteins and production of cytokines, which were remarkably similar among groups despite the vastly different exercise stimuli. We contend that alterations in inflammatory, circadian, ribosomal, and mitochondrial genes that occur in aSAT after each exercise session may trigger adaptations that contribute to preserved aSAT function and metabolism in regular exercisers. This work expands the understanding of genetic and molecular responses in aSAT triggered by a session of exercise that may contribute to the maintenance or remodeling of aSAT, which in turn may be an important factor underlying the preserved cardiometabolic health often attributed to regular exercise.

3.6 ACKNOWLEDGEMENT

The authors gratefully thank the contribution of the study participants. We thank OMRF Clinical genomics core for their technical assistance. We acknowledge the excellent clinical and technical assistance provided by all the members of the Substrate Metabolism Laboratory.

3.7 FIGURES

Fig 1A

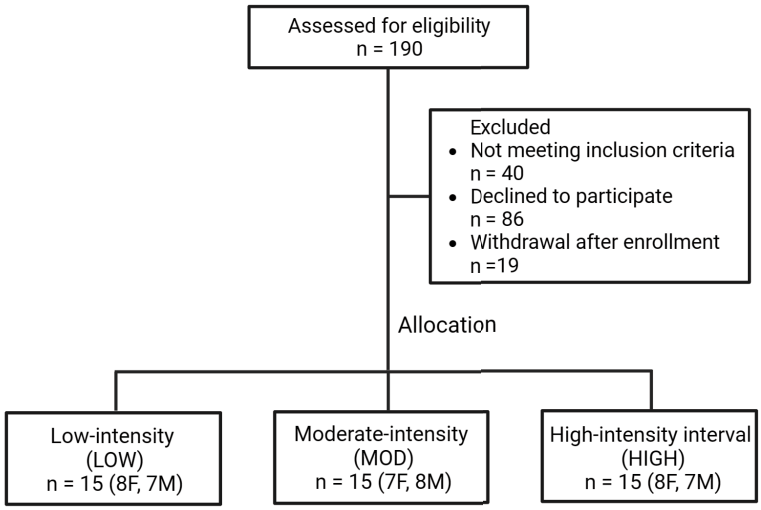

Fig 1B

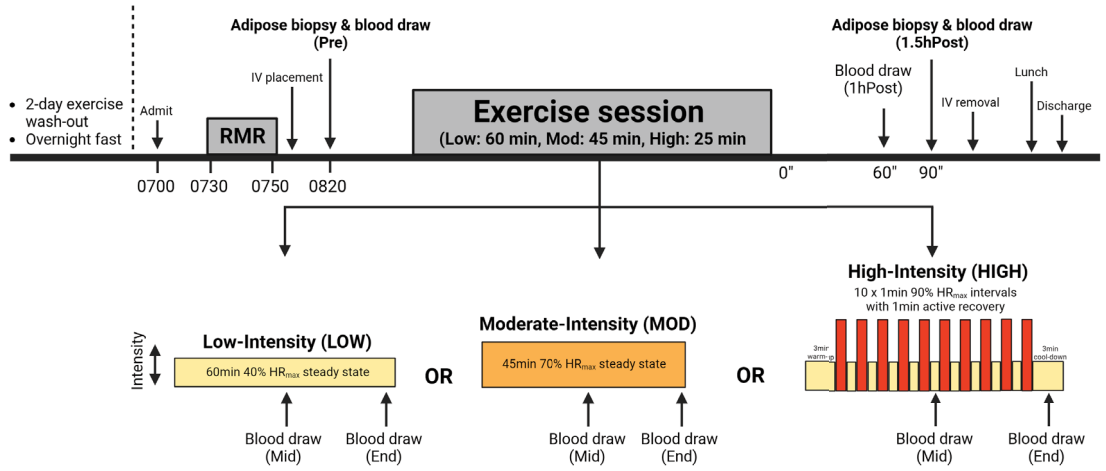

Figure 3-1 CONSORT diagram and study design

A) CONSORT diagram of the study. B) Schematic of study design.

Fig 2A

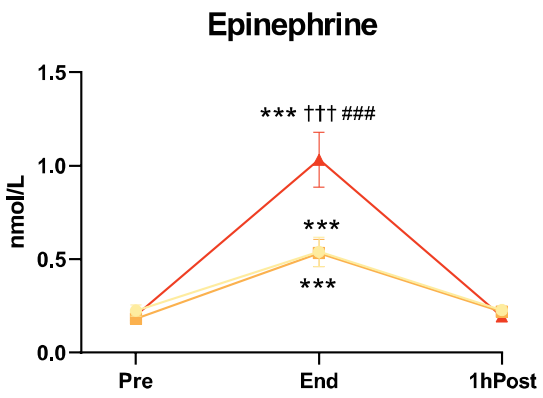

Fig 2B

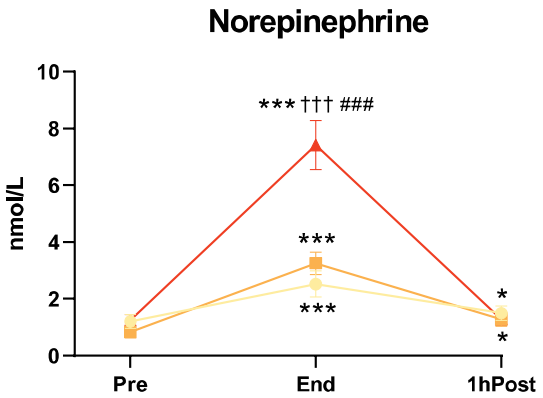

Fig 2C

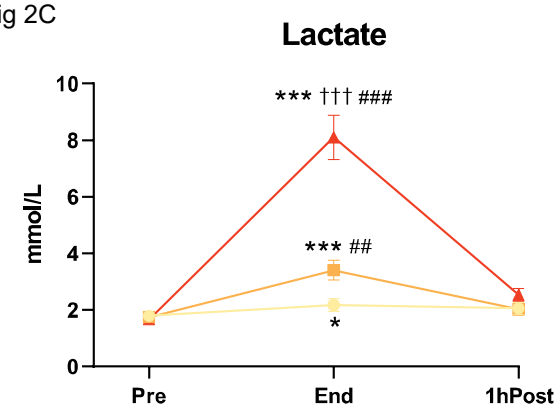

Fig 2D

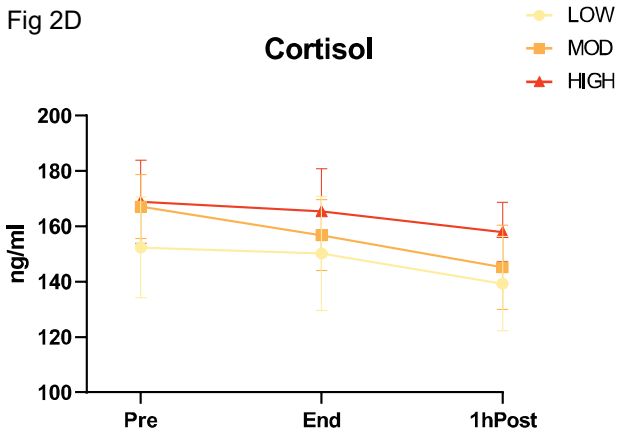

Figure 3-2 Humoral responses during and post LOW, MOD, and HIGH

A) Plasma epinephrine concentration. B) Plasma norepinephrine concentration. C) Plasma lactate concentration. D) Plasma cortisol concentration. *p<0.05 vs. Pre; **p <0.01 vs. Pre; ***p<0.001 vs. Pre; †p<0.05 vs. MOD; ††p<0.01 vs. MOD; †††p<0.001 vs. MOD; #p<0.05 vs. LOW; ##p<0.01 vs. LOW; ###p<0.001 vs. LOW. Significant Time x Group interaction effects were detected in epinephrine, norepinephrine, and lactate (p<0.001). Data is presented as Mean±SEM.

Fig 3A

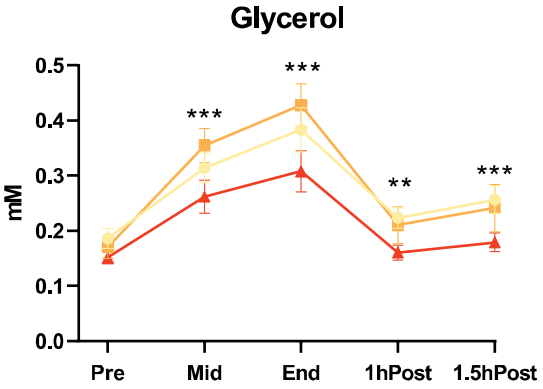

Fig 3B

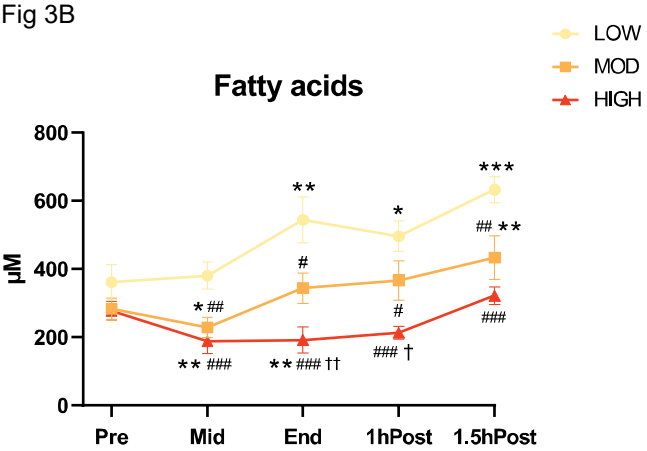

Figure 3-3 Lipolytic responses during and post LOW, MOD, and HIGH

A) Plasma glycerol concentration. B) Plasma fatty acid concentration. *p<0.05 vs. Pre; **p <0.01 vs. Pre; ***p<0.001 vs. Pre; †p<0.05 vs. MOD; ††p<0.01 vs. MOD; †††p<0.001 vs. MOD; #p<0.05 vs. LOW; ##p<0.01 vs. LOW; ###p<0.001 vs. LOW. A significant Time x Group interaction effect was detected in fatty acids (p<0.001). Data is presented as Mean±SEM.

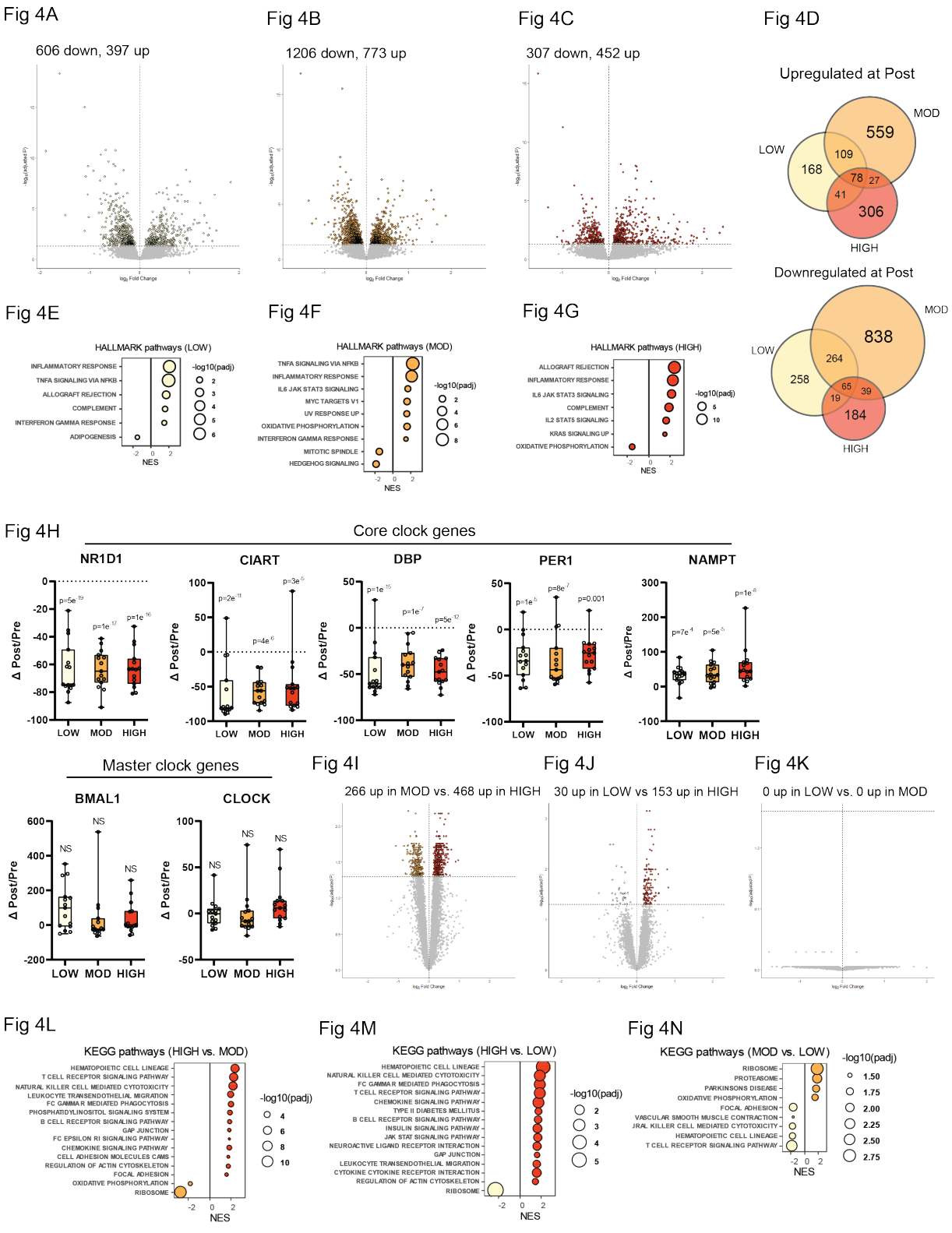

Figure 3-4 Transcriptomic responses in aSAT 1.5hour after LOW, MOD, and HIGH

A-C) Volcano plots of DEGs in LOW, MOD, and HIGH 1hPost vs. Pre (adjusted $p<0.05$). D) Venn diagram of upregulated and downregulated DEGs between LOW, MOD, and HIGH. E-G) Enriched pathways from GSEA (HALLMARK) in LOW, MOD, and HIGH 1hPost vs. Pre (adjusted $p<0.05$). H) ∆Post vs. Pre (% change) for selected core clock genes. There were no group differences. I-K) Volcano plots of DEGs comparing the acute effects of HIGH vs. MOD, HIGH vs. LOW, and MOD vs. LOW. L-N) Enriched pathways from GSEA (KEGG) in HIGH vs. MOD, HIGH vs. LOW, and MOD vs. LOW. Negative NES refers to significantly enriched pathways in MOD, LOW, and LOW, respectively.

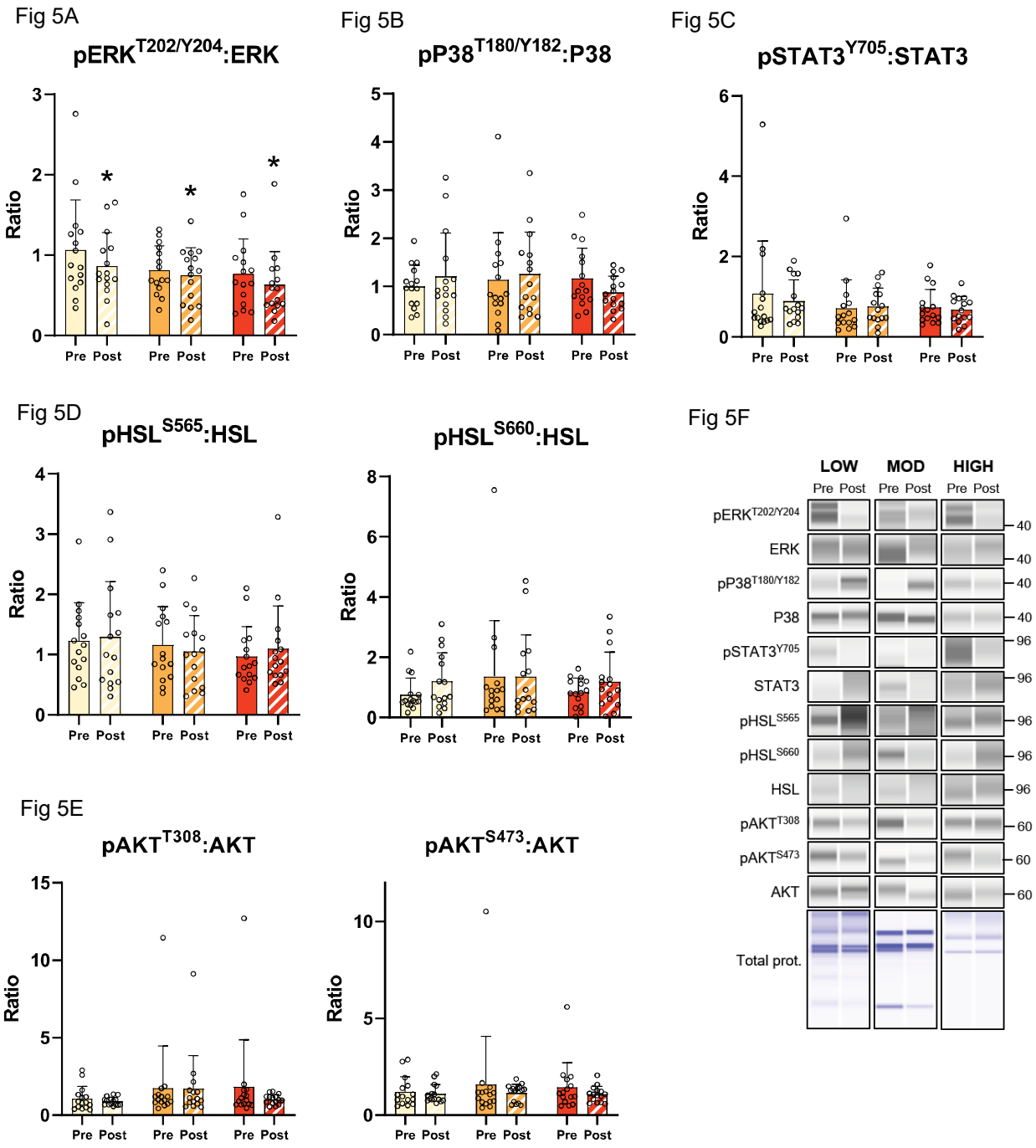

Figure 3-5 Protein phosphorylation of metabolic proteins in aSAT 1.5hour after LOW, MOD, and HIGH

A) Ratio of pERK$^{T202/Y204}$:ERK. B) Ratio of pP38$^{T180/Y182}$:P38. C) Ratio of pSTAT3^{Y705}:STAT3. D) Ratio of pHSL^{S565}:HSL and pHSL^{S660}:HSL. E) Ratio of pAKT^{T308}:AKT and pAKT^{S473}:AKT. F) Representative image of simple Western blot (JESS). *p<0.05 vs. Pre. There was no significant Time x Group interaction effect. Data is presented as Mean±SD.

Supplementary Fig 1

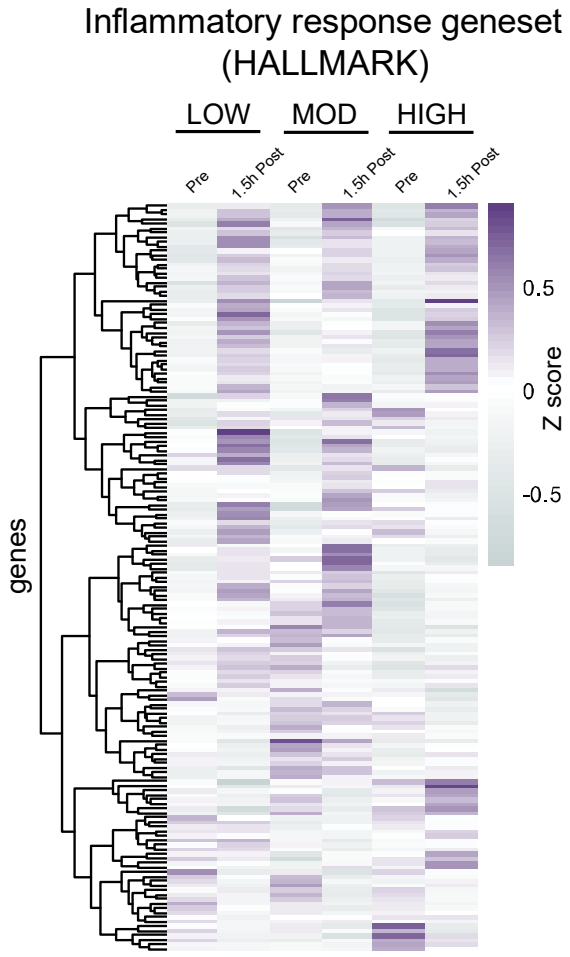

Figure 3-6 Supplementary Figure 1

Z-score heatmap of 165 genes from ‘HALLMARK_Inflammatory_response’ for Pre and Post in LOW, MOD, and HIGH.

3.8 TABLES

Table 3-1 Baseline subject characteristics and circulating metabolic biomarkers

	LOW (n=15)	**MOD (n=15)**	**HIGH (n=15)**	Difference between groups
Age (years)	31 ± 6	31 ± 6	30 ± 7	NS
Sex	8F, 7M	7F, 8M	8F, 7M	NS
Height (m)	1.72 ± 8.0	1.75 ± 8.8	1.73 ± 9.3	NS
Body mass (kg)	72.8 ± 9.0	74.5 ± 10.7	74.0 ± 11.2	NS
Body fat (%)	26 ± 6	26 ± 8	26 ± 8	NS
Fat mass (kg)	17.3 ± 6.1	17.3 ± 7.4	18.6 ± 7.3	NS
Lean mass (LM) (kg)	51.5 ± 8.2	52.9 ± 10.6	52.7 ± 10.8	NS
BMI (kg/m^2)	24.6 ± 2.2	24.4 ± 2.3	24.8 ± 2.6	NS
SBP (mmHg)	118 ± 8	124 ± 9	120 ± 11	NS
DBP (mmHg)	72 ± 7	78 ± 8	72 ± 9	NS
VO2peak (L/min)	2.6 ± 0.4	2.8 ± 0.6	2.9 ± 0.6	NS
VO2peak (mL/kg/min)	35.9 ± 4.5	37.4 ± 6.3	39.0 ± 5.6	NS
VO2peak (mL/kg LM/min)	50.8 ± 4.9	52.8 ± 6.5	55.1 ± 6.5	NS
Fat oxidation (µmol/min)	352 ± 79	349 ± 92	363 ± 73	NS
RMR (kcal/day)	1432 ± 160	1460 ± 250	1526 ± 244	NS
Fasting insulin (mU/L)	6.3 ± 2.7	5.4 ±2.5	5.6 ± 3.5	NS
Fasting glucose (mmol/L)	4.9 ± 0.7	5.1 ± 0.5	4.86 ± 0.5	NS
Fasting fatty acids (µM)	361 ± 200	283 ± 125	278 ± 106	NS
Fasting triglycerides (mM)	0.77 ± 0.28	0.89 ± 0.41	0.84 ± 0.40	NS

Table 3-2 Differentially expressed genes mostly affected (|log2FC|>1 & adjusted p<0.05) by LOW, MOD, and HIGH (Post vs. Pre)

LOW Post vs. Pre			MOD Post vs. Pre			HIGH Post vs. Pre		
GeneID	log2FC	padj	GeneID	log2FC	padj	GeneID	log2FC	padj
NR1D1	-1.61	5.40E-19	NR1D1	-1.56	1.38E-17	NR1D1	-1.51	1.57E-16
DBP	-1.10	1.04E-15	ADAMTS18	1.54	5.25E-07	CIART	-1.30	3.99E-05
CIART	-1.89	2.19E-11	NR4A3	1.60	3.99E-06	APOL4	1.39	1.58E-04
BHLHE41	-1.04	6.40E-10	CIART	-1.37	4.97E-06	IKZF4	1.06	2.91E-04
HK2	-1.08	6.96E-09	KCNA4	1.58	2.99E-05	SLC39A14	1.08	4.14E-04
ORC2	1.01	2.19E-08	FFAR3	1.20	8.12E-05	ANKRD20A5P	1.51	6.94E-04
APOL4	1.83	2.58E-08	C3orf52	1.88	1.15E-04	CR1	1.68	6.99E-04
ZBTB16	-1.04	4.21E-07	SLC39A14	1.11	1.26E-04	NR4A3	1.28	8.97E-04
ADAMTS18	1.51	4.67E-07	ABCC6P1	-1.19	2.21E-04	PROK2	2.44	0.002
MAP1LC3C	1.22	3.11E-06	APOL4	1.31	2.35E-04	MACIR	1.01	0.002
RPL7L1P9	-1.49	4.64E-05	KCNK6	1.20	2.91E-04	NFE2	2.04	0.003
THBS1	1.30	5.08E-05	RPL7L1P9	-1.29	5.75E-04	NCF1	1.48	0.003
LUZP2	-1.02	7.67E-05	MT1A	1.19	7.03E-04	KCNK6	1.05	0.004
CYP4F35P	1.10	1.34E-04	ANKRD20A8P	1.25	0.002	GRHL1	1.18	0.005
KCNA4	1.35	2.66E-04	THBS1	1.03	0.002	MGAM	2.04	0.005
KCNK6	1.20	2.66E-04	RPL11P3	1.19	0.017	PADI4	2.37	0.006
FFAR3	1.08	3.76E-04	HLA-V	1.01	0.018	C3orf52	1.42	0.007
ANKRD20A11P	1.03	0.001	C2CD4B	1.10	0.023	GAPT	1.77	0.010
C3orf52	1.54	0.002	SELE	1.55	0.029	FPR2	1.82	0.012
C5orf64	-1.11	0.002	NR4A1	1.11	0.044	FGF9	1.28	0.013
ANKRD20A5P	1.29	0.003				MT1A	1.01	0.013
PRR15	1.39	0.004				VNN2	1.53	0.013
MMP9	1.46	0.016				P2RY13	1.13	0.015
NWD2	1.01	0.031				NLRP12	1.89	0.016
						HAL	1.27	0.016
						AOAH	1.21	0.016
						GLT1D1	2.10	0.019
						LRG1	1.39	0.020
						CSF3R	1.41	0.021
						CCR1	1.06	0.023
						MNDA	1.34	0.025
						SH2D1A	1.38	0.026
						GFRA3	-1.01	0.027
						APOBEC3A	1.81	0.027
						MEFV	1.75	0.028
						CYP4Z1	1.21	0.031
						MKI67	1.07	0.032
						FCGR3B	1.44	0.036
						LILRA6	1.40	0.036
						JAML	1.10	0.037
						CASS4	1.10	0.039
						ADAM8	1.14	0.039
						NCF1B	1.42	0.041
						PELATON	1.58	0.041
						SLA	1.01	0.041
						IKZF3	1.10	0.041
						ADGRE3	1.80	0.044
						MIR223HG	1.31	0.047
						S100A8	1.47	0.047
						NCF1C	1.03	0.047
						TREM1	1.67	0.049

Table 3-3 Circulating cytokine responses during and post LOW, MOD, and HIGH

	LOW			MOD			HIGH			Group difference
	Pre	End	1.5hPost	Pre	End	1.5hPost	Pre	End	1.5hPost	
IL1β (pg/ml)	4.0 ± 1.5	4.7 ± 1.9**	4.6 ± 2.1	3.8 ± 1.4	4.3 ± 1.5**	4.4 ± 2.4	4.1 ± 1.8	5.3 ± 3.5**	4.6 ± 3.0	NS
IL10 (pg/ml)	30.0 ± 52.4	32.8 ± 52.4**	35.6 ± 57.6	27.6 ± 44.5	30.7 ± 42.9**	23.9 ± 28.0	27.1 ± 41.8	36.7 ± 63.0**	27.4 ± 40.6	NS
IL6 (pg/ml)	8.0 ± 12.9	8.6 ± 12.0**	10.3 ± 14.7***	5.9 ± 12.6	6.5 ± 12.1**	5.6 ± 7.1***	5.6 ± 10.3	7.3 ± 12.1**	6.8 ± 11.0***	NS
TNFα (pg/ml)	9.9 ± 3.1	11.5 ± 3.9**	11.7 ± 5.2*	9.4 ± 2.1	9.7 ± 2.9**	10.2 ± 2.6*	8.9 ± 2.3	10.7 ± 4.2**	9.5 ± 3.9*	NS
IFNγ (pg/ml)	34.3 ± 14.6	39.0 ± 18.5	36.3 ± 15.5	30.5 ± 10.3	32.2 ± 10.2	31.6 ± 12.4	33.9 ± 12.9	40.3 ± 28.6	33.8 ± 11.6	NS

*p<0.05 vs. Pre; **p<0.01 vs. Pre; ***p<0.001 vs. Pre. There was no significant Time x Group interaction effect. Sample sizes for IL10 – LOW: n=14; MOD: n=15; HIGH: n=14. Sample sizes for IL6 – LOW: n=10; MOD: n=14; HIGH: n=13. Data is presented as Mean±SD.

Chapter 4

Project 2
Effects of 12-Week Exercise Training on Subcutaneous Adipose Tissue Remodeling in Adults with Obesity without Weight Loss

4.1 ABSTRACT

Excessive adipose tissue mass underlies much of the metabolic health complications in obesity. Although exercise training is known to improve metabolic health in individuals with obesity, the effects of exercise training without weight loss on adipose tissue structure and metabolic function remain unclear. Thirty-six adults with obesity (BMI = 33±3 kg/m^2) were assigned to 12 wks (4d/wk) of either moderate-intensity continuous training (MICT; 70% HR max, 45min; n=17) or high-intensity interval training (HIIT; 90% HR max, 10 X 1min; n=19), maintaining their body weight throughout. Abdominal subcutaneous adipose tissue (aSAT) biopsy samples were collected once before and twice after training (1 day after the last exercise and again 4 days later). Exercise training modified aSAT morphology (i.e., reduced fat cell size, increased Collagen type 5a3, both $p \leq 0.05$, increased capillary density, $p=0.05$), and altered protein abundance of factors that regulate aSAT remodeling (i.e., reduced matrix metallopeptidase 9; $p=0.02$; increased angiopoietin-2; $p<0.01$). Exercise training also increased the protein abundance of factors that regulate lipid metabolism (e.g., hormone-sensitive lipase and fatty acid translocase; $p \leq 0.03$) and key proteins involved in the MAPK pathway when measured the day after the last exercise session. However, most of these exercise-mediated changes were no longer significant 4 days after exercise. Importantly, MICT and HIIT induced remarkably similar adaptations in aSAT. Collectively, even in the absence of weight loss, 12 weeks of exercise training induced changes in aSAT structure, as well as factors that regulate metabolism and inflammatory signal pathway in adults with obesity.

4.2 INTRODUCTION

Abdominal subcutaneous adipose tissue (aSAT) in obesity is usually characterized by hypertrophic adipocytes, accumulation of fibrotic collagen proteins in extracellular matrix (ECM), and relatively low capillary density (3, 96, 270), all of which are tightly linked with insulin resistance, cell necrosis, and inflammatory macrophage infiltration (271-273). The increased inflammation in aSAT is considered an important contributor to many systemic metabolic health complications (118, 274, 275). In addition, these aSAT abnormalities in obesity can limit fat storage capacity, resulting in the high rates of fatty acid release into the systemic circulation that underlies metabolically harmful ectopic lipid deposition commonly found in tissues such as the liver and skeletal muscle of many adults with obesity (180). Therefore, strategies aimed at remodeling aSAT to create more smaller adipocytes (i.e., adipogenesis), modify the content and composition of the ECM, increase capillarization (i.e., angiogenesis), reduce inflammatory pathway activation, and increase lipid storage capacity could lead to improved metabolic health outcomes, even in the absence of weight loss.

Exercise is one of the first-line strategies for treating obesity-related health complications, but how exercise “works” to improve metabolic health in obesity is still incompletely understood. Exercise training increases skeletal muscle mitochondria and oxidative capacity in adults with obesity (276-278). However, increasing muscle oxidative capacity, per se, is often found to do rather little to improve insulin sensitivity and other key markers of metabolic health in adults with obesity (10, 279). Alternatively, evidence from our lab and others suggests exercise triggers responses in aSAT that may lead to ECM remodeling, increased angiogenesis, and alterations in the inflammatory profile (15, 17, 280, 281). High-intensity interval training (HIIT) has garnered considerable attention because of its time efficiency and distinct physiological responses compared with more “conventional” moderate-intensity continuous training (MICT) (24, 282). However, whether and/or how the intensity of an exercise training program may modify adaptive responses within aSAT remains unclear. Differential effects of HIIT vs. MICT on circulating adipokine levels and adipocyte size in rodent models suggest a possibility that HIIT may induce more robust adaptations in aSAT morphology and metabolism compared with MICT (26, 283).

The primary aims of this study were to compare the effects of 12 weeks of MICT vs. HIIT on subcutaneous aSAT structure and whole-body fatty acid mobilization in adults with obesity. This project also examined the effects of MICT and HIIT on the factors that regulate aSAT remodeling (i.e., adipogenesis, ECM remodeling, angiogenesis), metabolism (i.e., lipolysis, esterification, mitochondrial adaptation), and inflammatory signal pathways. Importantly, because even modest changes in body weight and fat mass can induce some aSAT remodeling (97, 272, 284), this study was designed to require participants to maintain their body weight throughout the training intervention. We hypothesized that even without weight loss, 12 weeks of exercise training would induce detectable modifications to aSAT structure and metabolic regulation. Moreover, we hypothesized that these training-induced effects would be more pronounced in response to HIIT compared with MICT.

4.3 METHODS & MATERIALS

Subjects

Thirty-six adults with obesity (BMI: 30-40 kg/m^2) participated in the study. All subjects were sedentary and reported to have had a stable body weight at least 6 months before their first pre-training clinical measurement. Subjects were not taking any medications or supplements known to affect their metabolism except contraceptive medications for some female participants (n=16 out of 24). Eligible participants also had no history of cardiovascular or metabolic disease. All female participants were premenopausal and not pregnant or lactating. All subjects completed a detailed medical history survey and resting electrocardiogram, which were reviewed by a physician before any testing. Subjects participating in this study also participated in a related study from our laboratory, which focused primarily on the effects of 3 months of exercise training in whole-body insulin sensitivity and muscle lipid metabolism (278). Some of the methods (e.g., exercise training protocols) and results describing the basic responses to training (e.g., anthropometric characteristics, peak oxygen uptake) have been reported elsewhere (278) but are repeated here for convenience. Written informed consent was obtained from

all subjects before the study. This study conformed to the standards set by the Declaration of Helsinki, except for registration in a database. This study was approved by the University of Michigan Institutional Review Board and registered at clinicaltrials.gov (NCT02706093).

Study Design

Enrolled subjects were assigned to either moderate-intensity continuous training (MICT; n = 17) or high-intensity interval training (HIIT; n=19) groups in a counter balanced manner to optimize the matching of sex and baseline anthropometric characteristics and aerobic fitness between training groups. Before training, subjects underwent one "clinical trial" (i.e., hyperinsulinemic-euglycemic clamp, [1-^{13}C]palmitate tracer infusion to measure whole-body fatty acid mobilization, aSAT biopsies; see details in *Clinical trial* section, below). After 12 weeks of MICT or HIIT, subjects underwent two clinical trials, one conducted the day after the last exercise session (1d-Post training) and the other conducted after subjects refrained from exercise for 4 days (4d-Post training) to wash out the potential influence of the acute exercise effects. Importantly, subjects were required to maintain their body weight throughout the intervention (see details in *Training intervention* section, below). A schematic of the study design is presented in Figure 1.

Body composition and aerobic fitness testing

Before and after subjects completed the 12-week MICT or HIIT, body composition and aerobic fitness (i.e., peak oxygen uptake; VO_2peak) were measured. Fat mass and fat-free mass (FFM) were determined by dual-energy x-ray absorptiometry (Lunar DPX DEXA scanner, GE, WI). VO_2peak was assessed on a stationary cycle ergometer (Corvival, Lode, Netherlands) using an incremental exercise protocol starting at 40 watts for 4min and was increased by 20 watts each minute until volitional exhaustion. The rate of oxygen consumption was measured throughout this test using a metabolic cart (Max-II, Physiodyne Inc, NY) and VO_2peak was determined as the highest 30-second average before volitional fatigue. Measurements of respiratory exchange ratio (RER) ≥ 1.1 and maximal heart rate (HR_{max}) ≥ 90% of age-predicted values (i.e., 220-age) were used as secondary indices to help confirm maximal effort during these tests.

Training interventions

Training protocol.

Subjects in both groups exercised 4 days per week for 12 weeks. Each exercise training session for the MICT group consisted of continuous exercise for 45 minutes at 70% of their $HR_{max.}$ For the HIIT group, each training session involved a 3-minute warm-up at ~65% $HR_{max,}$ and then 10 x 1-minute intervals at 90% HR_{max} interspersed with 1 minute low-intensity active recovery. These high-intensity intervals were then followed by a 3-minute cool-down at 65% HR_{max}. Participants in both groups were allowed to select their preferred mode of exercise among stationary cycling, treadmill, elliptical, or rowing ergometers. Exercise time (MICT; 45 minutes, HIIT; 25 minutes) and energy expenditure (MICT; ~250 kcals, HIIT; ~150 kcals) between groups were considerably different to address the study goal of comparing the low-volume HIIT protocol (25) with a conventional and commonly prescribed steady-state exercise training program.

Training familiarization/ramp-up.

Subjects in both training groups followed a strictly regulated ramp-up protocol to gradually increase their exercise intensity and duration during the first two weeks of training. During the first week, participants in both groups performed 4 sessions of continuous 25-minute exercise at 65% HR_{max}. During the second week of the ramp-up, subjects in the MICT group performed 4 sessions of continuous 35-minute exercise at 70% HR_{max}, while participants in the HIIT group performed 4 sessions of exercise progressively increasing the number of 1-minute intervals at 90% HR_{max} (i.e., 2 x 1, 4 x 1, 6 x 1, 8 x 1). Both groups began their full training prescription at the beginning of week 3.

Monitoring of training adherence and weight maintenance.

Study staff supervised all exercise sessions for the first 3 weeks of training (total 12 sessions). For the remainder of the 12-week training program, subjects were required to be present for two supervised training sessions each week, with two unsupervised sessions monitored using downloadable telemetry heart rate devices (Polar, Finland) that

were provided to all participants, and were required to be worn during all exercise training sessions. Heart rate data during all sessions were reviewed by study staff to ensure the subjects' appropriate completion of all sessions at the assigned intensity and duration. To monitor weight stability, participants were weighed several times each week and if body mass deviated by 1-2% from their baseline, our research dietitian provided nutritional guidance to adjust their calorie intake to maintain their weight at their baseline levels.

Clinical trials

Subjects completed three separate clinical trials; Once before training (Pre-training) and twice after training (1d-Post training and 4d-Post training; Figure 4-1). For each of these three visits, subjects arrived at the Michigan Clinical Research Unit at 1730 h the evening before the clinical trial. For the 1d-Post training visit, participants performed their usual exercise session beginning at 1800 h (before dinner). Immediately after the exercise session, participants ingested a nutritional supplement drink, which was individually determined to replace the calories expended during their exercise session with their dinner (Boost Plus, Nestle, Switzerland; 50% carbohydrates, 35% fat, and 15% protein) to prevent an exercise-induced energy deficit state during the trial. During all trials, subjects were provided a standardized dinner (30% of estimated total daily energy expenditure) and snack (10% of estimated total daily energy expenditure) at 1900 h and 2200 h respectively. The macronutrient composition of the meal and snacks was 55% carbohydrates, 30% fat, and 15% protein. Participants had access to water ad libitum, but after their evening snack, they remained fasted until the completion of all measurements the next morning. Participants slept in their hospital room overnight.

At ~0700 h the next morning, intravenous catheters were inserted into a hand/forearm vein on each arm. A baseline blood sample was collected at ~0800 h. At ~0830 h we collected aSAT biopsy samples 10-15cm lateral to the umbilicus, as previously described (190). Briefly, we collected approximately 100mg of a core aSAT sample, which was immediately fixed in 10% formalin for histological analyses of aSAT morphology and structure (see details below), and another ~300mg of aSAT was collected via aspiration. These samples were immediately frozen in liquid nitrogen and

stored at −80°C for later quantification of specific proteins using Western blot analyses (see details below). At ~0900 h, we began continuous infusion of [1-^{13}C]palmitate (0.04 μmol/kg/min) to assess whole-body fatty acid mobilization. Beginning at ~0950 h, we collected 3 arterialized (heated hand technique) blood samples separated by 5 minutes each—these plasma samples were used to assess overnight fasted fatty acid mobilization. At ~1000 h, a ~2-hour hyperinsulinemic-euglycemic clamp began to determine anti-lipolytic sensitivity to insulin (285). Briefly, a primed, continuous infusion of insulin (40mU/m^2/min) was administered; blood glucose was assessed every 5 minutes, and 20% dextrose was infused at a variable rate to accommodate changes in blood glucose to maintain blood glucose at the participants' overnight fasted levels. After blood glucose concentration stabilized without further changes in the rate of D20 infusion for ≥ ~20 minutes (typically 100min after beginning the clamp procedure), five arterialized blood samples were collected every 5 minutes for the determination of steady-state plasma fatty acid kinetics.

Analytical procedures

Histological assessment of aSAT morphology and structure

The core aSAT samples that were fixed in 10% formalin at the time of the biopsy were later paraffin-embedded (Sakura Tissue Tek TEC, Japan). Embedded samples were sectioned in 10μm thickness by a microtome (#RM2235, Leica, Germany) and placed on a microscopy slide. Histological analysis was performed on samples collected before the 12-week training intervention and those collected 4d-Post training. To keep staining conditions as consistent as possible, samples from Pre-training and 4d-Post training visits were placed on the same slide. Sections were prepared for staining by being deparaffinized and dehydrated with xylene and a series of ethanol respectively, as described previously (286). To minimize variance between subjects, staining was performed in several batches and all the microscopy conditions (i.e., exposure time) were kept consistent.

Adipocyte size: Histological sample sections were stained with Harris' hematoxylin (#HHS16; Sigma Aldrich) and eosin (#318906; Sigma Aldrich) followed by dehydration by ethanol. Xylene-based permount was used to mount the slides. Images of the stained sections were obtained with a brightfield channel in 10x by Keyence BZ-X700 microscope (Keyence, Japan). Adipocyte size was determined by using Image J (NIH, USA) as described previously (286). The proportion of small adipocytes was measured by calculating the percentage of adipocytes with a mean size larger than 1000μm^2 and lower than 3000μm^2.

Extracellular matrix fibrosis: Deparaffinized sections were stained with Picro Sirius red (#36554-8; Sigma Aldrich) for 1 hour to determine total fibrosis in aSAT extracellular matrix. Sections were then rinsed with acidified water, followed by dehydration with ethanol, and mounted with a xylene-based permount. To determine the abundance of subtypes of collagen fibers in the ECM, we performed fluorescence immunohistochemistry. Deparaffinized sections were incubated in 0.5mM HCl-Glycine buffer (pH 3.0) at 90°C for 20 min for antigen retrieval. Sections were subsequently blocked with 3% hydrogen peroxide in methanol for 15 minutes followed by 5% normal goat serum in PBS for 1 hour. Sections were then incubated with primary antibodies overnight at 4°C, and then incubated with appropriate secondary antibodies in the dark. Sections were mounted with antifade mounting medium (Prolong Gold; Thermofisher Scientific). Images of the stained sections were obtained by Keyence BZ-X700 microscope (10x; fluorescence) and analyzed by using Image J. The proportions of each collagen were calculated by dividing the positively stained area by the entire section area. Primary antibodies were Collagen type 4 (Col4, #C1926, Sigma Aldrich), Collagen type 5a3 (Col5a3, #LS-C353420, LifeSpan BioSciences), Collagen type 6 (Col6, # ab6588, Abcam). Secondary antibodies were AlexaFlour 488 (# A11008, A21422, Thermofisher Scientific) and 555 (# A21428, Thermofisher Scientific).

Capillary density: Sections were incubated with anti-von Willebrand Factor (#AB7356; Abcam) primary antibody followed by incubation with HRP conjugated secondary antibody and DAB substrate for visualization. Hematoxylin was used for

counterstaining. Images were obtained in 10x by Keyence BZ-X700 microscope (brightfield). Image J was used to analyze capillary density (i.e., number of capillaries per section area and number of capillaries per adipocytes) and capillary size.

Protein abundance of factors regulating aSAT remodeling, metabolism, and inflammatory pathway.

A portion of each aspirated aSAT biopsy sample (~140mg wet weight) was homogenized in ice-cold 1X RIPA buffer (#9806, Cell Signaling Technology, MA) with freshly added protease and phosphatase inhibitors (P8340, P5726, and P0044; Sigma Aldrich) using two 5 mm steel beads (TissueLyser II, Qiagen, CA). Homogenates were rotated at 50 rpm for 60 min at 4°C and then centrifuged at 4°C for 3 x 15 minutes at 15,000g, disposing the lipid fraction between each centrifugation. Protein concentration was assessed using the bicinchoninic acid method (#23225, Thermofisher Scientific). Samples for Western blotting were prepared in 4x Laemmli buffer, heated for 5 minutes at 95°C, and equal amounts of protein (15μg) were loaded onto handcast gels ranging from 8 to 15%. Following separation by SDS-PAGE, proteins were transferred onto nitrocellulose membranes. Membranes were blocked for 2 hours with 5% bovine serum albumin in tris-buffered saline, 0.1% Tween 20 (TBST) at room temperature, and incubated with primary antibodies overnight at 4°C. After primary antibody incubation, membranes were washed and incubated with appropriate secondary antibodies (#7074 or #7076, Cell Signaling Technology). All blots were developed using enhanced chemiluminescence (#1705061, Biorad or #34095, Fisher) and imaged (Fluorchem E Imager, ProteinSimple, CA). Primary antibodies were Adipose triglyceride lipase (ATGL, #2138, Cell Signaling Technology), Hormone-sensitive lipase (HSL, #18381, Cell Signaling Technology), Comparative gene identification-58 (CGI-58, ab183739, Abcam), Glycerol-3-phosphate acyltransferase 1 (GPAT1, PA5-20524, Thermofisher Scientific), Diglyceride acyltransferase 1 (DGAT1, NB110-41487, Novus Biologics), CD36 (sc-9154, Santacruz biotechnology), Cytochrome c oxidase subunit IV (COX-IV, #4844, Cell Signaling Technology), Peroxisome Proliferator Activated Receptor Gamma (PPARγ, #2435, Cell Signaling Technology), CCAAT Enhancer Binding Protein Alpha (CEBPα, #8178, Cell Signaling Technology), Fatty acid-binding protein 4 (FABP4, sc-271529,

Santacruz Biotechnology), Matrix metalloproteinase 2 (MMP2, #87809, Cell Signaling Technology), Matrix metalloproteinase 9 (MMP9, #13667, Cell Signaling Technology), Tissue inhibitor metalloproteinase 1 (TIMP1, #8926, Cell Signaling Technology), Tissue inhibitor metalloproteinase 2 (TIMP2, #5738, Cell Signaling Technology), Vascular Endothelial Growth Factor A (VEGFα, ab46154, Abcam), Angiopoietin 1 (HPA018816, Sigma Aldrich), Angiopoietin 2 (sc-74403, Santacruz Biotechnology), p38 MAPK (#9212, Cell Signaling Technology), Phospho-p38 MAPK (Thr180/Tyr182) (#9211, Cell Signaling Technology), p44/42 MAPK (Erk1/2, #4695, Cell Signaling Technology), Phospho-p44/42 MAPK (Thr202/Tyr204) (phopho-Erk1/2, # 4376, Cell Signaling Technology), SAPK/JNK (#9252, Cell Signaling Technology), Phospho-SAPK/JNK (Thr183/Tyr185) (#9251, Cell Signaling Technology). To normalize proteins to the total protein level, Memcode (#24580, ThermoFisher Scientific) was used to stain total protein in the membranes (287). To reduce gel-to-gel variability, an internal standard sample (IS; composite aSAT lysate from 8 obese individuals) was also loaded onto each gel for normalization.

Circulating concentrations of adipokines and fatty acids.

Plasma concentrations of total adiponectin (DRP300, R&D Systems), high molecular weight (HMW) adiponectin (DHWAD0, R&D Systems), and leptin (EZHL-80SK, Sigma Aldrich) were assessed by ELISA. Plasma concentrations of fatty acids (NC9517309, NC9517311, Fujifilm Medical Systems) were measured using commercially available kits.

Plasma fatty acid kinetics.

Gas chromatography-mass spectroscopy (Agilent 5973 Networks, Mass Selective Detector, Agilent, DE) was used to determine the tracer-to-tracee ratio (TTR) for plasma palmitate and fatty acid rate of appearance (Ra) into plasma was calculated as we have reported previously (288).

Statistical analysis

Non-normally distributed data were log-transformed before statistical analysis. Linear mixed models were applied to examine the main effects of the training group (MICT

vs. HIIT) and training status (pre-training vs. 4d-Post training or pre-training vs. 1d-Post training vs. 4d-Post training) and training group x training status interactions (IBM Corp. Released 2019. IBM SPSS Statistics for Windows, Version 26.0. Armonk, NY: IBM Corp). Fisher's least significant different method was used for post hoc comparisons when significant interaction effects (i.e., training group x training status interaction) were observed. Pairwise comparisons were also conducted between different training statuses (i.e., Pre-training vs. 1d-Post training vs. 4d-Post training). In the few measurements where missing data were unavoidable due to inadequate tissue yield or tracer availability, data for these measurements from all trials were excluded and a specific sample size is reported for these few outcomes. All data are presented as mean ± SD.

4.4 RESULTS

Body weight, body composition, VO_2peak, and blood parameters in response to training

A total of 36 subjects with obesity completed the exercise training interventions (MICT; n = 17, HIIT; n = 19; Table 4-1). Both MICT and HIIT significantly increased both absolute (L/min) and relative (ml/kgFFM/min) VO_2peak ($p < 0.001$), and there was a trend for the increase in absolute VO_2peak in HIIT (11±5%) to be greater than MICT (6±8%) ($p=0.1$). As designed, body mass and fat-free mass did not change after training (Table 4-1), but there was a trend for body fat mass to be slightly lower after both HIIT and MICT ($p=0.06$), which was the result of very small ($\leq$ ~0.5kg), yet the consistent reduction in total body fat mass across subjects (Table 4-1).

Three months of exercise training without weight loss did not alter fasting plasma concentrations of fatty acids. Interestingly, fasting plasma concentrations of total adiponectin, HMW adiponectin, and leptin were all significantly reduced after training ($p=0.001$, $p=0.03$, $p=0.03$, respectively; Table 4-1) with no differences between MICT and HIIT.

Morphological and structural aSAT remodeling in response to training

Adipocyte cell size.

Twelve weeks of MICT and HIIT slightly (~10%), yet significantly reduced mean adipocyte size (p=0.002; Figure 4-2A and 2B) and increased the proportion of small adipocytes (p=0.018; Figure 4-2C). This was evidenced by a leftward shift in the frequency distribution for 4d-Post training adipocyte size (Figure 4-2D). There were no distinguishable differences between MICT and HIIT (Figure 4-2).

aSAT fibrosis and ECM collagen.

aSAT fibrosis (as assessed by Sirius Red staining) was not altered after training in either MICT or HIIT (Figure 4-3A and 3B). Using immunohistochemistry to assess potential changes in the abundance of some specific aSAT ECM proteins, we found a small, yet significant increase in Col5a3 4 days after training (p=0.04) with no differences between MICT and HIIT (Figure 4-3A and 3B). Conversely, the abundance of Col4 and 6 was not significantly altered by exercise training (Figure 4-3A and 3B).

aSAT capillarization.

Exercise training increased capillarization when expressed as the number of capillaries per mm^2 (Figure 4-4A and 4B; p=0.05). Conversely, the change of capillarization when expressed as the number of capillaries per adipocyte (Figures 4-4A and 4C), did not quite reach statistical significance (p=0.1). There were no differences in capillarization observed between MICT and HIIT. Additionally, the capillary cross-sectional area also did not change 4 days after training in either MICT or HIIT (Figure 4-4D).

Factors regulating aSAT remodeling

The morphological/structural measurements presented above were all measured in aSAT samples collected 4 days after the last exercise training session. However, because many longer-term adaptations to exercise training like these often stem from relatively short-lived responses to exercise, we measured changes in factors that regulate these structural adaptations both 1 day and 4 days after the last exercise training session.

Markers of adipogenesis regulation

The protein abundance of total PPARγ was not different after training in either group (Figure 4-5). However, we found a significant training group x training status interaction for CEBPα, another primary transcription factor for adipogenesis. Post-hoc testing revealed that the protein abundance of total CEBPα was significantly increased in aSAT 1 day and 4 days after the last exercise session in HIIT ($p=0.02$ and $p=0.03$ respectively) but not MICT (Figure 4-5). The protein abundance of FABP4, a marker for differentiated/mature adipocytes was significantly increased when measured 1 day after exercise ($p = 0.01$) and tended to remain elevated when measured 4 days after exercise ($p=0.09$) with no differences between MICT and HIIT.

Extracellular matrix regulators

Although we did not find an effect of exercise training on total aSAT fibrosis (as assessed by Sirius Red staining; Figure 4-3), we did find that the abundance of MMP9, one of the key proteins involved in ECM remodeling was reduced 4 days after exercise training ($p=0.02$). There was no significant difference in MMP9 abundance between MICT and HIIT. The protein abundance of MMP2, TIMP1, and TIMP2 were not altered either 1 day or 4 days after exercise training (Figure 4-5).

Angiogenesis regulators

Aligning with the observed increase in aSAT capillarization after both MICT and HIIT, protein abundance of the angiogenic regulator, Angiopoietin-2 was increased both 1 day and 4 days after exercise training ($p<0.01$) with no differences between groups (Figure 4-5). In contrast, we did not observe an increased abundance of VEGFα, which is widely considered a “master regulator” of angiogenic activity. Additionally, we found a significant training group x training status interaction for Angiopoietin-1, another angiogenic regulator. Post-hoc testing revealed that Angiopoietin-1 was significantly reduced below pre-training levels when measured 4 days after training after HIIT ($p=0.006$) but not MICT (Figure 4-5).

Whole-body fatty acid mobilization

After an overnight fast, fatty acid release from adipose tissue into the systemic circulation (fatty acid Ra) was not affected by either MICT or HIIT when measured either 1 day or 4 days after exercise training (Figure 4-6). During the insulin infusion, the potent antilipolytic effects of insulin reduced fatty acid Ra to levels ~70% below basal levels in both training groups ($p<0.001$), but there was no effect of exercise training on the antilipolytic effects of insulin when measured after 1 day and 4 days of exercise training (Figure 4-6).

Proteins regulating aSAT metabolism

In agreement with our observation that training did not affect fatty acid release from adipose tissue, protein abundance of the main triacylglycerol lipase protein, ATGL, and its primary activator, CGI-58 also did not change after training (Figure 4-7). Interestingly, however, abundance of HSL, which hydrolyzes diacylglycerol to monoacylglycerol, was significantly elevated above pre-training levels when measured 1 day after exercise ($p = 0.01$) and tended to remain elevated 4 days later ($p=0.06$; Figure 4-7). The protein abundance of the fatty acid trafficking protein, FAT/CD36 was significantly increased 1 day after exercise ($p=0.03$), which then returned to pre-training level 4 days later (Figure 4-7). Neither of the primary fatty acid esterification proteins, GPAT1 and DGAT1 were altered by training (Figure 4-7). Exercise training significantly increased the protein abundance of COX-IV, a classical marker of mitochondrial density ($p<0.01$). However, the protein abundance of SDHA, an enzyme involved in the citric acid cycle and electron transport chain, was not affected after exercise training. Importantly, we did not observe any differences between HIIT and MICT for any of these proteins that regulate aSAT metabolism (Figure 4-7).

Key signal proteins involved in the MAPK pathway

The protein abundance of phosphorylated P38 MAPK (Thr^{180} and Tyr^{182}) was significantly increased 1 day after exercise training ($p=0.02$) with no differences between MICT and HIIT (Figure 4-8). However, this exercise-induced increase in phosphorylated P38 was no longer evident when expressed relative to total P38 MAPK (Figure 4-8). We also found the total protein abundances of JNK and ERK1/2 to be significantly elevated

1 day after the last exercise session (both p=0.02) with no difference between MICT and HIIT. Importantly, when measured 4 days after the last exercise training session, we could no longer detect significant changes in the abundance of any of these proteins (total or phosphorylated forms) compared with pre-training levels (Figure 4-8).

4.5 DISCUSSION

The major findings of this study were that 12 weeks of exercise training, in the absence of changes in body weight and fat mass, reduced adipocyte size, modified the composition of ECM, and increased capillarization in aSAT. Accompanying the changes in ECM and capillarization, we found some key factors that regulate extracellular matrix remodeling (MMP9), and angiogenesis (ANGPTL2) were altered in response to exercise training. Additionally, many of the modest exercise-induced changes in factors that regulate aSAT metabolism (i.e., HSL and CD36) and inflammatory pathway activation (i.e., phosphorylated P38 MAPK, JNK, and ERK1/2) were evident the day after the last session of exercise but were reversed 4 days later. Importantly, despite the robust difference in training intensity and volume, metabolic and aSAT adaptations in response to MICT and HIIT were remarkably similar.

Adipose tissue with a greater proportion of smaller adipocytes is often considered to be more metabolically favorable in terms of lower pro-inflammatory macrophage infiltration (112), lower lipolytic rates (289), and enhanced sensitivity to insulin (290, 291). Some studies have reported adipocyte size to be smaller after exercise training (202, 292, 293), perhaps contributing to the exercise-induced improvement in metabolic health. However, most of these reductions in adipocyte size after exercise training were also accompanied by a meaningful amount of weight loss, thereby confounding the interpretation of the direct effects of exercise on adipocyte size. In contrast, by intentionally requiring our participants to maintain body weight throughout the 12-week training program, we were largely able to remove this confounding influence of weight loss on the effects of exercise training on adipocyte size. We must acknowledge that despite weight maintenance in our study, the very small, non-significant reduction in whole-body fat mass (~0.5kg) may have contributed to a portion of the ~10% reduction of adipocyte size we observed after training. However, it seems unlikely that we would be

able to detect this very small change in whole body fat mass at the adipocyte-level. This is supported by our observation that the reduction in adipocyte size in our study was not related to the reduction in fat mass (R^2 = 0.005, P = 0.7), suggesting factors other than loss of body fat (e.g., formation of more adipocytes) may also underlie the reduction of adipocyte size we observed. Our findings that some of the adipogenic markers were increased after training (i.e., a trend of increase in protein abundance of FABP4 and a significant increase in protein abundance of CEBPα in HIIT) provides some support for this notion. It is unclear why CEBPα was only increased in HIIT, but perhaps, the expression of adipogenic transcription factors may be differentially regulated by exercise intensity.

The potential role of exercise on aSAT ECM is important because ECM's fibrotic content is tightly associated with obesity-induced insulin resistance (294, 295). Because changes in body fat mass are known to induce remodeling of adipose ECM (294, 295), to accurately assess the effects of exercise on aSAT ECM, once again it is critical to tightly control body weight/body fat mass during exercise interventions. To our knowledge, only one previous study has examined the effects of exercise training on ECM remodeling independent of weight loss, and it was reported that in HFD-fed mice, four-months of exercise training markedly attenuated the increase in epididymal adipose tissue fibrosis despite identical gains in body weight and body fat mass between exercised and non-exercised animals (15). In contrast, our findings suggest that three-months of exercise training without weight loss may not induce meaningful modifications in aSAT fibrosis in human subjects with obesity. We recognize that our three-month exercise interventions may have been too short to induce meaningful changes in aSAT fibrotic deposition in humans. An alternative possibility to explain the apparent discrepancy between our findings and those of Kawanishi, et al (15) is that exercise may be effective in attenuating the increased fibrotic formation that often occurs in adipose tissue with weight gain but may not be as effective in reducing existing fibrosis. Importantly, however, our observation that exercise training modestly modified the composition of the collagens in aSAT samples may have important clinical implications. Although the increase in Col5a3 abundance may seem to conflict with the notion that increased extracellular matrix deposition is negatively associated with metabolic health,

evidence suggests that Col5a3 is a crucial signaling component in glucose homeostasis (296). Huang et al reported that isolated adipocytes from epididymal fat pads in Col5a3$^{-/-}$ mice exhibited impaired glucose uptake compared with that in wild type, suggesting the critical role of Col5a3 in adipose tissue glucose metabolism. Therefore, an increased abundance of Col5a3 in response to exercise training may still reflect a metabolically favorable adaptation.

High capillary density in adipose tissue enhances the capacity for oxygen and nutrient delivery (and metabolic by-product removal), possibly preventing local hypoxia, which can lead to increased fibrosis and inflammation (62, 297). Although we found an increase in aSAT capillarization after exercise training (i.e., when expressed as number of capillaries per mm^2) – this effect was rather modest and the increase in the number of capillaries per adipocyte did not quite reach statistical significance. One previous study reported that 12 weeks of endurance exercise training significantly increased the number of capillaries per adipocyte in human aSAT(14). However, this exercise-induced increase in aSAT capillarization was only found in their non-obese, insulin-sensitive subjects (BMI: 26 $\pm$ 0.72 kg/m^2) while aSAT capillarization did not increase significantly in their insulin-resistant subjects with obesity (BMI: 35.1 $\pm$ 0.9 kg/m^2) (14). This may help explain why we did not find a more robust increase in aSAT capillarization in our subjects. It is possible that insulin resistance may blunt angiogenesis by suppressing the expression of VEGFα (298). Additionally, our finding that Angiopoietin-2 protein abundance increased after both MICT and HIIT, suggests that exercise training may upregulate components of the angiogenic pathway - but perhaps 12 weeks of exercise training was not long enough to induce a robust increase in capillarization of the hypertrophied adipocytes in adults with obesity. While our finding that Angiopoietin-1 protein abundance in aSAT did not change after MICT is consistent with the previous exercise training study in humans (14), the reduction in HIIT suggests that aSAT Angiopoietin-1 may be differentially regulated by exercise intensity, although the underlying mechanisms for this phenomenon are unclear. Accompanying our observed trend for an increase in the number of capillaries per adipocyte in our study, the modest reduction in adipocyte diameter we observed after training may represent a favorable adaptation in the context of oxygen and nutrient delivery, by reducing diffusion distance in adipocytes.

Excessive fatty acid release/mobilization from aSAT into the systemic circulation that is common in obesity often results in ectopic fat deposition in other tissues (i.e., liver, skeletal muscle, heart, etc.) which underlies many obesity-related cardiometabolic complications (180, 299). Our findings that 12 weeks of exercise training without weight loss did not alter whole-body fatty acid mobilization rate is consistent with previous reports (211, 300). Our current findings extend on these previous studies by demonstrating that the anti-lipolytic effects of insulin were also not affected by 3 months of training. We acknowledge the possibility that our dose of insulin during the clamp (40 mU/m^2/min) may have been high enough to mask potential improvements in anti-lipolytic sensitivity to insulin after training. But based on previous work (301), we do not believe this to be the case. Our observations in this study are also specific to the conditions when exercise training is not accompanied by weight loss. We previously reported that when exercise training is accompanied by weight loss, systemic fatty acid mobilization declines (12). In fact, the reduction in lipolytic rate and systemic fatty acid mobilization was identical when adults with obesity lost 12% body weight with or without exercise training (12). Therefore, it appears that changes in systemic fatty acid mobilization are particularly responsive to weight loss but not exercise training, per se. Our finding that the protein expression of ATGL in aSAT was unaltered by training aligns with the lack of change in fatty acid Ra. Although the trend of increase in aSAT HSL we found in response to training may indicate increased lipolytic capacity, this may be only relevant under conditions when energy expenditure is high (e.g., during exercise) because fatty acid mobilization rate was not different while our subjects were at rest. Interestingly, we found a transient increase in the abundance of the fatty acid transporter, CD36 in aSAT 1 day after the last training session, which supports the notion of an adaptive response to increase the capacity of lipid handling in aSAT that the subjects experience during their regular exercise sessions. However, our observation that aSAT CD36 protein abundance returned to pre-training levels 4 days after the last session of exercise suggests this adaptation is transient.

Mitochondrial biogenesis and function are often compromised in aSAT in obesity, which has been associated with metabolic disturbances (141, 302, 303). These metabolic abnormalities linked to low mitochondria density in aSAT may attributed to increased endoplasmic reticulum stress, oxidative stress, and inflammation in response to nutritional

overload (242, 304, 305). Our finding that both MICT and HIIT increased the protein abundance of COX-IV in our obese subjects expands on previous works that indicate that exercise training may promote mitochondrial function and biogenesis in adipose tissue in both lean rodents (195, 196) and non-obese humans (53, 212). Unlike many of the other regulatory proteins we measured in our aSAT samples, the increase in COX-IV persisted at least 4 days after the last exercise training session, suggesting this was more than an acute/transient adaptation. It is also notable that the increase in aSAT COX-IV abundance was similar in both MICT and HIIT despite the large difference in exercise stimulus. Although COX-IV protein abundance is commonly used as a marker of mitochondrial content, we recognize that additional studies are needed to more comprehensively determine the effects of exercise training on aSAT mitochondrial adaptations in adults with obesity.

MAPK signaling in adipose tissue has been reported to be involved in adipogenesis, inflammation, and lipolysis, raising the possibility of an active role of MAPK signaling in aSAT remodeling (163, 260, 261, 266). The only previous study to our knowledge that examined the effects of exercise training on MAPK signaling in human aSAT reported a reduced expression of genes involved in the MAPK pathway after 6 months of exercise training in healthy adults (53). In contrast, we found no change in our markers of MAPK activity (i.e., the abundance of phosphorylated forms of P38, ERK1/2, and JNK relative to the total abundance of each protein) in response to training. Moreover, the transient increase in the total protein abundance of ERK1/2 and JNK we observed the day after the last exercise session suggests a possibility of an increase in the capacity for MAPK activity in aSAT. However, this potential for increased MAPK capacity was transient since the abundance of JNK and ERK all returned to pre-training levels after 4 days without exercise.

Leptin and adiponectin are two mostly well-studied peptides released from adipose tissue (“adipokines”). Obesity is often associated with high plasma leptin concentrations and low plasma adiponectin concentrations, and while the effects of weight loss on leptin (decrease) and adiponectin (increase) concentrations are quite consistent, evidence regarding the effects of exercise training on these adipokines is equivocal. Some studies report systemic leptin or adiponectin levels increase (306, 307), decrease (308-310),

while others report no change after training (311, 312). An important confounder to the interpretation of many of these exercise studies is the change in body fat mass that often occurred during these training interventions. Our finding that 12 weeks of exercise training without weight loss significantly reduced both systemic adiponectin and leptin levels suggests that these adipokines may be regulated by training independent of weight loss. However, the underlying mechanisms that explain the reduction in both adiponectin and leptin after training are unclear.

In contrast to our hypothesis, the metabolic and structural adaptations in aSAT were remarkably similar between HIIT and MICT, despite marked differences in the exercise stimulus. This finding may suggest that even though our MICT and HIIT protocols represent two rather distinct exercise training regimens – the difference in the exercise stimulus between MICT and HIIT was not large enough to evoke meaningful differences in adaptive responses to aSAT we measured in our study. Alternatively, it is possible that adaptations stemming from the more “conventional” 45 min of continuous exercise in our MICT protocol were closely matched by the brief high-intensity stimulus during HIIT, despite nearly 70% greater energy expenditure and 50% longer exercise time in MICT vs. HIIT. Regardless, the similar adaptations in aSAT structure and factors that regulate metabolic functions between HIIT and MICT were rather modest compared with previous findings that reported metabolic improvements (i.e., increased insulin sensitivity and reduced whole-body inflammation) and functional modifications in aSAT (189, 212, 313) after exercise training. We postulate the modest changes in aSAT structure and markers of metabolic function in our study compared with these others were largely a consequence of our study design to intentionally maintain body weight during our training program to assess the effects of exercise training independent of weight loss.

Although this was a well-controlled study to compare the effects of HIIT vs. MICT on lipid metabolism and aSAT structure and function independent of weight loss in obese adults, there are some important limitations. Despite the modest modifications in aSAT structure in response to exercise training even in the absence of weight loss, we acknowledge that 12 weeks of training intervention may be too short to induce major structural and morphological modifications given that aSAT remodeling may be a slow process (27). However, our findings suggest that even 3 months of exercise training may

increase the capacity of tissue remodeling (i.e., adipogenesis, angiogenesis, ECM remodeling) and it is possible that training-induced tissue remodeling may be even more robust after longer-term training. We did not tightly control dietary composition during the 12-week training intervention and therefore cannot completely rule out the possibility that the structural and metabolic adaptations in aSAT after training may be influenced by daily variations in nutrient content and/or timing of intake. Although we note that diet composition and meal timing could have some impact on aSAT metabolism (246, 314), we closely monitored body weight fluctuations in our participants enough to know that they didn't experience wide variations in diet composition or meal timing. Also, we successfully managed participants' body weight to keep it similar to their pre-training levels during the intervention period, which we contend to be the most impactful on our outcomes (315-317). As discussed in our previous report (278), we intentionally did not match total energy expenditure or exercise time between MICT and HIIT to compare two distinct exercise prescriptions that are commonly implemented in real-life environments. This allowed us to conclude that HIIT, even with lower energy expenditure and time commitment compared with MICT induced similar adaptations in aSAT.

In summary, our findings indicate that 12 weeks of exercise training, without weight loss, induced some remodeling within aSAT, as evidenced by a reduction in adipocyte cell size, altered ECM composition, and an increase in capillarization. However, these morphological/structural adaptations in aSAT were quite modest and did not culminate in measurable changes in whole-body fatty acid mobilization, which is a major factor underlying insulin resistance in obesity (12, 318). In line with this, in previously published work from this same overall project (278), we reported neither MICT nor HIIT induced a persistent increase in insulin sensitivity after 12 weeks of training. Therefore, perhaps adaptations to aSAT must be robust enough to lower systemic fatty acid mobilization to manifest into a measurable improvement in whole-body insulin sensitivity. We acknowledge that changes to aSAT structure and function may require an exercise intervention longer than 3 months. Alternatively, perhaps the independent effects of exercise training on aSAT structure and metabolic function are relatively subtle when not accompanied by weight loss, which is known to have a robust impact on many aspects of aSAT metabolism and morphology (55, 91, 97, 272). The transient nature in the

expression of some key factors that regulate aSAT fatty acid metabolism and inflammatory pathway activation (i.e., increased the day after the last exercise training session – but returned to pre-training levels 4 days later) supports the notion that the effects of exercise on aSAT metabolic function and inflammation are largely affected by the most recent session of exercise, rather than by longer-term adaptations to exercise training. Importantly, our findings also indicate that the effects of MICT and HIIT on aSAT structure, metabolism, and inflammatory pathway were remarkably similar despite marked differences in the energy expenditure, duration, and intensity of the exercise stimulus.

4.6 ACKNOWLEDGMENT

The authors gratefully thank the contribution of the study participants. We acknowledge excellent technical assistance provided by exercise training coordinators and supervisors; Dr. Benjamin Carr, Dr. Jacob Haus, Jeffrey Wysocki, RN; the staff at the Michigan Clinical Research Unit; and all the members of the Substrate Metabolism Laboratory.

4.7 FIGURES

Figure 4-1 Schematic of study design

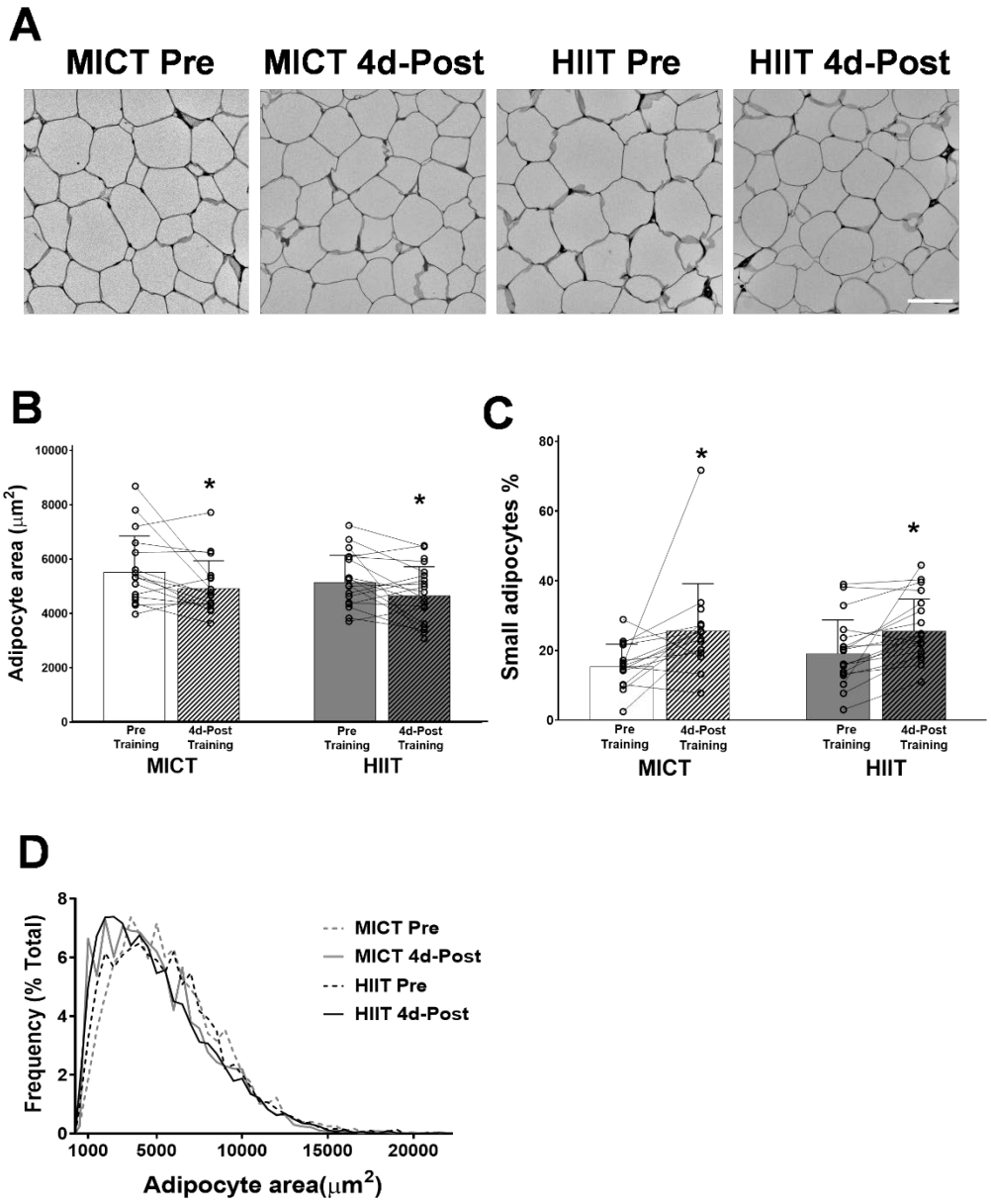

Figure 4-2 Changes in adipocyte cell size in response to training

A) Representative images of H&E stained aSAT. White scale bar refers to 100μm. B) Mean adipocyte area. C) Proportion of smaller adipocytes ($1000\mu m^2 \leq$ area $\leq 3000\mu m^2$). C) Frequency distribution of adipocyte area. Sample sizes were MICT n = 16 and HIIT = 18. *Significant main effect of training status ($p < 0.05$). ** Significant main effect of training status ($p < 0.01$). There were no significant effects of training group or training group x training status interactions.

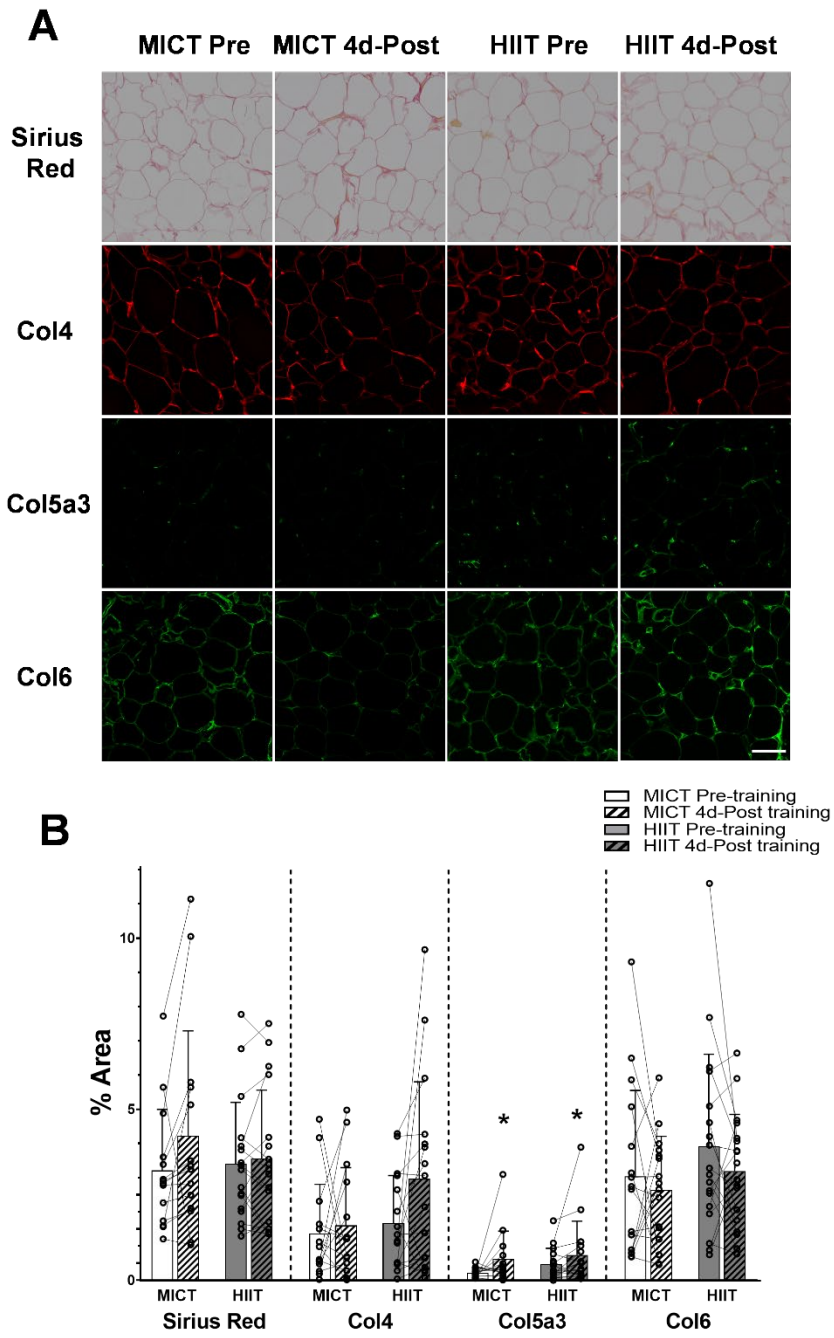

Figure 4-3 Adaptation of aSAT fibrosis and ECM proteins in response to training

A) Representative staining images of Sirius Red, Col4, Col5a3, and Col6 in aSAT section. The white scale bar refers to 100μm. B) Abundance of ECM proteins quantified from histology images. Sample sizes were MICT n = 14 and HIIT n = 17 for Sirius Red, MICT n = 14 and HIIT n = 16 for Col4 and Col5a3, and MICT n = 16 and HIIT n = 18 for Col6. *Significant main effect of training status ($p<0.05$). There were no significant effects of training group or training group x training status interactions.

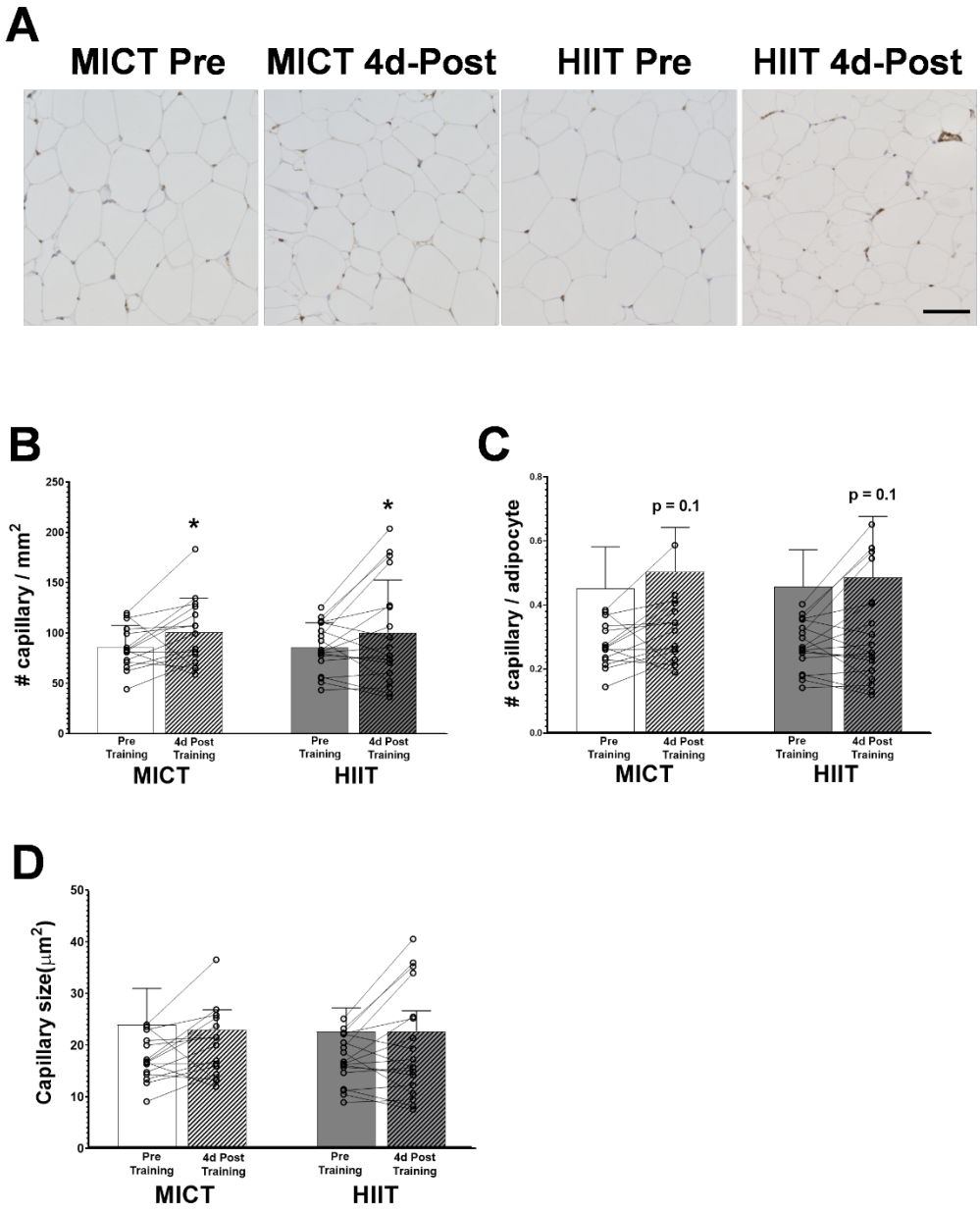

Figure 4-4 aSAT capillarization in response to training

A) Representative staining images of vWF in aSAT section. Capillaries are visible as dark-brown puncta. Black scale bar refers to 100μm. B) Number of capillaries per field area (mm^2). C) Number of capillaries per adipocytes. D) Mean capillary cross-sectional area (μm^2). *Significant main effect of training status ($p \leq 0.05$). Sample sizes were MICT n = 15 and HIIT = 18. There were no significant effects of training group or training group x training status interactions.

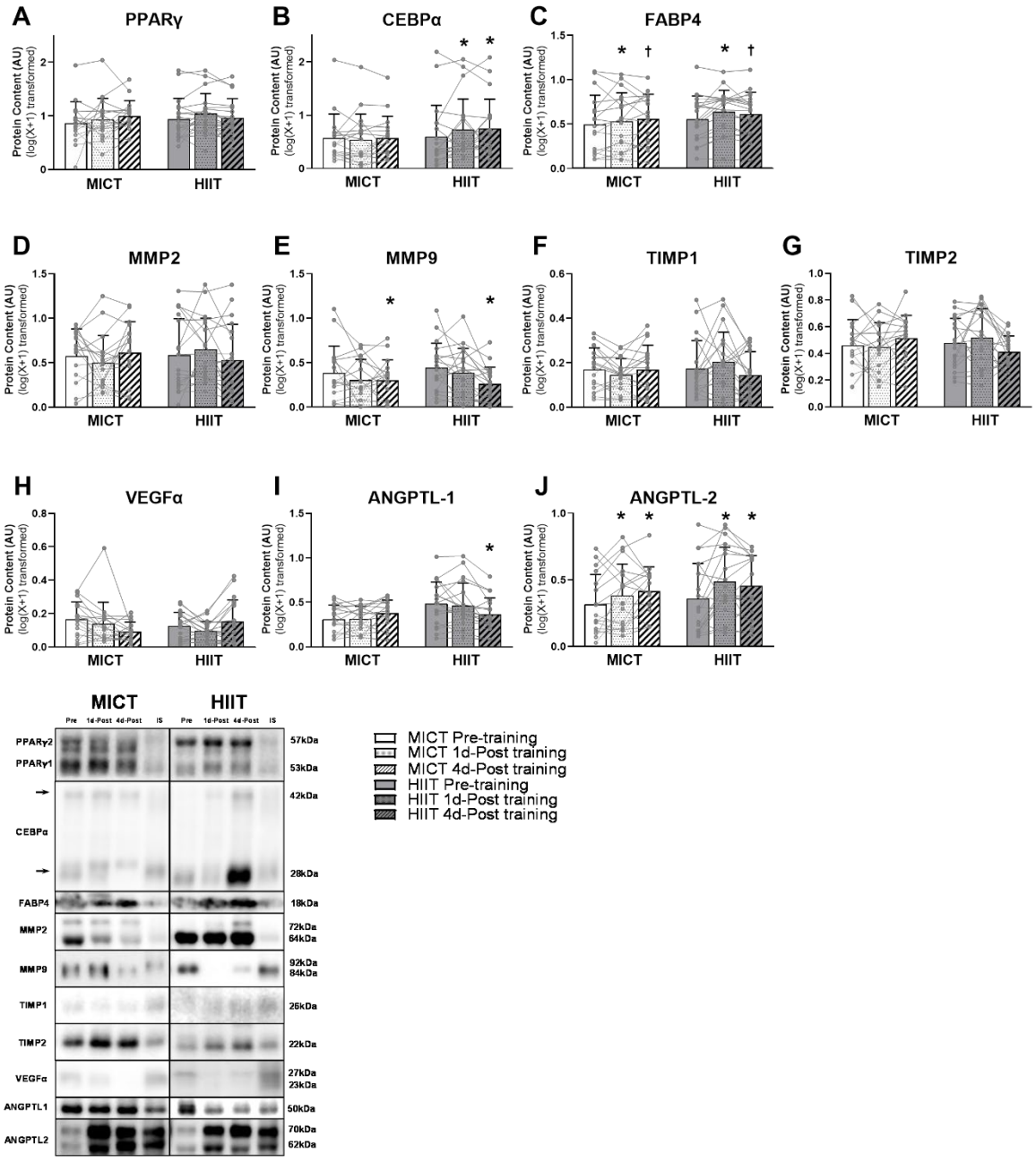

Figure 4-5 Adaptations in aSAT remodeling factors in response to exercise training

*Significant main effect of training status, with post-hoc analysis identifying a significant difference compared with Pre-training ($p<0.05$). † Trend of main effect of training status, with post-hoc analysis identifying a trend of difference compared with Pre-training ($0.05<p<0.1$). There were significant training group x training status interactions in the abundance of CEBPα ($p=0.046$) and Angiopoetin-1 ($p=0.002$).

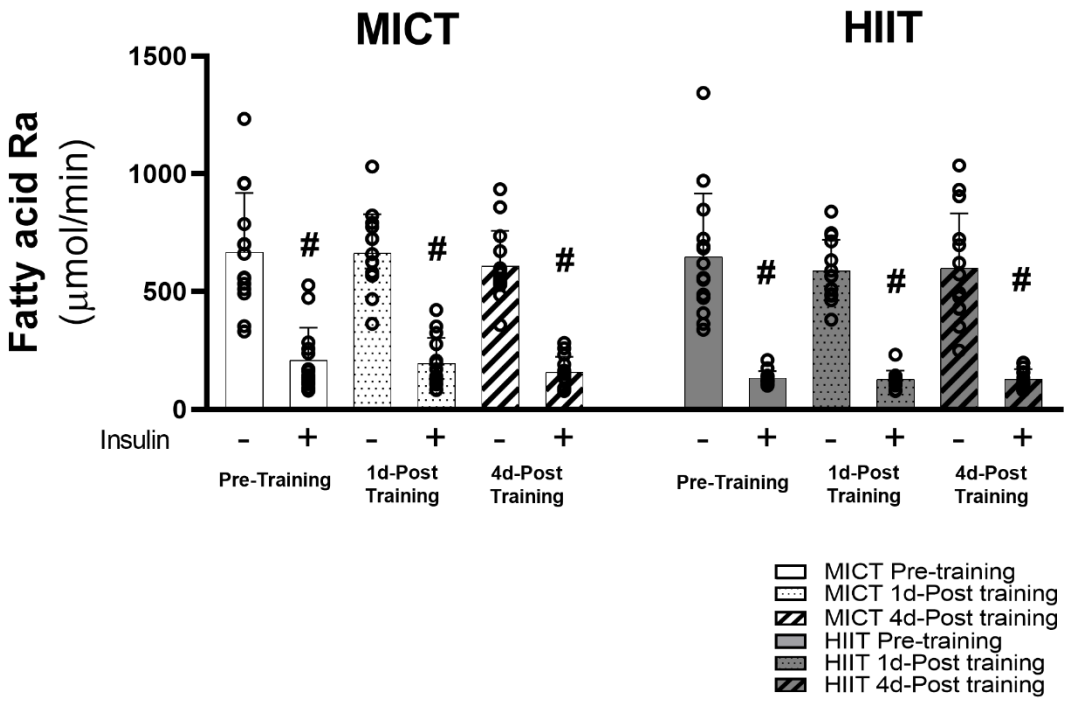

Figure 4-6 Whole body fatty acid mobilization rate in response to exercise training

Sample sizes were MICT n = 14 and HIIT = 14. Fatty acid rate of appearance in the systemic circulation after over-night fasting and insulin-stimulated conditions. #Significant main effect of insulin ($p<0.001$). There were no significant main effects of training group, training status, or training group x training status interactions.

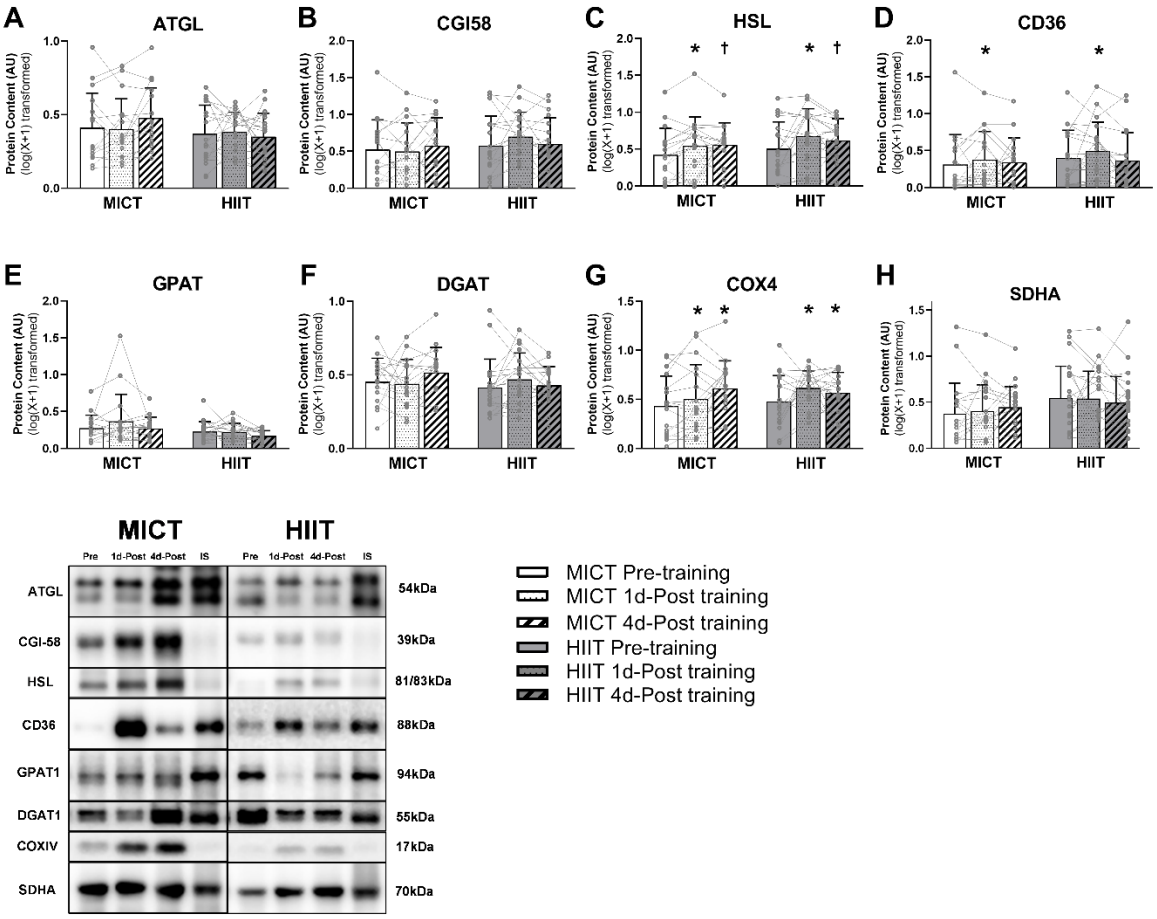

Figure 4-7 Adaptations in aSAT metabolic factors in response to exercise training

*Significant main effect of training status, with post-hoc analysis identifying a significant difference compared with Pre-Training ($p<0.05$). † Trend of main effect of training status, with post-hoc analysis identifying a trend of difference compared with Pre-Training ($0.05<p<0.1$). There were no significant main effects of training group or training group x training status interactions.

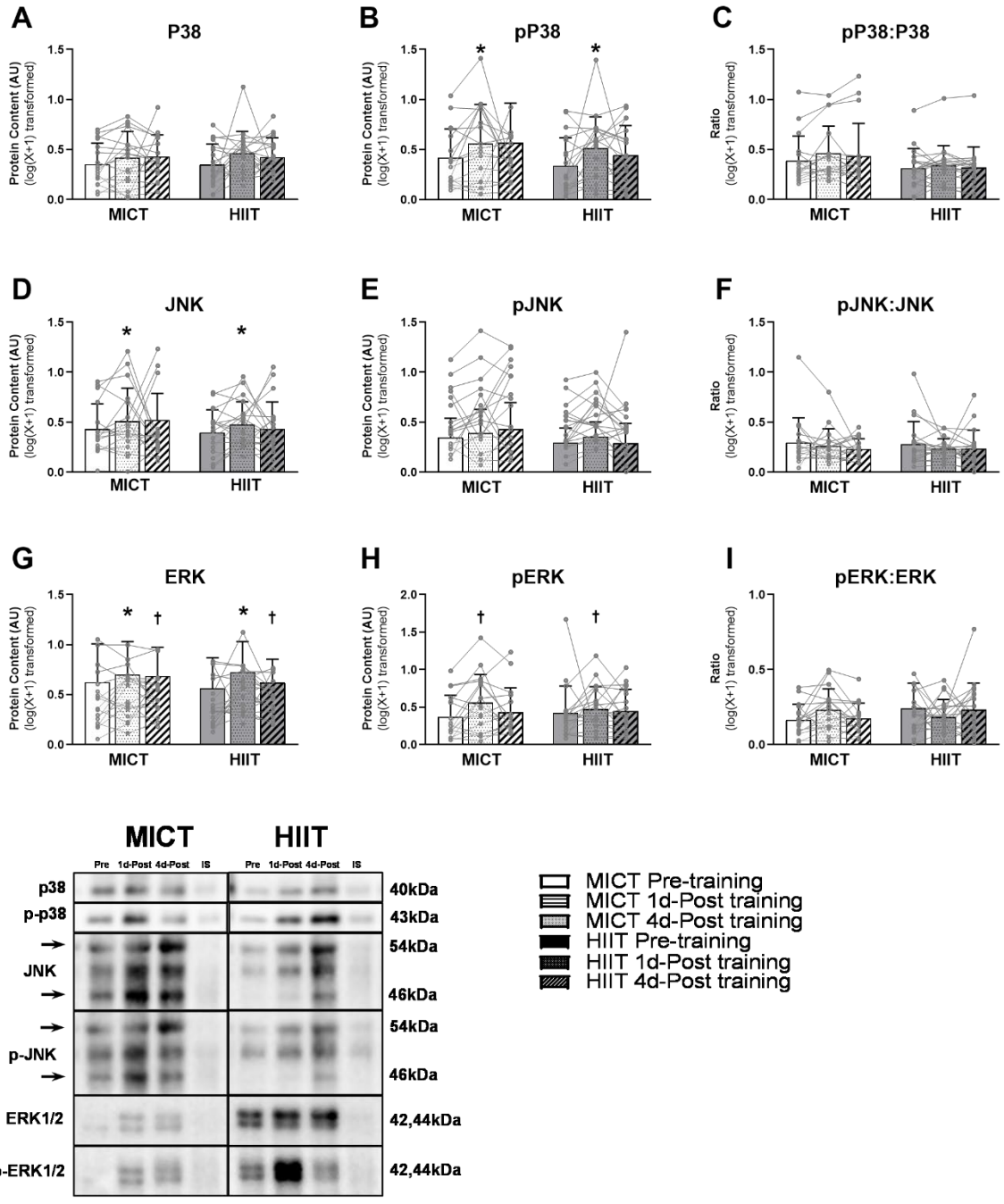

Figure 4-8 Adaptations in aSAT MAPK proteins in response to exercise training

*Significant main effect of training status, with post-hoc analysis identifying a significant difference compared with Pre-Training ($p<0.05$). † Trend of main effect of training status, with post-hoc analysis identifying a trend of difference compared with Pre-Training ($0.05<p<0.1$). There were no significant main effects of training group or training group x training status interactions

4.8 TABLES

Table 4-1 Subject characteristics and whole-body clinical biomarker measures before and after training

	MICT (n = 17)		**HIIT (n = 19)**	
Age (years)	30 ± 6		31 ± 7	
Sex	12 Women, 5 Men		12 Women, 7 Men	
Height (m)	1.71 ± 0.09		1.70 ± 0.08	
	Pre training	4d-Post Trained	Pre training	4d-Post Trained
Body mass (kg)	98.0 ± 11.6	97.6 ± 11.7	96.4 ± 13.7	96.6± 13.6
Fat mass (kg)	40.5 ± 7.1	40.1 ± 7.2	42.5 ± 7.7	42.0 ± 7.7
Fat-free mass (kg)	55.5 ± 9.3	55.6 ± 9.6	55.9 ± 10.5	56.5 ± 10.3
BMI (kg/m^2)	33.7 ± 3.2	33.4 ± 3.2	33.0 ± 2.9	33.1 ± 3.1
Body fat %	43.4 ± 6	43.1 ± 6.4*	42.1 ± 5.4	41.6 ± 5.4*
VO_2peak (L/min)	2.3 ± 0.5	2.5 ± 0.6***	2.5 ± 0.6	2.8 ± 0.6***
VO_2peak (ml/kgFFM /min)	41.9 ± 7.7	44.9 ± 7.7***	43.8 ± 6.1	48.5 ± 5.3***
Plasma fatty acids (uM)	392 ± 159	408 ± 118	433 ± 156	387 ± 122
Plasma total adiponectin (ug/ml)	4.7 ± 2.6	4.0 ± 2.3***	4.6 ± 1.9	3.9 ± 1.8***
Plasma HMW adiponectin (ug/ml)	2.6 ± 2.0	2.3 ± 1.8*	2.4 ± 1.3	2.0 ± 1.3*
Plasma leptin (ng/ml)	53.2 ± 25.1	48.5 ± 22.6*	49.0 ± 24.7	48.0 ± 27.2*

.

Chapter 5

Project 3
Effects of Years of Regular Exercise on Subcutaneous Adipose Tissue Remodeling in Adults with Overweight/Obesity

5.1 ABSTRACT

Abnormalities in the structure and metabolic function of abdominal subcutaneous adipose tissue (aSAT) underlie many obesity-related health complications. Regular exercise is known to improve cardiometabolic health in adults with overweight/obesity, but the long-term effects of regular exercise on aSAT are unclear. The primary aims of this study were to compare morphologic and proteomic differences in aSAT from adults with overweight/obesity who have exercised regularly for at least a few years (EX: ≥30min of moderate/vigorous endurance exercise, ≥4 days/week for > 2 years) vs. a well-match cohort of sedentary/non-exercisers (SED). To assess the effects of exercise independently of adiposity, histological and proteomic analyses were conducted on aSAT samples collected after an overnight fast from 16 EX (8F, 8M) and 16 SED (8F, 8M) adults with overweight/obesity (BMI: 30±3kg/m^2) who were tightly pair-matched for adiposity. Capillary density and protein abundance of the key angiogenic transcription factors, VEGFα, were significantly greater in aSAT samples from EX vs. SED ($p<0.05$). Conversely, the abundance of Col6a, and the macrophage markers CD14 and CD206, were significantly lower in EX vs SED ($p<0.05$). Global proteomics analysis revealed ribosomal, mitochondrial, and lipogenic proteins were upregulated, whereas complement and proteasomal proteins were downregulated in EX vs. SED (FDR <0.1). Moreover, phosphoproteomics indicated a greater abundance of phosphoproteins involved in protein translation, lipogenesis, and direct regulation of transcripts EX vs. SED ($p<0.01$). In exploratory *ex vivo* experiments, neo-vascular sprout density was greater in aSAT explants derived from exercisers ($p=0.01$). Additionally, lipid droplet size was larger in 3-dimensional spheroids cultured from the stromal vascular fraction isolated from

exercisers' aSAT samples, along with higher mRNA expression of lipogenic and esterification genes compared with non-exercisers ($p<0.05$). Overall, our findings suggest that regular exercise in adults with overweight/obesity favorably remodels the aSAT structure and proteomic profile in ways that may lead to improved lipid storage capacity, which can contribute to preserved cardiometabolic health.

5.2 INTRODUCTION

In adults with overweight/obesity, abnormalities in the morphology and metabolic function of aSAT are strongly linked with insulin resistance and related metabolic health complications (59, 319, 320). Some of these abnormalities in aSAT include: extracellular matrix (ECM) fibrosis, capillary rarefaction, pro-inflammatory macrophage infiltration, as well as alterations in metabolic function, such as dysregulated lipid metabolism and adipocytokine production (3, 104, 272). Importantly, some of these alterations can contribute to limiting fat storage capacity in aSAT, resulting in excessive systemic fatty acid availability that can lead to ectopic lipid deposition in other organs such as skeletal muscle and liver, which is known to underlie whole-body insulin resistance, local- and systemic inflammation and other obesity-related diseases (180). Therefore, strategies aimed at remodeling aSAT to enhance a more "healthful" storage capacity by increasing capillarization, reducing fibrotic ECM deposition and attenuating local inflammation may improve metabolic health in individuals with overweight/obesity. It is important to note that increasing the storage ***capacity*** of aSAT does not translate to increased body fat mass (this requires an energy surplus). Instead, increasing the effective storage capacity in aSAT can lower systemic fatty acid availability, which in turn can attenuate ectopic lipid deposition and tissue inflammatory pathway activation in individuals with the same amount of fat mass.

Regular endurance-type exercise is often recommended in the treatment and/or prevention of obesity-related health complications. Among the many health benefits of exercise, a growing body of evidence suggests that exercise training may induce favorable adaptations in aSAT morphology and metabolic function that may improve cardiometabolic health in adults with obesity (17, 189, 212). However, the direct effects of exercise on adaptations within aSAT are not completely understood, due in part to the profound impact that weight loss has on adipose tissue structure and function (284). As a result, the interpretation of many/most exercise training studies is confounded when exercise is accompanied by even a very modest degree of weight loss (57, 212). Additionally, although exercise training has been found to induce some modifications in aSAT even without weight loss (189, 321), limitations due to the relatively short duration of exercise interventions used in most interventional research studies (typically 3-6

months at most) may limit the detection of changes in aSAT that may take longer to manifest (27, 322). Therefore, investigating the effects of years of endurance-type exercise on aSAT, independently of adiposity, will enhance our understanding of how exercise may improve cardio-metabolic health outcomes in adults with obesity.

The main purpose of this study was to examine the effect of regular endurance exercise on aSAT structure/morphology, proteomic profile, and tissue remodeling capacity in adults with overweight/obesity. To achieve this, we conducted a cross-sectional study in which we recruited a cohort of adults with overweight/obesity who regularly participated in endurance-type exercise for at least a few years and a separate cohort of non-exercisers. Importantly, we tightly pair-matched subjects from each group for adiposity to examine exercise-induced adaptations in aSAT independent of variations in adiposity. We hypothesized that compared with aSAT from sedentary adults with overweight/obesity, aSAT from a well-matched group of regular exercisers would display distinct structural/morphological and proteomic characteristics – that may be more favorable for enhancing lipid storage capacity and lowering local and systemic inflammation.

5.3 METHODS & MATERIALS

Subjects

A total of 52 adults with overweight/obesity (BMI: 25-40 kg/m^2) were recruited for the study. Subjects completed a comprehensive behavior questionnaire and were categorized into either sedentary (n=28) or regular exerciser (n=24) based on their self-reported habitual physical activity behavior. Subjects who have been engaged in more than 2 years of at least 4 days/week of moderate to vigorous intensity aerobic exercise for >30 min were categorized as exercisers. All subjects reported having had a stable body weight at least 6 months prior to their enrollment. Eligible participants were not taking any medications or supplements known to affect their metabolism except contraceptive medications for some female participants. They did not have any history of cardiovascular or metabolic disease. All female participants were premenopausal and not pregnant or lactating. Written informed consent was obtained from all subjects before the

study. This study conformed to the standards set by the Declaration of Helsinki, except for registration in a database, and was approved by the University of Michigan Institutional Review Board.

Pair-matching strategy

16 sedentary (SED; 8F, 8M) and 16 regularly exercising (EX; 8F, 8M) adults with overweight/obesity were tightly pair matched for sex and adiposity (i.e., body fat % and fat mass) to allow pairwise comparison. Data for each of the 16 pair-matched subjects is provided in Supplementary Table 5-1. As a result, the mean difference in body fat % between well-matched SED vs EX was less than 0.7 ± 1.5% of body fat. The mean difference in fat mass was 0.01 ± 2.19kg (Figure 5-1C).

Body composition and aerobic fitness testing

Fat mass and fat-free mass were determined by bioelectrical impedance analysis (BIA, InBody, South Korea) or dual-energy x-ray absorptiometry (Lunar DPX DEXA scanner, GE, WI). The same measurement techniques were used for pair-matched SED (n=13) and EX (n=13) except for three pairs of subjects. Graded exercise testing was performed on a treadmill or a stationary cycle ergometer (Corvival, Lode, Netherlands) using an incremental exercise protocol. Modified Balke (323) protocol was used for treadmill testing, where the incline was increased by 2% every 2 min at a constant running pace. For cycle ergometer testing, the initial grade was set as 40W and was increased by 20W per minute. Testing was continued until volitional exhaustion. The rate of oxygen consumption was measured throughout this test using a metabolic cart (Max-II, Physiodyne Inc, NY) and peak oxygen uptake (VO_2peak) was determined as the highest 30-second average before volitional fatigue. Measurements of respiratory exchange ratio (RER) ≥ 1.2 and maximal heart rate (HR_{max}) ≥ 90% of age-predicted values (i.e., 220-age) were used as secondary indices to help confirm maximal effort during these tests.

Experimental trial

The night before the experimental trial, subjects ate a standardized dinner (30% of estimated total daily energy expenditure) at ~1900h and a snack (10% of estimated total

daily energy expenditure) at ~2200h. The next morning, after an overnight fast, subjects arrived at the clinical testing facility at 0700h for the experimental trial. An intravenous catheter was inserted into the antecubital vein on one arm. A baseline blood sample was collected at ~0730 h. At ~0800 h, approximately 100 mg of a core aSAT sample was collected by needle biopsy from ~10cm distal to the umbilicus, as described previously (190). The sample was immediately fixed in 10% formalin for histological analyses of adipose morphology and structure (see details below). Then, aspiration technique was used to collect another ~500mg of aSAT samples, which were snap-frozen in liquid nitrogen and stored at −80°C for later quantification of proteomes (untargeted global/phosphoproteomics and targeted immunoblots) (see details below). An additional portion of fresh aSAT samples were collected from a sub-cohort of the study participants (SED; n=24 and EX; n=19) for exploratory *ex vivo* assays. Approximately 200mg of aSAT was collected and followed the procedure for *ex vivo* angiogenesis assay (see details below). An additional ~400mg aSAT was collected and followed the procedure for *ex vivo* spheroid culture (see details below). These subjects also underwent a 2-hour oral glucose tolerance test (OGTT) following the biopsy. At ~0900 h, subjects drank a flavored solution containing 75g of glucose (Fisherbrand GTT Beverage), and blood was collected every 15 min for 2h. Blood samples were centrifuged at 2,000g at 4°C for 15 min. Serum and plasma were aliquoted and stored at −80°C until analysis for circulating factors.

Analytical procedures

Histological assessment of adipose tissue morphology and structure

The core adipose tissue samples that were fixed in 10% formalin at the time of the biopsy were later paraffin-embedded and processed (Sakura Tissue Tek TEC). Embedded samples were sectioned in 5 μm thickness by microtome (#RM2235, Leica) and placed on a microscopy slide (109508-WH, Thermofisher). Sections were prepared for staining by being deparaffinized and dehydrated with xylene and a series of ethanol as described previously (321). To minimize variance between subjects, staining was performed in a batch and all the microscopy conditions (i.e. exposure time) were kept consistent.

Adipocyte size: Sections were stained with fluorophore-conjugated Griffonia simplicifolia (GS) Lectin and mounted with an antifade medium (Prolong Gold, Thermofisher) and microscopic coverslip (2975, Corning). Images of the stained sections were taken in 10x with a widefield microscope (Keyence BZ-X700, IL, USA). Adipocyte size was determined by using Image J (NIH, USA) plugin AdipoQ (324).

Extracellular matrix fibrosis: Deparaffinized sections were stained with Picro Sirius red (#36554-8' Sigma-Aldrich) for 1 hour to determine total fibrosis in adipose tissue extracellular matrix. Sections were then rinsed with acidified water, followed by dehydration with ethanol, and mounted with xylene-based permount. To determine the abundance of subtypes of collagen fibers in the extracellular matrix which are the major components in adipose tissue extracellular matrix, we performed fluorescence immunohistochemistry (IHC). Deparaffinized sections were incubated in 0.5mM HCl-Glycine buffer (pH 3.0) at 90°C for 20 min for antigen retrieval. Sections were subsequently blocked with 3% hydrogen peroxide for 15 min and 5% normal goat serum (PI31872, Thermofisher) in PBS for 1 hour. Then the sections were incubated with primary antibodies overnight at 4°C and then incubated with appropriate secondary antibodies in dark. Sections were mounted with Prolong Gold. Images of the stained sections were obtained by Keyence BZ-X700 microscope (10x; fluorescence) and analyzed by using Image J. The proportions of each collagen were calculated by dividing the stained area by the field of view. Used primary antibodies were Col4a1 (C1926, Sigma), Col5a3 (LSC353420, LSbio), Col6a1 (ab6588, Abcam). Secondary antibodies used were AlexaFlour 488 (A11008, Invitrogen) and 647 (A21240, Invitrogen).

Capillary, innervation, macrophage (CD206+ and CD14+ Mϕ): After deparaffinization, sections were incubated in 0.5mM HCl-Glycine buffer (pH 3.0) at 90°C for 20 min for antigen retrieval. Sections were subsequently blocked with 3% hydrogen peroxide in methanol for 15 minutes, Streptavidin for 15 min, Biotin for 15 min, and 5% normal goat serum for 1 hour. For CD206+ Mϕ and CD14+Mϕ, goat serum blocking was performed overnight at 4°C and then the sections were incubated with primary antibodies overnight at 4°C. The following day, sections were incubated for 75min with a biotinylated

secondary antibody (NC9801827, Thermofisher), followed by HRP-linked streptavidin (S911, Thermofisher) for 45min. Tyramide Signal Amplification (B409533, Thermofisher) was applied to enhance the fluorescent signal for 10min. GS-lectin staining was used to stain for membrane, and nuclei were stained with Hoechst 33342 (H3570, Invitrogen). Sections were mounted with Prolong Gold. Images were taken in 10x with a fluorescent microscope (Keyence BZ-X700). Image J was used to analyze capillary and innervation density (i.e. number of capillaries per adipocytes), and macrophage abundance (i.e., CD206+ Mϕ and CD14 Mϕ per mm^2). Used primary antibodies were CD31 (#3528, Cell Signal Technology), Tyrosine Hydroxylase (P40101, Pel-Freez), CD206 (MAB25341, R&D), and CD14 (). TSA555 was used for CD31, Tyrosine Hydroxylase, and CD206 IHC, and TSA647 (B40958, Thermofisher) was used for CD14 IHC.

Untargeted global and phosphoproteomics

Liquid chromatography–tandem mass spectrometry proteomic analysis and quantification were completed by the Proteomics Resource Facility at the University of Michigan, Department of Pathology.

Protein Digestion and TMT labeling: A portion of each aspirated adipose biopsy sample (~50mg wet weight) was homogenized in ice-cold 1X RIPA buffer (89901, Thermofisher) with freshly added protease and phosphatase inhibitors (P8340, P5726, and P0044; Sigma) using two 5 mm steel beads (TissueLyser II, Qiagen, CA). Homogenates were rotated at 50 rpm for 60 min at 4°C and then centrifuged at 4°C for 3 x 15 minutes at 15,000g. Protein concentration was assessed using the bicinchoninic acid method (#23225, Thermofisher) after removing the supernatant. Samples (2µg/ul protein) were proteolyzed and labeled with TMT 16-plex (A44520, Thermofisher) essentially by following the manufacturer's protocol. Briefly, upon reduction (5 mM DTT, for 30 min at 45 C) and alkylation (15 mM 2-chloroacetamide, for 30 min at room temperature) of cysteines, proteins were precipitated by adding 6 volumes of ice-cold acetone followed by overnight incubation at -20° C. The precipitate was spun down, and the pellet was allowed to air dry. The pellet was resuspended in 0.1M TEAB and overnight (~16 h) digestion with trypsin/Lys-C mix (1:40 protease:protein; Promega) at 37° C was performed with constant mixing using a thermomixer. The TMT 16-plex reagents were

dissolved in 20µl of anhydrous acetonitrile and labeling was performed by transferring the entire digest to TMT reagent vial and incubating at room temperature for 1 hour. Reaction was quenched by adding 5µl of 5% hydroxyl amine and further 15 min incubation. Labeled samples were mixed, and dried using a vacufuge. Approximately 0.3 mg of the digest was used for high pH reversed-phase fractionation using a 90 min gradient of 50 mM Ammonium bicaronate/90% Acetontrile (Zorbax 300Extend-C18 column, 2.1x150 mm; Agilent). Ninety fractions were collected and combined into 12 fractions, dried, and reconstituted in 9µl of 0.1% formic acid/2% acetonitrile in preparation for Liquid chromatography-mass spectrometry (LC-MS/MS) analysis.

Phosphopeptide enrichment of TMT labeled samples: Remaining 1.3 mg of the TMT labeled peptides were desalted using SepPak C18 cartridge (Waters) and used for phosphopeptide enrichment using sequential metal- oxide and -affinity chromatography using TiO2 and Fe-NTA phosphoenrichment kits following manufacturer's protocol (High-Select TiO2; #A32993: and High-Select Fe-NTA phosphorinchment kit; A32992, ThermoScientific). Enriched phosphopeptides were further fractionated using an offline high pH reversed-phase fractionation kit according to the manufacturer's protocol (Pierce; Cat #84868). The fractions were immediately acidified with 10% TFA and dried.

LC-MS/MS analysis for global proteomic samples (LC-multinotch MS3): To obtain superior quantitation accuracy, we employed multinotch-MS3 (325) which minimizes the reporter ion ratio distortion resulting from fragmentation of co-isolated peptides during MS analysis. Orbitrap Fusion (Thermo Fisher Scientific) and RSLC Ultimate 3000 nano-UPLC (Dionex) were used to acquire the data. 2µl of the sample was resolved on a PepMap RSLC C18 column (75 µm i.d. x 50 cm; Thermo Scientific) at the flow-rate of 300 nl/min using 0.1% formic acid/acetonitrile gradient system (2-22% acetonitrile in 150 min;22-32% acetonitrile in 40 min; 20 min wash at 90% followed by 50 min re-equilibration) and directly spray onto the mass spectrometer using EasySpray source (Thermo Fisher Scientific). Mass spectrometer was set to collect one MS1 scan (Orbitrap; 120K resolution; AGC target 2x105; max IT 100 ms) followed by data-dependent, "Top Speed" (3 seconds) MS2 scans (collision-induced dissociation; ion trap; NCE 35; AGC 5x103;

max IT 100 ms). For multinotch-MS3, the top 10 precursors from each MS2 were fragmented by HCD followed by Orbitrap analysis (NCE 55; 60K resolution; AGC 5x104; max IT 120 ms, 100-500 m/z scan range).

LC-MS/MS analysis for phospho-proteomic samples: Q Exactive HF with EasySpray source (Thermo Fisher Scientific) and RSLC Ultimate 3000 nano-UPLC (Dionex) were used to acquire the data. 2µl of each fraction was resolved in the 2nd dimension on a nano-capillary reverse phase column (Acclaim PepMap C18, 2 micron, 75 µm i.d. x 25 cm, ThermoScientific) using a 0.1% formic/acetonitrile gradient at 300 nl/min (2-25% acetonitrile in 110 min;25-40% acetonitrile in 20 min; followed by a quick ramp up to 90% in 10 min and 10 min wash at 90% followed by 25 min re-equilibration). Mass spectrometer was set to collect one MS1 scan (Orbitrap; 120K resolution; AGC target 3x106; max IT 50 ms) followed by data-dependent MS/MS scans on the top 20 precursors were acquired (High-energy C-trap dissociation; 60K resolution; Normalized Collision Energy of 35; AGC 1x105; max IT 250 ms).

Data analysis: Proteome Discoverer (v2.4; Thermo Fisher) was used for data analysis. MS2 spectra were searched against UniProt protein database (downloaded on 2023.01.05) using the following search parameters: MS1 and MS2 tolerance were set to 10 ppm and 0.6 Da, respectively; carbamidomethylation of cysteines (57.02146 Da) and TMT labeling of lysine and N-termini of peptides (229.16293 Da) were considered static modifications; oxidation of methionine (15.9949 Da) and deamidation of asparagine and glutamine (0.98401 Da) were considered variable. Identified proteins and peptides were filtered to retain only those that passed ≤1% FDR threshold. Quantitation was performed using high-quality MS3 spectra (Average signal-to-noise ratio of 16 and <50% isolation interference). For phosphoproteomics data, the quantitation was performed using MS2 spectra.

Bioinformatics: For global proteomics, the abundance of proteins was median scaled. Differential expression analysis was conducted using the edgeR R package. Benjamini-Hochberg method was used to correct for multiple testing and a false discovery

rate (FDR) < 0.1 was applied for differential expressions. Kyoto Encyclopedia of Genes and Genomes (KEGG) pathway analysis for differentially expressed proteins was conducted by using Database for Annotation, Visualization, and Integrated Discovery (DAVID). KEGG pathway analysis for all identified proteins was conducted by using Search Tool for the Retrieval of Interacting Genes/Proteins (STRING). For phosphoproteomics, the abundance of phosphopeptides was median scaled. Imputation was performed by NAguideR (326) using *Impseq* algorithm. Differential expression analysis was conducted using edgeR R package and unadjusted P value<0.01 was used as the statistical threshold. To calculate significance score (π score), phosphoproteins that were missing phosphosite residue information were removed and π score was calculated as previously described (327). Pathway analysis on all identified phosphoproteins was conducted by using Reactome database. Kinase-substrate enrichment analysis was performed using KEA3 (328). P value<0.05 was used to determine significantly predicted kinases from differentially expressed phosphoproteins. Protein-protein interaction analysis was conducted by using Cytoscape (Institute of Systems Biology, WA, USA).

Targeted immunoblots

We used SDS-page based Western blot and capillary electrophoresis based Western blot (JESS, ProteinSimple, San Jose, CA) to measure the abundance of protein of interest in aSAT lysates. A portion of each aspirated adipose biopsy sample (~90 mg wet weight) was homogenized in ice-cold 1X RIPA buffer (89901, Thermofisher) with freshly added protease and phosphatase inhibitors (P8340, P5726, and P0044; Sigma) using two 5 mm steel beads (TissueLyser II, Qiagen, CA). Homogenates were rotated at 50 rpm for 60 min at 4°C and then centrifuged at 4°C for 3 x 15 minutes at 15,000g. Protein concentration was assessed using the bicinchoninic acid method (#23225, Thermofisher) after removing the supernatant. Samples for Western blotting were prepared in 4x Laemmli buffer, heated for 5 minutes at 95°C.

For SDS-page based Western blot, equal amounts of protein (15 ug) were loaded onto handcast gels ranging from 10 to 15%. Following separation by SDS-PAGE, proteins were transferred onto nitrocellulose membranes. Membranes were blocked for 2 hours at

room temperature and incubated with primary antibodies overnight at 4°C. After primary antibody incubation, membranes were washed and incubated with appropriate secondary antibody (#7074 or #7076, Cell Signaling Technology). All blots were developed using enhanced chemiluminescence (#1705061, Biorad or #34095, Fisher) and imaged (Fluorchem E Imager, ProteinSimple, CA). Primary antibodies used for SDS-page Western blot were Adipose triglyceride lipase (ATGL, #2138, Cell Signaling Technology), phospho-ATGL^{S406} (pATGL, a kind gift from Dr. Watt), Comparative gene identification-58 (CGI-58, ab183739, Abcam), G0/G1 switch 2 (G0S2, 12091-1-AP, Proteintech), Glycerol-3-phosphate acyltransferase 1 (GPAT1, PA5-20524, Thermofisher), Diglyceride acyltransferase 1 (DGAT1, NB110-41487, Novus Biologics), CD36 (sc-9154, Santacruz biotechnology), Fatty acid synthase (FASN, #3180, Cell Signaling Technology), Sterol regulatory element-binding protein 1(SREBP1, MA511685, Thermofisher), Ribosomal protein S3 (S3, #9528, Cell Signaling Technology), Ribosomal protein S6 (S6, #2217, Cell Signaling Technology), Total OXPHOS cocktail (NDUF8B, UQCRC2, ATP5A, and SDHB, ab110411, Abcam), Peroxisome Proliferator Activated Receptor Gamma (PPARγ, #2435, Cell Signaling Technology), CCAAT Enhancer Binding Protein Alpha (CEBPα, #8178, Cell Signaling Technology), Fatty acid-binding protein 4 (FABP4, sc-271529, Santacruz Biotechnology), Matrix metalloproteinase 2 (MMP2, #87809, Cell Signaling Technology), Matrix metalloproteinase 9 (MMP9, #13667, Cell Signaling Technology), Tissue inhibitor metalloproteinase 1 (TIMP1, #8926, Cell Signaling Technology), Tissue inhibitor metalloproteinase 2 (TIMP2, #5738, Cell Signaling Technology), Vascular Endothelial Growth Factor A (VEGFα, ab46154, Abcam), Angiopoietin 1 (HPA018816, Sigma Aldrich), Angiopoietin 2 (sc-74403, Santacruz Biotechnology), stress-activated protein kinase (SAPK)/c-Jun N-terminal kinase (JNK, #9252, Cell Signaling Technology), phospho-SAPK/JNK (Thr183/Tyr185) (pJNK$^{T183/Y185}$, #9251, Cell Signaling Technology). To normalize proteins to the total protein level, Memcode (#24580, ThermoFisher) was used to stain total protein in the membranes. To reduce gel-to-gel variability, an internal standard sample (composite aSAT lysate from 4 individuals) was also loaded on each gel for normalization.

For JESS, equal amounts of protein (0.16µg) were mixed with the Simple Western sample buffer and fluorescent mix and loaded in capillaries in 12-230 kDa JESS

separation module, 25 capillary cartridges (SW-W003). All experiments were performed on the automated JESS device by the manufacturer's instructions. Primary antibodies used for JESS were Hormone-sensitive lipase (HSL, #18381, Cell Signaling Technology), phospho-HSL (Ser565) (pHSL^{S565}, #4137, Cell Signaling Technology), phospho-HSL (Ser660) (pHSL^{S660}, #4126, Cell Signaling Technology), Protein kinase B (AKT, #9272, Cell Signaling Technology), phospho-AKT (Ser473) (pAKT^{S473}, #9271, Cell Signaling Technology), phospho-AKT (Thr308) (pAKT^{T308}, #13038, Cell Signaling Technology), p38 mitogen-activated protein kinase (P38, #9212, Cell Signaling Technology), phospho-P38 MAPK (Thr180/Tyr182) (pP38$^{T180/Y192}$, #9211, Cell Signaling Technology), p44/42 MAPK extracellular signal-regulated kinase (ERK, #4695, Cell Signaling Technology), phospho-p44/42 MAPK (Thr202/Tyr204) (pERK$^{T202/Y204}$, #4376, Cell Signaling Technology), Signal transducer and activator of transcription 3 (STAT3, #12640, Cell Signaling Technology), and phospho-STAT3 (Tyr705) (pSTAT3^{Y705}, #9145, Cell Signaling Technology).

Circulating concentrations of substrates, adipokines, and inflammatory biomarkers.

Plasma concentrations of glucose (TR-15221, ThermoFisher), plasma fatty acids (NC9517309, NC9517311; Fujifilm Medical Systems), total cholesterol (#999-02601, Wako Chemicals), HDL cholesterol (#997-01301, Wako Chemicals), triglycerides (T2449, Sigma) were assessed using commercially available kits. Serum insulin concentration was assessed using a chemiluminescent immunoassay (Siemens 1000). Plasma concentrations of total adiponectin (DRP300, R&D), high molecular weight (HMW) adiponectin (DHWAD0, R&D), and Leptin (DLP00, R&D) were assessed by enzyme-linked immunosorbent assays (ELISA). Plasma concentrations of IL1β, IL10, IL6, IFNγ, and TNFα were measured using a customized Luminex Multiplex kit (HSTCMAG-28SK).

***Ex vivo* angiogenesis assay**

Angiogenesis assay was conducted as previously described (329). Briefly, ~0.2g of core aSAT collected during biopsy was immediately stored in EGM-supplemented EBM-2 medium (CC3202, Lonza) and tissues were cut into small slices (each piece less than 1mm3) by using sterile forceps, and scalpel blades on a petri dish and embedded in

a 96 well plate with 40uL of Matrigel (356231, Corning). Embedded tissue slices were incubated at 37°C with 5% CO_2 until the harvest on day 11 post-seeding. On the day of harvesting, Z-stack images of capillary sprouts were taken by a brightfield microscope (Keyence, Japan). The sprout density was quantified by the area of sprouts relative to the area of the tissue slice using Image J.

***Ex vivo* spheroid culture**

Spheroid culture was conducted as previously described (330) with minor modifications. Briefly, ~0.5g of aspirated aSAT was stored in aMEM media (12571063, Thermofisher) upon collection. Collected aSAT was then minced with scissors until it became slurry. Slurred tissue was then incubated in a warm collagenase buffer for 50 min, followed by filtration for SVF isolation. Red cell lysis buffer was applied to remove red blood cells. Extracted SVF cells were reconstituted with endothelial growth medium-2 (EGM-2, 50306189, Thermofisher), and the cell number was counted by using a cell counter (Countess II, Life Technologies). 30,000 cells were seeded into 96 well ultra-low attachment (ULA) plates (12566490, Thermofisher) and incubated at 37ºC with 5% CO_2 with continuous horizontal shaking at a slow speed (70rpm). At day 6 post-seeding, aggregated spheroids were transferred into a 40µl matrigel droplet in 24-well low attachment plates (07200602, Thermofisher) and further incubated for 4 additional days with EGM2 media. After a total of 10 days of incubation with EGM-2 media, an adipogenic cocktail, aMEM based mixture with insulin, apotransferrin, BMP7, Fetal bovine serum, and intralipid, was applied to facilitate adipocyte differentiation. Media was changed every 2~3 days. Spheroids were collected 20 days and 27 days post-seeding.

Histochemistry: Spheroids were fixed in 4% formaldehyde and embedded in 4% agarose gel. Sections of spheroids were cut in 150µm by using a vibratome (VT1200, Leica) and placed on a microscopic slide. Sections were permeabilized in 0.2% Triton X-100 (T8787, Sigma), followed by 5% goat serum blocking for 1 hour. Primary antibody (i.e., Col6a) was applied overnight at 4°C, followed by BODIPY stain (P3922, Thermofisher) for 30min. Nuclei staining was performed with Hoechst and slides were mounted by using Prolong Gold. Capillaries were stained by using Alexa Flour 647

conjugated-Isolectin (I32450, Thermofisher) for 30min on a separate slide. 40X and 60X 30μm depth Z-stack images were acquired by a confocal microscope (Nikon A1, Tokyo, Japan). Lipid droplet and nucleus size were quantified using AdipoQ plugin in Image J. Stacked images for Col6a and isolectin were converted to a composite image by using Extended Depth of Field plugin in Image J, followed by quantification of stained area relative to the area of the spheroid area.

Spheroid mRNA expression: At least 6 spheroids from the same subject were pooled into a single Eppendorf tube on the day of harvest, dehydrated, and kept at -80°C until RNA extraction. RNA was extracted by using Qiagen Mini RNA extraction kit (74004, Qiagen). Extracted RNA (20ηg) was reverse transcribed to cDNA by using a High-Capacity cDNA RT kit (4368813; Life Technologies, Grand Island, NY). Real-time quantitative PCR with predesigned PrimeTime qPCR Assays (IDT) was used to assess the mRNA expression levels of the genes of interest. The qPCR data were normalized to the expression of two housekeeping genes, peptidylprolyl isomerase A (PPIA) and β2-microglobulin (B2M) using the −ΔCt method (331). Two samples whose housekeeping genes were undetected were removed.

Statistical analyses

Non-normally distributed data were log-transformed before statistical analysis. A paired Student's t-test was used to compare all measured variables between matched SED vs. EX cohorts. Independent Student's t-test was used to compare results from *ex vivo* assays between SED vs. EX. A two-way ANOVA linear mixed model was applied to examine the main effects of time, group, and time x group interaction effects in measured variables from spheroid culture (time; day20 vs., day27, group; SED vs., EX). Statistical analysis was done by using SPSS (Statistics for Windows, version 26.0; IBM Corp., Armonk, NY) or R (R, Vienna, Austria). P value ≤ 0.05 were considered statistically significant. Data are presented as mean ± SD unless noted otherwise.

5.4 RESULTS

Subject characteristics and whole-body clinical & metabolic biomarker measurements

Out of the 183 individuals we screened for this study, a total of 52 adults with overweight/obesity were enrolled in the study, and based on their self-reported physical activity behavior, these subjects were classified into sedentary (SED; n=28) or exerciser groups (EX; n=24) (Figure 5-1 A; Supplementary Table 5-2). From this larger cohort of subjects, we selected 16 SED (8M/8F) and 16 EX (8M/8F) who were tightly matched for adiposity (i.e., body fat% and fat mass) and who were also very similar in age, body weight, or body mass index (Figure 5-1B, C and Table 5-1). As designed, self-reported physical activity behavior (METs per week) was more than 8-fold greater in EX vs SED ($p=0.001$), and VO2peak (expressed relative to kg FFM) was also nearly 25% higher in EX vs SED ($p<0.001$) (Table 5-1). Several markers of metabolic health were also different between EX and SED (Table 5-1). For example, indices of insulin resistance at the whole-body level (HOMA-IR) and in adipose tissue (Adipo-IR) were significantly lower in EX vs SED (both $p \leq 0.05$) whereas HDL cholesterol was greater in EX compared with SED ($p \leq 0.05$). Interestingly, despite similar adiposity between groups, total adiponectin concentration was significantly higher in EX ($p<0.05$), but plasma concentrations of HMW adiponectin and leptin were not significantly different between groups (Table 5-1).

Regular exercise induced capillarization and ECM remodeling.

Adipocyte size distribution was nearly identical in EX and SED (Figure 5-2A) and mean adipocyte size was also very similar between groups (3308 ± 797 vs 2972 ± 561 μm^2, $P=0.25$). Protein abundance of PPARγ and CEBPα, which are the major transcription factors for adipogenesis (75) were not different between groups (Figure 5-2B), but we did find a strong trend ($p=0.06$) for a greater protein abundance of FABP4, a marker of adipocyte proliferation (332) in EX vs SED ($p=0.06$) (Figure 5-2B). Interestingly, capillary density in aSAT was significantly greater in EX vs SED ($p=0.03$) (Figure 5-2C), and this was accompanied by a greater protein abundance of VEGFα ($p=0.02$) (Figure 5-2D), which is commonly considered a master regulator of angiogenesis (333). In contrast,

protein abundances of other factors involved in angiogenic regulation, ANGPTL-1 and ANGPTL-2 (334), were not different between groups (Figure 5-2D). Our assessments of ECM deposition also yielded some contrasting results. For example, although pericellular fibrotic content, assessed by Sirius Red histochemistry, was not different between groups (Figure 5-2E), the abundance of Col6a (the type collagen in aSAT most commonly linked with metabolic abnormalities (105)) was significantly lower in EX vs SED ($p=0.04$) (Figure 5-2E). The abundance of some other collagen subtypes (i.e., Col4a and Col5a3) was not different between groups (Figure 5-2E). In agreement with the similar pericellular fibrotic content between groups, we did not find a statistical difference in the protein abundance of MMP-2 or MMP-9, which are key proteins involved in ECM remodeling (Figure 5-2F). However, the protein abundance of TIMP-1, one of the enzymes that directly inhibit the activity of MMPs was significantly higher in EX compared with SED ($p=0.02$), while the protein abundance of TIMP-2 was not different between groups (Figure 5-2F). Innervation density was not different between the two groups (Supplementary Figure 5-1A).

Exercise induced changes in aSAT macrophages.

Protein abundance of the adipose tissue macrophage markers, CD14 and CD206 were significantly lower in aSAT samples from EX compared with SED ($p=0.05$ and $p=0.01$ respectively) (Figure 5-3A). In contrast, some of the main MAPK proteins known to regulate inflammatory response and adipocyte differentiation in aSAT (i.e., P38, ERK1/2, and JNK) (264, 335), were not different between groups in either their total protein abundance or the abundance of the phosphorylated state of these proteins (Figure 5-3B). In addition, plasma concentrations of many key circulating pro/anti-inflammatory cytokines (IL-1β, IL-6, IL-10, IFN-γ, and TNFα) were also not different between EX and SED (Figure 5-3D).

Global/phosphoproteomics in aSAT

In our untargeted global proteomics and phosphoproteomics analyses comparing a subset of our well-matched SED (4F, 4M) and EX (4F, 4M) subjects, a total of 2536 proteins were identified, where 158 of them were differentially expressed between EX vs. SED (84 proteins were upregulated - and 74 proteins were downregulated in EX vs SED;

FDR<0.1) (Figure 5-4A). Interestingly, ribosomal and mitochondrial proteins represented the greatest proportion of upregulated proteins; out of the 84 proteins upregulated in EX vs. SED, 20 of these were ribosomal proteins and 22 were mitochondrial proteins (Figure 5-4A). Several factors that regulate fatty acid metabolism were also upregulated in EX vs. SED (e.g., ABHD5, TECR, SLC25A20) (Figure 5-4A). In agreement with our histological findings, abundance of the macrophage marker MRC2 (i.e., CD206) was lower in EX vs SED, and some complement cascade proteins (i.e., CA3, CA8), known to participate in macrophage activation, were also downregulated in EX (Figure 5-4B). Additionally, ECM proteins that are often associated with the highly fibrotic ECM (i.e., THBS1 and CLC) were downregulated in EX vs SED (Figure 5-4A). Pathway analysis based on differentially expressed proteins suggested that 'Ribosome', 'Thermogenesis', 'Oxidative phosphorylation', 'Fatty acid elongation', and 'Fatty acid metabolism' were enriched in EX, while 'Complement and coagulation cascades' and 'Purine metabolism' were enriched in SED (Figure 5-4B). Using all identified proteins (2536 proteins), rank-based pathway analysis additionally identified 'Citrate cycle', and 'Fatty acid synthesis/degradation' as significantly enriched pathways in EX and 'Proteolysis' enriched in SED (Figure 5-4C). Among the 2637 identified phosphopeptides, 96 phosphopeptides were differentially expressed between EX vs SED (36 upregulated and 60 downregulated in EX vs SED; $p < 0.01$) (Figure 5-4D). Differentially expressed phosphopeptides were ranked by significance score (Π score; a product of magnitude (logFC) and FDR) which allows the identification of robustly enriched phosphopeptides (327) (Figure 5-4E). Top Π scored phosphopeptides that were upregulated in EX included STAT5B (signal transducer and activator of transcription 5B; a transcription factor), and some RNA binding proteins (e.g., Matrin3; MATR3, AlkB Homolog 5; ALKBH5, and RNA Binding Motif Protein X-linked; RBMX) (Figure 5-4E). Conversely, PGM1 (phosphoglucomutase1), an enzyme that is involved in fatty acid synthesis by catalyzing the interconversion of G1P and G6P and EIF4EBP1, a protein translation repressor, were downregulated in EX (Fig 5-4E). Pathway analysis conducted on all identified phosphopeptides suggested half of the significantly enriched pathways in EX compared with SED were key events in post-transcriptional modifications such as 'mRNA splicing', 'Processing of Capped Intron-Containing Pre-mRNA', 'RNA polymerase II transcription

termination', and 'mRNA 3'-end processing' (Figure 5-4F). Additionally, 'Fatty acid metabolism' and 'RAC GTPase cycles' which regulate cytoskeleton reorganization and cell proliferation, were also significantly enriched in EX (Figure 5-4F). Kinase-substrate enrichment analysis predicted a total of 21 kinases based on differentially expressed phosphoproteins where 13 were predicted in EX and 8 in SED ($p < 0.05$) (Figure 5-4G, Supplementary Figure 5-2B). Predicted kinases in EX included PRKAA1 and PRKAA2, which function as the catalytic subunits of AMPK, and PRKG1 and PRKG2, which were previously reported to be involved in the regulation of the nitric oxide system in human adipose tissue (336) (Figure 5-4G). Expected enriched pathways based on the predicted kinases in EX included 'AMPK signaling', 'Regulation of lipolysis in adipocytes, and 'Adipocytokine signaling' pathways and enriched pathways in SED included 'Wnt signaling', 'PI3K-Akt signaling', and 'T-cell receptor signaling' pathways (Figure 5-4H).

Targeted immunoblot analyses in aSAT

We also measured protein abundance of specific proteins involved in key metabolic pathways, as well as to help verify some of the global proteomics findings. Aligning with our global proteomics findings regarding the upregulation of ribosomal proteins in EX vs SED, we also found protein abundance of S3 ribosome ($p=0.04$) and S6 ribosome ($p=0.05$) to be significantly greater in EX measured by immunoblot analysis (Figure 5-5A). Similarly, protein abundance of oxidative phosphorylation subunits NDFUB8 (complex I), SDHB (complex II), UQCRC2 (complex III), and ATP5A (complex V) was also significantly greater in EX ($p<0.05$) (Figure 5-5B). In contrast, we did not find a difference in the protein abundance of UCP1, a key thermogenic protein in mitochondria (Supplementary Figure 5-3A). The protein abundance of FASN ($p<0.01$) and active form of SREBP1 ($p=0.02$), which are the key lipogenic regulators were also significantly higher in EX (Figure 5-5C). Conversely, the protein abundances of esterification enzymes (i.e., GPAT1 and DGAT1) and fatty acid translocase (i.e., CD36) were not different between groups (Figure 5-5C). Protein abundance of key lipolytic regulators, ATGL, HSL, G0S2, as well as phosphorylated forms of ATGL and HSL were also not different between groups (Figure 5-5C and Supplementary Figure 5-3B). We did observe a strong trend for a greater protein abundance of CGI-58 (the primary activator of ATGL) in EX vs SED

(p=0.06; Figure 5-5C), which is in line with our global proteomics findings. We also measured the abundance of AKT, which is one of the key downstream proteins activated by insulin that regulates lipid metabolism, where we observed no difference in the protein abundance of AKT and its phosphorylation (i.e., $pAKT^{T308}$ and $pAKT^{S473}$) between groups (Supplementary Figure 5-3C). However, interestingly, $pAKT^{T308}$:AKT ratio, but not $pAKT^{S473}$:AKT, was significantly lower in EX compared with SED (p=0.01) (Supplementary Figure 5-5B). We did not observe differences in the abundance of STAT3 and phosphorylated STAT3 between groups (Supplementary Figure 5-3D).

Ex vivo functional assays reveal distinct aSAT remodeling capacity in exercisers.

Because we did not have access to fresh aSAT samples from many of the well-matched EX and SED subjects described above, our exploratory *ex vivo* (ev) experiments were conducted on fresh adipose tissue samples collected from a different sub-cohort of exercisers ("EX^{ev}"; n=19) and sedentary subjects ("SED^{ev}"; n=24) from our larger pool of recruited subjects (Figure 5-1A and Figure 5-6A). Although BMI was similar between EX^{ev} and SED^{ev}, unlike our main sub-cohorts of EX and SED subjects described above, %body fat and fat mass were lower, and fat-free mass was greater in EX^{ev} vs SED^{ev} (Table 5-2). Whole-body insulin sensitivity index (i.e., Matsuda index) and antilipolytic sensitivity to insulin assessed from the 2-hour oral glucose tolerance test (OGTT) were significantly higher in EX^{ev} (Table 5-2 and Supplementary Figure 5-4C). Intriguingly, our *ex vivo* angiogenic capacity assay demonstrated that after 11 days of incubation, the density of neo-vascular sprouts was significantly greater in aSAT explants derived from EX^{ev} vs SED^{ev} (p=0.01; Figure 5-6B), suggestive of a greater angiogenic capacity in EX^{ev}. This finding is in agreement with the greater capillary density and elevated protein abundance of VEGFα reported in our main group of well-matched EX vs SED subjects (Figure 5-2). In our 3D culture experiments, we observed evidence of active maturation of spheroids derived from the stromal vascular fraction (SVF) of fresh aSAT samples. This was demonstrated by a marked increase in lipid droplet size (Figure 5-6C) and increased mRNA expression of some key regulatory, metabolic, and inflammatory factors (e.g., CEBPα, PNPLA2, DGAT1, TNFα) between day 20 and day 27 of incubation in both EX^{ev} and SED^{ev} (main effect for time; p<0.05) (Figure 5-6D). The spheroids derived from EX^{ev}

exhibited some distinct characteristics compared with spheroids originating from SEDev, including greater lipid droplet size in EXev at both day 20 and day 27 (main effect for group; p=0.03; Figure 5-6C). In line with the larger lipid droplets in EX^{ev}, there was a strong trend for DGAT1 mRNA expression to be greater in EX^{ev} vs SED^{ev} (main effect of group; p=0.06) (Figure 5-6D). We also found that mRNA expression of SREBF1 (coding gene for SREBP) and CD11c both increased significantly between day 20 and day 27 in EX^{ev} ($p<0.01$) but not SED^{ev}. Additionally, the mRNA expression of COL1 was significantly lower in EX^{ev} than SED^{ev}. (main effect of group; p=0.02) and there was a trend of lower mRNA expression of TNFα in EX^{ev} compared with SED^{ev} (main effect of group; p=0.08) (Figure 5-6D).

5.5 DISCUSSION

Our cross-sectional study design allowed us to examine the effects of long-term regular exercise on aSAT remodeling that may contribute to improved cardiometabolic health in adults with overweight/obesity. By tightly matching our sedentary and exercise cohorts, we examined the structural and functional adaptations in aSAT in response to regular exercise independent of sex and adiposity. The major findings of this study were that even with the same degree of adiposity, aSAT from regular exercisers with overweight/obesity exhibit higher capillarization, altered ECM protein content, fewer macrophages, higher lipogenic capacity, and enhanced protein translation capacity compared with sedentary adults with overweight/obesity. Using cutting-edge ex vivo techniques, we found distinct aSAT remodeling capacity in regular exercisers by demonstrating higher angiogenic capacity in aSAT strips and higher lipid storage capacity in adipose spheroids that were generated from isolated SVF from fresh aSAT samples collected from exercisers and non-exercisers. The distinct aSAT morphology, proteomic profile, and remodeling capacity we observed in regular exercisers may contribute to their enhanced indices of cardiometabolic health.

The enlarged adipocytes commonly found in aSAT from adults with obesity often result in a relatively low capillary density in the tissue, which in turn can induce local hypoxia in aSAT along with an accompanying increase in local inflammation and fibrosis

(62, 196, 297). Although adipocyte size was similar in EX vs SED, the greater capillary density we found in aSAT from EX suggests regular exercise enhances the capacity for oxygen and nutrient delivery to their relatively large adipocytes. The greater protein abundance of VEGFα in aSAT from EX vs SED that accompanied the higher capillary density suggests regular exercise may upregulate the primary angiogenic pathway. We (17, 280) and others (337) have reported an increase in VEGFA mRNA in adipose tissue after a single session of exercise, suggesting the adaptive increase in aSAT angiogenesis with exercise training is triggered after each session of exercise. Further evidence for an exercise-induced enhancement in the regulation of angiogenesis in adipose tissue stems from our kinase-substrate enrichment analysis indicating that PRKG-1 and -2 (key mediators of nitric oxide signaling that regulate angiogenesis) were predicted to be enriched in EX (338). Moreover, the greater density of capillary sprouts in aSAT explant samples from EX^{ev} vs SED^{ev} in our *ex vivo* angiogenesis experiments further supports the notion of a robust enhancement in angiogenic capacity with regular exercise. Although previous work suggests that each session of exercise may trigger an increase in angiogenic pathway activation (189, 280), the number of weeks or months of exercise training required before a measurable increase in capillarization in aSAT from adults with overweight/obesity can be detected remains uncertain. To our knowledge, only two previous studies have examined the longitudinal effects of exercise training on adipose tissue capillarization in humans (including Project 2), and even only a few months of exercise training appear to modestly increase capillarization in some subjects (14, 321). Walton et al., (14) reported that 3 months of aerobic training increased aSAT capillary density in healthy, lean subjects, however, 3 months of training did not result in a detectable increase in aSAT capillarization in subjects with obesity and insulin resistance. In Project 2 (321), we found 3 months of exercise training increased capillary density per tissue area in adults with obesity, but the number of capillaries per adipocyte did not change significantly. The cross-sectional design of the present study expands on these earlier findings by suggesting a more prolonged exposure to exercise training may be necessary to detect an increase in capillarization in adults with overweight/obesity.

Remodeling the fibrotic content and/or composition of aSAT ECM can improve the metabolic function of the tissue and attenuate inflammation that is common in

overweight/obesity (104). Our finding that pericellular ECM fibrotic content (as measured by Sirius Red) was similar in EX vs SED is in contrast to some earlier work reporting that endurance exercise can reduce excessive fibrotic protein accumulation in adipose tissue (57, 339). However, the reduction in ECM proteins reported in participants in some of these previous exercise studies (57, 339) may be due at least in part to their modest reduction in body fat, which is known to reduce ECM protein content (284, 340). Importantly, even in the absence of reduced fibrotic content in aSAT, modifications in the relative abundance of different types/subtypes of fibrotic proteins can also impact metabolic function and the inflammatory profile within adipose tissue (105, 296). For example, a relatively high abundance of Col6a and THBS1 has been linked with metabolic dysregulation in aSAT and poor cardiometabolic health outcomes (99, 319), and deletion of Col6a has been found to improve lipid storage capacity in adipose tissue, which in turn led to protection against the development of insulin resistance in obese rats (105). Therefore, our observation of lower Col6a and THBS1 in aSAT from EX vs SED suggests that regular exercise may induce favorable adaptations to the composition of aSAT ECM. Additionally, although some of the key ECM regulators such as MMPs were not different between EX and SED, our finding of higher TIMP1 in EX suggests regular exercise may regulate collagen degradation pathways in aSAT.

The fibrotic content and composition of aSAT ECM is intimately linked with adipose tissue macrophages (ATM), whereby the ECM has been found to be involved in the recruitment and infiltration of ATMs (105, 340), as well as phenotypic switching of ATMs from anti-inflammatory M2 to pro-inflammatory M1 type (340, 341), while ATM accumulation within aSAT can drive further ECM synthesis (109). Our finding that the pro-inflammatory ATM marker, CD14 was lower in EX vs. SED aligns with several previous studies (56, 342) demonstrating an exercise training-induced reduction in M1 macrophage abundance in aSAT. However, our observation that the anti-inflammatory ATM marker, CD206 was also lower EX vs SED conflicts with some previous studies (56, 201, 215). Factors underlying this discrepancy are unclear, but our observation that both pro- and anti-inflammatory ATMs were lower in EX vs SED may be indicative of an immunosuppressive role of regular exercise in aSAT of our subjects. The downregulated complement system proteins such as C3 and C8, that we observed in EX vs SED reflect

the lower overall ATM infiltration because complement system promotes the clearance of damaged cells by macrophages (343). Interestingly, circulating C3 has been reported to augment insulin secretion (344), and because adipose tissue is a main source of circulating C3 (along with the liver), perhaps, a lower C3 production by aSAT may contribute to the lower fasting insulin concentration we observed in EX. Although our measurements suggest regular exercise may attenuate some inflammatory pathways in adipose tissue, this did not manifest in lower systemic inflammation, as indicated by similar concentrations of circulating cytokines in EX vs SED. This supports the notion that ATM may not always be an accurate predictor of systemic inflammation, but rather they may be primarily involved in aSAT remodeling (268).

The exercise-induced morphological adaptations we observed, such as increased capillarization, lower Col6, and ATM are particularly intriguing because these adaptations can enhance the capacity for fatty acid storage and release, which are the primary functions of aSAT, and these processes are often poorly regulated in obesity (180). Lipid storage in aSAT requires the esterification of fatty acids to form triacylglycerol (TAG), and although we did not find the main esterification proteins, GPAT1 and DGAT1, to be different between EX and SED, we cannot rule out the possibility that esterification activity could still be modified independently of protein abundance (345). For fatty acids to be released from the TAGs stored in aSAT, fatty acids must be hydrolyzed from TAG (i.e., lipolysis), but neither the total protein abundances of the main lipases ATGL and HSL nor the phosphorylated state of these proteins were different in aSAT from EX and SED. Interestingly, the observation that phosphorylated forms of ATGL and HSL were not lower in EX vs SED despite lower circulating insulin in EX, along with the lower abundance of phosphorylated AKT (AKT^{T308}), an insulin-activated downstream kinase that is instrumental in the potent insulin-mediated reduction in lipase phosphorylation/activity, may reflect a greater antilipolytic sensitivity to insulin of aSAT in EX vs SED. Additionally, even though we found regular exercise did not increase markers for the density of sympathetic nervous system innervation, the strong trend for a greater abundance of the ATGL co-activator, CGI-58 in EX vs SED along with increased capillarization suggests regular exercise may ‘prime’ aSAT for more effective release of fatty acids when

stimulated (e.g., exercise-induced catecholamine). Thus, regular exercise may modestly modify aSAT for a more effective release of fatty acids.

Fatty acid biosynthesis pathways had the highest enrichment score for EX vs SED in our ranked KEGG analysis, and although most de novo lipogenesis (DNL) occurs in the liver (346), DNL does play an important role in adipose tissue. In contrast to the liver, where DNL is commonly found to be elevated in obesity, adipose tissue DNL is often reported to be lower in individuals with obesity (347, 348). Importantly, low rates of DNL in adipose tissue have been linked with insulin resistance (349), perhaps via reduced formation of insulin-sensitizing fatty acids such as palmitoleate and fatty acid esters of hydroxy–fatty acids (350, 351). Our finding that the abundance of the key lipogenic proteins FASN and the active form of SREBP1 were greater in EX vs SED suggests the possibility of a favorable training-induced adaptation on factors regulating DNL. Enhanced oxidative function in aSAT has also been identified as an important adaptive response to exercise training that may improve metabolic health by combating cellular stress common in overweight/obesity (242, 304). Our findings that the abundance of several mitochondrial proteins was greater in aSAT from EX vs SED suggests favorable adaptations in aSAT mitochondria (i.e., potentially enhanced oxidative capacity) in response to regular exercise, which agrees with Project 2 (321) and others (53, 212). The underlying mechanism for mitochondrial biogenesis in aSAT in response to exercise is not clearly understood, but the high ATP requirements for TAG/fatty acid futile cycling that occurs with repetitive exercise sessions may help drive this adaptation (352). Elevated TAG/FA futile cycling in response to exercise also aligns with findings from our kinase-substrate enrichment analysis predicting that the AMPK-signaling pathway was enriched in aSAT from EX vs SED because energy costs of re-esterification have been found to increase AMPK activation in adipose tissue (353). Similarly, the high energy costs of TAG re-esterification may have contributed to our finding that the thermogenic pathway was enriched in EX vs SED. However, it is important to acknowledge that the upregulated thermogenic pathway along with the downregulated purine metabolism pathway (which was also found in our proteomic analysis) have been linked with increased energy dissipation in the context of adipose ‘browning’ (354). Although many studies performed in rodent models report increased brown or beige/brite adipose tissue

in response to exercise (222, 355, 356), most human studies do not (53, 199, 357), and our finding that protein abundance of UCP1 was not different in EX vs SED further supports this.

Protein translation is the fundamental biological process that allows the cells to respond to stress or metabolic perturbation by generating the proteins that are needed to react against or adapt to the stimuli, and ribosomes play a critical role in this process by regulating protein translation (358, 359). The robust upregulation of ribosomal proteins we found in EX vs SED is in agreement with some previous work (53, 360) suggesting that regularly performed exercise may enhance protein translation capacity in aSAT. In turn, enhanced translational capacity may underlie the increased capillary structure, mitochondrial biogenesis, and metabolic proteins we observed in aSAT samples from our exercisers, similar to that found in exercise-trained skeletal muscle (361). The potential exercise-induced increase in translational capacity in aSAT is further supported by our observation that the phosphorylation of translation repressor protein EIF4EBP1 was downregulated in aSAT from EX vs SED The lower phosphorylation of EIF4EBP1 in EX vs SED is also intriguing because EIF4EBP1 is a key mediator of adipose tissue development and energy homeostasis. Our findings from the pathway analysis conducted on the phosphoproteomic data suggest the altered post-transcriptional regulation in EX vs SED, may extend beyond the translation machinery and encompass direct regulation of transcripts. We observed upregulated phosphorylation of numerous RNA binding proteins (RBP) (e.g., MATR3, RBMX, RBM14, etc), which form ribonucleoprotein complexes that can directly regulate transcripts by splicing pre-mRNA or adenylating mRNA (362) in aSAT from EX vs SED, suggesting enhanced post-transcriptional modification capacity in aSAT by regular exercise. For example, RBMX was recently described as the most interactive RBP that induces alternative splicing in more than 200 RNAs (363) and emerging evidence reports numerous RBPs in adipose tissue can promote adipogenesis and alter metabolic function via RNA stabilization or alternative splicing (364). Although the roles of most of the differentially expressed RBPs we found in aSAT from EX and SED are yet to be elucidated, our findings provide insights into the vast modifications that may link cellular modulation with the chronic aSAT remodeling we observed from our EX.

Bioengineered 3-dimensional spheroids cultured from adipose tissue SVF, whose structure resembles that of *in vivo* adipose tissue, have recently been suggested as an alternative system to model the progression of obesity (330, 365). To our knowledge, this is the first time the spheroid model has been used to compare adipose tissue remodeling capacity in adults with overweight/obesity whose exercise status and metabolic characteristics were distinct. Our finding that spheroids derived from regular exercisers exhibited larger lipid droplets and higher expressions of esterification (DGAT1) and lipogenic (SREBF1) genes, suggests they may have a higher lipid storage capacity than spheroids from non-exercisers. Although we did not find a difference in VEGFα, ANGPTL-2, and -4 mRNA expressions between spheroids derived from exercisers vs non-exercisers (which may have been attribute to the fact that spheroids were not given endothelial cell growth stimulation after initial SVF aggregation period), our finding of lower TNFα and COL1A mRNA expression in spheroids from the exercisers aligns with the notion that regular exercise may attenuate local inflammation and ECM deposition in aSAT. The distinct characteristics of spheroids cultured from the SVF of exercisers vs non-exercisers in this *ex vivo* experiment appear to parallel some functional differences observed *in vivo*. For example, signs for greater lipid storage capacity and lower inflammatory stress that we observed in spheroids from the exercisers vs. sedentary may reflect *in vivo* aSAT milieu that is often associated with improved insulin sensitivity (105, 366). This may be associated with, or even underlie the enhanced antilipolytic response to insulin we observed *in vivo*, where the liberation of fatty acids during the OGTT was lower in exercisers vs sedentary despite lower plasma insulin concentrations during the test.

Although the cross-sectional design of this study provided the only truly feasible approach to assess adaptations to adipose tissue after years of exercise training, it is important to acknowledge some of the limitations inherent to cross-sectional studies. In our exercise cohort, although all subjects regularly performed endurance-type exercise, we did not control for factors such as the intensity, frequency, mode, or duration of their routine exercise sessions, and other than requiring they consistently engaged in an endurance exercise program for at least 2 years, we did not include an upper-limit to the number of years these subjects had been training. Additionally, while our rigorous

strategy to tightly match our EX and SED cohorts for adiposity helped reduce the influence of what would be a major confounder to the interpretation of the effects of years of exercise on aSAT adaptations, this approach may have also introduced some selection bias. For example, people who have engaged in regular exercise for several years, yet still retain a relatively high body fat mass may have some metabolic/physiologic alterations compared with non-exercisers with the same degree of adiposity. Also, we did not preserve fresh aSAT samples from all of our well-matched cohorts of EX and SED subjects for our *ex vivo* experiments, and the subjects used for these *ex vivo* experiments were not as well-matched for adiposity. However, secondary analysis from angiogenesis assay on a subset of 7 EX^{ev} and 7 SED^{ev} subjects who were well-matched for adiposity, indicated the sprout density was still statistically higher ($p=0.01$) in EX^{ev} vs SED^{ev}, corroborating the notion that increased angiogenesis in aSAT may be an exercise-induced adaptation independently of adiposity. The intriguing findings from our 3-dimensional spheroid experiments suggest adipose tissue remodeling capacity in exercisers vs sedentary may parallel some differences in metabolic profile observed between these groups *in vivo*, yet these preliminary findings are not conclusive. Follow-up studies examining functional outcomes in the spheroids (e.g., antilipolytic response to insulin) are warranted to more thoroughly assess whether spheroids cultured from adipose tissue SVF from exercisers and non-exercisers recapitulate the tissue and whole-body metabolic profiles of the donor.

In summary, our findings indicate that adults with overweight/obesity who exercised regularly for at least a few years exhibit structural and proteomic remodeling in aSAT, as evidenced by higher capillarization, altered ECM contents, fewer ATM, upregulated proteins/phosphoproteins involved in metabolism (lipogenesis, fat storage and release, and oxidative phosphorylation), protein translation, and post-transcriptional modifications. Moreover, our *ex vivo* experiments suggest regular exercise may enhance adipose tissue remodeling capacity. Our work expands the understanding of the sustained role of exercise on aSAT structure and metabolic function, which is often limited by relatively brief exercise interventions in most longitudinal studies (212) or confounding covariates (sex and adiposity) that can significantly influence aSAT function and metabolism (284, 367). Additionally, our findings suggest that altered protein translation

capacity and transcript regulation capacity in aSAT may be induced by regular exercise, and this may underlie the proteomic and functional remodeling of aSAT. Overall, we contend that although some early modifications in aSAT may be induced after a few weeks or months of endurance exercise training (212, 321, 368), more impactful, chronic adaptations to aSAT structure, function, and proteomic profile may require consistent exercise for much longer to manifest and further contribute to improved and/or preserved cardiometabolic health.

5.6 ACKNOWLEDGEMENT

The authors gratefully thank the contribution of the study participants. We thank the Proteomics Resource Facility at the University of Michigan for their excellent technical assistance. We acknowledge the excellent clinical and technical assistance provided by all the members of the Substrate Metabolism Laboratory.

5.7 FIGURES

Fig 1A

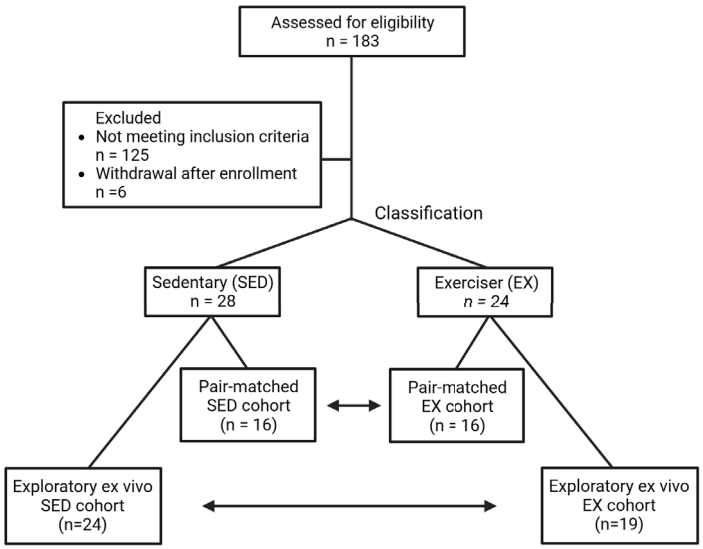

Fig 1B

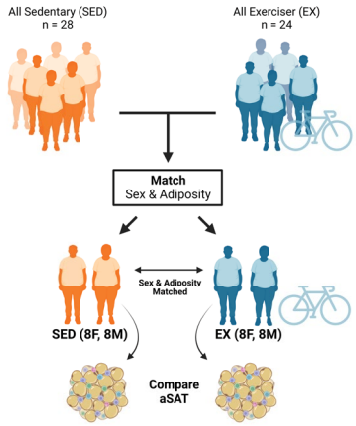

Fig 1C

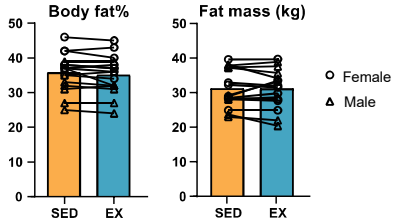

Figure 5-1 CONSORT diagram and study design

A) CONSORT diagram of the study. B) Schematic of study design. C) Body fat % and fat mass comparison between well-matched pairs of SED and EX subjects. Matched pairs are shown with connecting lines. Female (○) and male (Δ).

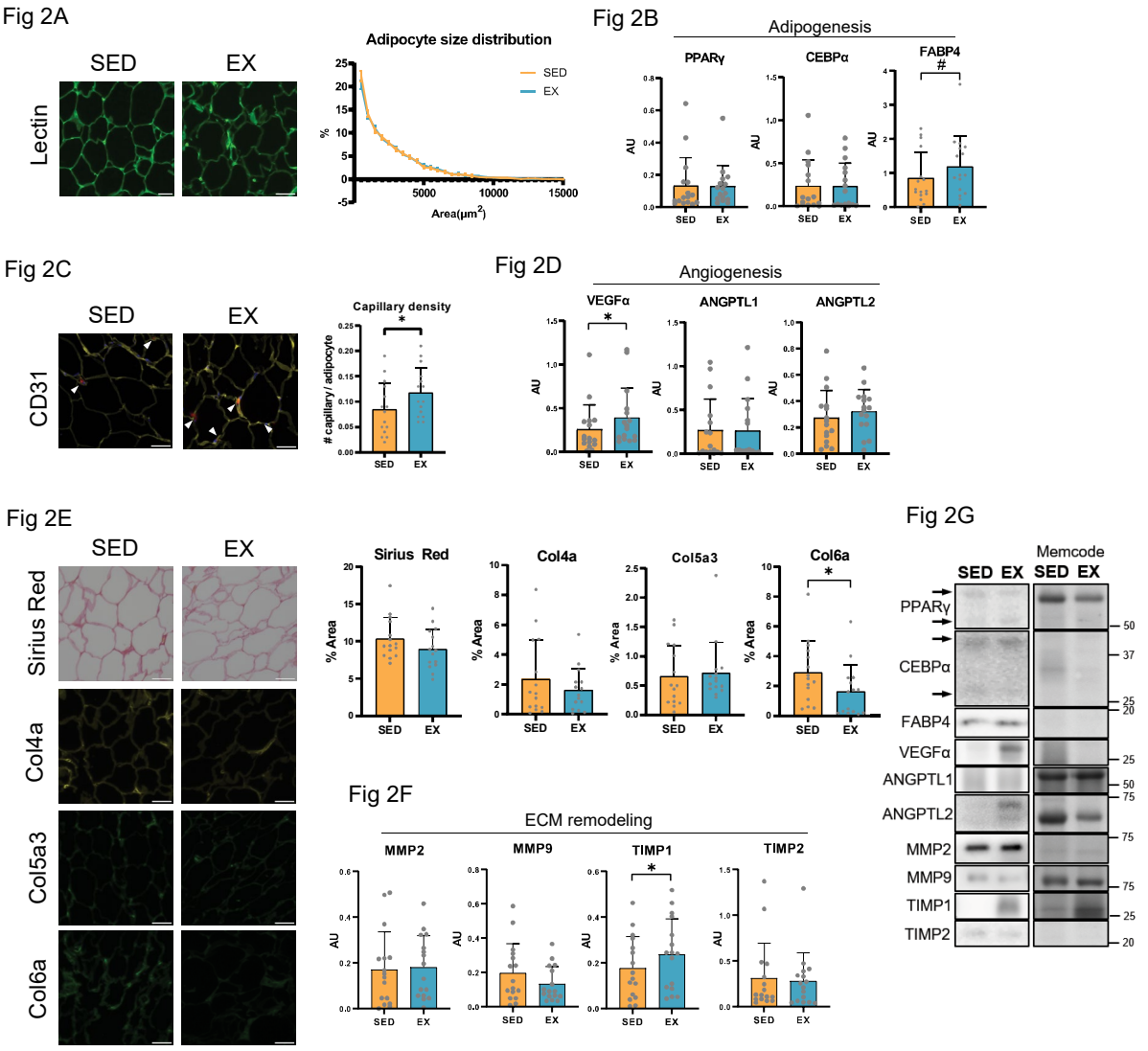

Figure 5-2 Structural and morphological comparison of aSAT in SED vs EX

A) Representative images of adipocyte membrane in aSAT section stained by GS-lectin, and histogram of adipocyte area distribution. B) Protein abundance of factors that are involved in adipogenesis and cell proliferation. C) Representative images of CD31 in aSAT section, and quantification of capillary density (number of capillaries per adipocyte). D) Protein abundance of factors that are involved in angiogenesis. E) Representative images of Sirius Red, Col4a, Col5a3, and Col6a in aSAT section, and quantification of their abundance (% positive stain area relative to section area). F) Protein abundance of ECM regulators. White scale bars indicate 50μm. *p<0.05. Immunoblot data was visualized after log(X+1) transformation. SED: n=15 and EX: n=15. AU; Arbitrary Units.

Fig 3A

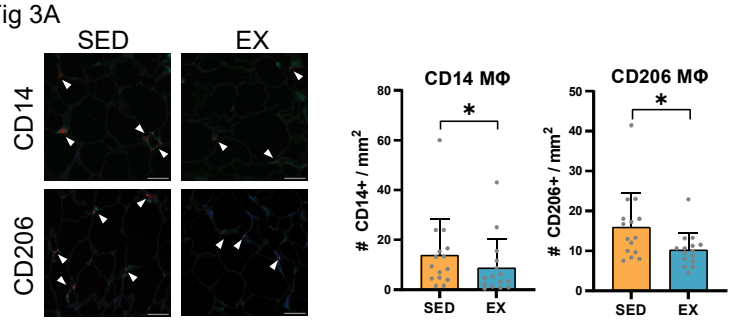

Fig 3B

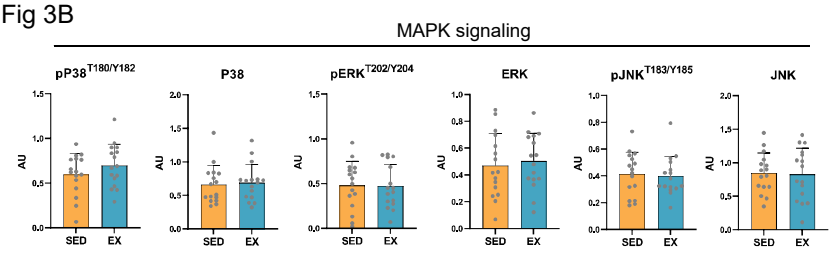

Fig 3C

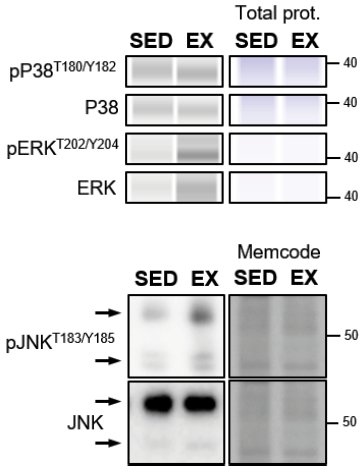

Fig 3D

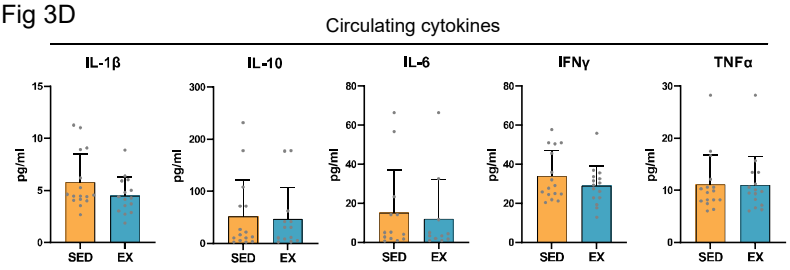

Figure 5-3 Comparison of macrophage and inflammatory pathway in aSAT and circulating inflammatory markers in SED vs EX

A) Representative images of CD14+ Mϕ and CD206+ Mϕ in aSAT section, and quantification of their abundance (number of Mϕ per field area (mm^2)). SED: n=15 and EX: n=15. B) Protein abundance of key MAPK proteins. SED: n=16 and EX: n=16. C) Representative blots of key MAPK proteins. D) Circulating cytokine abundances. Because some cytokines were not detected in a few samples, sample sizes for IL-1β, IFN-γ, and TNFα were SED: n=16 and EX: n=15; sample sizes for IL-10 were SED: n=15 and EX: n=13, and sample size for IL-6 were SED: n=13 and EX: n=11. MAPK; Mitogen-activated protein kinases. Mϕ; Macrophage

Fig 4A

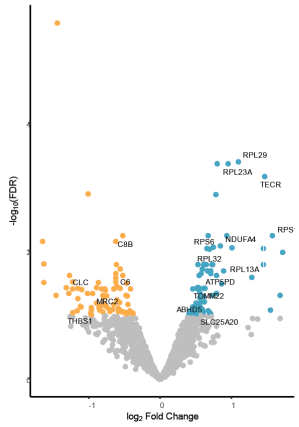

Fig 4B

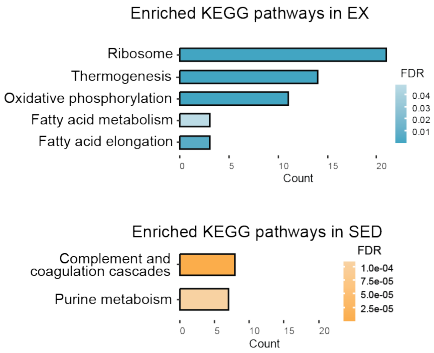

Fig 4C

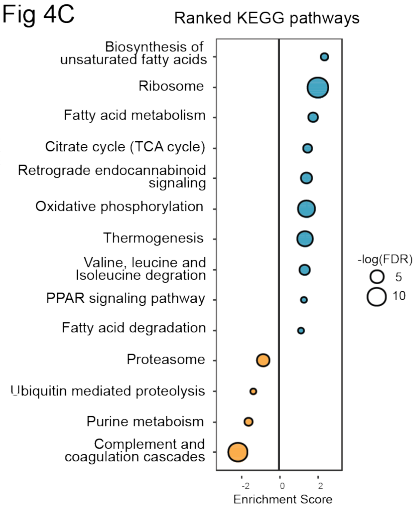

Fig 4D

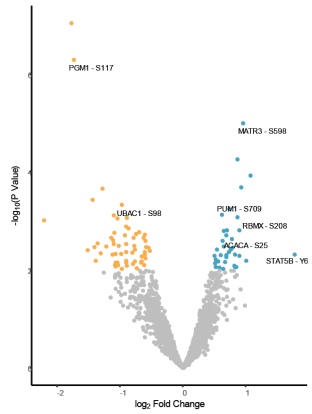

Fig 4E

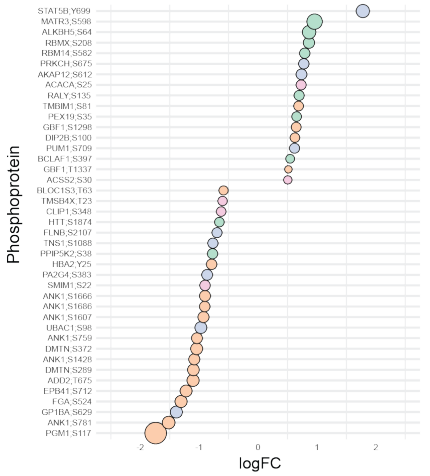

Fig 4F

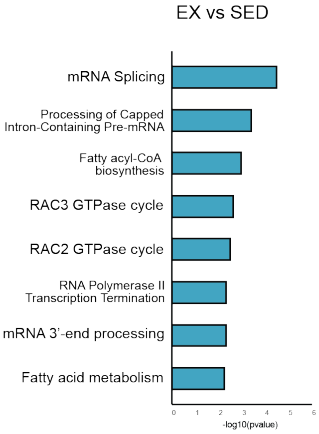

Fig 4G

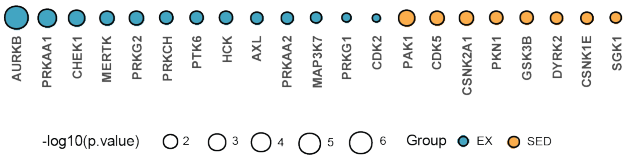

Fig 4H

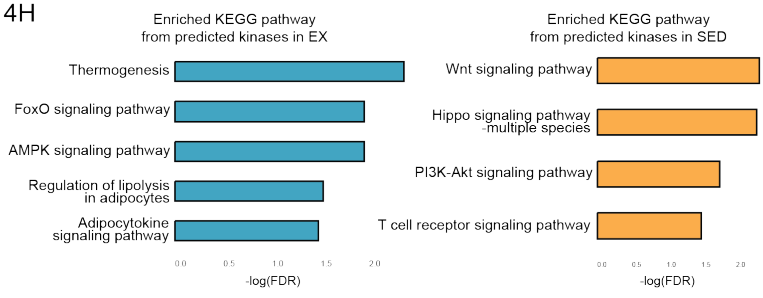

Figure 5-4 Comparison of aSAT proteomes by untargeted global/phosphoproteomics in SED vs EX

A) Volcano plot of differentially expressed proteins (FDR<0.1). B) KEGG pathway analysis conducted on differentially expressed proteins (n=158) between SED vs. EX. (FDR < 0.05). C) KEGG pathway analysis conducted on all identified proteins (n=2536). (FDR < 0.05). D) Volcano plot of differentially expressed phosphoproteins (p value<0.01; corresponding FDR≤0.25). E) Significance score based on fold change and FDR of the 41 differentially expressed phosphosites. F) Reactome pathway analysis conducted on all identified phosphoproteins showing enriched pathways in EX relative to SED. (p < 0.01). G) Kinase enrichment analysis of the differentially expressed phosphoproteins. (p < 0.05). H) KEGG pathway analysis conducted on predicted kinases (p < 0.01). Samples sizes - SED: n=8 and EX: n=8. FDR; False Discovery Rate.

Fig 5A

Fig 5B

Fig 5C

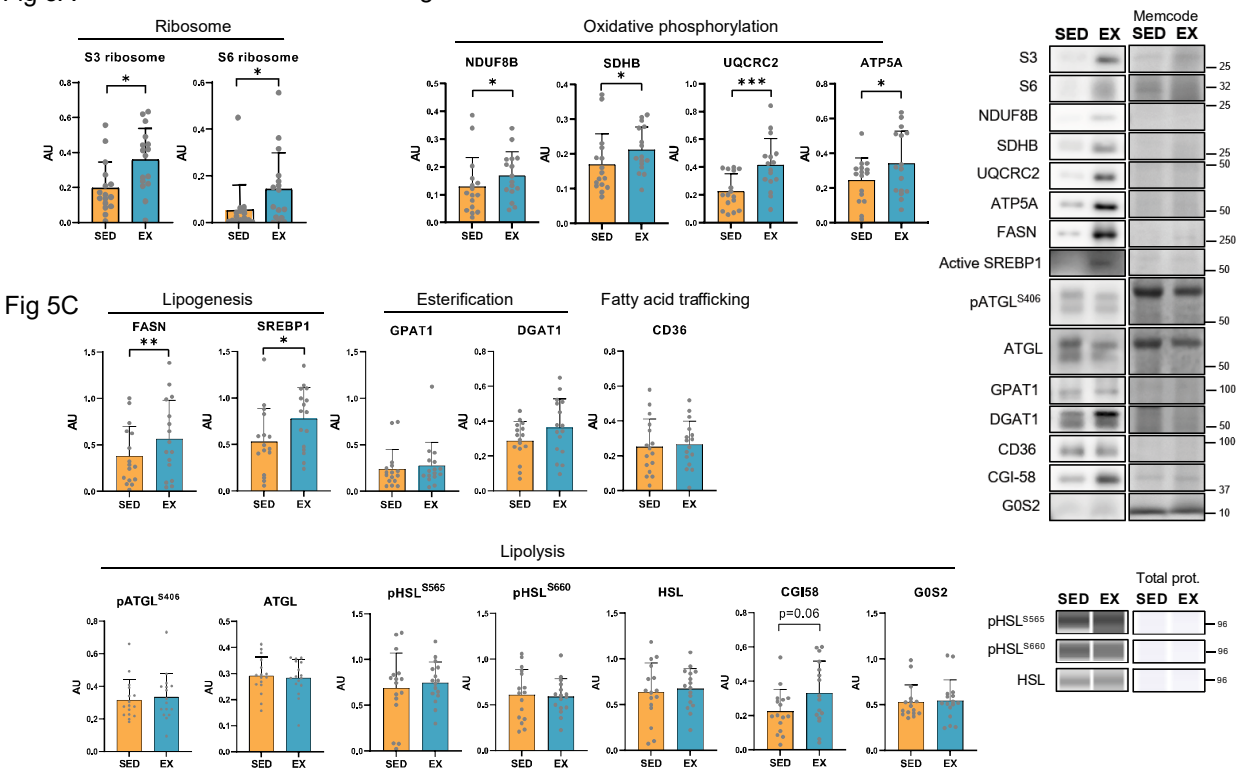

Figure 5-5 Comparison of aSAT proteomes by targeted immunoblots in SED vs EX

A) Protein abundance of ribosomal proteins. B) Protein abundance of oxidative phosphorylation subunits. C) Protein abundance of factors involved in lipid metabolism. Representative blot images from SDS-page Western blot and JESS are presented separately. *p<0.05, **p<0.01, ***p<0.001. Immunoblot data except ratio data were visualized after log(X+1) transformation. Sample sizes – SED: n=16 and EX: n=16. AU; Arbitrary Units.

Fig 6A

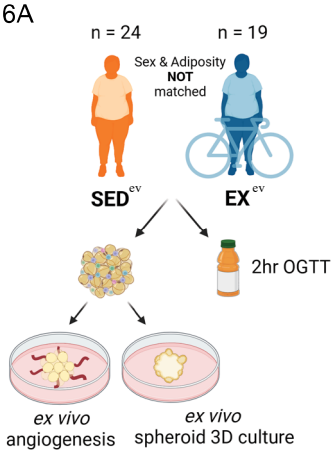

Fig 6B

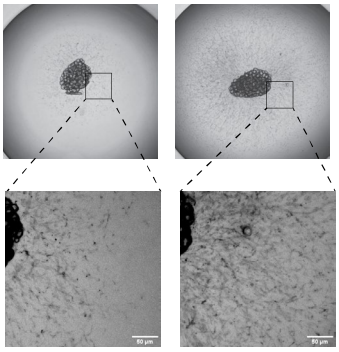

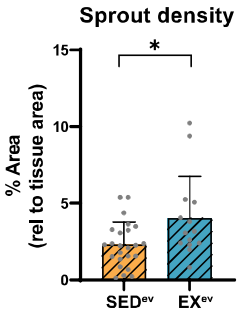

Fig 6C

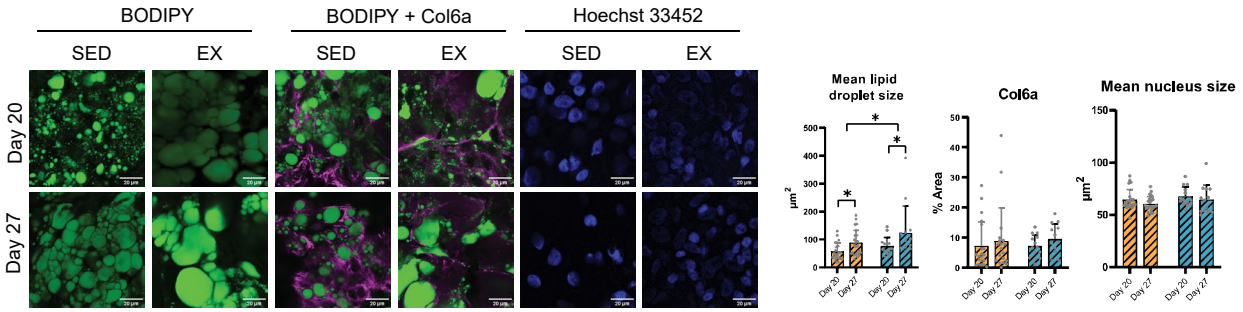

Fig 6D

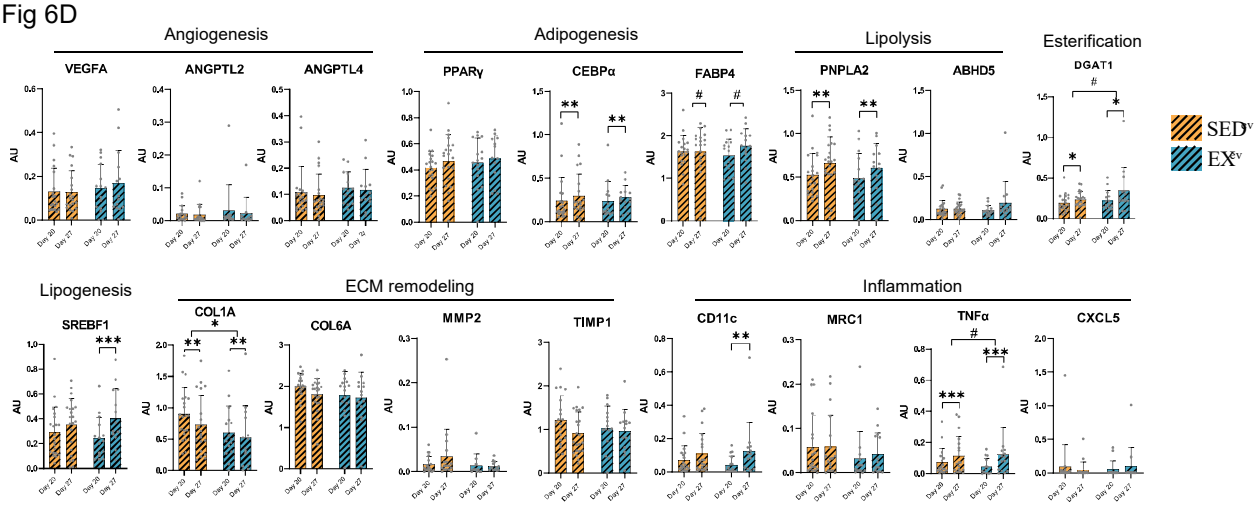

Figure 5-6 Comparison of aSAT remodeling capacity in EX^{ev} vs SED^{ev}

A) Overview of cohort comparison and analytic procedures. B) Representative images of sprouted capillaries from aSAT strips, and quantification of sprout density (% area of sprouts relative to tissue area). *p<0.05. Sample sizes were EX^{ev}: n=14 and SED^{ev}: n=24. C) Representative images of lipid droplet, Col6a, and nuclei in adipose spheroid sections at day20 and day27 post seeding in EX^{ev} and SED^{ev}, and quantification of mean lipid droplet size, Col6a (% stained area relative to section area), and mean nucleus size. Sample sizes were EX^{ev}; n=15 and SED^{ev}: n=24. D) mRNA expression of genes involved in adipose remodeling, metabolic function, and inflammation. Sample sizes were EX^{ev}: n=16 and SED^{ev}: n=24. Connecting lines between Day20 and Day27 indicate main effect of time and lines between EX^{ev} and SED^{ev}

indicate main effect of group. *p≤0.05, **p≤0.01, ***p≤0.001, #p<0.1. There were significant time x group interaction effects in the mRNA expression of SREBF1 and CD11c. Gene expression data were visualized after log(X+1) transformation. AU; Arbitrary Units.

Supplementary Fig 1A

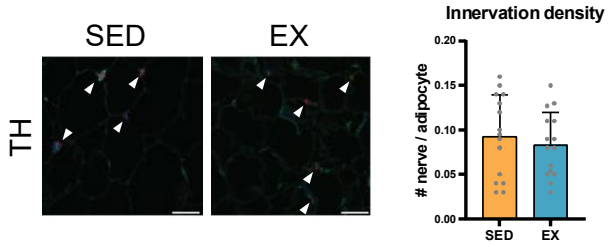

Figure 5-7 Supplementary Figure 1

A) Representative images of Tyrosine hydroxylase in aSAT section, and quantification of innervation density (number of nerves per adipocyte). Sample sizes – SED: n=15 and EX: n=15

Supplementary Fig 2A

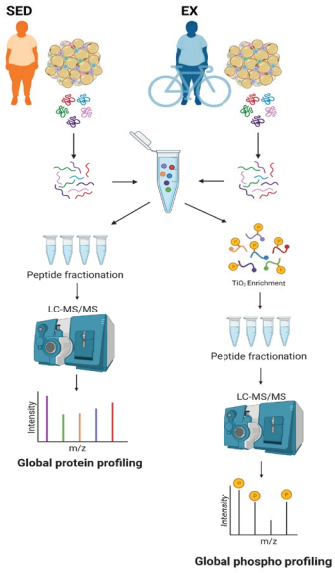

Supplementary Fig 2B

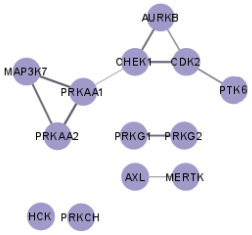

EX

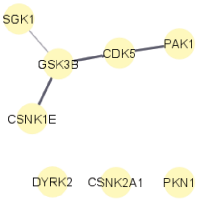

SED

Figure 5-8 Supplementary Figure 2

A) Overview of global/phosphoproteomic workflow. B) Protein-protein interaction of predicted kinases in aSAT rendered by Cytoscape. Sample sizes – SED: n=8 and EX: n=8.

Supplementary Fig 3A

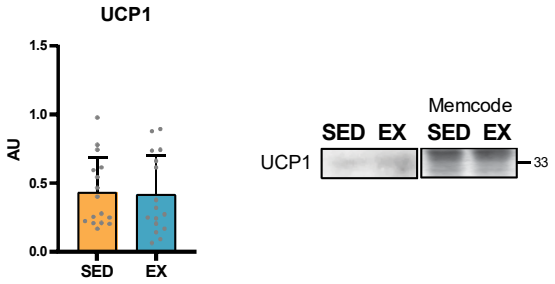

Supplementary Fig 3B

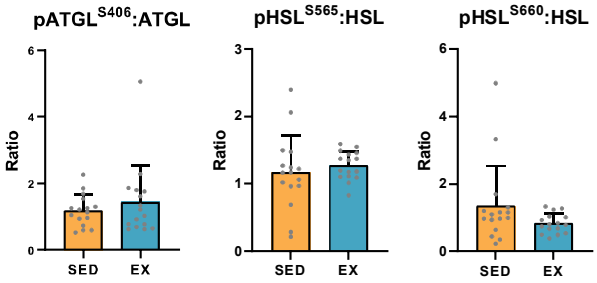

Supplementary Fig 3C

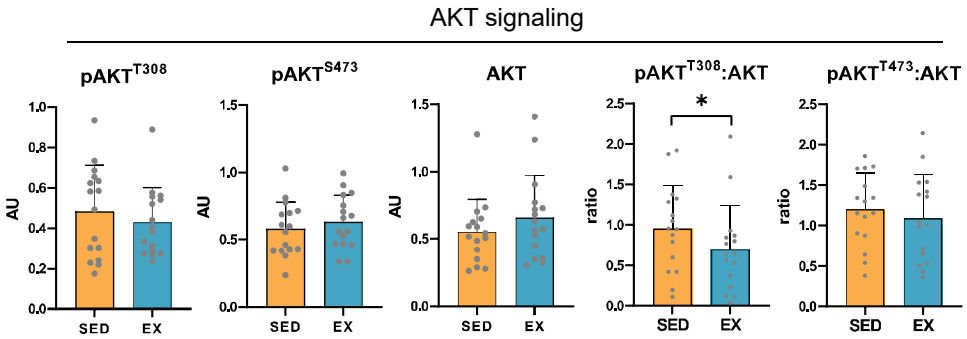

Supplementary Fig 3D

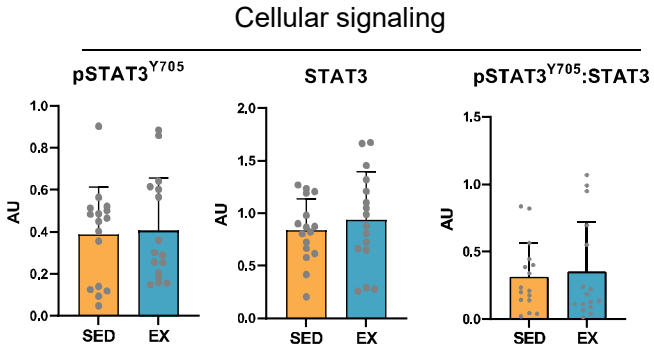

Supplementary Fig 3E

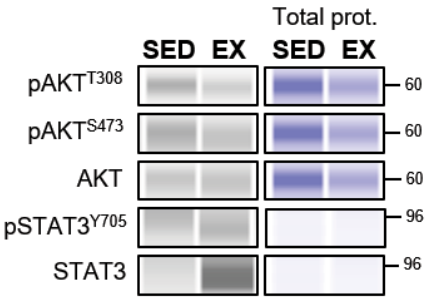

Figure 5-9 Supplementary Figure 3

A) Protein abundance of AKT and its phosphorylation, and ratio of phosphorylation to total AKT. B) Protein abundance of STAT3 and its phosphorylation. Sample sizes – SED: n=16 and EX: n=16.

Supplementary Fig 4A

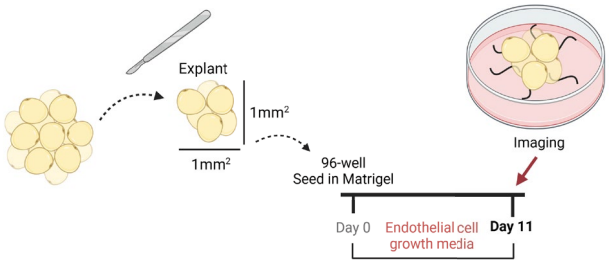

Supplementary Fig 4B

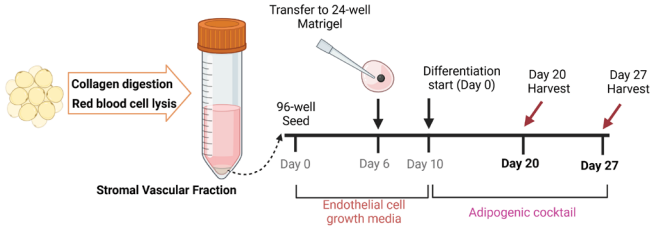

Supplementary Fig 4C

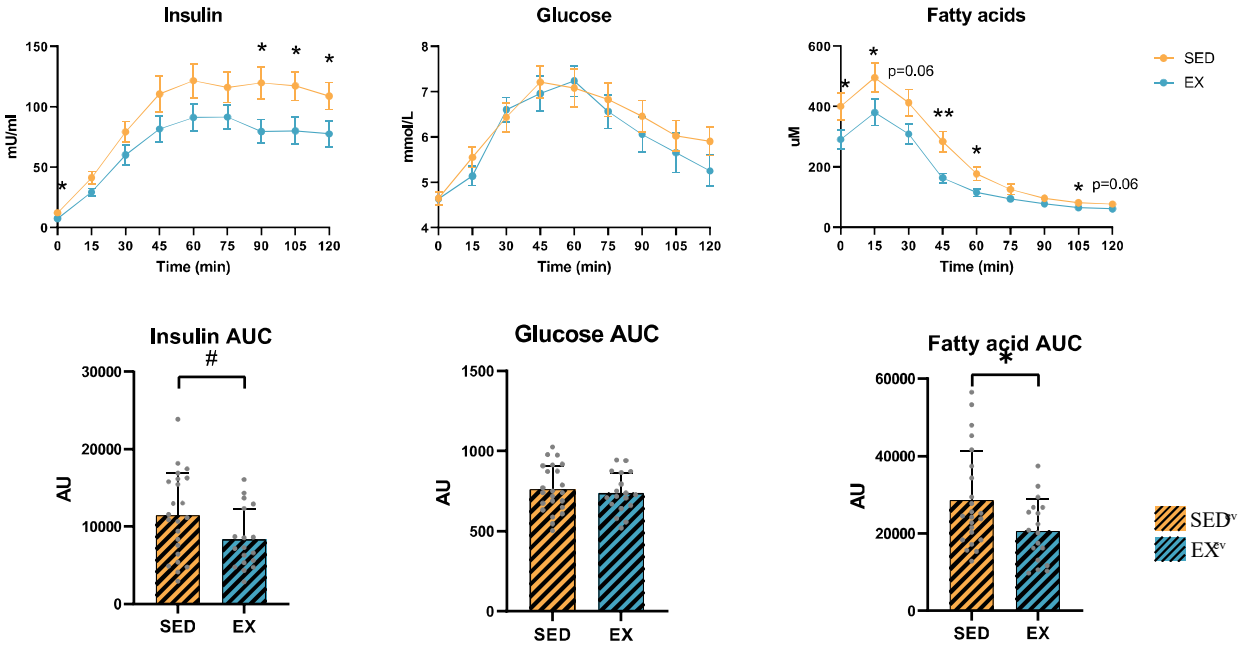

Figure 5-10 Supplementary Figure 4

A) Workflow for ex vivo angiogenesis assay. B) Workflow for ex vivo spheroid culture. C) Insulin, glucose, and fatty acid kinetics from 2hr OGTT. *p<0.05 and #p<0.1 between SED vs. EX. Sample sizes – SED: n=23 and EX: n=18. OGTT; Oral glucose tolerance test, AUC; Area under curve. Data is expressed as mean ± SEM.

5.8 TABLES

Table 5-1 Subject characteristics and whole-body clinical biomarker measures between well-matched EX vs SED

	SED (n =16)	EX (n=16)	Between groups p-value
Age (years)	31 ± 6	30 ± 5	NS
Sex	8F, 8M	8F, 8M	NS
Height (m)	1.71 ± 0.09	1.72 ± 0.07	NS
Body mass (kg)	87.8 ± 12.8	90.0 ± 13.0	NS
Body fat (%)	35.9 ± 5.5	35.2 ± 5.5	NS
Fat mass (kg)	31.1 ± 5.5	31.1 ± 5.7	NS
Fat-free mass (kg)	56.6 ± 10.6	58.9 ± 10.5	NS
BMI (kg/m^2)	29.5 ± 2.6	30.4 ± 3.5	NS
SBP (mmHg)	124 ± 11	127 ± 7	NS
DBP (mmHg)	77 ± 8	79 ± 6	NS
VO2peak (L/min)	2.5 ± 0.5	3.2 ± 0.7	$p < 0.001$
VO2peak (mL/kg/min)	28.7 ± 4.0	35.5 ± 6.5	$P < 0.001$
VO2peak (mL/kg FFM/min)	44.5 ± 4.3	54.1 ± 7.0	$p < 0.001$
MET (kcal/kg/week)	5.8 ± 6.0	57.6 ± 44.8	$p = 0.001$
Fasting insulin (mU/L)	13.1 ± 6.1	8.8 ± 7.0	$p < 0.05$
Fasting glucose (mmol/L)	4.9 ± 0.8	4.6 ± 0.8	NS
Fasting fatty acids (mM)	3.1 ± 1.4	3.0 ± 1.5	NS
HOMA-IR	2.8 ± 1.6	1.9 ± 1.7	$p < 0.05$
Adipo-IR	3913 ± 3143	2364 ± 2145	$p = 0.05$
Total cholesterol (mg/dl)	103.5 ± 37.5	103.4 ± 31.1	NS
HDL cholesterol (mg/dl)	34.7 ± 11.2	42.1 ± 13.1	$p = 0.05$
Total adiponectin (ng/ml)	7017 ± 2824	10869 ± 4680	$p < 0.05$
HMW adiponectin (ng/ml)	4371 ± 2466	5753 ± 2752	NS
Leptin (ng/ml)	25.2 ± 14.3	24.7 ± 17.0	NS

Table 5-2 Subject characteristics and whole-body clinical biomarker measures in EX^{ev} vs SED^{ev}

	SED^{ev} (n =24)	**EX^{ev} (n=19)**	**Between groups p-value**
Age (years)	33 ± 6	32 ± 5	NS
Sex	17F, 7M	8F, 11M	NS
Height (m)	1.67 ± 0.08	1.70 ± 0.10	NS
Body mass (kg)	86.1 ± 9.8	86.4 ± 16.5	NS
Body fat (%)	39.5 ± 6.1	31.2 ± 5.7	$p < 0.001$
Fat mass (kg)	33.8 ± 5.9	27.0 ± 7.4	$p < 0.01$
Fat-free mass (kg)	52.4 ± 8.9	59.4 ± 12.0	$p < 0.05$
BMI (kg/m^2)	30.9 ± 2.6	29.6 ± 3.7	NS
SBP (mmHg)	124 ± 9	122 ± 8	NS
DBP (mmHg)	79 ± 6	74 ± 7	$p < 0.05$
VO2peak (L/min)	2.4 ± 0.5	3.4 ± 0.8	$p < 0.0001$
VO2peak (mL/kg/min)	28.2 ± 4.6	39.4 ± 6.9	$p < 0.0001$
VO2peak (mL/kg FFM/min)	46.2 ± 4.4	57.1 ± 7.1	$p < 0.0001$
MET (kcal/kg/week)	7.4 ± 8.6	59.0 ± 46.3	$p < 0.0001$
Fasting insulin (mU/L)	11.8 ± 6.3	6.8 ± 3.8	$p < 0.01$
Fasting glucose (mmol/L)	4.6 ± 0.7	4.6 ± 0.6	NS
Fasting fatty acids (mM)	3.9 ± 2.1	2.9 ± 1.3	NS
HOMA-IR	2.5 ± 1.5	1.4 ± 0.9	$p < 0.01$
Adipo-IR	4684 ± 3717	1920 ± 1196	$p < 0.001$
Matsuda index	4.3 ±3.0	5.9 ± 2.1	$p = 0.01$
Total cholesterol (mg/dl)	92.7 ± 20.4	97.0 ± 21.9	NS
HDL cholesterol (mg/dl)	38.2 ± 12.6	40.7 ± 9.8	NS
Total adiponectin (ng/ml)	10382 ± 4788	10406 ± 7230	NS
HMW adiponectin (ng/ml)	6295 ± 2852	5942 ± 5077	NS
Leptin (ng/ml)	36.0 ± 21.8	16.2 ± 13.6	$p < 0.001$

Table 5-3 Supplementary Table 1. Detailed subject characteristics for SED (n=16) and EX (n=16).

Subject	Sex (M/F)	Age (yrs)	height (cm)	body mass (kg)	% body fat	fat mass (kg)	fat free mass (kg)	BMI (kg/m^2)
SED 1	F	31	162	76.6	42%	32.0	44.6	29.2
SED 2	F	22	164	76.1	38%	28.9	47.2	28.5
SED 3	F	34	170	77.2	37%	28.5	48.7	26.7
SED 4	F	39	159	70.6	35%	24.9	45.7	27.9
SED 5	F	37	161	86.4	46%	39.6	46.8	33.2
SED 6	F	19	160	75.7	37%	28.1	47.6	29.6
SED 7	F	39	164	85.7	38%	32.9	52.8	31.9
SED 8	F	39	162	74.9	42%	31.2	43.7	28.6
SED 9	M	34	184	106.4	35%	37.2	69.2	31.5
SED 10	M	34	178	87.1	32%	28.0	59.1	27.5
SED 11	M	34	170	96.7	39%	37.3	59.4	33.5
SED 12	M	35	179	103.2	37%	38.1	65.1	32.4
SED 13	M	34	180	114.2	33%	37.8	76.4	35.1
SED 14	M	30	175	93.6	31%	29.2	64.4	30.4
SED 15	M	23	176	83.6	28%	23.0	60.6	27.0
SED 16	M	29	187	96.3	25%	23.7	72.6	27.4
MEAN	8F, 8M	32.0	170.7	87.8	0.4	31.3	56.5	30.0
SD		6.1	9.3	12.8	0.1	5.4	10.8	2.6

Subject	Sex (M/F)	Age (yrs)	height (cm)	body mass (kg)	% body fat	fat mass (kg)	fat free mass (kg)	BMI (kg/m^2)
EX 1	F	29	166	81.2	40%	31.5	49.7	29.5
EX 2	F	25	165	89.5	37%	33.5	56.0	32.9
EX 3	F	41	166	77.8	36%	28.1	49.7	28.2
EX 4	F	34	166	76.2	34%	24.9	51.3	27.5
EX 5	F	27	165	89.3	45%	39.7	49.6	32.8
EX 6	F	23	177	76.8	38%	27.7	49.1	24.6
EX 7	F	25	168	87.5	37%	32.0	55.5	31.0
EX 8	F	29	170	73.0	43%	29.8	43.2	25.3
EX 9	M	32	169	100.1	36%	35.7	64.4	35.0
EX 10	M	29	163	94.0	31%	29.0	65.0	35.3
EX 11	M	34	174	95.8	39%	37.6	58.2	31.5
EX 12	M	33	179	105.3	32%	34.1	71.2	33.0
EX 13	M	27	189	120.9	32%	38.9	82.0	33.8
EX 14	M	39	177	104.6	32%	33.2	71.4	33.5
EX 15	M	27	176	81.4	27%	22.0	59.4	26.3
EX 16	M	31	176	86.5	24%	20.4	66.1	27.9
MEAN	8F, 8M	30.3	171.6	90.0	0.4	31.1	58.9	30.5
SD		5.0	6.9	13.0	0.1	5.7	10.4	3.5

Table 5-4 Supplementary Table 2. Subject characteristics for the entire study subjects.

	N = 52
Age (years)	31 ± 6
Sex	32 F, 20 M
Height (m)	1.69 ± 0.09
Body mass (kg)	85.9 ± 12.8
Body fat (%)	36 ± 7
Fat mass (kg)	30.9 ± 7.1
Fat-free mass (kg)	55.0 ±10.7
BMI (kg/m^2)	30.2 ± 3.2
SBP (mmHg)	125 ± 9
DBP (mmHg)	78 ± 7
VO2peak (L/min)	2.8 ± 0.8
VO2peak (mL/kg/min)	32.5 ± 7.7
VO2peak (mL/kg FFM/min)	50.3 ± 8.0
MET (kcal/kg/week)	32 ± 41
Group	28 SED, 24 EX

Chapter 6

Overall Discussion

6.1 INTRODUCTION

The overall findings from my dissertation projects contribute to our understanding of how exercise can induce modifications in abdominal subcutaneous adipose tissue (aSAT) at various time points: a few hours after exercise, 12 weeks into an exercise training program, and after more than two years of long-term, regular exercise. Furthermore, this dissertation offers insights into how different types of endurance exercises commonly practiced in real-life settings may lead to distinct adaptations in aSAT. In this chapter, I will provide a summary of the key findings from all three dissertation projects and integrate them to gain a comprehensive understanding of the adaptations that occur in aSAT in response to exercise. Subsequently, I will address some important questions that should be considered for future studies.

6.2 SUMMARY OF KEY FINDINGS

Project 1: *The effects of a single session of low-intensity, moderate-intensity, and high-intensity exercise on adipose tissue transcriptome, protein phosphorylation, and cytokine production.*

In Project 1, RNA sequencing was used to identify transcriptomic changes in aSAT 1.5hours after a single session of low-intensity continuous (LOW), moderate-intensity continuous (MOD), or high-intensity interval (HIGH) exercise in non-obese regular exercisers. Additionally, phosphorylation of some key metabolic proteins and concentrations of circulating cytokines were also assessed to compare the acute effects of three different exercise modalities on metabolic modifications in aSAT.

Key findings:

- High-intensity exercise triggered more pronounced changes in inflammatory genes in aSAT compared with LOW and MOD, while low- and moderate-intensity exercise modality upregulated genes involved in the ribosome and oxidative phosphorylation.
- Gene sets involved in inflammation and circadian rhythm were globally altered 1.5 hours after all three modalities.
- Concentrations of pro-inflammatory (IL1β, IL6, TNFα) and anti-inflammatory (IL10) cytokines in the circulation significantly increased after acute exercise.
- Phosphorylation of ERK in aSAT was reduced 1.5 hours after acute exercise.

Overall, this project identified early signals in aSAT that are induced by a session of exercise that may contribute to the favorable maintenance of aSAT function in regular exercisers.

Project 2: *The effects of 12-week exercise training on adipose tissue remodeling in adults with obesity without weight loss.*

In project 2, aSAT samples were collected before and after 12 weeks of moderate-intensity continuous training (MICT) or high-intensity interval training (HIIT) from adults with obesity who were required to not lose weight during intervention. aSAT morphology was measured by histochemistry and protein abundance of factors that regulate structural and metabolic remodeling of aSAT was measured by immunoblotting. Antilipolytic sensitivity to insulin was measured in vivo through a hyperinsulinemic-euglycemic clamp.

Key findings:

- 12 weeks of moderate-intensity continuous training (MICT) and 12 weeks of high-intensity interval training (HIIT) both increased capillarization, reduced fat cell size, and altered ECM composition even without weight loss.
- 12 weeks of moderate-intensity continuous training (MICT) and 12 weeks of high-intensity interval training (HIIT) both increased the protein abundance of markers of angiogenesis, adipogenesis, mitochondrial biogenesis, and altered protein

abundance of ECM regulator and key proteins involved in the MAPK pathway, but the exercise effects were transient.

- The modest modifications in adipose tissue structure in response to 12 weeks of MICT or HIIT did not lead to changes in the rate of fatty acid release from adipose tissue.

Overall, these results expand our understanding of the effects of two commonly used exercise training prescriptions (MICT and HIIT) on adipose tissue remodeling that may lead to advanced strategies for improving metabolic health outcomes in adults with obesity.

Project 3: *Effects of long-term, regular exercise on adipose tissue structure, proteome, and remodeling capacity in adults with overweight/obesity.*

In project 3, aSAT structure and proteomic profile were compared between regularly exercising adults with overweight/obesity and well-matched sedentary/non-exercising adults. Histochemistry was used to compare aSAT morphology and structure. Untargeted global and phosphoproteomics were used to compare aSAT proteome. As an exploratory aim, angiogenic capacity and lipid storage capacity were compared by *ex vivo* angiogenesis assay and 3-dimensional spheroid culture.

Key findings:

- Compared with well-matched sedentary adults with overweight/obesity, aSAT from regular exercisers with overweight/obesity has higher capillarization, less Col6a, and markers of macrophages.
- Compared with well-matched sedentary adults with overweight/obesity, aSAT from regular exercisers with overweight/obesity has a higher abundance of ribosomal, mitochondrial, and lipogenic proteins.
- Compared with well-matched sedentary adults with overweight/obesity, aSAT from regular exercisers with overweight/obesity has a higher abundance of phosphoproteins involved in protein translation, lipogenesis, and direct regulation of transcripts.

- Compared with well-matched sedentary adults with overweight/obesity, aSAT explants from regular exercisers with overweight/obesity exhibited higher angiogenic capacity.
- Compared with well-matched sedentary adults with overweight/obesity, spheroids bioengineered from the isolated stromal vascular fraction of aSAT from regular exercisers with overweight/obesity had larger lipid droplets and higher mRNA expression of lipogenic and esterification genes.

Overall, findings from Project 3 suggest that regular exercise in adults with overweight/obesity favorably remodels the aSAT structure and proteomic profile that may lead to improved lipid storage capacity in ways, which can contribute to preserved cardiometabolic health.

6.3 INTEGRATED INTERPRETATION OF RESULTS

Effects of exercise on adipose tissue vascularization

Greater capillary density in adipose tissue enhances oxygen and nutrient delivery capacity, potentially averting local hypoxia, a condition that can lead to heightened extracellular matrix (ECM) deposition and inflammation (62). Findings from Project 2 that capillary density (number of capillaries per mm^2) and the protein abundance of pro-angiogenic regulator ANGPTL2 were increased after 12 weeks of exercise training in adults with obesity indicate that increased capillarization in aSAT may be a part of the early structural adaptations induced by exercise training.

In Project 3, we observed higher capillarization and increased protein abundance of VEGFα in regular exercisers with overweight/obesity when compared with well-matched non-exercising adults. This aligns with the findings from Project 2 and suggests that robust angiogenesis and vascularization may require an extended period of exercise stimuli to manifest. This might explain the somewhat modest increase in capillarization observed in Project 2. Furthermore, our exploratory *ex vivo* angiogenesis assay demonstrated increased angiogenic capacity when stimulating aSAT explants with endothelial cell growth factors. Hence, the findings from Project 2 and 3 collectively

suggest that regular exercise training may induce vascularization in aSAT among adults with obesity, and this effect appears to be independent of variations in adiposity.

Effects of exercise on adipose tissue inflammation

One of the important aims of my dissertation projects was to determine whether exercise may reduce aSAT inflammation because it is well-known that chronic augmentation of aSAT inflammation is tightly associated with dysregulated aSAT function and cardiometabolic health risk factors, particularly in adults with obesity (369). In Project 3, we found that the markers of macrophages (CD14 and CD206) and complement proteins that promote the clearance of damaged cells by macrophages were lower in regularly exercising adults with overweight/obesity compared with well-matched non-exercising cohorts. This suggests a possibility that regular exercise may lower the inflammatory potential in aSAT. However, lower macrophage abundance did not lead to lower concentrations of some markers of systemic inflammation (pro-inflammatory cytokines).

Although findings from Project 2 that 12-week exercise training without weight loss modified some key MAPK proteins (ERK and JNK) in aSAT from adults with obesity that mediate inflammatory signaling in adipose tissue (261), I was unable to assess more direct evidence of aSAT inflammation such as macrophage abundance, or cytokine abundance due to technical limitations. Therefore, it is unclear whether aSAT inflammation can be reduced by 12-week exercise training in adults with obesity, especially in the absence of weight loss.

Paradoxically, acute inflammatory response in aSAT may be necessary for healthy adipose tissue remodeling (125). In this regard, our finding from Project 1 that acute exercise induced global inflammatory responses in aSAT may be an early important signal induced by exercise that contributes to the maintenance of aSAT function in non-obese regular exercisers. An important related question that should be addressed is whether the acute inflammatory response in aSAT after exercise may also occur in adults with obesity. Our lab previously reported that a session of both HIIT and MICT upregulated aSAT inflammatory genes in adults with obesity who had been trained for 6 weeks (18). Subjects in this study were a sub-cohort of the subjects who participated in

Project 2, whose aSAT was favorably modified by 12 weeks of MICT or HIIT. Although we are limited to making a direct connection between the transient inflammatory response after acute exercise and training-induced morphological and proteomic adaptations, it is intriguing that our lab's findings may collectively support the notion that exercise-induced inflammatory response could be beneficial or even necessary for healthy remodeling in obesity. Additionally, high-intensity interval (HIGH) exercise may be more effective in triggering inflammatory response than moderate- (MOD) or low-intensity (LOW) continuous exercises.

Overall, findings from my projects suggest that regular exercise may favorably modify aSAT inflammatory status by attenuating infiltration of adipose tissue macrophages but also highlight an important possibility that bouts of exercise may trigger pro-inflammatory responses in aSAT that might be essential in healthy maintenance of aSAT function.

Effects of exercise on extracellular matrix (ECM) remodeling

The fibrotic content and composition of aSAT ECM is linked with aSAT dysfunction (i.e. limited lipid storage capacity) and inflammation in obesity (96, 104). Some preclinical studies have demonstrated that exercise training per se may attenuate ECM deposition in HFD-induced obesity (15). However, findings from Project 2 and 3 indicate that the overall fibrotic content in aSAT ECM (measured by Sirius Red histochemistry) may not be directly altered by regular exercise without weight change. We still found some evidence that exercise training may modify the specific composition of ECM. For example, the abundance of Col5a3, which was reported to be crucial in glucose homeostasis (296) was increased after 12-week exercise training in adults with obesity (Project 2). Additionally, we observed a lower abundance of Col6a, a highly enriched collagen type in adipose tissue that is often associated with metabolic health complications (105), in regularly exercising adults with overweight/obesity (Project 3). Lower abundance of Col6a was associated with fewer markers of macrophages and higher capillarization in aSAT supporting the notion that the regular exercise-induced adaptations in aSAT ECM that we observed from Project 3 may be metabolically favorable (49).

Alterations in aSAT ECM composition by 12-week exercise training (Project 2) and years of regular exercise (Project 3) were accompanied by modifications in key enzymes that regulate ECM (e.g., reduced abundance of MMP9 in Project 2 and higher abundance of TIMP1 in exercisers in Project 3). This suggests that the compositional change of aSAT ECM could have resulted from dynamic ECM remodeling induced by exercise training. Overall, our data suggests that regular exercise may directly induce ECM remodeling that may favorably contribute to improving aSAT function, which could lead to improved cardiometabolic health in obesity.

Effects of exercise on adipose tissue lipid metabolism

The lipid storage capacity of aSAT is directly linked with cardiometabolic health and systemic inflammation because excessive fatty acid mobilization that results from limited lipid storage of aSAT can lead to ectopic lipid accumulation in other organs such as skeletal muscle, liver, and endothelium which in turn, leads to metabolic health complications such as insulin resistance, systemic inflammation, and atherosclerosis (180, 299). Therefore, an overarching aim of my projects was to examine whether fatty acid mobilization can be directly regulated by exercise in obesity.

Consistent with the previous findings (211, 300), the finding in Project 2 that 12 weeks of exercise training without weight loss did not alter whole-body basal fatty acid mobilization in adults with obesity. Project 2 additionally confirmed that insulin-stimulated fatty acid mobilization in adults with obesity was not affected by exercise training. This suggests that exercise training per se may not modify fatty acid release capacity. Exercise training may reduce fatty acid mobilization in obesity when weight loss is accompanied, but the reduction in fatty acid release is probably driven by the loss of fat mass (12). However, increased protein abundance of HSL and CD36 1 day after exercise training suggested a possibility that exercise training may enhance fatty acid release or handling capacity in aSAT even without weight loss.

Our findings from Project 3 greatly expanded our understanding of the potential effects of regular endurance exercise on aSAT lipid metabolism in adults with overweight/obesity. Interestingly, proteomes involved in fatty acid synthesis (e.g., FASN and active form of SREBP1) were strongly upregulated in the regular exercisers. Although

de novo lipogenesis (DNL) in adipose tissue has not garnered a lot of attention partially due to its low contribution to total fatty acid synthesis (370) (the liver is the central site for DNL) and technical difficulties in studying DNL in adipose tissue *in vivo*, some evidence suggests that lipogenic gene expression in aSAT is suppressed in obesity (347, 348). This suggests maintaining adipose DNL may be metabolically beneficial in obesity. Perhaps, the production of insulin-sensitizing fatty acids (e.g., palmitoleate and fatty acid esters of hydroxyl-fatty acids) or more effective conversion of glucose to fatty acid, which is a favorable form of substrate to be stored in adipose tissue could result in from increased DNL. In addition, we also found a strong trend of greater protein abundance of CGI-58, an ATGL co-activator from regular exercisers. This indicates that regular exercise may modify aSAT for more effective release of fatty acids especially when stimulated during exercise. Overall, although findings from my projects indicate that exercise training may not directly regulate whole-body fatty acid mobilization, it may remodel aSAT proteome for more effective fatty acid release and storage.

Effects of exercise on adipose tissue oxidative phosphorylation

A robust increase in mitochondrial density and oxidative capacity is a well-known exercise-induced adaptation in skeletal muscle (52). Findings from my projects suggest that exercise may induce similar mitochondrial adaptations in aSAT as well. An acute session of exercise increased oxidative phosphorylation genes (Project 1) and repeated bouts of exercise increased the mitochondrial protein abundance (Project 2 and 3). Although we did not measure mitochondrial respiration, these data collectively suggest that exercise may favorably modify aSAT oxidative metabolism that may help combat cellular stress common in overweight/obesity (242, 304). It is important to note that despite the evidence of increased mitochondrial density and enhanced oxidative capacity in aSAT, these do not seem to lead to adipose tissue browning based on our finding that the protein abundance of UCP1 was not different between regular exercisers and non-exercisers in Project 3, which is consistent with many previous studies (53, 199, 357).

Effects of exercise on ribosome biogenesis/remodeling

A novel finding from my projects is that increased ribosomal biogenesis may be a regular exercise-induced adaptation in aSAT. In Project 3, we found that ribosomal proteins were significantly upregulated in aSAT from regularly exercising adults with overweight/obesity. In Project 1, acute MOD and LOW induced upregulation of ribosomal genes in aSAT from regular exercisers demonstrating a possibility that the acute transcriptomic alterations in ribosomal genes may manifest into robust proteomic adaptation in aSAT. Interestingly, the ribosome pathway was not upregulated 1 hour after a session of MICT or HIIT in the sub-cohort of Project 2 even though subjects were participating in exercise training intervention for 6 weeks (18). Perhaps, upregulation of ribosomal genes may not be induced in the early period of exercise training and may require an extended period of training (e.g., 6 months) (53). The finding of robust ribosomal adaptation in aSAT is potentially important because the enhanced protein translation capacity may explain the molecular adaptation that underlies regular exercise-induced structural or metabolic modifications in aSAT as it was observed from skeletal muscle (361).

6.4 DIRECTIONS FOR FUTURE RESEARCH

Single cell-based analysis in adipose tissue

Overall findings from my projects suggest a possibility that exercise may induce favorable adaptations in adipose tissue. However, cell-specific adaptations in response to exercise were not addressed, which is a very important area that needs to be further investigated. Mature adipocytes account for more than 90% of the total tissue volume (371), but may only take up 20~50% of the total cell population in adipose tissue, indicative of the heterogeneity of adipose tissue. The stromal vascular fraction of adipose tissue consists of various cells such as preadipocytes, fibro-adipogenic progenitors, immune cells, etc. It is well known that obesity drives the phenotypical change in adipose tissue immune cells (111) that can lead to exacerbated inflammation in response to cellular stimuli (e.g., nutritional overload or exercise). Previous research from our lab reported that the phenotype of adipose progenitor cells was altered 12 hours after acute exercise (190). A recent study revealed that Pdgfra-positive cells (abundant in fibro-

adipogenic progenitor cells) were the most responsive cells in response to exercise (372). Given that adipose tissue is a primary reservoir of fibro-adipogenic progenitors and fibroblasts (373), it is certainly possible that exercise response in adipose tissue may largely be driven by certain cells. Therefore, single cell-based analysis such as single nuclei RNA sequencing (snRNA-seq) has the potential to greatly expand our understanding of exercise-induced remodeling of adipose tissue and provide insights into therapeutic applications.

Functional measurement of adipose tissue remodeling

One of the novel findings in Project 3 was that we were able to demonstrate some parts of exercise-induced adipose tissue remodeling (angiogenesis, lipid droplet expansion, ECM collagen synthesis) through functional *ex vivo* experiments. Although our attempt to conduct the *ex vivo* experiments was exploratory and thus the experimental techniques may be further developed to better mimic the *in vivo* microenvironment, it showed a possibility that tissue remodeling capacities may be assessed by cutting-edge functional assays. Incorporation of specific gene silencing (via siRNA) techniques or drug treatments may allow functional identification of specific components in adipose tissue.

6.5 OVERALL CONCLUSIONS

Abnormalities in the structure and metabolic function of adipose tissue underlie many obesity-related health complications. Whether or how exercise may favorably modify adipose tissue independently of variations in adiposity was the primary aim of the dissertation projects. Project 1 provided evidence that a single session of three different exercise intensities can directly trigger distinct transcriptomic signals particularly involved in inflammation, circadian rhythm, ribosome, and oxidative phosphorylation. Project 2 showed that 12 weeks of endurance exercise training induced some early structural and metabolic adaptations in adipose tissue in adults with obesity. Even without weight loss, exercise training reduced adipocyte size, increased capillary density, and induced ECM remodeling. Project 3 demonstrated that at least two years of regular exercise increased capillary density, induced ECM remodeling, and attenuated macrophage infiltration in

adipose tissue in adults with overweight/obesity. Importantly, we found that regular exercise induced robust proteomic adaptations in the ribosome, mitochondria, and fatty acid synthesis that could contribute to the preserved cardiometabolic health in regular exercisers. Overall, findings from my dissertation projects provide a comprehensive approach to identifying potential exercise-induced adaptations in adipose tissue in a timely fashion. Exercise effects were examined within 2 hours after an acute exercise, after 3 months of training, and after years of regular exercise training, identifying important adaptations in adipose tissue that could contribute to improving or preserving cardiometabolic health in overweight/obesity.

Bibliography

1. Hales CM, Carroll MD, Fryar CD, and Ogden CL. Prevalence of obesity among adults and youth: United States, 2015–2016. 2017.
2. Guh DP, Zhang W, Bansback N, Amarsi Z, Birmingham CL, and Anis AH. The incidence of co-morbidities related to obesity and overweight: a systematic review and meta-analysis. *BMC public health.* 2009;9(1):1-20.
3. Sun K, Kusminski CM, and Scherer PE. Adipose tissue remodeling and obesity. *The Journal of clinical investigation.* 2011;121(6):2094-101.
4. Guo Z, Hensrud DD, Johnson CM, and Jensen MD. Regional postprandial fatty acid metabolism in different obesity phenotypes. *Diabetes.* 1999;48(8):1586-92.
5. Jensen MD, Cryer PE, Johnson CM, and Murray MJ. Effects of epinephrine on regional free fatty acid and energy metabolism in men and women. *American Journal of Physiology-Endocrinology And Metabolism.* 1996;270(2):E259-E64.
6. Heilbronn L, Smith S, and Ravussin E. Failure of fat cell proliferation, mitochondrial function and fat oxidation results in ectopic fat storage, insulin resistance and type II diabetes mellitus. *International journal of obesity.* 2004;28(4):S12-S21.
7. Kunz HE, Hart CR, Gries KJ, Parvizi M, Laurenti M, Dalla Man C, et al. Adipose tissue macrophage populations and inflammation are associated with systemic inflammation and insulin resistance in obesity. *American Journal of Physiology-Endocrinology and Metabolism.* 2021;321(1):E105-E21.
8. Knowler WC, Barrett-Connor E, Fowler SE, Hamman RF, Lachin JM, Walker EA, et al. Reduction in the incidence of type 2 diabetes with lifestyle intervention or metformin. 2002.
9. Myers J. Exercise and cardiovascular health. *Circulation.* 2003;107(1):e2-e5.
10. Østergård T, Andersen JL, Nyholm B, Lund S, Nair KS, Saltin B, et al. Impact of exercise training on insulin sensitivity, physical fitness, and muscle oxidative

capacity in first-degree relatives of type 2 diabetic patients. *American Journal of Physiology-Endocrinology and Metabolism.* 2006;290(5):E998-E1005.

11. Short KR, Vittone JL, Bigelow ML, Proctor DN, Rizza RA, Coenen-Schimke JM, et al. Impact of aerobic exercise training on age-related changes in insulin sensitivity and muscle oxidative capacity. *Diabetes.* 2003;52(8):1888-96.
12. Schenk S, Harber MP, Shrivastava CR, Burant CF, and Horowitz JF. Improved insulin sensitivity after weight loss and exercise training is mediated by a reduction in plasma fatty acid mobilization, not enhanced oxidative capacity. *The Journal of physiology.* 2009;587(20):4949-61.
13. Varshney P, Guth LM, Anderson CM, Raajendiran A, Watt MJ, and Horowitz JF. 287-OR: Acute Exercise Enhances the Differentiation Rate of Human Adipocyte Precursor Cells. *Diabetes.* 2019;68(Supplement_1).
14. Walton RG, Finlin BS, Mula J, Long DE, Zhu B, Fry CS, et al. Insulin-resistant subjects have normal angiogenic response to aerobic exercise training in skeletal muscle, but not in adipose tissue. *Physiological reports.* 2015;3(6):e12415.
15. Kawanishi N, Niihara H, Mizokami T, Yano H, and Suzuki K. Exercise training attenuates adipose tissue fibrosis in diet-induced obese mice. *Biochemical and biophysical research communications.* 2013;440(4):774-9.
16. Egan B, Hawley JA, and Zierath JR. SnapShot: exercise metabolism. *Cell Metabolism.* 2016;24(2):342-. e1.
17. Van Pelt DW, Guth LM, and Horowitz JF. Aerobic exercise elevates markers of angiogenesis and macrophage IL-6 gene expression in the subcutaneous adipose tissue of overweight-to-obese adults. *Journal of Applied Physiology.* 2017;123(5):1150-9.
18. Ludzki AC, Schleh MW, Krueger EM, Taylor NM, Ryan BJ, Baldwin TC, et al. Inflammation and metabolism gene sets in subcutaneous abdominal adipose tissue are altered 1 hour after exercise in adults with obesity. *Journal of Applied Physiology.* 2021;131(4):1380-9.
19. Shen Y, Zhou H, Jin W, and Lee H. Acute exercise regulates adipogenic gene expression in white adipose tissue. *Biology of sport.* 2016;33(4):381.

20. Oliveira AG, Araujo TG, Carvalho BM, Guadagnini D, Rocha GZ, Bagarolli RA, et al. Acute exercise induces a phenotypic switch in adipose tissue macrophage polarization in diet-induced obese rats. *Obesity.* 2013;21(12):2545-56.
21. Kraniou GN, Cameron-Smith D, and Hargreaves M. Acute exercise and GLUT4 expression in human skeletal muscle: influence of exercise intensity. *Journal of applied physiology.* 2006;101(3):934-7.
22. AL Mulla N, Simonsen L, and Bülow J. Post-exercise adipose tissue and skeletal muscle lipid metabolism in humans: the effects of exercise intensity. *The Journal of physiology.* 2000;524(3):919-28.
23. Horowitz JF. Fatty acid mobilization from adipose tissue during exercise. *Trends in Endocrinology & Metabolism.* 2003;14(8):386-92.
24. Little JP, Jung ME, Wright AE, Wright W, and Manders RJF. Effects of high-intensity interval exercise versus continuous moderate-intensity exercise on postprandial glycemic control assessed by continuous glucose monitoring in obese adults. *Applied physiology, nutrition, and metabolism.* 2014;39(7):835-41.
25. Gibala MJ, Little JP, MacDonald MJ, and Hawley JA. Physiological adaptations to low-volume, high-intensity interval training in health and disease. *The Journal of physiology.* 2012;590(5):1077-84.
26. Sun L, Li F-H, Li T, Min Z, Yang L-D, Gao H-E, et al. Effects of high-intensity interval training on adipose tissue lipolysis, inflammation, and metabolomics in aged rats. *Pflügers Archiv-European Journal of Physiology.* 2020;472(2):245-58.
27. Arner E, Westermark PO, Spalding KL, Britton T, Rydén M, Frisén J, et al. Adipocyte turnover: relevance to human adipose tissue morphology. *Diabetes.* 2010;59(1):105-9.
28. Organizations WH. https://www.who.int/news-room/fact-sheets/detail/obesity-and-overweight.
29. Must A, Spadano J, Coakley EH, Field AE, Colditz G, and Dietz WH. The disease burden associated with overweight and obesity. *Jama.* 1999;282(16):1523-9.
30. Nguyen NT, Nguyen X-MT, Lane J, and Wang P. Relationship between obesity and diabetes in a US adult population: findings from the National Health and Nutrition Examination Survey, 1999–2006. *Obesity surgery.* 2011;21(3):351-5.

31. Thompson D, Karpe F, Lafontan M, and Frayn K. Physical activity and exercise in the regulation of human adipose tissue physiology. *Physiological reviews.* 2012.
32. Virtue S, and Vidal-Puig A. Adipose tissue expandability, lipotoxicity and the metabolic syndrome—an allostatic perspective. *Biochimica et Biophysica Acta (BBA)-molecular and cell biology of lipids.* 2010;1801(3):338-49.
33. Gray SL, and Vidal-Puig AJ. Adipose tissue expandability in the maintenance of metabolic homeostasis. *Nutrition reviews.* 2007;65(suppl_1):S7-S12.
34. Kohlgruber A, and Lynch L. Adipose tissue inflammation in the pathogenesis of type 2 diabetes. *Current diabetes reports.* 2015;15(11):1-11.
35. Jensen MD. Adipose tissue and fatty acid metabolism in humans. *Journal of the Royal society of medicine.* 2002;95(Suppl 42):3.
36. Henry SL, Bensley JG, Wood-Bradley RJ, Cullen-McEwen LA, Bertram JF, and Armitage JA. White adipocytes: more than just fat depots. *The international journal of biochemistry & cell biology.* 2012;44(3):435-40.
37. Sacks H, and Symonds ME. Anatomical locations of human brown adipose tissue: functional relevance and implications in obesity and type 2 diabetes. *Diabetes.* 2013;62(6):1783-90.
38. Tsiloulis T, and Watt MJ. Exercise and the regulation of adipose tissue metabolism. *Progress in molecular biology and translational science.* 2015;135:175-201.
39. Nye C, Kim J, Kalhan SC, and Hanson RW. Reassessing triglyceride synthesis in adipose tissue. *Trends in Endocrinology & Metabolism.* 2008;19(10):356-61.
40. Lee M-J, Wu Y, and Fried SK. Adipose tissue heterogeneity: implication of depot differences in adipose tissue for obesity complications. *Molecular aspects of medicine.* 2013;34(1):1-11.
41. Choe SS, Huh JY, Hwang IJ, Kim JI, and Kim JB. Adipose tissue remodeling: its role in energy metabolism and metabolic disorders. *Frontiers in endocrinology.* 2016;7:30.
42. Lin D, Chun T-H, and Kang L. Adipose extracellular matrix remodelling in obesity and insulin resistance. *Biochemical pharmacology.* 2016;119:8-16.

43. Kawai T, Autieri MV, and Scalia R. Adipose tissue inflammation and metabolic dysfunction in obesity. *American Journal of Physiology-Cell Physiology.* 2021;320(3):C375-C91.
44. Lemoine AY, Ledoux S, and Larger E. Adipose tissue angiogenesis in obesity. *Thrombosis and haemostasis.* 2013;110(10):661-9.
45. Suganami T, Tanaka M, and Ogawa Y. Adipose tissue inflammation and ectopic lipid accumulation. *Endocrine journal.* 2012:EJ12-0271.
46. Carey DG, Jenkins AB, Campbell LV, Freund J, and Chisholm DJ. Abdominal fat and insulin resistance in normal and overweight women: direct measurements reveal a strong relationship in subjects at both low and high risk of NIDDM. *Diabetes.* 1996;45(5):633-8.
47. Iacobini C, Pugliese G, Fantauzzi CB, Federici M, and Menini S. Metabolically healthy versus metabolically unhealthy obesity. *Metabolism.* 2019;92:51-60.
48. Blüher M. Metabolically healthy obesity. *Endocrine reviews.* 2020;41(3):bnaa004.
49. Crewe C, An YA, and Scherer PE. The ominous triad of adipose tissue dysfunction: inflammation, fibrosis, and impaired angiogenesis. *The Journal of clinical investigation.* 2017;127(1):74-82.
50. Carpentier AC. 100th anniversary of the discovery of insulin perspective: insulin and adipose tissue fatty acid metabolism. *American Journal of Physiology-Endocrinology and Metabolism.* 2021;320(4):E653-E70.
51. Reilly SM, and Saltiel AR. Adapting to obesity with adipose tissue inflammation. *Nature Reviews Endocrinology.* 2017;13(11):633-43.
52. Holloszy JO, and Coyle EF. Adaptations of skeletal muscle to endurance exercise and their metabolic consequences. *Journal of applied physiology.* 1984;56(4):831-8.
53. Rönn T, Volkov P, Tornberg Å, Elgzyri T, Hansson O, Eriksson KF, et al. Extensive changes in the transcriptional profile of human adipose tissue including genes involved in oxidative phosphorylation after a 6-month exercise intervention. *Acta physiologica.* 2014;211(1):188-200.

54. Stanford KI, Middelbeek RJ, Townsend KL, Lee M-Y, Takahashi H, So K, et al. A novel role for subcutaneous adipose tissue in exercise-induced improvements in glucose homeostasis. *Diabetes.* 2015;64(6):2002-14.
55. Larson-Meyer DE, Heilbronn LK, Redman LM, Newcomer BR, Frisard MI, Anton S, et al. Effect of calorie restriction with or without exercise on insulin sensitivity, β-cell function, fat cell size, and ectopic lipid in overweight subjects. *Diabetes care.* 2006;29(6):1337-44.
56. Dieli-Conwright CM, Parmentier J-H, Sami N, Lee K, Spicer D, Mack WJ, et al. Adipose tissue inflammation in breast cancer survivors: effects of a 16-week combined aerobic and resistance exercise training intervention. *Breast cancer research and treatment.* 2018;168:147-57.
57. Čížková T, Štěpán M, Daďová K, Ondrůjová B, Sontáková L, Krauzová E, et al. Exercise training reduces inflammation of adipose tissue in the elderly: cross-sectional and randomized interventional trial. *The Journal of Clinical Endocrinology & Metabolism.* 2020;105(12):e4510-e26.
58. De Glisezinski I, Crampes F, Harant I, Berlan M, Hejnova J, Langin D, et al. Endurance training changes in lipolytic responsiveness of obese adipose tissue. *American Journal of Physiology-Endocrinology And Metabolism.* 1998;275(6):E951-E6.
59. Klöting N, Fasshauer M, Dietrich A, Kovacs P, Schön MR, Kern M, et al. Insulin-sensitive obesity. *American Journal of Physiology-Endocrinology and Metabolism.* 2010;299(3):E506-E15.
60. Smith GI, Mittendorfer B, and Klein S. Metabolically healthy obesity: facts and fantasies. *The Journal of clinical investigation.* 2019;129(10):3978-89.
61. Guilherme A, Henriques F, Bedard AH, and Czech MP. Molecular pathways linking adipose innervation to insulin action in obesity and diabetes mellitus. *Nature Reviews Endocrinology.* 2019;15(4):207-25.
62. Halberg N, Khan T, Trujillo ME, Wernstedt-Asterholm I, Attie AD, Sherwani S, et al. Hypoxia-inducible factor 1α induces fibrosis and insulin resistance in white adipose tissue. *Molecular and cellular biology.* 2009;29(16):4467-83.

63. Salans LB, Knittle JL, and Hirsch J. The role of adipose cell size and adipose tissue insulin sensitivity in the carbohydrate intolerance of human obesity. *The Journal of clinical investigation.* 1968;47(1):153-65.
64. Yang J, Eliasson B, Smith U, Cushman SW, and Sherman AS. The size of large adipose cells is a predictor of insulin resistance in first-degree relatives of type 2 diabetic patients. *Obesity.* 2012;20(5):932-8.
65. Lönn M, Mehlig K, Bengtsson C, and Lissner L. Adipocyte size predicts incidence of type 2 diabetes in women. *The FASEB journal.* 2010;24(1):326-31.
66. Carobbio S, Pellegrinelli V, and Vidal-Puig A. Adipose tissue function and expandability as determinants of lipotoxicity and the metabolic syndrome. *Obesity and lipotoxicity.* 2017:161-96.
67. Nguyen MA, Favelyukis S, Nguyen A-K, Reichart D, Scott PA, Jenn A, et al. A subpopulation of macrophages infiltrates hypertrophic adipose tissue and is activated by free fatty acids via Toll-like receptors 2 and 4 and JNK-dependent pathways. *Journal of biological chemistry.* 2007;282(48):35279-92.
68. Vishvanath L, and Gupta RK. Contribution of adipogenesis to healthy adipose tissue expansion in obesity. *The Journal of clinical investigation.* 2019;129(10):4022-31.
69. Hammarstedt A, Gogg S, Hedjazifar S, Nerstedt A, and Smith U. Impaired adipogenesis and dysfunctional adipose tissue in human hypertrophic obesity. *Physiological reviews.* 2018;98(4):1911-41.
70. Kim J-Y, Van De Wall E, Laplante M, Azzara A, Trujillo ME, Hofmann SM, et al. Obesity-associated improvements in metabolic profile through expansion of adipose tissue. *The Journal of clinical investigation.* 2007;117(9):2621-37.
71. Lu Q, Li M, Zou Y, and Cao T. Induction of adipocyte hyperplasia in subcutaneous fat depot alleviated type 2 diabetes symptoms in obese mice. *Obesity.* 2014;22(7):1623-31.
72. Wang QA, Tao C, Gupta RK, and Scherer PE. Tracking adipogenesis during white adipose tissue development, expansion and regeneration. *Nature medicine.* 2013;19(10):1338-44.

73. Allister CA, Liu L-f, Lamendola CA, Craig CM, Cushman SW, Hellerstein MK, et al. In vivo 2H2O administration reveals impaired triglyceride storage in adipose tissue of insulin-resistant humans1. *Journal of lipid research.* 2015;56(2):435-9.
74. Ghaben AL, and Scherer PE. Adipogenesis and metabolic health. *Nature reviews Molecular cell biology.* 2019;20(4):242-58.
75. Christodoulides C, Lagathu C, Sethi JK, and Vidal-Puig A. Adipogenesis and WNT signalling. *Trends in Endocrinology & Metabolism.* 2009;20(1):16-24.
76. Lotta LA, Gulati P, Day FR, Payne F, Ongen H, Van De Bunt M, et al. Integrative genomic analysis implicates limited peripheral adipose storage capacity in the pathogenesis of human insulin resistance. *Nature genetics.* 2017;49(1):17-26.
77. Chu AY, Deng X, Fisher VA, Drong A, Zhang Y, Feitosa MF, et al. Multiethnic genome-wide meta-analysis of ectopic fat depots identifies loci associated with adipocyte development and differentiation. *Nature genetics.* 2017;49(1):125-30.
78. Isakson P, Hammarstedt A, Gustafson B, and Smith U. Impaired preadipocyte differentiation in human abdominal obesity: role of Wnt, tumor necrosis factor-α, and inflammation. *Diabetes.* 2009;58(7):1550-7.
79. Majithia AR, Flannick J, Shahinian P, Guo M, Bray M-A, Fontanillas P, et al. Rare variants in PPARG with decreased activity in adipocyte differentiation are associated with increased risk of type 2 diabetes. *Proceedings of the National Academy of Sciences.* 2014;111(36):13127-32.
80. Tang W, Zeve D, Suh JM, Bosnakovski D, Kyba M, Hammer RE, et al. White fat progenitor cells reside in the adipose vasculature. *Science.* 2008;322(5901):583-6.
81. Hausman G, and Richardson R. Adipose tissue angiogenesis. *Journal of animal science.* 2004;82(3):925-34.
82. Lijnen HR. Angiogenesis and obesity. *Cardiovascular research.* 2008;78(2):286-93.
83. Lee YS, Kim J-w, Osborne O, Sasik R, Schenk S, Chen A, et al. Increased adipocyte O2 consumption triggers HIF-1α, causing inflammation and insulin resistance in obesity. *Cell.* 2014;157(6):1339-52.

84. Xue Y, Petrovic N, Cao R, Larsson O, Lim S, Chen S, et al. Hypoxia-independent angiogenesis in adipose tissues during cold acclimation. *Cell metabolism.* 2009;9(1):99-109.
85. Zhang Q-X, Magovern CJ, Mack CA, Budenbender KT, Ko W, and Rosengart TK. Vascular endothelial growth factor is the major angiogenic factor in omentum: mechanism of the omentum-mediated angiogenesis. *Journal of Surgical Research.* 1997;67(2):147-54.
86. Tam J, Duda DG, Perentes JY, Quadri RS, Fukumura D, and Jain RK. Blockade of VEGFR2 and not VEGFR1 can limit diet-induced fat tissue expansion: role of local versus bone marrow-derived endothelial cells. *PloS one.* 2009;4(3):e4974.
87. Sun K, Asterholm IW, Kusminski CM, Bueno AC, Wang ZV, Pollard JW, et al. Dichotomous effects of VEGF-A on adipose tissue dysfunction. *Proceedings of the National Academy of Sciences.* 2012;109(15):5874-9.
88. Sung H-K, Doh K-O, Son JE, Park JG, Bae Y, Choi S, et al. Adipose vascular endothelial growth factor regulates metabolic homeostasis through angiogenesis. *Cell metabolism.* 2013;17(1):61-72.
89. Bråkenhielm E, Cao R, Gao B, Angelin B, Cannon B, Parini P, et al. Angiogenesis inhibitor, TNP-470, prevents diet-induced and genetic obesity in mice. *Circulation research.* 2004;94(12):1579-88.
90. Mammoto T, Jiang A, Jiang E, and Mammoto A. Role of Twist1 phosphorylation in angiogenesis and pulmonary fibrosis. *American journal of respiratory cell and molecular biology.* 2016;55(5):633-44.
91. Rupnick MA, Panigrahy D, Zhang C-Y, Dallabrida SM, Lowell BB, Langer R, et al. Adipose tissue mass can be regulated through the vasculature. *Proceedings of the National Academy of Sciences.* 2002;99(16):10730-5.
92. Hunyenyiwa T, Hendee K, Matus K, Kyi P, Mammoto T, and Mammoto A. Obesity Inhibits Angiogenesis Through TWIST1-SLIT2 Signaling. *Frontiers in cell and developmental biology.* 2021;9.
93. Fujisaka S, Usui I, Ikutani M, Aminuddin A, Takikawa A, Tsuneyama K, et al. Adipose tissue hypoxia induces inflammatory M1 polarity of macrophages in an

HIF-1α-dependent and HIF-1α-independent manner in obese mice. *Diabetologia.* 2013;56(6):1403-12.

94. Williams AS, Kang L, and Wasserman DH. The extracellular matrix and insulin resistance. *Trends in Endocrinology & Metabolism.* 2015;26(7):357-66.
95. Hynes RO. The extracellular matrix: not just pretty fibrils. *Science.* 2009;326(5957):1216-9.
96. Chun T-H. Peri-adipocyte ECM remodeling in obesity and adipose tissue fibrosis. *Adipocyte.* 2012;1(2):89-95.
97. Kos K, Wong S, Tan B, Gummesson A, Jernas M, Franck N, et al. Regulation of the fibrosis and angiogenesis promoter SPARC/osteonectin in human adipose tissue by weight change, leptin, insulin, and glucose. *Diabetes.* 2009;58(8):1780-8.
98. Ryan MC, and Christiano AM. The functions of laminins: lessons from in vivo studies. *Matrix biology.* 1996;15(6):369-81.
99. Pasarica M, Gowronska-Kozak B, Burk D, Remedios I, Hymel D, Gimble J, et al. Adipose tissue collagen VI in obesity. *The Journal of Clinical Endocrinology & Metabolism.* 2009;94(12):5155-62.
100. Buechler C, Krautbauer S, and Eisinger K. Adipose tissue fibrosis. *World journal of diabetes.* 2015;6(4):548.
101. Bonnans C, Chou J, and Werb Z. Remodelling the extracellular matrix in development and disease. *Nature reviews Molecular cell biology.* 2014;15(12):786-801.
102. Christiaens V, and Lijnen HR. Role of the fibrinolytic and matrix metalloproteinase systems in development of adipose tissue. *Archives of physiology and biochemistry.* 2006;112(4-5):254-9.
103. Marcelin G, Silveira ALM, Martins LB, Ferreira AV, and Clément K. Deciphering the cellular interplays underlying obesity-induced adipose tissue fibrosis. *The Journal of clinical investigation.* 2019;129(10):4032-40.
104. Sun K, Tordjman J, Clément K, and Scherer PE. Fibrosis and adipose tissue dysfunction. *Cell metabolism.* 2013;18(4):470-7.

105. Khan T, Muise ES, Iyengar P, Wang ZV, Chandalia M, Abate N, et al. Metabolic dysregulation and adipose tissue fibrosis: role of collagen VI. *Molecular and cellular biology.* 2009;29(6):1575-91.
106. Chun T-H, Inoue M, Morisaki H, Yamanaka I, Miyamoto Y, Okamura T, et al. Genetic link between obesity and MMP14-dependent adipogenic collagen turnover. *Diabetes.* 2010;59(10):2484-94.
107. Traurig MT, Permana PA, Nair S, Kobes S, Bogardus C, and Baier LJ. Differential expression of matrix metalloproteinase 3 (MMP3) in preadipocytes/stromal vascular cells from nonobese nondiabetic versus obese nondiabetic Pima Indians. *Diabetes.* 2006;55(11):3160-5.
108. Tinahones FJ, Coín-Aragüez L, Mayas MD, Garcia-Fuentes E, Hurtado-del-Pozo C, Vendrell J, et al. Obesity-associated insulin resistance is correlated to adipose tissue vascular endothelial growth factors and metalloproteinase levels. *BMC physiology.* 2012;12(1):1-8.
109. Henegar C, Tordjman J, Achard V, Lacasa D, Cremer I, Guerre-Millo M, et al. Adipose tissue transcriptomic signature highlights the pathological relevance of extracellular matrix in human obesity. *Genome biology.* 2008;9(1):1-32.
110. Spencer M, Yao-Borengasser A, Unal R, Rasouli N, Gurley CM, Zhu B, et al. Adipose tissue macrophages in insulin-resistant subjects are associated with collagen VI and fibrosis and demonstrate alternative activation. *American Journal of Physiology-Endocrinology and Metabolism.* 2010.
111. Lumeng CN, Bodzin JL, and Saltiel AR. Obesity induces a phenotypic switch in adipose tissue macrophage polarization. *The Journal of clinical investigation.* 2007;117(1):175-84.
112. Weisberg SP, McCann D, Desai M, Rosenbaum M, Leibel RL, and Ferrante AW. Obesity is associated with macrophage accumulation in adipose tissue. *The Journal of clinical investigation.* 2003;112(12):1796-808.
113. Xu H, Barnes GT, Yang Q, Tan G, Yang D, Chou CJ, et al. Chronic inflammation in fat plays a crucial role in the development of obesity-related insulin resistance. *The Journal of clinical investigation.* 2003;112(12):1821-30.

114. Gundra UM, Girgis NM, Ruckerl D, Jenkins S, Ward LN, Kurtz ZD, et al. Alternatively activated macrophages derived from monocytes and tissue macrophages are phenotypically and functionally distinct. *Blood, The Journal of the American Society of Hematology.* 2014;123(20):e110-e22.
115. Shaul ME, Bennett G, Strissel KJ, Greenberg AS, and Obin MS. Dynamic, M2-like remodeling phenotypes of CD11c+ adipose tissue macrophages during high-fat diet–induced obesity in mice. *Diabetes.* 2010;59(5):1171-81.
116. Kratz M, Coats BR, Hisert KB, Hagman D, Mutskov V, Peris E, et al. Metabolic dysfunction drives a mechanistically distinct proinflammatory phenotype in adipose tissue macrophages. *Cell metabolism.* 2014;20(4):614-25.
117. Pandolfi JB, Ferraro AA, Sananez I, Gancedo MC, Baz P, Billordo LA, et al. ATP-induced inflammation drives tissue-resident Th17 cells in metabolically unhealthy obesity. *The Journal of Immunology.* 2016;196(8):3287-96.
118. Hotamisligil GS, Shargill NS, and Spiegelman BM. Adipose expression of tumor necrosis factor-alpha: direct role in obesity-linked insulin resistance. *Science.* 1993;259(5091):87-91.
119. Lumeng CN, and Saltiel AR. Inflammatory links between obesity and metabolic disease. *The Journal of clinical investigation.* 2011;121(6):2111-7.
120. Olefsky JM, and Glass CK. Macrophages, inflammation, and insulin resistance. *Annual review of physiology.* 2010;72:219-46.
121. Ahmed B, Sultana R, and Greene MW. Adipose tissue and insulin resistance in obese. *Biomedicine & Pharmacotherapy.* 2021;137:111315.
122. Rotter V, Nagaev I, and Smith U. Interleukin-6 (IL-6) induces insulin resistance in 3T3-L1 adipocytes and is, like IL-8 and tumor necrosis factor-α, overexpressed in human fat cells from insulin-resistant subjects. *Journal of Biological Chemistry.* 2003;278(46):45777-84.
123. Weisberg SP, Hunter D, Huber R, Lemieux J, Slaymaker S, Vaddi K, et al. CCR2 modulates inflammatory and metabolic effects of high-fat feeding. *The Journal of clinical investigation.* 2006;116(1):115-24.

124. Lee YS, Li P, Huh JY, Hwang IJ, Lu M, Kim JI, et al. Inflammation is necessary for long-term but not short-term high-fat diet–induced insulin resistance. *Diabetes.* 2011;60(10):2474-83.
125. Asterholm IW, Tao C, Morley TS, Wang QA, Delgado-Lopez F, Wang ZV, et al. Adipocyte inflammation is essential for healthy adipose tissue expansion and remodeling. *Cell metabolism.* 2014;20(1):103-18.
126. Xu X, Grijalva A, Skowronski A, van Eijk M, Serlie MJ, and Ferrante Jr AW. Obesity activates a program of lysosomal-dependent lipid metabolism in adipose tissue macrophages independently of classic activation. *Cell metabolism.* 2013;18(6):816-30.
127. Caslin HL, Bhanot M, Bolus WR, and Hasty AH. Adipose tissue macrophages: Unique polarization and bioenergetics in obesity. *Immunological reviews.* 2020;295(1):101-13.
128. Cedikova M, Kripnerová M, Dvorakova J, Pitule P, Grundmanova M, Babuska V, et al. Mitochondria in white, brown, and beige adipocytes. *Stem cells international.* 2016;2016.
129. De Pauw A, Tejerina S, Raes M, Keijer J, and Arnould T. Mitochondrial (dys) function in adipocyte (de) differentiation and systemic metabolic alterations. *The American journal of pathology.* 2009;175(3):927-39.
130. Heinonen S, Jokinen R, Rissanen A, and Pietiläinen KH. White adipose tissue mitochondrial metabolism in health and in obesity. *Obesity Reviews.* 2020;21(2).
131. Kusminski CM, and Scherer PE. Mitochondrial dysfunction in white adipose tissue. *Trends in endocrinology & metabolism.* 2012;23(9):435-43.
132. Rosen ED, and Spiegelman BM. PPARγ: a nuclear regulator of metabolism, differentiation, and cell growth. *Journal of Biological Chemistry.* 2001;276(41):37731-4.
133. Rosen ED, and Spiegelman BM. Molecular regulation of adipogenesis. *Annual review of cell and developmental biology.* 2000;16(1):145-71.
134. Vankoningsloo S, De Pauw A, Houbion A, Tejerina S, Demazy C, de Longueville F, et al. CREB activation induced by mitochondrial dysfunction triggers triglyceride

accumulation in 3T3-L1 preadipocytes. *Journal of cell science.* 2006;119(7):1266-82.

135. Kajimoto K, Terada H, Baba Y, and Shinohara Y. Essential role of citrate export from mitochondria at early differentiation stage of 3T3-L1 cells for their effective differentiation into fat cells, as revealed by studies using specific inhibitors of mitochondrial di-and tricarboxylate carriers. *Molecular genetics and metabolism.* 2005;85(1):46-53.
136. Tormos KV, Anso E, Hamanaka RB, Eisenbart J, Joseph J, Kalyanaraman B, et al. Mitochondrial complex III ROS regulate adipocyte differentiation. *Cell metabolism.* 2011;14(4):537-44.
137. Newsholme P, Cruzat VF, Keane KN, Carlessi R, and de Bittencourt Jr PIH. Molecular mechanisms of ROS production and oxidative stress in diabetes. *Biochemical Journal.* 2016;473(24):4527-50.
138. Rani V, Deep G, Singh RK, Palle K, and Yadav UC. Oxidative stress and metabolic disorders: Pathogenesis and therapeutic strategies. *Life sciences.* 2016;148:183-93.
139. Kono T, Robinson FW, Blevins TL, and Ezaki O. Evidence that translocation of the glucose transport activity is the major mechanism of insulin action on glucose transport in fat cells. *Journal of Biological Chemistry.* 1982;257(18):10942-7.
140. May JM, and De Haen C. Insulin-stimulated intracellular hydrogen peroxide production in rat epididymal fat cells. *Journal of Biological Chemistry.* 1979;254(7):2214-20.
141. Heinonen S, Buzkova J, Muniandy M, Kaksonen R, Ollikainen M, Ismail K, et al. Impaired mitochondrial biogenesis in adipose tissue in acquired obesity. *Diabetes.* 2015;64(9):3135-45.
142. Yin X, Lanza IR, Swain JM, Sarr MG, Nair KS, and Jensen MD. Adipocyte mitochondrial function is reduced in human obesity independent of fat cell size. *The Journal of Clinical Endocrinology & Metabolism.* 2014;99(2):E209-E16.
143. Xu XJ, Gauthier M-S, Hess DT, Apovian CM, Cacicedo JM, Gokce N, et al. Insulin sensitive and resistant obesity in humans: AMPK activity, oxidative stress, and

depot-specific changes in gene expression in adipose tissue. *Journal of lipid research.* 2012;53(4):792-801.

144. Koh EH, Park J-Y, Park H-S, Jeon MJ, Ryu JW, Kim M, et al. Essential role of mitochondrial function in adiponectin synthesis in adipocytes. *Diabetes.* 2007;56(12):2973-81.
145. Carrière A, Carmona M-C, Fernandez Y, Rigoulet M, Wenger RH, Pénicaud L, et al. Mitochondrial reactive oxygen species control the transcription factor CHOP-10/GADD153 and adipocyte differentiation: a mechanism for hypoxia-dependent effect. *Journal of Biological Chemistry.* 2004;279(39):40462-9.
146. Carrière A, Fernandez Y, Rigoulet M, Pénicaud L, and Casteilla L. Inhibition of preadipocyte proliferation by mitochondrial reactive oxygen species. *FEBS letters.* 2003;550(1-3):163-7.
147. Porte Jr D, Baskin DG, and Schwartz MW. Leptin and insulin action in the central nervous system. *Nutrition reviews.* 2002;60(suppl_10):S20-S9.
148. Ryu V, and Bartness TJ. Short and long sympathetic-sensory feedback loops in white fat. *American Journal of Physiology-Regulatory, Integrative and Comparative Physiology.* 2014;306(12):R886-R900.
149. Garretson JT, Szymanski LA, Schwartz GJ, Xue B, Ryu V, and Bartness TJ. Lipolysis sensation by white fat afferent nerves triggers brown fat thermogenesis. *Molecular metabolism.* 2016;5(8):626-34.
150. Chi J, Wu Z, Choi CHJ, Nguyen L, Tegegne S, Ackerman SE, et al. Three-dimensional adipose tissue imaging reveals regional variation in beige fat biogenesis and PRDM16-dependent sympathetic neurite density. *Cell metabolism.* 2018;27(1):226-36. e3.
151. Johnson M, Young AD, and Marriott I. The therapeutic potential of targeting substance P/NK-1R interactions in inflammatory CNS disorders. *Frontiers in cellular neuroscience.* 2017;10:296.
152. Russell FA, King R, Smillie S-J, Kodji X, and Brain S. Calcitonin gene-related peptide: physiology and pathophysiology. *Physiological reviews.* 2014;94(4):1099-142.

153. Bartness TJ, Liu Y, Shrestha YB, and Ryu V. Neural innervation of white adipose tissue and the control of lipolysis. *Frontiers in neuroendocrinology.* 2014;35(4):473-93.
154. Kuo LE, Kitlinska JB, Tilan JU, Li L, Baker SB, Johnson MD, et al. Neuropeptide Y acts directly in the periphery on fat tissue and mediates stress-induced obesity and metabolic syndrome. *Nature medicine.* 2007;13(7):803-11.
155. Burnstock G, and Gentile D. The involvement of purinergic signalling in obesity. *Purinergic signalling.* 2018;14(2):97-108.
156. Wang P, Loh KH, Wu M, Morgan DA, Schneeberger M, Yu X, et al. A leptin–BDNF pathway regulating sympathetic innervation of adipose tissue. *Nature.* 2020;583(7818):839-44.
157. Xanthos DN, and Sandkühler J. Neurogenic neuroinflammation: inflammatory CNS reactions in response to neuronal activity. *Nature Reviews Neuroscience.* 2014;15(1):43-53.
158. Scherer T, O'Hare J, Diggs-Andrews K, Schweiger M, Cheng B, Lindtner C, et al. Brain insulin controls adipose tissue lipolysis and lipogenesis. *Cell metabolism.* 2011;13(2):183-94.
159. Oral EA. Lipoatrophic diabetes and other related syndromes. *Reviews in Endocrine and Metabolic Disorders.* 2003;4(1):61-77.
160. Schweiger M, Eichmann TO, Taschler U, Zimmermann R, Zechner R, and Lass A. Measurement of lipolysis. *Methods in enzymology.* 2014;538:171-93.
161. Arner P, and Langin D. Lipolysis in lipid turnover, cancer cachexia, and obesity-induced insulin resistance. *Trends in Endocrinology & Metabolism.* 2014;25(5):255-62.
162. Watt MJ, Steinberg GR, Chan S, Garnham A, Kemp BE, and Febbraio MA. β-adrenergic stimulation of skeletal muscle HSL can be overridden by AMPK signaling. *The FASEB journal.* 2004;18(12):1445-6.
163. Greenberg AS, Shen W-J, Muliro K, Patel S, Souza SC, Roth RA, et al. Stimulation of lipolysis and hormone-sensitive lipase via the extracellular signal-regulated kinase pathway. *Journal of Biological Chemistry.* 2001;276(48):45456-61.

164. Choi SM, Tucker DF, Gross DN, Easton RM, DiPilato LM, Dean AS, et al. Insulin regulates adipocyte lipolysis via an Akt-independent signaling pathway. *Molecular and cellular biology.* 2010;30(21):5009-20.
165. Degerman E, Smith CJ, Tornqvist H, Vasta V, Belfrage P, and Manganiello V. Evidence that insulin and isoprenaline activate the cGMP-inhibited low-Km cAMP phosphodiesterase in rat fat cells by phosphorylation. *Proceedings of the National Academy of Sciences.* 1990;87(2):533-7.
166. Langin D, and Arner P. Importance of TNFα and neutral lipases in human adipose tissue lipolysis. *Trends in Endocrinology & Metabolism.* 2006;17(8):314-20.
167. Ryden M, and Arner P. Tumour necrosis factor-α in human adipose tissue–from signalling mechanisms to clinical implications. *Journal of internal medicine.* 2007;262(4):431-8.
168. Yang X, Zhang X, Heckmann BL, Lu X, and Liu J. Relative contribution of adipose triglyceride lipase and hormone-sensitive lipase to tumor necrosis factor-α (TNF-α)-induced lipolysis in adipocytes. *Journal of Biological Chemistry.* 2011;286(47):40477-85.
169. Wang H, and Eckel RH. Lipoprotein lipase: from gene to obesity. *American Journal of Physiology-Endocrinology and Metabolism.* 2009;297(2):E271-E88.
170. Campbell PJ, Carlson MG, Hill J, and Nurjhan N. Regulation of free fatty acid metabolism by insulin in humans: role of lipolysis and reesterification. *American Journal of Physiology-Endocrinology And Metabolism.* 2006;263(6):E1063-E9.
171. Coleman RA, and Lee DP. Enzymes of triacylglycerol synthesis and their regulation. *Progress in lipid research.* 2004;43(2):134-76.
172. Yen C-LE, Stone SJ, Koliwad S, Harris C, and Farese RV. Thematic review series: glycerolipids. DGAT enzymes and triacylglycerol biosynthesis. *Journal of lipid research.* 2008;49(11):2283-301.
173. Brunzell JD, Schwartz RS, Eckel RH, and Goldberg AP. Insulin and adipose tissue lipoprotein lipase activity in humans. *International journal of obesity.* 1981;5(6):685-94.

174. Bódis K, and Roden M. Energy metabolism of white adipose tissue and insulin resistance in humans. *European journal of clinical investigation.* 2018;48(11):e13017.
175. Reilly SM, Hung C-W, Ahmadian M, Zhao P, Keinan O, Gomez AV, et al. Catecholamines suppress fatty acid re-esterification and increase oxidation in white adipocytes via STAT3. *Nature metabolism.* 2020;2(7):620-34.
176. McDevitt RM, Bott SJ, Harding M, Coward WA, Bluck LJ, and Prentice AM. De novo lipogenesis during controlled overfeeding with sucrose or glucose in lean and obese women. *The American journal of clinical nutrition.* 2001;74(6):737-46.
177. Riemens S, Sluiter W, and Dullaart R. Enhanced escape of non-esterified fatty acids from tissue uptake: its role in impaired insulin-induced lowering of total rate of appearance in obesity and Type II diabetes mellitus. *Diabetologia.* 2000;43(4):416-26.
178. Coppack S, Evans R, Fisher R, Frayn K, Gibbons G, Humphreys S, et al. Adipose tissue metabolism in obesity: lipase action in vivo before and after a mixed meal. *Metabolism.* 1992;41(3):264-72.
179. Frayn K, Humphreys S, and Coppack S. Net carbon flux across subcutaneous adipose tissue after a standard meal in normal-weight and insulin-resistant obese subjects. *International journal of obesity and related metabolic disorders: journal of the International Association for the Study of Obesity.* 1996;20(9):795-800.
180. McQuaid SE, Hodson L, Neville MJ, Dennis AL, Cheeseman J, Humphreys SM, et al. Downregulation of adipose tissue fatty acid trafficking in obesity: a driver for ectopic fat deposition? *Diabetes.* 2011;60(1):47-55.
181. Stinkens R, Goossens GH, Jocken JW, and Blaak EE. Targeting fatty acid metabolism to improve glucose metabolism. *Obesity Reviews.* 2015;16(9):715-57.
182. Tuvdendorj D, Chandalia M, Batbayar T, Saraf M, Beysen C, Murphy EJ, et al. Altered subcutaneous abdominal adipose tissue lipid synthesis in obese, insulin-resistant humans. *American Journal of Physiology-Endocrinology and Metabolism.* 2013;305(8):E999-E1006.
183. Ranganathan G, Unal R, Pokrovskaya I, Yao-Borengasser A, Phanavanh B, Lecka-Czernik B, et al. The lipogenic enzymes DGAT1, FAS, and LPL in adipose

tissue: effects of obesity, insulin resistance, and TZD treatment. *Journal of lipid research.* 2006;47(11):2444-50.

184. Pedersen BK, and Febbraio MA. Muscles, exercise and obesity: skeletal muscle as a secretory organ. *Nature Reviews Endocrinology.* 2012;8(8):457-65.
185. Egan B, and Zierath JR. Exercise metabolism and the molecular regulation of skeletal muscle adaptation. *Cell metabolism.* 2013;17(2):162-84.
186. Richter EA, and Hargreaves M. Exercise, GLUT4, and skeletal muscle glucose uptake. *Physiological reviews.* 2013.
187. Cartee GD. Mechanisms for greater insulin-stimulated glucose uptake in normal and insulin-resistant skeletal muscle after acute exercise. *American journal of physiology-endocrinology and metabolism.* 2015;309(12):E949-E59.
188. Dantas WS, Roschel H, Murai IH, Gil S, Davuluri G, Axelrod CL, et al. Exercise-induced increases in insulin sensitivity after bariatric surgery are mediated by muscle extracellular matrix remodeling. *Diabetes.* 2020;69(8):1675-91.
189. Fabre O, Ingerslev LR, Garde C, Donkin I, Simar D, and Barres R. Exercise training alters the genomic response to acute exercise in human adipose tissue. *Epigenomics.* 2018;10(08):1033-50.
190. Ludzki AC, Krueger EM, Baldwin TC, Schleh MW, Porsche CE, Ryan BJ, et al. Acute aerobic exercise remodels the adipose tissue progenitor cell phenotype in obese adults. *Frontiers in physiology.* 2020;11:903.
191. Contrepois K, Wu S, Moneghetti KJ, Hornburg D, Ahadi S, Tsai M-S, et al. Molecular choreography of acute exercise. *Cell.* 2020;181(5):1112-30. e16.
192. Kershaw EE, and Flier JS. Adipose tissue as an endocrine organ. *The Journal of Clinical Endocrinology & Metabolism.* 2004;89(6):2548-56.
193. Stanford KI, Middelbeek RJ, and Goodyear LJ. Exercise effects on white adipose tissue: beiging and metabolic adaptations. *Diabetes.* 2015;64(7):2361-8.
194. Cannon B, and Nedergaard J. Brown adipose tissue: function and physiological significance. *Physiological reviews.* 2004.
195. Sutherland LN, Bomhof MR, Capozzi LC, Basaraba SAU, and Wright DC. Exercise and adrenaline increase PGC-1α mRNA expression in rat adipose tissue. *The Journal of physiology.* 2009;587(7):1607-17.

196. Trevellin E, Scorzeto M, Olivieri M, Granzotto M, Valerio A, Tedesco L, et al. Exercise training induces mitochondrial biogenesis and glucose uptake in subcutaneous adipose tissue through eNOS-dependent mechanisms. *Diabetes.* 2014;63(8):2800-11.
197. Camera DM, Anderson MJ, Hawley JA, and Carey AL. Short-term endurance training does not alter the oxidative capacity of human subcutaneous adipose tissue. *European journal of applied physiology.* 2010;109(2):307-16.
198. Nakhuda A, Josse AR, Gburcik V, Crossland H, Raymond F, Metairon S, et al. Biomarkers of browning of white adipose tissue and their regulation during exercise-and diet-induced weight loss. *The American journal of clinical nutrition.* 2016;104(3):557-65.
199. Tsiloulis T, Carey AL, Bayliss J, Canny B, Meex RC, and Watt MJ. No evidence of white adipocyte browning after endurance exercise training in obese men. *International journal of obesity.* 2018;42(4):721-7.
200. Despres J, Bouchard C, Savard R, Tremblay A, Marcotte M, and Theriault G. The effect of a 20-week endurance training program on adipose-tissue morphology and lipolysis in men and women. *Metabolism.* 1984;33(3):235-9.
201. Kolahdouzi S, Talebi-Garakani E, Hamidian G, and Safarzade A. Exercise training prevents high-fat diet-induced adipose tissue remodeling by promoting capillary density and macrophage polarization. *Life sciences.* 2019;220:32-43.
202. Gollisch KSC, Brandauer J, Jessen N, Toyoda T, Nayer A, Hirshman MF, et al. Effects of exercise training on subcutaneous and visceral adipose tissue in normal- and high-fat diet-fed rats. *American Journal of Physiology-Endocrinology and Metabolism.* 2009;297(2):E495-E504.
203. Marker JC, Hirsch I, Smith LJ, Parvin C, Holloszy J, and Cryer P. Catecholamines in prevention of hypoglycemia during exercise in humans. *American Journal of Physiology-Endocrinology And Metabolism.* 1991;260(5):E705-E12.
204. Laurens C, De Glisezinski I, Larrouy D, Harant I, and Moro C. Influence of Acute and Chronic Exercise on Abdominal Fat Lipolysis: An Update. *Frontiers in Physiology.* 2020;11:1606.

205. Coggan AR, Raguso CA, Gastaldelli A, Sidossis LS, and Yeckel CW. Fat metabolism during high-intensity exercise in endurance-trained and untrained men. *Metabolism.* 2000;49(1):122-8.
206. Stich V, De Glisezinski I, Crampes F, Hejnova J, Cottet-Emard J-M, Galitzky J, et al. Activation of α2-adrenergic receptors impairs exercise-induced lipolysis in SCAT of obese subjects. *American Journal of Physiology-Regulatory, Integrative and Comparative Physiology.* 2000;279(2):R499-R504.
207. Ryden M, Bäckdahl J, Petrus P, Thorell A, Gao H, Coue M, et al. Impaired atrial natriuretic peptide-mediated lipolysis in obesity. *International Journal of Obesity.* 2016;40(4):714-20.
208. Mauriege P, Prud'Homme D, Marcotte M, Yoshioka M, Tremblay A, and Despres J. Regional differences in adipose tissue metabolism between sedentary and endurance-trained women. *American Journal of Physiology-Endocrinology And Metabolism.* 1997;273(3):E497.
209. Riviere D, Crampes F, Beauville M, and Garrigues M. Lipolytic response of fat cells to catecholamines in sedentary and exercise-trained women. *Journal of Applied Physiology.* 1989;66(1):330-5.
210. Crampes F, Riviere D, Beauville M, Marceron M, and Garrigues M. Lipolytic response of adipocytes to epinephrine in sedentary and exercise-trained subjects: sex-related differences. *European journal of applied physiology and occupational physiology.* 1989;59(4):249-55.
211. Horowitz JF, Braudy RJ, Martin Iii WH, and Klein S. Endurance exercise training does not alter lipolytic or adipose tissue blood flow sensitivity to epinephrine. *American Journal of Physiology-Endocrinology And Metabolism.* 1999.
212. Riis S, Christensen B, Nellemann B, Møller AB, Husted AS, Pedersen SB, et al. Molecular adaptations in human subcutaneous adipose tissue after ten weeks of endurance exercise training in healthy males. *Journal of Applied Physiology.* 2019;126(3):569-77.
213. Crampes F, Beauville M, Riviere D, and Garrigues M. Effect of physical training in humans on the response of isolated fat cells to epinephrine. *Journal of Applied Physiology.* 1986;61(1):25-9.

214. Garritson JD, and Boudina S. The Effects of Exercise on White and Brown Adipose Tissue Cellularity, Metabolic Activity and Remodeling. *Frontiers in physiology.* 2021:1938.
215. Kawanishi N, Yano H, Yokogawa Y, and Suzuki K. Exercise training inhibits inflammation in adipose tissue via both suppression of macrophage infiltration and acceleration of phenotypic switching from M1 to M2 macrophages in high-fat-diet-induced obese mice. *Exercise immunology review.* 2010;16.
216. Hayashino Y, Jackson JL, Hirata T, Fukumori N, Nakamura F, Fukuhara S, et al. Effects of exercise on C-reactive protein, inflammatory cytokine and adipokine in patients with type 2 diabetes: a meta-analysis of randomized controlled trials. *Metabolism.* 2014;63(3):431-40.
217. Perry CG, Lally J, Holloway GP, Heigenhauser GJ, Bonen A, and Spriet LL. Repeated transient mRNA bursts precede increases in transcriptional and mitochondrial proteins during training in human skeletal muscle. *The Journal of physiology.* 2010;588(23):4795-810.
218. Mahoney D, Parise G, Melov S, Safdar A, and Tarnopolsky M. Analysis of global mRNA expression in human skeletal muscle during recovery from endurance exercise. *The FASEB journal.* 2005;19(11):1498-500.
219. Pilegaard H, Saltin B, and Neufer PD. Wiley Online Library; 2003.
220. Brandao CFC, de Carvalho FG, Souza AdO, Junqueira-Franco MVM, Batitucci G, Couto-Lima CA, et al. Physical training, UCP1 expression, mitochondrial density, and coupling in adipose tissue from women with obesity. *Scandinavian journal of medicine & science in sports.* 2019;29(11):1699-706.
221. Matta L, Fonseca TS, Faria CC, Lima-Junior NC, De Oliveira DF, Maciel L, et al. The effect of acute aerobic exercise on redox homeostasis and mitochondrial function of rat white adipose tissue. *Oxidative Medicine and Cellular Longevity.* 2021;2021.
222. Khalafi M, Mohebbi H, Symonds ME, Karimi P, Akbari A, Tabari E, et al. The impact of moderate-intensity continuous or high-intensity interval training on adipogenesis and browning of subcutaneous adipose tissue in obese male rats. *Nutrients.* 2020;12(4):925.

223. Swain DP, and Leutholtz BC. Heart rate reserve is equivalent to% VO2 reserve, not to% VO2max. *Medicine and science in sports and exercise.* 1997;29(3):410-4.
224. Harrow J, Frankish A, Gonzalez JM, Tapanari E, Diekhans M, Kokocinski F, et al. GENCODE: the reference human genome annotation for The ENCODE Project. *Genome research.* 2012;22(9):1760-74.
225. Langmead B, Trapnell C, Pop M, and Salzberg SL. Ultrafast and memory-efficient alignment of short DNA sequences to the human genome. *Genome biology.* 2009;10(3):1-10.
226. Jiang H, and Wong WH. Statistical inferences for isoform expression in RNA-Seq. *Bioinformatics.* 2009;25(8):1026-32.
227. Salzman J, Jiang H, and Wong WH. Statistical modeling of RNA-Seq data. *Statistical science: a review journal of the Institute of Mathematical Statistics.* 2011;26(1).
228. Love MI, Huber W, and Anders S. Moderated estimation of fold change and dispersion for RNA-seq data with DESeq2. *Genome biology.* 2014;15(12):1-21.
229. Hohorst H-J. Determination of L-lactate with LDH and DPN. *Methods of enzymatic analysis.* 1965:265-70.
230. Dill DB, and Costill DL. Calculation of percentage changes in volumes of blood, plasma, and red cells in dehydration. *Journal of applied physiology.* 1974;37(2):247-8.
231. Alis R, Sanchis-Gomar F, Primo-Carrau C, Lozano-Calve S, Dipalo M, Aloe R, et al. Hemoconcentration induced by exercise: Revisiting the D ill and C ostill equation. *Scandinavian journal of medicine & science in sports.* 2015;25(6):e630-e7.
232. Asher G, and Sassone-Corsi P. Time for food: the intimate interplay between nutrition, metabolism, and the circadian clock. *Cell.* 2015;161(1):84-92.
233. Anafi RC, Lee Y, Sato TK, Venkataraman A, Ramanathan C, Kavakli IH, et al. Machine learning helps identify CHRONO as a circadian clock component. *PLoS biology.* 2014;12(4):e1001840.

234. Gekakis N, Staknis D, Nguyen HB, Davis FC, Wilsbacher LD, King DP, et al. Role of the CLOCK protein in the mammalian circadian mechanism. *Science.* 1998;280(5369):1564-9.
235. Macpherson RE, Huber JS, Frendo-Cumbo S, Simpson JA, and Wright DC. Adipose tissue insulin action and IL-6 signaling after exercise in obese mice. *Medicine & Science in Sports & Exercise.* 2015;47(10):2034-42.
236. Castellani L, Perry CG, Macpherson RE, Root-McCaig J, Huber JS, Arkell AM, et al. Exercise-mediated IL-6 signaling occurs independent of inflammation and is amplified by training in mouse adipose tissue. *Journal of Applied Physiology.* 2015;119(11):1347-54.
237. Keller C, Keller P, Marshal S, and Pedersen BK. IL-6 gene expression in human adipose tissue in response to exercise–Effect of carbohydrate ingestion. *The Journal of physiology.* 2003;550(3):927-31.
238. Hodgetts V, Coppack SW, Frayn KN, and Hockaday T. Factors controlling fat mobilization from human subcutaneous adipose tissue during exercise. *Journal of Applied Physiology.* 1991;71(2):445-51.
239. Yu C, Chen Y, Cline GW, Zhang D, Zong H, Wang Y, et al. Mechanism by which fatty acids inhibit insulin activation of insulin receptor substrate-1 (IRS-1)-associated phosphatidylinositol 3-kinase activity in muscle. *Journal of Biological Chemistry.* 2002;277(52):50230-6.
240. Marcinko K, Sikkema SR, Samaan MC, Kemp BE, Fullerton MD, and Steinberg GR. High intensity interval training improves liver and adipose tissue insulin sensitivity. *Molecular metabolism.* 2015;4(12):903-15.
241. Bianco C, and Mohr I. Ribosome biogenesis restricts innate immune responses to virus infection and DNA. *Elife.* 2019;8:e49551.
242. Wang T, Si Y, Shirihai OS, Si H, Schultz V, Corkey RF, et al. Respiration in adipocytes is inhibited by reactive oxygen species. *Obesity.* 2010;18(8):1493-502.
243. Cox KH, and Takahashi JS. Circadian clock genes and the transcriptional architecture of the clock mechanism. *Journal of molecular endocrinology.* 2019;63(4):R93-R102.

244. Goriki A, Hatanaka F, Myung J, Kim JK, Yoritaka T, Tanoue S, et al. A novel protein, CHRONO, functions as a core component of the mammalian circadian clock. *PLoS biology.* 2014;12(4):e1001839.
245. Zhang R, Lahens NF, Ballance HI, Hughes ME, and Hogenesch JB. A circadian gene expression atlas in mammals: implications for biology and medicine. *Proceedings of the National Academy of Sciences.* 2014;111(45):16219-24.
246. Shostak A, Meyer-Kovac J, and Oster H. Circadian regulation of lipid mobilization in white adipose tissues. *Diabetes.* 2013;62(7):2195-203.
247. Paschos GK, Ibrahim S, Song W-L, Kunieda T, Grant G, Reyes TM, et al. Obesity in mice with adipocyte-specific deletion of clock component Arntl. *Nature medicine.* 2012;18(12):1768-77.
248. Bray MS, and Young ME. Circadian rhythms in the development of obesity: potential role for the circadian clock within the adipocyte. *Obesity reviews.* 2007;8(2):169-81.
249. Hunter AL, Pelekanou CE, Barron NJ, Northeast RC, Grudzien M, Adamson AD, et al. Adipocyte NR1D1 dictates adipose tissue expansion during obesity. *Elife.* 2021;10:e63324.
250. Nielsen KN, Peics J, Ma T, Karavaeva I, Dall M, Chubanava S, et al. NAMPT-mediated NAD+ biosynthesis is indispensable for adipose tissue plasticity and development of obesity. *Molecular metabolism.* 2018;11:178-88.
251. Dreher SI, Irmler M, Pivovarova-Ramich O, Kessler K, Jürchott K, Sticht C, et al. Acute and long-term exercise adaptation of adipose tissue and skeletal muscle in humans: a matched transcriptomics approach after 8-week training-intervention. *International Journal of Obesity.* 2023;47(4):313-24.
252. Strączkowski M, Stefanowicz M, Nikołajuk A, and Karczewska-Kupczewska M. Subcutaneous adipose tissue circadian gene expression: Relationship with insulin sensitivity, obesity, and the effect of weight-reducing dietary intervention. *Nutrition.* 2023;115:112153.
253. Dollet L, and Zierath JR. Interplay between diet, exercise and the molecular circadian clock in orchestrating metabolic adaptations of adipose tissue. *The Journal of Physiology.* 2019;597(6):1439-50.

254. Pivovarova O, Gögebakan Ö, Sucher S, Groth J, Murahovschi V, Kessler K, et al. Regulation of the clock gene expression in human adipose tissue by weight loss. *International journal of obesity.* 2016;40(6):899-906.
255. Keller M, Mazuch J, Abraham U, Eom GD, Herzog ED, Volk H-D, et al. A circadian clock in macrophages controls inflammatory immune responses. *Proceedings of the National Academy of Sciences.* 2009;106(50):21407-12.
256. Christiansen T, Bruun JM, Paulsen SK, Ølholm J, Overgaard K, Pedersen SB, et al. Acute exercise increases circulating inflammatory markers in overweight and obese compared with lean subjects. *European journal of applied physiology.* 2013;113:1635-42.
257. Sim M, Dawson B, Landers G, Swinkels DW, Tjalsma H, Trinder D, et al. Effect of exercise modality and intensity on postexercise interleukin-6 and hepcidin levels. *International journal of sport nutrition and exercise metabolism.* 2013;23(2):178-86.
258. Lira FS, Dos Santos T, Caldeira RS, Inoue DS, Panissa VL, Cabral-Santos C, et al. Short-term high-and moderate-intensity training modifies inflammatory and metabolic factors in response to acute exercise. *Frontiers in physiology.* 2017;8:856.
259. MacNeil LG, Tarnopolsky MA, and Crane JD. Acute, exercise-induced alterations in cytokines and chemokines in the blood distinguish physically active and sedentary aging. *The Journals of Gerontology: Series A.* 2021;76(5):811-8.
260. Hu E, Kim JB, Sarraf P, and Spiegelman BM. Inhibition of adipogenesis through MAP kinase-mediated phosphorylation of PPARγ. *Science.* 1996;274(5295):2100-3.
261. Trujillo ME, Lee M-J, Sullivan S, Feng J, Schneider SH, Greenberg AS, et al. Tumor Necrosis Factor α and Glucocorticoid Synergistically Increase Leptin Production in Human Adipose Tissue: Role for p38 Mitogen-Activated Protein Kinase. *The Journal of Clinical Endocrinology & Metabolism.* 2006;91(4):1484-90.
262. Zhang Y, Li R, Meng Y, Li S, Donelan W, Zhao Y, et al. Irisin stimulates browning of white adipocytes through mitogen-activated protein kinase p38 MAP kinase and ERK MAP kinase signaling. *Diabetes.* 2014;63(2):514-25.

263. Stephenson EJ, Lessard SJ, Rivas DA, Watt MJ, Yaspelkis III BB, Koch LG, et al. Exercise training enhances white adipose tissue metabolism in rats selectively bred for low-or high-endurance running capacity. *American Journal of Physiology-Endocrinology and Metabolism.* 2013;305(3):E429-E38.
264. Bost F, Aouadi M, Caron L, and Binétruy B. The role of MAPKs in adipocyte differentiation and obesity. *Biochimie.* 2005;87(1):51-6.
265. Sale E, Atkinson P, and Sale G. Requirement of MAP kinase for differentiation of fibroblasts to adipocytes, for insulin activation of p90 S6 kinase and for insulin or serum stimulation of DNA synthesis. *The EMBO Journal.* 1995;14(4):674-84.
266. Camp HS, and Tafuri SR. Regulation of peroxisome proliferator-activated receptor γ activity by mitogen-activated protein kinase. *Journal of Biological Chemistry.* 1997;272(16):10811-6.
267. Ahn C, Ryan BJ, Gillen JB, Ludzki A, Schleh MW, Reinheimer BA, et al. 721-P: Exercise Training Alters Subcutaneous Adipose Tissue Morphology in Obese Adults Even without Weight Loss. *Diabetes.* 2019;68(Supplement_1).
268. Jia Q, Morgan-Bathke ME, and Jensen MD. Adipose tissue macrophage burden, systemic inflammation, and insulin resistance. *American Journal of Physiology-Endocrinology and Metabolism.* 2020;319(2):E254-E64.
269. Sadler D, Mattacks CA, and Pond CM. Changes in adipocytes and dendritic cells in lymph node containing adipose depots during and after many weeks of mild inflammation. *Journal of anatomy.* 2005;207(6):769-81.
270. Summers LKM, Samra JS, Humphreys SM, Morris RJ, and Frayn KN. Subcutaneous abdominal adipose tissue blood flow: variation within and between subjects and relationship to obesity. *Clinical science.* 1996;91(6):679-83.
271. Després J-P. Abdominal obesity as important component of insulin-resistance syndrome. *Nutrition (Burbank, Los Angeles County, Calif).* 1993;9(5):452-9.
272. ClÉment K, Viguerie N, Poitou C, Carette C, Pelloux V, Curat CA, et al. Weight loss regulates inflammation-related genes in white adipose tissue of obese subjects. *The FASEB Journal.* 2004;18(14):1657-69.

273. Cinti S, Mitchell G, Barbatelli G, Murano I, Ceresi E, Faloia E, et al. Adipocyte death defines macrophage localization and function in adipose tissue of obese mice and humans. *Journal of lipid research.* 2005;46(11):2347-55.
274. Shimomura I, Funahasm T, Takahashi M, Maeda K, Kotani K, Nakamura T, et al. Enhanced expression of PAI–1 in visceral fat: Possible contributor to vascular disease in obeisty. *Nature medicine.* 1996;2(7):800-3.
275. Kern PA, Ranganathan S, Li C, Wood L, and Ranganathan G. Adipose tissue tumor necrosis factor and interleukin-6 expression in human obesity and insulin resistance. *American Journal of Physiology-Endocrinology And Metabolism.* 2001;280(5):E745-E51.
276. Tremblay A, Simoneau J-A, and Bouchard C. Impact of exercise intensity on body fatness and skeletal muscle metabolism. *Metabolism.* 1994;43(7):814-8.
277. Menshikova EV, Ritov VB, Toledo FGS, Ferrell RE, Goodpaster BH, and Kelley DE. Effects of weight loss and physical activity on skeletal muscle mitochondrial function in obesity. *American journal of physiology-endocrinology and metabolism.* 2005;288(4):E818-E25.
278. Ryan BJ, Schleh MW, Ahn C, Ludzki AC, Gillen JB, Varshney P, et al. Moderate-intensity exercise and high-intensity interval training affect insulin sensitivity similarly in obese adults. *The Journal of Clinical Endocrinology & Metabolism.* 2020;105(8):e2941-e59.
279. Hutchison SK, Teede HJ, Rachoń D, Harrison CL, Strauss BJ, and Stepto NK. Effect of exercise training on insulin sensitivity, mitochondria and computed tomography muscle attenuation in overweight women with and without polycystic ovary syndrome. *Diabetologia.* 2012;55(5):1424-34.
280. Ludzki AC, Pataky MW, Cartee GD, and Horowitz JF. Acute endurance exercise increases Vegfa mRNA expression in adipose tissue of rats during the early stages of weight gain. *Applied Physiology, Nutrition, and Metabolism.* 2018;43(7):751-4.
281. Cullberg KB, Christiansen T, Paulsen SK, Bruun JM, Pedersen SB, and Richelsen B. Effect of weight loss and exercise on angiogenic factors in the circulation and in adipose tissue in obese subjects. *Obesity.* 2013;21(3):454-60.

282. Weston KS, Wisløff U, and Coombes JS. High-intensity interval training in patients with lifestyle-induced cardiometabolic disease: a systematic review and meta-analysis. *British journal of sports medicine.* 2014;48(16):1227-34.
283. Shirvani H, and Arabzadeh E. Metabolic cross-talk between skeletal muscle and adipose tissue in high-intensity interval training vs. moderate-intensity continuous training by regulation of PGC-1α. *Eating and Weight Disorders-Studies on Anorexia, Bulimia and Obesity.* 2020;25(1):17-24.
284. Magkos F, Fraterrigo G, Yoshino J, Luecking C, Kirbach K, Kelly SC, et al. Effects of moderate and subsequent progressive weight loss on metabolic function and adipose tissue biology in humans with obesity. *Cell metabolism.* 2016;23(4):591-601.
285. DeFronzo RA, Tobin JD, and Andres R. Glucose clamp technique: a method for quantifying insulin secretion and resistance. *American Journal of Physiology-Endocrinology And Metabolism.* 1979;237(3):E214.
286. Parlee SD, Lentz SI, Mori H, and MacDougald OA. Quantifying size and number of adipocytes in adipose tissue. *Methods in enzymology.* 2014;537:93-122.
287. Moritz CP. Tubulin or not tubulin: heading toward total protein staining as loading control in western blots. *Proteomics.* 2017;17(20):1600189.
288. Newsom SA, Schenk S, Thomas KM, Harber MP, Knuth ND, Goldenberg N, et al. Energy deficit after exercise augments lipid mobilization but does not contribute to the exercise-induced increase in insulin sensitivity. *Journal of applied physiology.* 2010.
289. Laurencikiene J, Skurk T, Kulyté A, Hedén P, Åström G, Sjölin E, et al. Regulation of lipolysis in small and large fat cells of the same subject. *The Journal of Clinical Endocrinology & Metabolism.* 2011;96(12):E2045-E9.
290. Olefsky JM. The effects of spontaneous obesity on insulin binding, glucose transport, and glucose oxidation of isolated rat adipocytes. *The Journal of clinical investigation.* 1976;57(4):842-51.
291. Olefsky JM. Insensitivity of large rat adipocytes to the antilipolytic effects of insulin. *Journal of lipid research.* 1977;18(4):459-64.

292. Despres JP, Pouliot MC, Moorjani S, Nadeau A, Tremblay A, Lupien PJ, et al. Loss of abdominal fat and metabolic response to exercise training in obese women. *American Journal of Physiology-Endocrinology And Metabolism.* 1991;261(2):E159-E67.
293. Américo ALV, Muller CR, Vecchiatto B, Martucci LF, Fonseca-Alaniz MH, and Evangelista FS. Aerobic exercise training prevents obesity and insulin resistance independent of the renin angiotensin system modulation in the subcutaneous white adipose tissue. *PloS one.* 2019;14(4).
294. Divoux A, Tordjman J, Lacasa D, Veyrie N, Hugol D, Aissat A, et al. Fibrosis in human adipose tissue: composition, distribution, and link with lipid metabolism and fat mass loss. *Diabetes.* 2010;59(11):2817-25.
295. Spencer M, Unal R, Zhu B, Rasouli N, McGehee Jr RE, Peterson CA, et al. Adipose tissue extracellular matrix and vascular abnormalities in obesity and insulin resistance. *The Journal of Clinical Endocrinology & Metabolism.* 2011;96(12):E1990-E8.
296. Huang G, Ge G, Wang D, Gopalakrishnan B, Butz DH, Colman RJ, et al. α3 (V) collagen is critical for glucose homeostasis in mice due to effects in pancreatic islets and peripheral tissues. *The Journal of clinical investigation.* 2011;121(2):769-83.
297. Krishnan J, Danzer C, Simka T, Ukropec J, Walter KM, Kumpf S, et al. Dietary obesity-associated Hif1α activation in adipocytes restricts fatty acid oxidation and energy expenditure via suppression of the Sirt2-NAD+ system. *Genes & development.* 2012;26(3):259-70.
298. Pasarica M, Sereda OR, Redman LM, Albarado DC, Hymel DT, Roan LE, et al. Reduced adipose tissue oxygenation in human obesity: evidence for rarefaction, macrophage chemotaxis, and inflammation without an angiogenic response. *Diabetes.* 2009;58(3):718-25.
299. Ravussin E, and Smith SR. Increased fat intake, impaired fat oxidation, and failure of fat cell proliferation result in ectopic fat storage, insulin resistance, and type 2 diabetes mellitus. *Annals of the New York Academy of Sciences.* 2002;967(1):363-78.

300. Horowitz JF, Leone TC, Feng W, Kelly DP, and Klein S. Effect of endurance training on lipid metabolism in women: a potential role for PPARα in the metabolic response to training. *American Journal of Physiology-Endocrinology And Metabolism.* 2000;279(2):E348-E55.
301. Shojaee-Moradie F, Baynes K, Pentecost C, Bell J, Thomas E, Jackson N, et al. Exercise training reduces fatty acid availability and improves the insulin sensitivity of glucose metabolism. *Diabetologia.* 2007;50(2):404-13.
302. Semple RK, Crowley VC, Sewter CP, Laudes M, Christodoulides C, Considine RV, et al. Expression of the thermogenic nuclear hormone receptor coactivator PGC-1 α is reduced in the adipose tissue of morbidly obese subjects. *International journal of obesity.* 2004;28(1):176-9.
303. Hammarstedt A, Jansson PA, Wesslau C, Yang X, and Smith U. Reduced expression of PGC-1 and insulin-signaling molecules in adipose tissue is associated with insulin resistance. *Biochemical and biophysical research communications.* 2003;301(2):578-82.
304. Chen X-H, Zhao Y-P, Xue M, Ji C-B, Gao C-L, Zhu J-G, et al. TNF-α induces mitochondrial dysfunction in 3T3-L1 adipocytes. *Molecular and cellular endocrinology.* 2010;328(1-2):63-9.
305. Marycz K, Kornicka K, Szlapka-Kosarzewska J, and Weiss C. Excessive endoplasmic reticulum stress correlates with impaired mitochondrial dynamics, mitophagy and apoptosis, in liver and adipose tissue, but not in muscles in EMS horses. *International Journal of Molecular Sciences.* 2018;19(1):165.
306. Shadid S, Stehouwer CDA, and Jensen MD. Diet/Exercise versus pioglitazone: effects of insulin sensitization with decreasing or increasing fat mass on adipokines and inflammatory markers. *The Journal of Clinical Endocrinology & Metabolism.* 2006;91(9):3418-25.
307. Markofski MM, Carrillo AE, Timmerman KL, Jennings K, Coen PM, Pence BD, et al. Exercise training modifies ghrelin and adiponectin concentrations and is related to inflammation in older adults. *Journals of Gerontology Series A: Biomedical Sciences and Medical Sciences.* 2014;69(6):675-81.

308. Polak J, Klimcakova E, Moro C, Viguerie N, Berlan M, Hejnova J, et al. Effect of aerobic training on plasma levels and subcutaneous abdominal adipose tissue gene expression of adiponectin, leptin, interleukin 6, and tumor necrosis factor α in obese women. *Metabolism.* 2006;55(10):1375-81.
309. Ozcelik O, Celik H, Ayar A, Serhatlioglu S, and Kelestimur H. Investigation of the influence of training status on the relationship between the acute exercise and serum leptin levels in obese females. *Neuroendocrinology Letters.* 2004;25(5):381-5.
310. Yatagai T, Nishida Y, Nagasaka S, Nakamura T, Tokuyama K, Shindo M, et al. Relationship between exercise training-induced increase in insulin sensitivity and adiponectinemia in healthy men. *Endocrine journal.* 2003;50(2):233-8.
311. Hulver MW, Zheng D, Tanner CJ, Houmard JA, Kraus WE, Slentz CA, et al. Adiponectin is not altered with exercise training despite enhanced insulin action. *American Journal of Physiology-Endocrinology And Metabolism.* 2002;283(4):E861-E5.
312. Ligibel JA, Giobbie-Hurder A, Olenczuk D, Campbell N, Salinardi T, Winer EP, et al. Impact of a mixed strength and endurance exercise intervention on levels of adiponectin, high molecular weight adiponectin and leptin in breast cancer survivors. *Cancer Causes & Control.* 2009;20(8):1523-8.
313. Marcell TJ, McAuley KA, Traustadóttir T, and Reaven PD. Exercise training is not associated with improved levels of C-reactive protein or adiponectin. *Metabolism.* 2005;54(4):533-41.
314. Hernández EÁ, Kahl S, Seelig A, Begovatz P, Irmler M, Kupriyanova Y, et al. Acute dietary fat intake initiates alterations in energy metabolism and insulin resistance. *The Journal of clinical investigation.* 2017;127(2):695-708.
315. Sjöström L, and Björntorp P. Body composition and adipose tissue cellularity in human obesity. *Acta Medica Scandinavica.* 1974;195(1-6):201-11.
316. Smith SR, Lovejoy JC, Greenway F, Ryan D, deJonge L, de la Bretonne J, et al. Contributions of total body fat, abdominal subcutaneous adipose tissue compartments, and visceral adipose tissue to the metabolic complications of obesity. *Metabolism-Clinical and Experimental.* 2001;50(4):425-35.

317. Eriksson-Hogling D, Andersson DP, Bäckdahl J, Hoffstedt J, Rössner S, Thorell A, et al. Adipose tissue morphology predicts improved insulin sensitivity following moderate or pronounced weight loss. *International journal of obesity.* 2015;39(6):893-8.
318. Roden M, Price TB, Perseghin G, Petersen KF, Rothman DL, Cline GW, et al. Mechanism of free fatty acid-induced insulin resistance in humans. *The Journal of clinical investigation.* 1996;97(12):2859-65.
319. Schleh MW, Ryan BJ, Ahn C, Ludzki AC, Varshney P, Gillen JB, et al. Metabolic dysfunction in obesity is related to impaired suppression of fatty acid release from adipose tissue by insulin. *Obesity.* 2023.
320. Åkra S, Aksnes TA, Flaa A, Eggesbø HB, Opstad TB, Njerve IU, et al. Markers of remodeling in subcutaneous adipose tissue are strongly associated with overweight and insulin sensitivity in healthy non-obese men. *Scientific Reports.* 2020;10(1):14055.
321. Ahn C, Ryan BJ, Schleh MW, Varshney P, Ludzki AC, Gillen JB, et al. Exercise training remodels subcutaneous adipose tissue in adults with obesity even without weight loss. *The Journal of Physiology.* 2022;600(9):2127-46.
322. Spalding KL, Arner E, Westermark PO, Bernard S, Buchholz BA, Bergmann O, et al. Dynamics of fat cell turnover in humans. *Nature.* 2008;453(7196):783-7.
323. Balke B, and Ware RW. An experimental study of physical fitness of Air Force personnel. *United States Armed Forces Medical Journal.* 1959;10(6):675-88.
324. Sieckmann K, Winnerling N, Huebecker M, Leyendecker P, Juliana Silva Ribeiro D, Gnad T, et al. AdipoQ—a simple, open-source software to quantify adipocyte morphology and function in tissues and in vitro. *Molecular Biology of the Cell.* 2022;33(12):br22.
325. McAlister GC, Nusinow DP, Jedrychowski MP, Wühr M, Huttlin EL, Erickson BK, et al. MultiNotch MS3 enables accurate, sensitive, and multiplexed detection of differential expression across cancer cell line proteomes. *Analytical chemistry.* 2014;86(14):7150-8.

326. Wang S, Li W, Hu L, Cheng J, Yang H, and Liu Y. NAguideR: performing and prioritizing missing value imputations for consistent bottom-up proteomic analyses. *Nucleic acids research.* 2020;48(14):e83-e.
327. Xiao Y, Hsiao T-H, Suresh U, Chen H-IH, Wu X, Wolf SE, et al. A novel significance score for gene selection and ranking. *Bioinformatics.* 2012;30(6):801-7.
328. Kuleshov MV, Xie Z, London ABK, Yang J, Evangelista John E, Lachmann A, et al. KEA3: improved kinase enrichment analysis via data integration. *Nucleic Acids Research.* 2021;49(W1):W304-W16.
329. Rojas-Rodriguez R, Gealekman O, Kruse ME, Rosenthal B, Rao K, Min S, et al. *Methods in enzymology*. Elsevier; 2014:75-91.
330. Muller S, Ader I, Creff J, Leménager H, Achard P, Casteilla L, et al. Human adipose stromal-vascular fraction self-organizes to form vascularized adipose tissue in 3D cultures. *Scientific reports.* 2019;9(1):7250.
331. Schmittgen TD, and Livak KJ. Analyzing real-time PCR data by the comparative CT method. *Nature protocols.* 2008;3(6):1101-8.
332. Lowe CE, O'Rahilly S, and Rochford JJ. Adipogenesis at a glance. *Journal of cell science.* 2011;124(16):2681-6.
333. Melincovici CS, Boşca AB, Şuşman S, Mărginean M, Mihu C, Istrate M, et al. Vascular endothelial growth factor (VEGF)-key factor in normal and pathological angiogenesis. *Rom J Morphol Embryol.* 2018;59(2):455-67.
334. Hato T, Tabata M, and Oike Y. The role of angiopoietin-like proteins in angiogenesis and metabolism. *Trends in cardiovascular medicine.* 2008;18(1):6-14.
335. Kyriakis JM, and Avruch J. Mammalian mitogen-activated protein kinase signal transduction pathways activated by stress and inflammation. *Physiological reviews.* 2001;81(2):807-69.
336. Engeli S, Janke J, Gorzelniak K, Böhnke J, Ghose N, Lindschau C, et al. Regulation of the nitric oxide system in human adipose tissue. *Journal of lipid research.* 2004;45(9):1640-8.
337. Czarkowska-Paczek B, Zendzian-Piotrowska M, Bartlomiejczyk I, Przybylski J, and Gorski J. The influence of physical exercise on the generation of TGF-β1,

PDGF-AA, and VEGF-A in adipose tissue. *European journal of applied physiology.* 2011;111:875-81.

338. Ridnour LA, Isenberg JS, Espey MG, Thomas DD, Roberts DD, and Wink DA. Nitric oxide regulates angiogenesis through a functional switch involving thrombospondin-1. *Proceedings of the National Academy of Sciences.* 2005;102(37):13147-52.
339. Li L, Wei Y, Fang C, Liu S, Zhou F, Zhao G, et al. Exercise retards ongoing adipose tissue fibrosis in diet-induced obese mice. *Endocrine connections.* 2021;10(3):325-35.
340. Liu Y, Aron-Wisnewsky J, Marcelin G, Genser L, Le Naour G, Torcivia A, et al. Accumulation and changes in composition of collagens in subcutaneous adipose tissue after bariatric surgery. *The Journal of Clinical Endocrinology.* 2016;101(1):293-304.
341. Springer NL, Iyengar NM, Bareja R, Verma A, Jochelson MS, Giri DD, et al. Obesity-associated extracellular matrix remodeling promotes a macrophage phenotype similar to tumor-associated macrophages. *The American Journal of Pathology.* 2019;189(10).
342. Bruun JM, Helge JW, Richelsen B, and Stallknecht B. Diet and exercise reduce low-grade inflammation and macrophage infiltration in adipose tissue but not in skeletal muscle in severely obese subjects. *American Journal of Physiology-Endocrinology and Metabolism.* 2006;290(5):E961-E7.
343. Phieler J, Garcia-Martin R, Lambris JD, and Chavakis T. *Seminars in immunology*. Elsevier; 2013:47-53.
344. Fiorentino T, Hribal M, Andreozzi F, Perticone M, Sciacqua A, Perticone F, et al. Plasma complement C3 levels are associated with insulin secretion independently of adiposity measures in non-diabetic individuals. *Nutrition, Metabolism and Cardiovascular Diseases.* 2015;25(5):510-7.
345. Morgan-Bathke M, Chen L, Oberschneider E, Harteneck D, and Jensen MD. Sex and depot differences in ex vivo adipose tissue fatty acid storage and glycerol-3-phosphate acyltransferase activity. *American Journal of Physiology-Endocrinology and Metabolism.* 2015;308(9):E830-E46.

346. Shrago E, Glennon JA, and Gordon ES. Comparative aspects of lipogenesis in mammalian tissues. *Metabolism.* 1971;20(1):54-62.
347. Ortega FJ, Mayas D, Moreno-Navarrete JM, Catalán V, Gómez-Ambrosi J, Esteve E, et al. The gene expression of the main lipogenic enzymes is downregulated in visceral adipose tissue of obese subjects. *Obesity.* 2010;18(1):13-20.
348. Diraison F, Dusserre E, Vidal H, Sothier M, and Beylot M. Increased hepatic lipogenesis but decreased expression of lipogenic gene in adipose tissue in human obesity. *American Journal of Physiology-Endocrinology and Metabolism.* 2002;282(1):E46-E51.
349. Vijayakumar A, Aryal P, Wen J, Syed I, Vazirani RP, Moraes-Vieira PM, et al. Absence of carbohydrate response element binding protein in adipocytes causes systemic insulin resistance and impairs glucose transport. *Cell reports.* 2017;21(4):1021-35.
350. Cao H, Gerhold K, Mayers JR, Wiest MM, Watkins SM, and Hotamisligil GS. Identification of a lipokine, a lipid hormone linking adipose tissue to systemic metabolism. *Cell.* 2008;134(6):933-44.
351. Yore MM, Syed I, Moraes-Vieira PM, Zhang T, Herman MA, Homan EA, et al. Discovery of a class of endogenous mammalian lipids with anti-diabetic and anti-inflammatory effects. *Cell.* 2014;159(2):318-32.
352. Rognstad R, and Katz J. The balance of pyridine nucleotides and ATP in adipose tissue. *Proceedings of the National Academy of Sciences.* 1966;55(5):1148-56.
353. Townsend LK, Knuth CM, and Wright DC. Cycling our way to fit fat. *Physiological reports.* 2017;5(7):e13247.
354. NICHOLLS DG. Hamster Brown-Adipose-Tissue Mitochondria: Purine Nucleotide Control of the Ion Conductance of the Inner Membrane, the Nature of the Nucleotide Binding Site. *European Journal of Biochemistry.* 1976;62(2):223-8.
355. Boström P, Wu J, Jedrychowski MP, Korde A, Ye L, Lo JC, et al. A PGC1-α-dependent myokine that drives brown-fat-like development of white fat and thermogenesis. *Nature.* 2012;481(7382):463-8.

356. Tanimura R, Kobayashi L, Shirai T, and Takemasa T. Effects of exercise intensity on white adipose tissue browning and its regulatory signals in mice. *Physiol Rep.* 2022;10(5):e15205.
357. Vosselman M, Hoeks J, Brans B, Pallubinsky H, Nascimento E, Van Der Lans A, et al. Low brown adipose tissue activity in endurance-trained compared with lean sedentary men. *International Journal of obesity.* 2015;39(12):1696-702.
358. Mauro VP, and Edelman GM. The ribosome filter hypothesis. *Proceedings of the National Academy of Sciences.* 2002;99(19):12031-6.
359. Komili S, Farny NG, Roth FP, and Silver PA. Functional specificity among ribosomal proteins regulates gene expression. *Cell.* 2007;131(3):557-71.
360. Song G, Chen J, Deng Y, Sun L, and Yan Y. TMT Labeling Reveals the Effects of Exercises on the Proteomic Characteristics of the Subcutaneous Adipose Tissue of Growing High-Fat-Diet-Fed Rats. *ACS Omega.* 2023.
361. Robinson MM, Dasari S, Konopka AR, Johnson ML, Manjunatha S, Esponda RR, et al. Enhanced protein translation underlies improved metabolic and physical adaptations to different exercise training modes in young and old humans. *Cell metabolism.* 2017;25(3):581-92.
362. Glisovic T, Bachorik JL, Yong J, and Dreyfuss G. RNA-binding proteins and post-transcriptional gene regulation. *FEBS letters.* 2008;582(14):1977-86.
363. Louis JM, Agarwal A, Aduri R, and Talukdar I. Global analysis of RNA–protein interactions in TNF-α induced alternative splicing in metabolic disorders. *FEBS letters.* 2021;595(4):476-90.
364. Zhang P, Wu W, Ma C, Du C, Huang Y, Xu H, et al. RNA-Binding Proteins in the Regulation of Adipogenesis and Adipose Function. *Cells.* 2022;11(15):2357.
365. Hu W, and Lazar MA. Modelling metabolic diseases and drug response using stem cells and organoids. *Nature Reviews Endocrinology.* 2022;18(12):744-59.
366. Koliwad SK, Streeper RS, Monetti M, Cornelissen I, Chan L, Terayama K, et al. DGAT1-dependent triacylglycerol storage by macrophages protects mice from diet-induced insulin resistance and inflammation. *The Journal of clinical investigation.* 2010;120(3):756-67.

367. Karastergiou K, Smith SR, Greenberg AS, and Fried SK. Sex differences in human adipose tissues–the biology of pear shape. *Biology of sex differences.* 2012;3(1):1-12.
368. Verboven K, Stinkens R, Hansen D, Wens I, Frederix I, Eijnde BO, et al. Adrenergically and non-adrenergically mediated human adipose tissue lipolysis during acute exercise and exercise training. *Clinical Science.* 2018;132(15):1685-98.
369. Makki K, Froguel P, and Wolowczuk I. Adipose tissue in obesity-related inflammation and insulin resistance: cells, cytokines, and chemokines. *International Scholarly Research Notices.* 2013;2013.
370. Wallace M, and Metallo CM. *Seminars in Cell & Developmental Biology*. Elsevier; 2020:65-71.
371. Corvera S. Cellular heterogeneity in adipose tissues. *Annual review of physiology.* 2021;83:257-78.
372. Wei W, Riley NM, Lyu X, Shen X, Guo J, Raun SH, et al. Organism-wide, cell-type-specific secretome mapping of exercise training in mice. *Cell Metabolism.* 2023.
373. Han J, Koh YJ, Moon HR, Ryoo HG, Cho C-H, Kim I, et al. Adipose tissue is an extramedullary reservoir for functional hematopoietic stem and progenitor cells. *Blood, The Journal of the American Society of Hematology.* 2010;115(5):957-64.